

**Explaining satellite-derived
Actual evapotranspiration patterns
In
Homogeneously cropped large fields
(Naivasha-Kenya)**

BY

Tesfay Alemseged

**February 2002
Enschede, The Netherlands**

**Explaining satellite-derived Actual evapotranspiration patterns
In
Homogeneously cropped large fields**
(Remote sensing and ground survey perspective)

By

Tesfay Alemseged

Supervisor
Prof. Dr. A.M.J. Meijerink

This thesis submitted to the International Institute for Geo-information Science and Earth Observation (ITC), in partial fulfillment of the requirements for the degree of Master of Science in **Water Resources and Environmental Management (WREM)** with specialization in **Environmental System Analysis and Management (ESAM)**. Enschede, The Netherlands.

Degree Assessment Board

Dr. Ir. E.O. Seyhan (external examiner)
Free University Amsterdam
Prof.Dr. A.M.J. Meijerink (Chairman- Supervisor)
Water resources survey division (ITC)
Dr.Ir. C.M.M. Mannaerts (Member)
Water resources survey division (ITC)
Dr.Ir. G.R. Henneman (Member)
Soil survey division (ITC)



**INTERNATIONAL INSTITUTE FOR GEO-INFORMATION SCIENCE AND
EARTH OBSERVATION
ENSCHDE, THE NETHERLANDS**

February 2002

Disclaimer

This document describes work undertaken as part of a programme of study at the International institute of Geo-information science and earth observation. All views and opinions expressed therein remain the sole responsibility of the author, and do not necessarily represent those of the institute.

This work is dedicated to my father

Alemseged Tesfay

(1924-1975)

Abstract

Actual evapotranspiration (ETa) on a pixel basis was calculated using a Thematic Mapper image data of 18 May 2000 of Ndabibi wheat farm in Kenya with the aid of the surface energy balance method. The year 2000 was a dry year and only some fields with a 6-weeks old wheat crop received sufficient rain for the crop to grow and transpire.

The ETa estimates indicate important within and between fields' variabilities. Analysis of between and within-field ETa variability in Agricultural fields requires collecting large quantities of data to describe the variability present and to document the effects of site-specific crop management strategies on that variability. The purpose of this study was to detect the spatial relationship between the performance of the crops denoted by the actual evapotranspiration and soil chemical and physical properties.

During September 2001 field sampling was done for some general physical and chemical variables, during a wet period in two selected fields with a –next- wheat crop. Pixel scale (60 m) ETa Map was used as a base in sampling ground- based data with the aid of Global positioning system (GPS). Grid and landscape directed soil sampling were chosen for the upper and lower wheat plots respectively to reveal the observed ETa patterns.

124 observation points with two horizons were sampled in both fields, special observation points were chosen within the sampling grid based on the land shape and observed ETa patterns within the same field for determining soil physical properties such as: bulk density (Bd), saturated hydraulic conductivity (Ks), soil characterization, particle size (texture), slope steepness, depth of the topsoil and soil chemical properties such as: the readily available nutrients (Magnesium, sodium, Potassium and calcium) and percentage of organic carbon and organic matter on the various ETa patterns.

Soil heterogeneity was observed in both sampling fields ranging from clay loam to sandy clay loam in the upper field and from sandy loam-to-silt loam in the lower field. Multivariate statistics and stepwise regression were applied to analyze the relationship between the ETa patterns (18 May 2000) and field-measured (September, 2001) data.

Hence, the experimental conditions were poor. Despite that, the results of stepwise multiple regressions show that much of the variation of ETa can be explained by organic matter content, pH and bulk density of the root zone. This suggests that a single image with ETa values is more worth than just an instantaneous view of the crop, controlled by weather conditions preceding the satellite overpass.

Acknowledgements

Other things cannot be described in words. Above all, I thank my God for giving me every thing I was wishing but I have nothing to give him except thank you. I wish to express my gratitude to the Commission for Sustainable Agriculture and Environmental Rehabilitation in Tigray (Co-SAERT), and the Netherlands Government for granting me the opportunity to pursue this course of study.

I wish to extend my sincere gratitude to my supervisor prof. Dr. A.M.J. Maijerk for showing kindness and the passion of hydrology and practicality in his guidance during the fieldwork and thesis writing as well as during the lectures in the course, I am very happy to get a small part of his wide knowledge.

I would like to thanks also to Drs. Robert Becht for his good fieldwork co-ordination and help. I wish to thank also Miss. Sara Higgins and Mr. Fergus (farm Manager) supplying vital information related to their farm system.

I would like to convey my sincere and special thanks to Dr. Mannearts ,Dr. Henneman ,Dr.Rossiter, Dr. Dénes Kovács and Dr. Zoltán Vekerdy for their valuable comments and advice during the finalization of this thesis.

Many thanks to the program director Ir. A.M. van Lieshout, water resources survey division staff, G. Parod , Barbara Cassentini, Matthias spalivero and others for their assistance during my stay in ITC. Thanks to the cluster managers (Polman & Mulder) for their continuous up-keep of my computer.

I am forever grateful to my beloved parents, Ato Alemseged Tesfay and W/o Webet Berhe, who taught me the principles of life. My special heartfelt gratitude also goes to my sisters Mebrat, Tebletse, Mulu, Yergalem, Metslal, Alganesh, Genet and my brother Abraha for their warm affection, support and continuous encouragement.

Finally, my thanksgiving of my heart goes to my beloved wife Helen and my son Mikias who through their prayers and encouragement kept me going. I really appreciate the hard ship she faced due to my absence.

TABLE OF CONTENT

Chapter 1. Introduction	1
1.1. Objectives	2
1.2. Research questions.....	2
1.3. Hypothesis.....	2
1.4. General approach	2
Chapter 2. Literature Review	4
2.1. Evapotranspiration	4
2.2. Soil properties	7
2.3. Statistical analysis.....	12
Chapter 3. General overview of the study area.....	14
3.1. Location	14
3.2. Parent material	14
3.3. Climate.....	14
3.4. Ndabibi wheat farms	19
3.5. Soils.....	20
Chapter 4. Materials and methods.....	24
4.1. Field work and post field work	25
4.2. Field sampling and laboratory work.	26
4.3. Research method.....	27
Chapter 5. Analysis of evapotranspiration (RS & GIS applications).....	30
5.1. Data acquisition and preprocessing (parameters used)	30
5.2. Data analysis	32
5.3. Classification of crop performance zones	36
Chapter 6. Statistical analysis, single variables	42
6.1. Upper field	42
6.2. Lower field.....	54
6.3. Mixed data (both fields).....	64
Chapter 7. Multivariate analysis	73
7.1. Introduction.....	73
7.2. Upper wheat field.....	74
7.3. Lower wheat field	80
7.4. Combined data (both fields).....	84
Chapter 8. Results	89
8.1. Upper field regression results	89
8.2. Lower field regression results	90
8.3. Combined data (fields) regression results	90
Chapter 9. Discussion	91
Chapter 10. Conclusions and Recommendations.....	93
10.1. Conclusions.....	93
10.2. Recommendations.....	94
References.....	96
Appendix.....	99
Appendix A Soil profile description	99
Appendix B Statistical methods.....	112
Appendix C. Naivasha weather data (Temperature and wind speed graphs).....	115

Appendix D LANDSAT-ETM+ Image Preprocessing..... 116
Appendix E Field data (upper and lower fields) a) upper field..... 117
Appendix F Summary of Analytical methods..... 122

List of Figures

Figure 1 Effect of soil pH on availability of soil nutrients.....	10
Figure 2 Location map of the study area.....	14
Figure 3 Mean monthly values of meteorological observations for the Lake Naivasha area (recorded in.....	15
Figure 4 Illustration of Rainfall variability	16
Figure 5 illustration of rainfall variation around Ndabibi area.....	17
Figure 6 Temporal variation of rainfall and soil temperature (source: Naivasha meteorological station, 2001).....	17
Figure 7 Monthly (May) rainfall records across 36 years.....	19
Figure 8 Land use map of the study area.....	21
Figure 9 Geological map of the study area (sub-mapped from Clarke1990).	22
Figure 10 Soils map of the study area (Kijabe fields are indicated on the left side)	23
Figure 11 Data analysis method (spatial analysis)	27
Figure 12 Location of sampling points for both upper and lower wheat fields (respectively)	28
Figure 13 Flow diagram (methodology and materials).....	29
Figure 14 Estimation of actual evapotranspiration patterns.....	31
Figure 15 Images showing NDVI (a), surface temperature (b) and radiated temperature (c) of the study area on.....	34
Figure 16 Images showing evaporative fraction and daily ETa values of the study area on Landsat TM image window of 18 May 2000 (part of lake Naivasha is indicated on the right side).....	35
Figure 17 Descriptive statistics and normal probability plot of ETa (Both fields).....	36
Figure 18 Box plot to compare the variability of ETa in both fields	37
Figure 19 within field variability patterns (upper field) 19a: Kijabe wheat field sliced ETa patterns.....	38
Figure 20 3D views of actual evapotranspiration and NDVI patters	38
Figure 21 Box plot and sliced crop performance zones (Upper wheat field)	39
Figure 22 within field variability patterns (lower field)	40
Figure 23 ETa and NDVI patterns of the lower field.....	40
Figure 24 Box plot and sliced crop performance zones (Lower wheat field)	41
Figure 25 Location of sampling points for upper wheat field.....	42
Figure 26 scatter plot of ETa regressed by pH_10 cm depth (Upper field).....	45
Figure 27 scatter plot of ETa regressed by %pH_30 cm depth (upper field)	45
Figure 28 Soil pH map of the upper field (using ordinary Kriging).	46
Figure 29 Descriptive statistics and normal probability plots for all samples in the upper field.....	47
Figure 30 Descriptive statistics and normal probability plot for soil %OM in the upper wheat field.....	49
Figure 31 Location of sampling points for the lower wheat field.....	54
Figure 32 Descriptive statistics and normal probability plots for the lower field samples	57
Figure 33 scatter plot of ETa regressed by pH_10 (Lower field).....	57
Figure 34 Descriptive statistics and normal probability plots for NDVI and ETa (mixed data).	64
Figure 35 Descriptive statistics and normal probability plot of soil pH at 10 cm. (Mixed data)	65
Figure 36 scatterplot of ETa regressed by pH_10 (Mixed field data).....	65
Figure 37 Descriptive statistics and normal probability plot of EC at 10 cm depth (mixed data)	66
Figure 38 Descriptive statistics and normal probability plots of all soluble cations (mixed data)	66
Figure 39 Descriptive statistics and normal probability plot of %OM_10 (mixed data).	68
Figure 40 Descriptive statistics and normal probability plot of Bd in both horizons (mixed data).....	69
Figure 41 Descriptive statistics and normal probability plot of Ks (mixed data).....	69
Figure 42 Descriptive statistics and normal probability plot of topsoil depth (mixed data)	70
Figure 43 Descriptive statistics and normal probability plot of sand percentages (mixed data)	70
Figure 44 Descriptive statistics and normal probability plot of slope percentages (mixed data)	71
Figure 45 Statistical analysis steps (Multivariate statistics)	73

<i>Figure 46 Eigen values and Scree plot (upper field variables)</i>	75
<i>Figure 47 Eigen values and Scree plot (lower field variables)</i>	81
<i>Figure 48 Eigen values and Scree plot (mixed field variables)</i>	85
<i>Figure 49 Regression plot of the Observed (satellite derived) against predicted ETa values</i>	90
<i>Figure 50 Regression plot of the Observed (satellite derived) against predicted ETa values (Both fields)</i>	90
<i>Figure 51 Temperature, Relative humidity and wind speed, source Oserian farm Naivasha.</i>	115
<i>Figure 52 Fieldwork time wind speed record (sept. 20, 2001), source Oserian farm Naivasha</i>	115

List of Plates

<i>Plate 1 Partial view of the Upper Kijabe field covered by 52 days old wheat (August 20, 2001)</i>	46
<i>Plate 2 Partial view of the Lower Kijabe field covered by 112 days old (matured) wheat (September 3, 2001)</i>	56
<i>Plate 3. Profile of the study area</i>	124

LIST OF TABLES

<i>Table 1 illustration of the spatial variability of RF. (sept. 16-29) ...</i>	<i>Table 2 Nine months RF record</i>	17
<i>Table 3 Two-sample T test for upper field ETa [mm/d] vs. lower field ETa (mm/d)</i>		36
<i>Table 4 One-way Analysis of variance of the sliced actual evapotranspiration zone (Upper wheat field)</i>		39
<i>Table 5 One-way Analysis of variance of the sliced actual evapotranspiration zone (Lower wheat field)</i>		41
<i>Table 6 Correlations of soil chemical parameters (upper field)</i>		43
<i>Table 7 Correlation Pearson of ETa and physical soil parameters (Upper field)</i>		50
<i>Table 8 Analysis results of chemical and physical predictors in the upper wheat plot at</i>		53
<i>Table 9 Analysis results of log transformed chemical and physical predictors in the upper wheat plot at</i>		53
<i>Table 10 Correlation (Pearson) of soil chemical variables</i>		55
<i>Table 11 Correlation (Pearson) analysis of soil physical Variables</i>		60
<i>Table 12 Analysis results (summary) of chemical and physical predictors in the lower wheat plot at</i> <i>α =0.05</i>		62
<i>Table 13 Analysis results of log transformed chemical and physical predictors in the lower wheat plot</i>		63
<i>Table 14 Correlation (Pearson) of chemical variables (mixed data i.e. upper & lower wheat fields)</i>		65
<i>Table 15 Correlation (Pearson) of physical variables (both fields)</i>		68
<i>Table 16 Analysis results of chemical and physical predictors in the both wheat plots (mixed) at</i> <i>α =0.05</i>		71
<i>Table 17 Analysis results of log transformed chemical and physical variables (mixed data) at α =0.05</i>		72
<i>Table 18 Principal component analysis (upper field)</i>		74
<i>Table 19 Stepwise Regression of upper wheat plot chemical Parameters</i>		77
<i>Table 20 Stepwise Regression of upper wheat plot physical Parameters</i>		78
<i>Table 21 Stepwise Regression of the upper wheat plot in general</i>		79
<i>Table 22 Principal component analysis (lower field)</i>		80
<i>Table 23 Stepwise Regression of lower field chemical parameters</i>		81
<i>Table 24 Stepwise Regression of lower field physical parameters</i>		82
<i>Table 25 Stepwise Regression lower field of general soil properties</i>		83
<i>Table 26 Principal component analysis (combined data)</i>		84
<i>Table 27 Stepwise Regression mixed fields (chemical soil properties)</i>		85
<i>Table 28 Stepwise Regression mixed fields (physical soil properties)</i>		86
<i>Table 29 Stepwise Regression mixed fields (mixed soil properties)</i>		87

List of Abbreviations

Abbreviations

ANOVA	Analysis of Variance
ET	EvapoTranspiration
ET _a	Actual EvapoTranspiration
ET _c	Crop Potential EvapoTranspiration
ET _{ref}	Grass reference EvapoTranspiration
E-R	Energy Balance Residual
FAO	Food and Agricultural Organization
LAI	Leaf Area Index
NIR	Near Infrared Radiation
NDVI	Normalized Difference Vegetation Index
SAVI	Soil Adjusted Vegetation Index
LANDSAT	LAND remote sensing SATellite
TM	Thematic Mapper
AVHRR	A Very High Resolution Radiometer
NOAA	National Oceanic and Atmospheric Administration
PC	Principal Component

Symbol (General)	Description	Units
------------------	-------------	-------

K _c	Crop Coefficient	[-]
λE or LE	Latent heat flux	[W m ⁻²]
H	Sensible heat flux	[W m ⁻²]
G	Soil heat flux	[W m ⁻²]
α	The Priestley-Taylor coefficient	[-]
n	Bright sunshine hours in a day	[hours]
N	Total daytime hours in a day	[hours]
R ²	Coefficient of regression	[-]
R _o ²	Coefficient of determination	[-]
E	Efficiency factor	[-]
t	Calculated t-statistic value	[-]
t-critical	Critical t-statistic value	[-]
Z	Number of data pairs	[-]
∇	Level of significance	[-]
a	Slope of regression line forced to pass through origin	[-]
V _c	Fractional vegetation cover	[-]
A	Land surface altitude	[km]

Symbol (Radiation)	Description	Units
--------------------	-------------	-------

R _n	Net radiation flux	[W m ⁻²]
K _↓ ^{TOA}	Incoming extraterrestrial shortwave radiation flux	[W m ⁻²]
K _↓	Incoming shortwave radiation flux	[W m ⁻²]
L _↓	Incoming longwave radiation flux	[W m ⁻²]
K _↑	Outgoing shortwave radiation flux	[W m ⁻²]
L _↑	Outgoing longwave radiation flux	[W m ⁻²]
K _n	Net shortwave radiation	[W m ⁻²]
L _n	Net longwave radiation	[W m ⁻²]
R _{n24}	Net radiation flux per day	[W m ⁻²]
K _{↓24}	Incoming shortwave radiation flux per day	[W m ⁻²]

$K_{\downarrow 24}^{TOA}$	Incoming extraterrestrial shortwave radiation per day	[W m ⁻²]
L_{n24}	Net longwave radiation flux per day	[W m ⁻²]
τ_{sw}'	Single-way transmittance in the shortwave range	[-]
τ_{sw}''	Two-way transmittance in the shortwave range	[-]
τ_{sw24}'	Single-way daily transmittance in the shortwave range	[-]
T_o	Surface temperature	[K]
T_a	Air temperature at reference height	[K]
T_{mean}	Mean daily air temperature	[K]
T_{max}	Maximum daily air temperature	[K]
T_{min}	Minimum daily air temperature	[K]
α_o	Daily surface albedo	[-]
α_{inst}	Instantaneous surface albedo	[-]
ϵ_o	Surface broadband emissivity	[-]
ϵ'	Net broadband emissivity between atmosphere and surface	[-]
ϵ_a	Atmosphere broadband emissivity	[-]
σ	Stefan-Boltzmann Constant (5.67*10 ⁻⁸)	[W m ⁻² K ⁻⁴]
EF	Evaporative fraction	[-]
I_{sc}	The solar constant (1367)	[W m ⁻²]
Γ	Day angle	[rad]
E_o	Eccentricity	[-]
ω	Hour angle	[rad]
H	Altitude of satellite	[km]
R	Radius of earth (6370)	[km]

Symbol (Meteorological)	Description	Units
λ_v	Latent heat of vaporization	[MJ kg ⁻¹]
P_a	Atmospheric vapor pressure	[k Pa]
ρ_a	Density of air	[Kg m ⁻³]
c_p	Specific heat of air at constant pressure	[J kg ⁻¹ K ⁻¹]
d	Zero plane displacement	[m]
k	Von Karman's constant (0.41)	[-]
e_a	Atmospheric water vapor pressure at reference height	[k Pa]
$e_{a,sat}$	Saturation vapor pressure of air at reference height	[k Pa]
$e_{o,sat}$	Saturation vapor pressure near surface	[k Pa]
D	Vapor pressure deficit at reference height ($e_{a,sat} - e_a$)	[k Pa]
RH	Relative humidity	[%]
r_{ah}	Aerodynamic resistance to heat transport	[s m ⁻¹]
r_{av}	Aerodynamic resistance to water vapor transport	[s m ⁻¹]
r_a	Aerodynamic resistance ($r_{ah} \approx r_{av}$)	[s m ⁻¹]
Δ	Slope of saturation vapor pressure	[k Pa °C ⁻¹]
u	Wind speed at reference height	[m s ⁻¹]
Z_{oh}	Roughness length for heat transport	[m]
Z_{om}	Roughness length for momentum transport	[m]
γ	Psychrometric constant	[k Pa °C ⁻¹]
Ψ_m	Intergrated stability function for momentum transfer	[-]
Ψ_h	Intergrated stability function for heat transfer	[-]
d	Displacement height	[m]
Z	Reference height (1.75)	[m]

Symbol (Soil & plant)	Description	Units
d	Soil depth	[cm]
θ_d	Soil moisture content (by volume) at depth d	[%]
A_h	Depth topsoil soil (A horizon)	[cm]
h	Crop height	[m]
me/100g	milliequivalents per 100-gram	
EC	Electrical conductivity	[μ s/cm]
Symbol (Geometry)	Description	Units
θ_z	Solar zenith angle, incidence angle on a horizontal plane [deg]	
ϕ_z	Satellite zenith angle	[deg]
ϕ_{view}	Off-nadir angle	[deg]

Chapter 1. Introduction

Satellite data can be used to calculate actual evapotranspiration (ET_a) on a pixel basis by the surface energy balance method. The work of e.g. Bastiaanssen et al. (1998a,b), Caselles, V., M.M. Artigao, E. Hurtado, C. Coll, A. Brasa 1998 and others have made general application possible by the development of approximations for physical parameters and by transfer functions. Several studies have shown the validity of the method when applied to cropped lands (Bastiaanssen et al 2000)

The accuracy of the actual evapotranspiration in mm.d⁻¹ by the method depends on the available data concerning air temperature at standard height (2 m), incoming radiation, relative humidity and ground heat flux measurement, to name the most important ones.

The method is not free of complications because the instantaneous values during overpass have to be extrapolated over the day when clouds appear after the overpass and the evaporative fraction may not be constant. Furthermore, interpolation between satellite overpasses has to be made. Farah (2001) worked on providing solutions of those problems, but they require continuous recording of some meteorological parameters.

However, an estimate of ET_a using satellite data can be made by using air temperature and estimation of incoming short wave radiation during a sunny day for the area concerned. That ET_a estimate provides the spatial variation of the relative evapotranspiration within a realistic range.

In practice, neither time series of images may be available, nor on-site continuous meteorological data. To complicate the matter further, preferably soil moisture has to be measured during the satellite overpass at many sample points, which is very difficult to achieve.

However, it is common knowledge that within-field or within-farm variation of crop performance tends to be persistent, because of the soil qualities, which do not have much year to year variation, except for soil moisture.

In this study an attempt is made to relate some easily measurable soil physical and chemical variables, sampled during a year with normal rainfall, to patterns of relative ET_a as calculated with satellite data of a previous, dry year.

The experimental conditions can be qualified as being poor. The field sampling was done with a different wheat crop grown under supervision of a new farm manager and during the fieldwork frequent rains occurred, so that the measurement of the spatial variation in soil moisture lost its significance. During the dry year of the satellite overpass most of the fields had a crop failure. Only a few fields in the upper part of a large wheat farm selected for this study had a crop and in the lower part of the farm only one field had a partial crop. There is evidence of significant spatial variation of rainfall within the wheat farm because of orographic effects, but rainfall was not recorded in the farm during the year 2000.

However, the fields are about 1 km² in size, allowing a study of the within-field variability with one variety of wheat per field, sown during a short period of time with only minor variation in practice.

The problems analyzed was, whether under these conditions the ET_a patterns be related to easily measurable soil variables. If so, a single image would be worth more than an instantaneous view.

1.1. Objectives

- To investigate whether pixel scale ETa estimates generated using the energy balance Equations (satellite derived) can be related to terrain and soil data under uniform crop.
- To explain whether results of the analysis can be used for site-specific management at field scale.

1.2. Research questions

- To what extent the within field variation of ETa estimates (using the energy balance approach) can be explained by soil physical and chemical factors.
- To investigate whether explanatory relationships as derived from one field can be used for extrapolation to the near by fields.
- To draw conclusions as to the feasibility of using ETa values at pixel scale for site specific management.

1.3. Hypothesis

- There are significant spatial crop performance differences within fields of a given soil and crop setting.
- ETa variation at a single day and at field scale can be explained from terrain and soil properties.

1.4. General approach

It is logical that management practices used in one field may not necessarily produce the same results in another field because of the interaction of several physical characteristics. In addition, this complex interaction between management practices and physical characteristics changes across years. This in turn causes more challenge in planning and making appropriate management decisions.

Knowledge of the relationship between the spatial variability of crop performance and the most likely attributes is an essential approach to determine what set of practices will produce the best outcome for meeting environmental goals of a specific farm zone while maintaining productivity and profitability.

This paper does not attempt to evaluate the effect of all the various parameters towards the yield variability rather the results of this study could contribute in evaluating the effect of selected soil-water parameters (texture, soil organic matter content, water holding capacity and nutrient availability) and topographic effects towards the observed spatial crop performance variations (in an instantaneous actual evapotranspiration results).

The results that are expected from this study will be helpful in identifying the relationship between the crop performance (actual evapotranspiration) and the spatial distribution of soil physical and chemical properties for that particular season.

Chapter 2. Literature Review

Definitions

•**Actual evapotranspiration (ET_a)** is a real amount of water what is consumed by crops. ET_a depends on climatological factors, type of crops and the amount of water available for consumption in the soil root zone.

Theoretical background

"Soil evaporation is a direct pathway for water to move from soil to the atmosphere as water vapor. Over the course of a certain rainy season, soil evaporation is 20-30 percent of total ET. Soil evaporation rates are highest after rainfall. At those times the soil surface is wet and the water readily evaporates" (Brady and Weil.1996).

As the soil dries the soil evaporation rates decline. Plant transpiration is evaporation of water from leaf and plant surfaces. Transpiration is the last step in a continuous water pathway from soil, into plant roots, through plant stems and leaves, and out into the atmosphere. Water conditions "drive" the system by pulling the water "uphill" through the entire pathway. Since water in this pathway also carries nutrients, transpiration is an essential process in plant life. In fact evapotranspiration is highly variable hour to hour and day to day, however, only instantaneous recording was available. For sunny days, as in May 18, 2000, evaporative fraction is constant.

2.1. Evapotranspiration

To date, the only practical means of mapping the spatial distribution of ET on a regional or local scale is to use remotely sensed multispectral data from satellite-based sensors (Moran et al., 1989). Satellite imagery has been widely used for large-area estimation of mass and energy fluxes and review of many of these applications is given by Bastiaanssen (1998), Moran and Jackson (1991), also included in the AHAS package (Parodi, 2000). The techniques traditionally involved combination of atmospheric corrections, models of resistance to mass and energy, and detailed spatial information of major surface and climate variables.

An operational application of this technology, however, is often limited due to the inherent complexity of this procedure. Remote sensors are designed to quantify energy in specific ranges of the radiometric spectrum. The ranges coincide with atmospheric windows where the atmosphere is almost transparent and the perturbation caused by its components is minimum.

The evaporation process of land surfaces is a consequence of energetic changes of fluxes that tend to balance. The energy playing the role derived from remote sensors (Parodi, 2001), The thermodynamic process ruling the energetic equilibrium is expressed in energy balance equation (EBE).

Estimation of actual evapotranspiration using the spatial energy balance approach is an application of the Principle of conservation of energy where the surface energy balance is considered as the main boundary condition to be satisfied in the analysis.

For a unit horizontal area the energy budget is defined as:

$$R_n = G_o + H + \lambda E \quad (1)$$

Where: R_n (W m⁻²) is the net incoming radiation flux density,

H (W m⁻²) is the sensible heat flux density,

G_o (W m⁻²) is the sensible heat flux density and

λE (W m⁻²) is the latent heat flux density

The parameter λ is the latent heat of vaporization of water (J kg⁻¹) and E is the vapor flux density (kg m⁻² s⁻¹).

The measure of spatial distribution of Evapotranspiration is expressed in equivalent of water depth over a period of time. The main challenge of the energy balance approach of computing evapotranspiration is the determination of the latent heat flux λE sensible heat H out of the total available energy ($R_n - G_o$).

The energy balance equation neglects the energy required for photosynthesis and heat stored in the vegetation.

Computation of the sensible heat flux i.e. the energy used to warm up the surrounding environment and the plant itself is the most sensitive and challenging part in partitioning the remaining (available) energy in to a sensible and latent heat flux density.

The evaporative fraction $\Lambda = \lambda E / (R_n - G_0)$ is used for partitioning the remaining energy.

The net radiation R_n is the difference between all incoming and outgoing radiative fluxes. Radiation is divided into short wave and long wave. The amount of incoming short-wave radiation varies with the positions on the earth's surface (i.e. latitude) in relation to the sun.

The determination of actual evapotranspiration requires quantification of the latent heat flux (λE) term, since this represents the energy required to convert water to vapor. Since latent heat depends on the soil water content, it is the most difficult parameter to measure. The method relies on estimating the other terms in equation (1)

Another way of defining the net radiation is given by the relation:

$$R_n = K_{\downarrow} - K_{\uparrow} + L_{\downarrow} - L_{\uparrow} \quad (2)$$

where, K_{\downarrow} : Incoming short-wave radiation [$W m^{-2}$]

K_{\uparrow} : Outgoing short-wave radiation [$W m^{-2}$]

$$K_{\uparrow} = \rho_o K_{\downarrow}$$

ρ_o : albedo, derived from the six visible and near infrared bands (b(1-5) and b7)

L_{\downarrow} : Incoming long-wave radiation [$W m^{-2}$], which depends on the thermic Structure of the layered Atmosphere, influenced by the atmospheric emissivity, ϵ_a and air temperature (T_a)

$$L_{\uparrow} = \sigma \cdot \epsilon_a T_a^4$$

σ : Stefan_Boltzmann constant ($5.669 \cdot 10^{-8} W \cdot m^{-2} K^{-4}$)

L_{\uparrow} : Out going long-wave radiation which depends on the emissivity of the surface (ϵ_o) and surface temperature (T_o) which is expressed as:

$$L_{\uparrow} = \sigma \cdot \epsilon_o T_o^4$$

L -The emissivity is dependent on the albedo values (both broad-band and minimal planetary) and the double way atmospheric transmittances.

$$\rho_o = \frac{\rho_p - \rho_a}{\tau^2} \quad (3)$$

Where, ρ_a : broad band planetary albedo (derived from the six visible and near infrared bands TM bands 1,2,3,4,5 and 7)

ρ_p : Minimal planetary albedo (derived from the six visible and near infrared bands TM bands 1,2,3,4,5 and 7)

τ^2 : double way atmospheric transmittance

The actual amount of incoming short wave radiation varies with the positions of the earth's surface (i.e. altitude) in relation to the sun. The reflected and absorbed portion of short wave radiation from the surface of the earth is also influenced by the surface characteristics and land wetness condition.

Similarly the incoming and out going long wave radiations are emitted by the atmosphere and the earth's surface respectively. A portion of the incoming long-wave radiation is reflected back to the atmosphere.

Where the symbol ϵ_o and $(1 - \epsilon_o)$ represents the emissivity of a specific body in the thermal ranges, and the net incoming short wave radiation $\rho_o K_{\downarrow}$ is reflected out of the total incoming short wave radiation.

The energy balance equation there for can be also given in its final form as:

$$R_n = (1 - \rho_o) K \downarrow \sigma \cdot \varepsilon T_a^4 - \sigma \cdot \varepsilon_o T_o^4 + \varepsilon_o \sigma \cdot \varepsilon T_a^4 \quad (4)$$

Among the different components of the energy balance the soil heat flux (G) could not be determined from satellite sensors. Determination of the soil heat flux therefore requires an empirical formula derived from remotely sensed parameters such as the vegetation indexes (NDVI), surface temperature, and surface albedo.

Estimate of soil heat flux is given using the relation:

$$\frac{G_o}{Rn} = 1.430 \frac{T_o^c}{100 \rho_o} (0.32 \rho_o \text{mean} + 0.62 \rho_o \text{mean}^2) (1 - 0.978 \text{NDVI}^4) \quad (5)$$

The sensible heat flux (H) is expressed as:

$$H = \rho_{air} C_p \frac{(T_o - T_a)}{r} \quad (6)$$

Where r : aerodynamic roughness (L)
 ρ_{air} : Moist air density (m/L^3)
 C_p : air specific heat at constant pressure ($\text{J/kg} \cdot ^\circ\text{k}$)

Estimation of actual evapotranspiration using satellite imagery involves another important relationship with instantaneous evaporative fraction Λ , and the daily average net radiation, Rn_{24} . The evaporative fraction can be computed from the instantaneous surface energy balance on a pixel-by-pixel basis (Bastiaanssen et al., 1999):

The latent heat flux λE , being the residual term is useful to compute the evaporative fraction.

$$\lambda E = R_n - G_o - H \quad (\text{W/m}^2) \quad (7)$$

Where the evaporative fraction is given by:

$$\Lambda = \frac{\lambda E}{\lambda E + H} = \frac{\lambda E}{R_n - G_o} \quad (8)$$

The evaporative fraction is a ratio of the actual to wet area evapotranspiration when the atmospheric moisture conditions are in equilibrium with the soil moisture conditions.

The value of evaporative fraction is assumed to be the same as the daily values and the soil heat flux (G) assumed to be zero on a daily basis. Considering the above points and substituting equation (eq. 1) in equation (eq.2) leads to the following form:

$$\lambda E_{day} = \Lambda_{inst} \cdot Rn_{day}$$

$$Rn_{day} = K \downarrow_{day} - \rho_o K \downarrow + \Delta L \quad (9)$$

As an alternative to the ground (station) right time pyranometer reading the incoming short wave radiation has been obtained using a model, taking in to account the geographic location, solar zenith angle and time of satellite overpass.

Where, the fraction of short wave radiation reaching the ground surface has been estimated from the total extra-terrestrial radiation (Ra) using the emissivity ratio.

$$K \downarrow_{day} = 0.718 Ra \quad (10)$$

The daily actual evapotranspiration for the area has been obtained by using the following relationship:

$$ETa_{day} = \frac{\Lambda_{inst} * Rn_{day}}{28} \quad (11)$$

For the purpose of visualizing the wheat performance variations the Actual evapotranspiration map has been produced (equations 1-11) using the Landsat TM image taken on 18 May 2000. However, it should be noted that due to the absence of the right time pyranometric reading of the incoming short-wave radiation evapotranspiration estimate was done using a model, which accounts the geographic location, solar zenith angle and time of satellite overpass.

The estimation of actual evapotranspiration values were made mainly based on simplified assumptions involving the ground data including air temperature and wind speed records from the near by stations and the remote sensed data. There fore, the value obtained is appropriate. However, the ETa pattern thus obtained is valid for the comparison with site factor patterns.

The other limitation of this study is overlooking the temporal dimension of the dynamic nature of soil properties, i.e. soil properties measured during the field work (September 2001), are used to explain actual evapotranspiration patterns derived from satellite image of May 18,2000.

The final ETa map is considered to be essential to give a relative variation of the within and between field variation of the wheat evapotranspiration values classified as High, Medium and Lower crop performance ranges based on the estimates for May 18 2000.

2.2. Soil properties

General aspects of topsoil classification and fertility classification methods are discussed in FAO (1998): Topsoil characterization for sustainable land management, Eroconsult (1989): Agricultural compendium for rural development in the tropics and Subtropics, Booker (1991): tropical soil manual, e.t.c.However, some specific aspects are mentioned here because of their relevance to this study.

2.2.1.Topsoil classification

FAO, 1998 groups topsoils by texture and the following dominant features: organic material, organic matter status, physical, chemical and biological features, drainage features, land use, erosion or degradation, external physical conditions, and slope class.

The lower limit of the topsoil is set at 30cm depth, or at a root growth-inhibiting layer whichever shallower soil may be. This layer can be hard rock, a pedogenetically indurated layer, a chemically unfavorable layer, or a strongly contrasting layer. Litter, if existent, occurs above the topsoil (FAO, 1998).

"The topsoil is strongly influenced by soil forming factors, both externally and internally. The characterization and subsequent stratification of topsoils, therefore, has to take into account all these factors, which are interdependent, they are related to each other and influence one another.

The factors climate, vegetation and organic matter, topography and physiography, mineralogical soil constituents, surface processes, biological activity and human activity" (FAO, 1998).

2.2.2.Soil moisture

It is generally known that mountainous areas play an important role at water resources forming and runoff generation. Water content in the unsaturated zone of soil profile is a basic parameter at water flow partition in water balance, at surface runoff generation and groundwater recharge and at actual evapotranspiration calculation that is the main loss component besides surface runoff. Soil water content is a time dynamic variable responding to climatic inputs variability. However, some general spatial distribution patterns dependent on topography, hydrography, pedology and vegetation are evident considering long term average. The potential for predicting the spatial distribution of soil water content in mountain catchment is related to soil type, vegetation type, relative height, slope, aspect and distance from water streams.

2.2.3.Fertility capability classes (FCC)

Characterizing soil resources in terms of their spatial variability of fertility levels is an essential method in identifying the main attributes of within and between field variability of field conditions as well as crop performance.

Mapping and analyzing this variability based on differential capability levels and linking the spatial relationships to management action, places production agriculture at the cutting edge of GIS applications.

According to the FAO, 1998 Fertility Capability Classification (FCC) system Soil Management practices are largely limited to the ploughed layer, as a result the FAO recommends characterization of the topsoils be preferably done based on FCC. The FAO system groups soils according to their fertility constraints in a quantitative manner. Since each soil type has properties that are intrinsic. The numbers of viable management options are confined by these properties.

The FCC provides a checklist of identifiable properties that influence the effectiveness of specific management practices. The importance of each soil property varies with the crop and management system and therefore no priorities are assigned or intended. However, beyond its use as an important guide as practice of concern, the system by itself is not sufficient to provide precise and enough information for implementation of soil management practices (Smith 1989).

The FCC classifies the topsoils quantitatively based on their fertility constraints: type (topsoil texture 0-20cm), substrata type (subsoil texture 20-60cm), and 15 modifiers. Class designations from the three categorical levels are combined to form an FCC unit.

2.2.4. Vegetation and organic matter

The influence of vegetation cover on soil fertility of particular relevance to this study is the relation to within and between fields' variations of soil fertility, because the upper portion of the study area was part of the existing thick forest 7 years ago.

The FAO 1998 topsoil characterization describes vegetation and organic matter Similar to the other top soil property influencing factors i.e. biological activities, surface processes, topography and physiography, mineralogical soil constituents and human activities as a basic source of soil variability.

According to the FAO 1998, Vegetation contributes in several ways to the formation of topsoil characteristics:

- penetrating roots loosen the soil and improve porosity and aeration
- Litter, decaying branches and stems are transformed into organic matter (OM).

The replenishment of nutrients in the topsoil is largely determined by the chemical constituents of litter; and a vegetation cover and protects the surface against the impact of raindrops and wind.

More over, Vegetation may eventually be transformed into soil organic matter (%OM) and this when intimately mixed with soil mineral particles:

- Enhances aggregation
- Increases structural stability
- Increases water holding capacity
- Contributes to the nutrient holding capacity
- Buffers against potential acidification
- Binds toxic substances to the soil complex, e.g. an excess of Al and Fe; and
- Provides the soil with N, P and S and other nutrients which were stored in the above ground

Biomass.

The volume of solid particles in organic soils is much lesser than in mineral soils. For management purposes organic soils provide greater space for retaining more pore water availing for plants. The amount of water retained at very low tensions is much greater for organic soils (FAO 1988b). The total pore space in fibric organic topsoils is high which allows a high rate of water movement because of the large pores usually present. These large pores collapse on progressive decomposition and total pore space decreases on drainage the porosity of organic soils changes drastically.

According to the FAO, 1998 top soil characterization, Soil organic matter is central to the maintenance of soil fertility: mineralization of N, P and S, the soil's ability to hold nutrients cations, structural stability and water holding capacity are all affected by OM content. Nutrients can be easily supplied where fertilizers are available. Organic matter is one of the most important aggregate stabilizing agents in the soil. The very high OM decomposition rates in the warmer climates make it difficult to maintain high carbon levels in cultivated soils. A decrease in OM increases the erosion risk.

Water erosion preferentially removes soil colloids, including humified OM. Decreasing OM content also increases the susceptibility to crusting, which further enhances the erosion risk. The soil erosion risk is also increased by the reduction of soil faunal activity, which decreases with decreasing OM content.

2.2.5. Saturated hydraulic conductivity

Saturated flow through soils is a hydraulic flow through a soil profile under a completely saturated condition; that is, all pores, large and small, are filled with water. The lower horizons of poorly drained soils are often saturated, as are portions of well-drained soils above stratified layers of clay. During and

immediately following a heavy rain or irrigation, pores in the upper soil zones are filled entirely with water.

The principle of an inverse Auger method applies the same principle in determining the quantity of water (Q) flowing through a column of saturated soil expressed by the Darcy's law as follows:

$$Q = \frac{K_s * A * \Delta P}{L}$$

Where K_s is the saturated hydraulic conductivity, A is area of the column through which the water flows, P the hydrostatic pressure difference from the top to the bottom of the column. Since area A and length L of a given column are fixed, the hydraulic force ΔP determines the rate of flow, driving the water through the soil (commonly gravity) and the hydraulic conductivity K_s or case with which the pores permit water movement.

The saturated hydraulic conductivity K_s of a uniform saturated soil remains fairly constant over time, and is dependent on the size and configuration of the soil pores, all of which are filled with water. This is in contrast to the value of K in an unsaturated soil; which decreases as the water content decreases.

2.2.6.Texture

“The sizes of the mineral particles profoundly affect the physical properties of soils: drainage, the water-holding capacity and the ease with which the soil can be cultivated. Coarse-textured soils and gravelly soils do have a low soil moisture storage capacity because of their high porosity and high infiltration rates as well as excessive internal drainage. This low moisture storage capacity has a considerably negative effect on crop growth and yields in semi-arid and sub-humid areas, where rains are often variable in time and space and dry spells within the main cropping season are frequent, because excess moisture from previous rains cannot be stored sufficiently long in the soil profile”(FOA soil classification, 1998b).

There are cases where, the Field level (hand test) and laboratory texture analysis results show variation in some portions of the field, in such cases laboratory measured values are applied for the purpose of the study. However, no texture variables were used for statistical modeling.

2.2.7.Soil chemistry

High rainfall contributes towards the leaching of the soil cations such as Mg and Ca. Water (H_2O) combines with carbon dioxide (CO_2) to form a weak acid-carbonic acid (H_2CO_3). The weak acid ionizes, releasing hydrogen (H^+) and bicarbonate (HCO_3^-). The released hydrogen ions replace the calcium ions held by soil colloids, causing the soil to become acid.

The displaced calcium (Ca^{++}) ions combine with the bicarbonate ions to form calcium bicarbonate, which, being soluble, is leached from the soil. The net effect is increased soil acidity.

When clay colloids are saturated by H ions, they behave as a weak acid. The more hydrogen ions held by the exchange complex of a soil in relation to the basic ions (Ca, Mg, K) held, the greater the acidity of the soil (Cliff Synder, 2001).

According to the Hand book of tropical soil manual, Knowledge about the level of Individual exchangeable cations in soil are of immediate value in advisory work than CEC, because they not only indicate existing nutrient status, but can also be used to assess balance amongst cations.

This is of great importance because many effects, for example soil structure and nutrient uptake by crops, are influenced by the relative concentrations of cations as well as by their absolute levels.

Magnesium

The level of soluble magnesium or magnesium deficiency in a crop may not only be associated with low magnesium content in the soil, but also with the presence of large amounts of other cations, particularly Ca and K.

With increasing Ca:Mg ratios above about 5:1, the magnesium may become increasingly less available to plants, although soils can remain fertile over a very wide range of Ca:Mg ratios.

Deficiency symptoms resulting from absolute values of exchangeable Mg, rather than cation imbalance, are being reported in acid, coarse textured soils having exchangeable Mg levels of <0.2 me/100 gram soil (Heald, 1965 as cited in Booker Tate 1991).

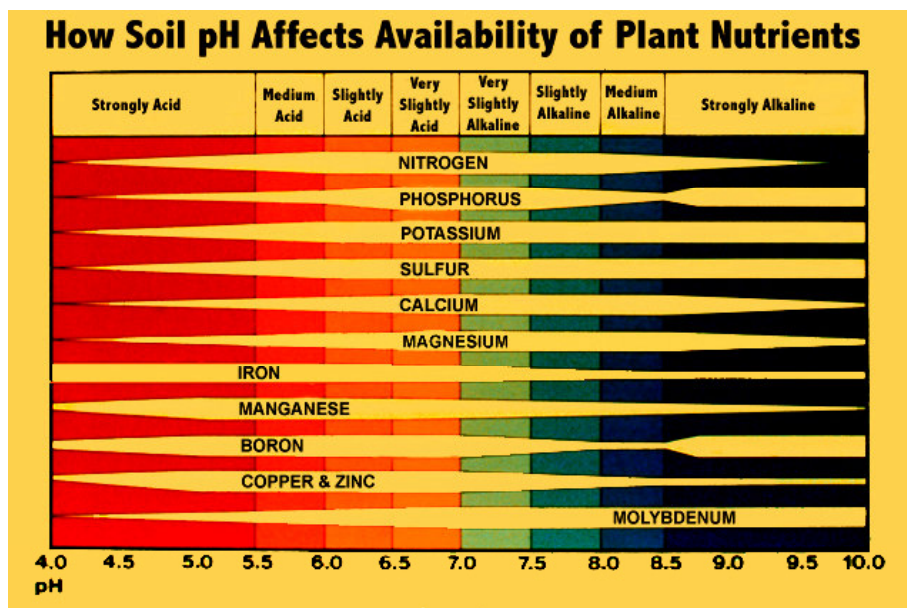
Nitrogen sources (fertilizers, manures, legumes), which contain or form ammonium, increase soil acidity unless the plant directly absorbs the ammonium ions. The greater the nitrogen fertilization rates with these sources, the greater the soil acidification. As ammonium is converted to nitrate in the soil (nitrification), H ions are released. For each 453.59 grams of nitrogen as ammonium or forming ammonium in urea, ammonium nitrate, and anhydrous ammonia, it takes approximately 816.47 grams of pure calcium carbonate to neutralize the residual acidity. Also, the nitrate that is provided or that which forms can combine with basic cations like calcium, magnesium, and potassium and leach from the topsoil into the subsoil. As these bases are removed and replaced by H ions, soils become more acid.

According to Cliff synder (2001), even if the top six inches of soil show a pH above 6.0, the subsoil may be extremely acid. When sub-soil pH's drop below 5.0, aluminum and manganese in the soil become much more soluble and in some soils may be toxic to plant growth. Wheat is an example of a crop that is sensitive to high soluble aluminum levels in the subsoil and crop yields may be reduced under conditions of low subsoil pH.

There fore the pH values measured at 10 and 30 cm depth was used in the statistical analysis. The primary effect of low pH values relate to the availability of toxic elements and plant nutrients. Toxic elements like aluminum and manganese are the major causes of crop failure in acid soils. These elements are a problem in acidic soils since they dissolve more readily and are more available for plant uptake at low pH. The primary problem with low pH for wheat production is aluminum toxicity, which results in poor root development.

Figure 1 Effect of soil pH on availability of soil nutrients

(Source: After Truog (1948) as site in Booker Tate, 1991)



2.2.8. Bulk density

Bulk density is a measure of the weight of the soil per unit volume (g/cc), usually given on an oven-dry (110° C) basis. Variation in bulk density is attributable to the relative proportion and specific gravity of solid organic and inorganic particles and to the porosity of the soil. According to Booker (1991), most mineral soils have bulk densities between 1.0 and 2.0. Although bulk densities are seldom measured, they are important in quantitative soil studies. Such data are especially necessary, in calculating soil moisture movement within a profile and rates of clay formation and carbonate accumulation.

2.2.9. Andic soils

According to Brady Nico van Breemen and Peter Buurman (1998), Andosols are soils developed in volcanic ash, tuff, pumic and other volcanic ejects of various compositions. They are commonly found at high elevations near the volcanic source. Since the volcanic materials have been deposited in recent geological time, Andosols have not been highly weathered. The rapid weathering of the porous parent

material results in the accumulation of amorphous clays with a high specific surface. Andosols are young soils-having been developed for only 5,000-10,000 years. They have a unique set of properties due to a common type of parent materials.

The silicate minerals allophane and imogolite and/or Aluminum-humus complexes dominate the colloidal fraction of at least the upper 35 cm. The combination of these minerals and the high organic matter results in high water holding capacity. The upper layers are characteristically dark in colour and have low bulk densities (Brady Weil.1996)

General Andosols have a fluffy consistency and a dark colour. These soils are further characterized by their high porosity, high permeability and their large soil moisture storage capacity. They are rich in nutrients, but show a great affinity for phosphate ions that they bind and which become unavailable for crops.

Andosols suborders: based on the explanation given by Brady (1996), which are formed as result of soil moisture regime (Ustands) and humid climate (Udands) occur in a significant areas along the rift valley of east Africa.

During the laboratory analysis additional treatment and time was required to oxidize the high organic matter content of the soil samples.

2.2.10.Wheat performance

According to FAO 1977, better farming series, Wheat is a cereal that is chiefly grown in cold countries. In Africa wheat grows in regions where there is a very cold season, mainly on the edges of the desert, near rivers and lakes: such as the Mauritania and Senegal, along the Senegal River; in Mali and Niger, along the Niger River; in Chad, near to Lake Chad; as well as in mountainous and hilly regions such as: eastern Zaire; Rwanda and Burundi.

East African highlands specifically Ethiopia and Kenya are also known for growing wheat as a staple food; making bread. Wheat is a common name of which the scientific name is *Triticum spp* based on the FAO, 1977, the indicative annual yield is 4-6 tones per hectare and plant density for broadcast is 100-140 kg ha⁻¹.

Wheat is a grass (monocot); it has mostly fine roots, and no taproot. It would therefore be fairly sensitive to compaction. It is also known to be quite sensitive to salts and Aluminum (beginning at pH< 5.8 or so). For good yields it needs quite some N, which can be supplied partly by OM; it needs a good supply of cations, especially Ca⁺², Mg⁺², K⁺ (not Na⁺). It is sensitive to micronutrient deficiencies (especially Cu⁺²). It is not especially drought-sensitive; wheat yield suffers if drought occurs at key times. Water requirement increases during the vegetative stage through flowering, and then decreases after grain set, during translocation.

Soil compaction and possible Crusting can prevent seedling emergence to the extent that a substantial amount of seed may be wasted and resowing may be necessary if production of a crop is to be worthwhile. This occurs because the mechanical strength of a crust maybe too great for seedling shoots to penetrate so that emergence is impossible.

According to Booker 1991 the maximum rooting depth for winter wheat is in the range of 150-200 cm where the nutrient and water uptake ranges between 100-150. Actual root penetration depends on cultivars, water regime (rainfall intensity and frequency) and soil conditions,

The average rooting pattern of winter wheat in tropical soils can be generalized as; lateral spread of roots is in the range of 15-25 cm and 50-60% water uptake horizon is ≤30cm, readily available soil water (% of total AWC) demand is 50% during the growth period and 90% during the ripening period.

According to Agricultural compendium for rural development in the tropics 1989, Suitable climate for wheat growth is a minimum of 250 mm well-distributed rainfall, where ear initiation stage is the most critical period as regard to water supply.

2.2.11.Spatial variations within large fields

The heterogeneous nature of agricultural lands is observed causing within field variability of agricultural yields under uniform fertilizer application. The use of remote sensing and geographic information system for Evaluation of Agricultural land potentials (relative fertility levels) is essential and cheaper approach for implementing variable-rate strategies of fertilizer application. In fact, this thesis deals with aspects of within field variability.

The crop management system known as site-specific agricultural management relies on geo-spatial information to facilitate the treatment of small portions of field as individuals management units. Although agriculturalists have long known that fields are heterogeneous, only recently have technologies become available that allow production practices to efficiently take this variability into account. Key technologies include GPS, GIS, electronic sensors, and ruggedized computers for within-field data acquisition and operation control that can be added, the calculation of actual evapotranspiration, as it is done in this study.

Statistical analysis of soil characteristics, topography and rainfall parameters indicates that among the various reasons for the nested variation in crop actual evapotranspiration, it is possible to sense the effect of the fertility (Nutrient deficiency) and inferior moisture holding capacity of soils in reducing the evapotranspiration potentials in the rain fed wheat fields.

Mapping the surveyed area by classes of soil fertility from remote sensing using limited ground-based data is advantageous to assess the magnitudes of crop yield losses and associated economic losses caused by spatially uniform fertilizer application and lack of within field operation control.

Information pertaining to spatial transpiration-nutrient uptake level relationship of agricultural fields on the other hand is essential to document and evaluate key spatial crop performance variability attributes of targeted potential agricultural fields.

If so, then it should be possible to compare performance across agricultural fields in a number of crop type, soil quality, soil texture etc. settings to understand where we presently stand with respect to productive utilization of land and water, to compare relative performance of crops, and to identify where performance can be improved.

Apart from the above-mentioned variables such as application of agrochemicals, planting date, crop types etc. Crop management and other factors play an important role. Although this study area was aimed for explaining the ETa variation using the soil properties, variations of ETa due to a single day heavy rain and water logging during sensitive crop stages was observed in some portion of the lower field.

2.3. Statistical analysis

In explaining the spatial Variation of actual evapotranspiration based on the geo-referenced field data appropriate statistical analysis methods should be chosen. Testing the quality of the field data however, is a prior step in deciding to perform a certain statistical analysis of the field data and evapotranspiration estimates of each sampling point.

Many standard statistical procedures such as the t-test assumes that the samples were drawn from a normal distribution before performing a certain statistical analysis, there fore testing the distribution of the field data is a prior step in the overall processes. Normality Test generates a normal probability plot and performs a hypothesis test to examine whether or not the observations follow a normal distribution.

Different descriptive statistical methods have been devised to aid in understanding the population of a given data set, including the mean, median, range, histogram etc. Statistical hypotheses is used for claiming about the existing data set collected using the grid and transect sampling where descriptive statistics may be used to infer information about the population.

The “mean” is used as a measure of central tendency in a data set, but the use of the mean requires an underlying assumption that the data set has an almost symmetrical distribution (Wonnacott, 1990), i.e. normal distribution in statistical analysis testing for differences of means of two populations is much used test, such as t-test.

Normal probability plot is a common statistical method devised to measure how far the plot points fall from the fitted line in a probability plot. The statistic is a weighted squared distance from the plot points to the fitted line with larger weights in the tails of the distribution. Among others the Anderson-Darling and Ryan-Joiner tests have similar power for detecting non-normality related to other tests such as the - Smirnov test, which has relatively lesser power (Minitab, 2000).

The common null hypothesis for these three tests is H_0 : data follow a normal distribution. If the p-value of the test is less than the alpha level, H_0 is rejected. The vertical axis of the displayed plots has a probability scale; the horizontal axis, a data scale. A least-squares line is fit to the plotted points and

drawn on the plot for reference. The line forms an estimate of the cumulative distribution function for the population from which data are drawn. Numerical estimates of the population parameters, $\bar{\sigma}$ and $\bar{\mu}$, are displayed with the plot.

Anderson-Darling test that can be processed by the Minitab software applies an empirical cumulative distribution function, for generating a normal probability plot and performs a hypothesis test to examine whether or not the observations follow a normal distribution. For the normality test, the hypotheses are,

H0: the data follow normal distribution vs.

H1: the data do not follow a normal distribution

The grid on the graph resembles the grids found on normal probability paper. The vertical axis has a probability scale; the horizontal axis, a data scale. A least-squares line is fit to the plotted points and drawn on the plot for reference. The line forms an estimate of the cumulative distribution function for the population from which data are drawn. Numerical estimates of the population parameters, μ and σ are displayed with the plot.

2-Sample t-test computes a confidence interval and performs a hypothesis test of the difference between two population means when σ 's are unknown and samples are drawn independently from each other. This procedure is based upon the t-distribution, and for small samples it works best if data were drawn from distributions that are normal or close to normal. The two-sample t-test with pooled variances is slightly more powerful than the two-sample t-test with unequal variances.

2-Sample t test is commonly used to perform a hypothesis test of two independent samples and compute a confidence interval of the difference between two population means when the population standard deviations, σ 's, are unknown. For a two-tailed two-sample t

$$H_0: \mu_1 - \mu_2 = \delta_o \text{ versus } H_1: \mu_1 - \mu_2 \neq \delta_o$$

Where μ_1 and μ_2 are the population means and

δ_o ; is the hypothesized difference between the two population means.

The two-sample rank test is slightly less powerful (the confidence interval is wider on the average) than the two-sample t-test with pooled sample variance when the populations are normal, and considerably more powerful (confidence interval is narrower, on the average) for many other populations. If the populations have different shapes or different standard deviations, a 2-Sample t without pooling variances may be more appropriate”.

Other standard statistical methods are also found important in analysis of the relationship of different parameters in the fields of hydrology and agriculture. Correlation in this context calculates the Pearson product moment coefficient of correlation (also called the correlation coefficient or correlation) for pairs of variables.

Confirming whether it is different or not different from zero uses the correlation coefficient. The p value obtained within the correlation coefficients is used to test whether the evidence is sufficient or not.

Standard statistical methods such as the principal component analysis, stepwise regression, analysis of variance as well as geo-statistical techniques are widely used in this study.

Literature concerning these statistical methods is available in standard statistical books such as Wonnacott 1990, Webster, R. and Oliver, M. A. (1990). However, additional notes relevant to this study are also given in appendix G.

Chapter 3. General overview of the study area

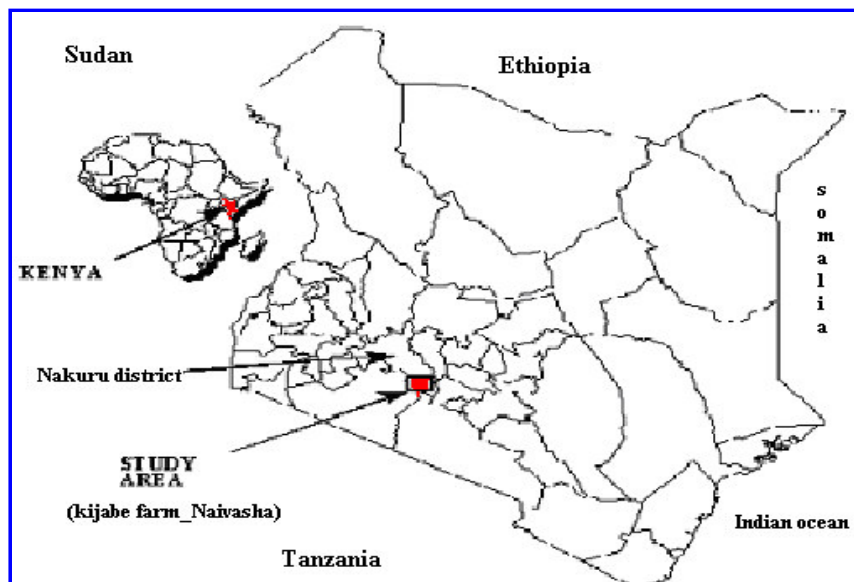
3.1. Location

The location of the study area lies between the following UTM coordinates of zone 37,0190318-183493 East-west: or $(36^{\circ}13'04.33'' - 36^{\circ}09'23.95'' E)$ and 9915314 to 9923545 South-North: or $(00^{\circ}45'55.23'' - 00^{\circ}41'27.28'' S)$ (figure 2).

Kijabe wheat farm is located on the lower part of the Eburru Mountains, at the center of an undulating plateau with an overall gently sloping foot slope, traversed by a few gentle valleys. Slope steepness varies from 5 % on the valley walls to 12 % on the very broad interfluves. The farm comprises a uniformly cropped wheat fields lying in an area of about 35 km squared.

Kijabe farm is one of the most extensive commercial wheat farms in Kenya, located about 57 km west of Naivasha town, within the rift valley province, Nakuru district of Kenya. Naivasha is a small lakeside town located in the southern part of the district, nearly 100 km northwest of the national capital, Nairobi.

Figure 2 Location map of the study area



3.2. Parent material

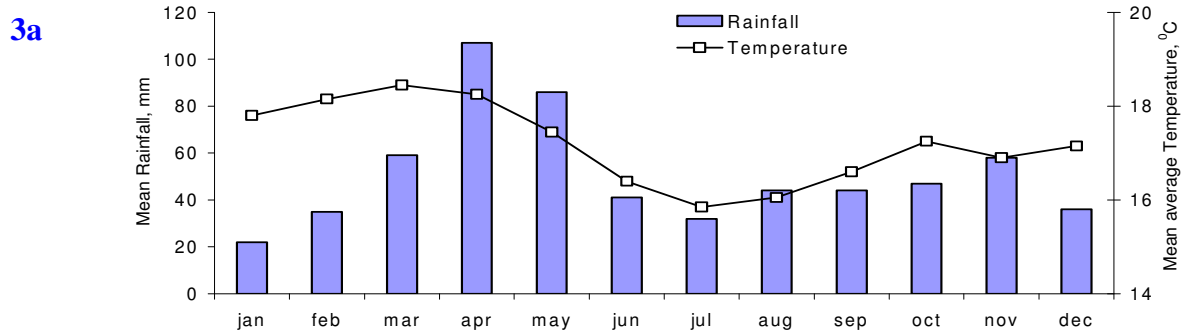
The geology of the Kijabe area is highly faulted pumic, originated from volcanic tuff and ash fall deposits consisting pantellite and trachyte pumic commonly known as the Eburru pumic. Based on the geological report and map of Naivasha area (1:100,000 scale) by Clarke and Woodhall, 1988, the Kijabe hill is identified within the Eburru volcanic complex of geological age mid/late Pleistocene-Holocene (<0.45 my BP).

3.3. Climate

Two rainy seasons and large annual temperature variations are typical characteristics of the climate in the area. The aridity index (precipitation / potential evapotranspiration), around the lake, is about 0.3 - 0.5. The mean monthly values of some meteorological state variables are shown in figure 3a, 3b & 3c.

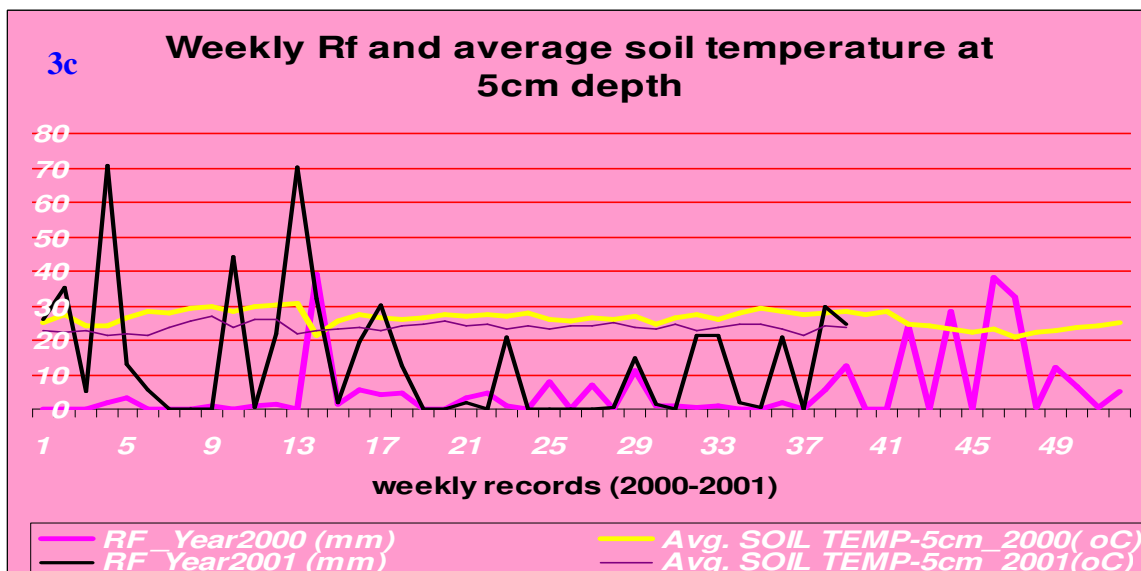
Being close to the equator, the mean monthly temperature at Elsemere station, which is the closest to the farm, but at lower altitude, varies, only a little, from 8 to 18.5 and the mean monthly rainfall is fairly well distributed. The wettest two months (Elsemere station) are April and May with 107 mm and 86 mm respectively and the driest month of January, February and July receives 22, 35 and 32 mm respectively on the average.

Figure 3 Mean monthly values of meteorological observations for the Lake Naivasha area (recorded in Naivasha Meteorological Station). Source: FAO's CROPWAT database.



3b

	Jan	Feb	Mar	Apr	May	Jun	Jul	Aug	Sep	Oct	Nov	Dec
Mean Rainfall, mm	22	35	59	107	86	41	32	44	44	47	58	36
Maximum Temperature, °c	17.8	18.1	18.5	18	18	16	16	16	17	17	17	17.2
Minimum temperature, °C	8	8.1	9.7	12	11	9.8	9.2	9.3	8.7	9	9.2	8.6
Relative Humidity, %	62	61	65	75	80	79	77	76	74	72	77	72
Windspeed, Km day ⁻¹	104	104	104	104	121	121	121	130	130	130	104	104
Sunshine, hours	5.9	5.9	5.3	4.7	4.9	4.8	4.2	4.7	5.4	5.5	4.4	4.2
Solar Radiation, W m ⁻²	171	186	179	164	157	150	143	159	177	179	158	152



3.3.1. Analysis of rainfall

The year of the satellite image used, 2000 was a drought year.

Rainfall prior to the satellite overpass (May 2000) is of course of major influence on the ETa. However, the rainfall record nearest to the investigated wheat fields is that of the Elsemere station, which did not

record any rain during May 2000 (see figure.4). That value cannot be used for the wheat fields because of spatial variation of the rainfall and generally the wheat fields, which are at higher elevation, receive more rain than the Elsemere station.

Two stations were installed after May 2000 on the Kijabe wheat farm with an overlapping period of record of 9 months in 2001, as shown in figure 4. The position of the upper and lower field in relation to the upper and lower Kijabe farm gauges (no standard meteorological gauges) is shown in the map of figure 4. A difference of some 111 mm during the 9 months can be noted over a distance of only 4.1 km. For only 8 days during the fieldwork a tipping bucket gauge was installed close to the upper wheat field (ITC gauge, see table 1).

During that period frequent rains occurred and although the distance to the upper Kijabe gauge was only 2.4 km, about double the amount of rain was measured, see table 2.

The spatial variability of the rainfall was pointed out by the local people, who mentioned that apart from more rain with increasing altitude, there were certain tracks of the rain depending on prevailing wind direction during the morning hours. As the clouds are forced onto the Eburru mountains isolated showers start generally early afternoon. The rainfall-altitude relationship for the 9 months period is confirmed by the figures in Table 3. It is likely that the upper wheat field at the highest altitude receives most rainfall.

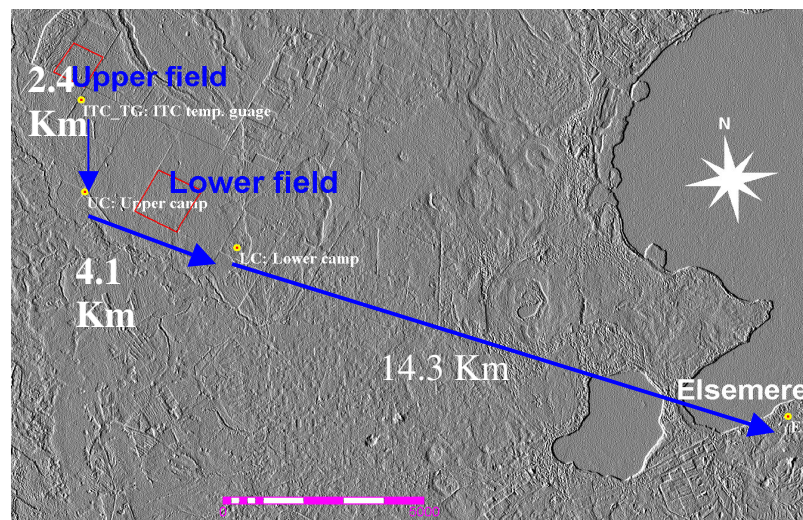
The ETa patterns as derived from the TM image of 18 May 2000 reflect the orographic trend of the rainfall. The upper wheat field must have received sufficient rain for the crops to grow. In fact, the farm manager confirmed that only the upper field had a reasonable harvest that year. It should be noted that the fields around the upper Kijabe gauge has low ETa, suggesting that the orographic effect is strong in the upper zone.

It cannot be excluded that even within the fields studied in detail spatial rainfall influences the variability of ETa, but it is unknown by how much because of lack of rainfall data.

Furthermore, the indirect reconstruction of the effect of rainfall during May 2000 by analyzing the spatial patterns of soil moisture of the soils could not be done because of frequent rainfall during the fieldwork period. However, even within the 1-km² fields, variations in rainfall could have an effect on the crop.

Figure 4 Illustration of Rainfall variability

Rainfall in mm (Upper & lower camp gauges)		
Months	Lower c.	Upper c.
January	139.75	140.2
February	17.8	30.66
March	59.1	80.3
April	172.58	209.4
May	9.8	20
June	45.58	47.4
July	53.4	25.3
August	59.21	60.1
September	42.9	98.4
October		
November		
December		
January		
Tot.	600.12	711.76



Legend
ITC Temporary gauge Elevation~2225 m.a.s.l. RF (15 days)=98 mm
Upper gauge (camp) Elevation~2179 m.a.s.l.RF (9 months)=711 mm
Lower gauge (camp) Elevation~2050 m.a.s.l.RF (9months)=600mm
Elsemere (lake shore) Elevation~1921 m.a.s.l. RF (9 months)=529mm

3.3.2. Spatial Variability

During a period of 9 months in 2001 daily rainfall data of two non-standard rain gauges (Upper gauge and Lower gauge) within the farm are available. The variation of monthly rainfall with altitude and the distances of the rain gauges, see figure 4.

A tipping bucket gauge (ITC gauge) was installed during the short fieldwork period only closer to the upper wheat field selected for sampling, at an altitude of 2225 m. The rainfall measured there was 62 % more than the rainfall over the corresponding period at the Upper Camp farm gauge, suggesting that the orographic effect extends further to the upper most of the farm. Distances of the rain gauges, figure 4.

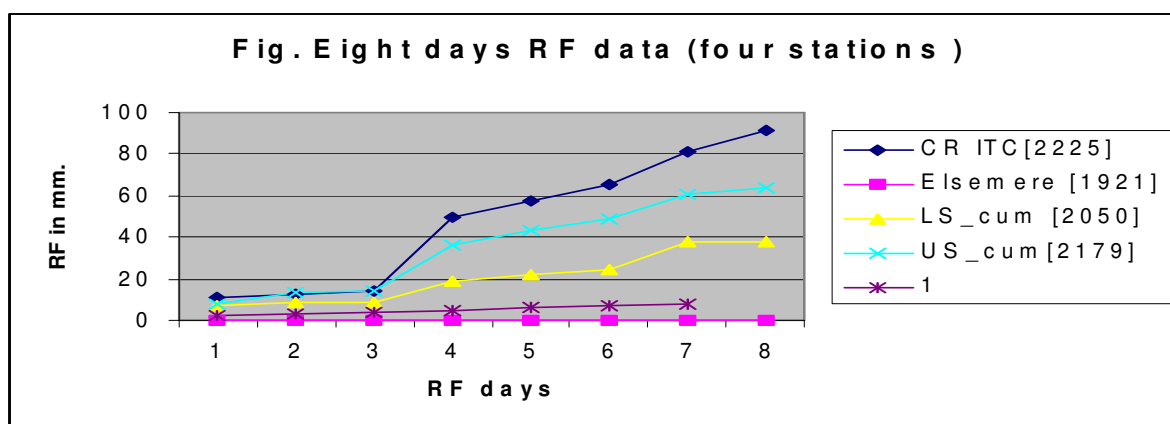
Table 1 illustration of the spatial variability of RF. (sept. 16-29)

	Lower Kijabe	Upper Kijabe	ITC temp.ID	Elsemer
.. RF mm	0	40.5	98	44.5
Elevation [m.a.s.l]	2050	2179	2225	1921

Table 2 Nine months RF record

	Lower ca.	Upper c.	Elsemer
RF mm	600.12	711.76	528.81
Elevation [m.a.s.l]	2050	2179	1921

Figure 5 illustration of rainfall variation around Ndabibi area



3.3.3. Rainfall daily 2000.

Comparing to the previous 10 consecutive years, Naivasha area in general Kijabe fields in particular, the year 2000 was known as a drought year, however, It was not possible to get properly recorded precipitation data from the farm, the existing farm level gauges were installed in the beginning of January 2001.

According to the local inhabitants and farm workers no precipitation was received around the Kijabe fields for about seven days before the day of satellite overpass i.e. May 18,2000. Therefore, in such periods of moisture stress, variation of soil Water holding capacity could possibly be a constraint in crop performance.

Figure 6 Temporal variation of rainfall and soil temperature (source: Naivasha meteorological station, 2001)

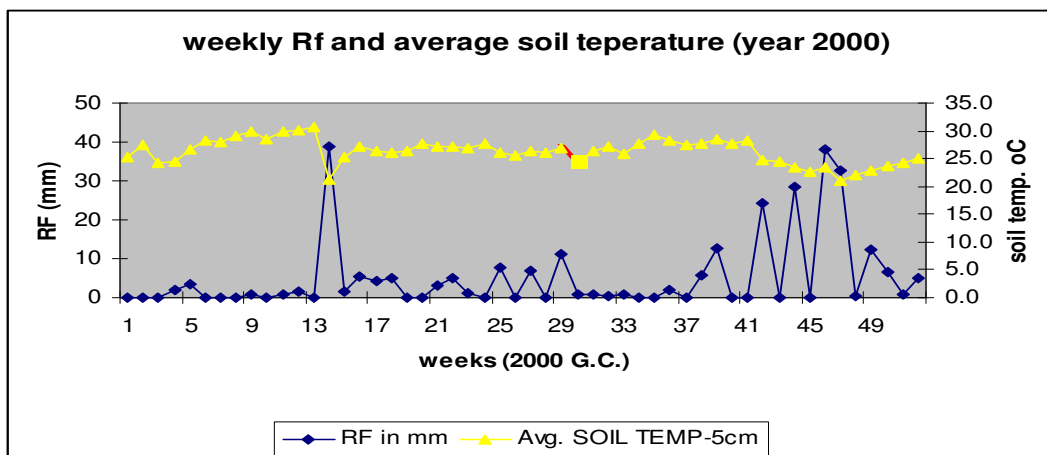
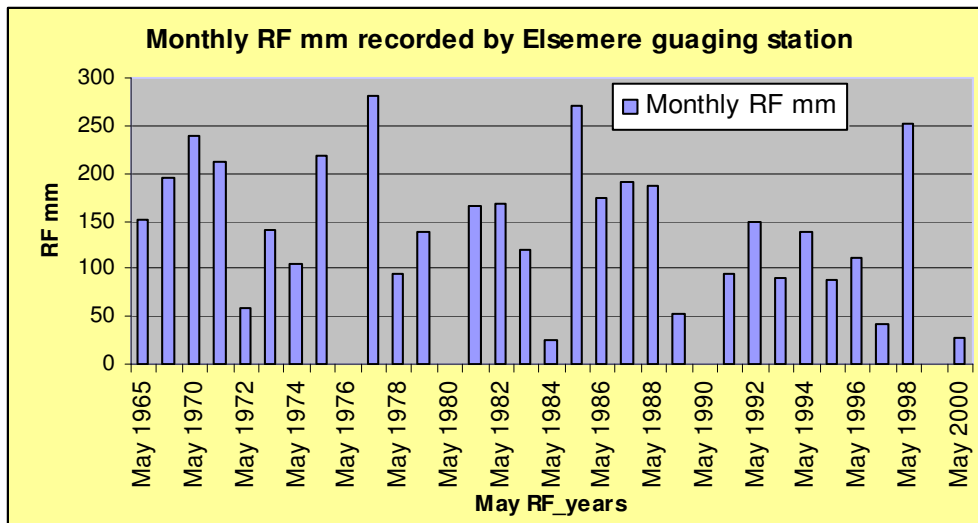


Figure 7 Monthly (May) rainfall records across 36 years.



3.4. Ndabibi wheat farms

The slopes of the Mau escarpment and the adjoining Eburru Mountain as well as portions of the highest parts on the western deep slopes are heavily forested. The forests open out into grassy glades in the lower reaches, and in the lower grounds adjoining the Kijabe fields. The forest is largely confined to the deeper valleys. Local inhabitants stated that the lower parts of the Kijabe wheat field is highly porous and more vulnerable to drought causing crop failure due to moisture stress compared to the upper thicker soils. The fast draining steeper streams, once flown to the Ndabibi plains disappears on their way down due to cracks, which have opened up.

Sufforion (drainage by surface tunnels) is common, at different depth and magnitude; at several places collapse depressions are found. Here the lower farmhouse, two bore halls were made at close distance one was dry while the other encountered flowing water.

The porous nature of the rocks in the Eburru Mountains probably aids in the taping off of the streams-waters as they plunge down the slopes towards the main Rift floor. The hydrological behavior of the surface flow within the wheat fields (Kijabe farms) on the other hand is influenced by the nature of the topography and the vegetative cover. On a convex slope and undulating landscape, such as the shoulder or a ridge, gradient increases down the slope and runoff tends to accelerate as it flows down the slope. Soil on the lower part of the slope tends to dispose of water by runoff more rapidly than the soil above it. The soil on the lower part of a convex slope is subject to greater erosion than that of the higher part. Soil erosion by runoff during land preparation and early crop growth, is experienced in the area, there fore extensive soil conservation measures were taken since the last 5 years.

Wheat is grown under modern management practices in staggered operation throughout the year. The wheat variety per field is adjusted to soil conditions and altitude. Fertilizers are applied based on soil data aggregated per field. Only minor within-field variations in conditions can be attributed to non-soil factors, such as non-optimal aircraft spraying, wildlife damage, and localized re-sowing due to water logging in a part of a valley bottom.

Site description and agronomic practices

The two sampling areas consisted of a one killometer square each (total of 200 hectares) is a portion of the vast Kijabe wheat field (~35 Km. squared). The lower fields have been cropped to wheat for more than 50 years. Soils are variable containing three soil map units and considerable spatial variability organic matter contents. The major soil types in the experimental areas identified are clay loam to sandy clay loam in the upper field and sandy clay-to-clay loam in the lower field.

Based on the historical records of the farm the lower part of the field have been a grazing land after it was deforested, firstly by the local community and a commercial dairy farmers were using the plateau as a main source of forage.

Crop production was introduced since the last 50 years by growing maize by small farmers and finally for growing wheat. Before it was sold to commercial farmers the Ndabibi wheat field was owned by the Kenyan government, later it was considered as one of the less productive and bankrupt state owned farms. The actual size of the Kijabe wheat farm is a result of step-by-step expansion towards the northeastern boundaries. Some of the upper reach wheat fields are indicated as forest areas in the ten-year-old aerial photos.

Wheat is grown as continuous wheat monoculture in Kijabe farms, In order to maximize production, the farm management makes wise choices regarding every thing in their capacity from the variety of wheat used to the type of tillage system plantation dates.

These factors and others affect the successful production of wheat crop in the area. Planting time in each field is so flexible throughout the year and mainly depends on the microclimate of the area and relative moisture holding capacity of the plots. The main wheat varieties that are produced two times a year include: Mexica and Nyangume other varieties such as Mbuni, Pasa, Hiore, Kwala, Hoire are also widely used. According to the Kijabe farm management records, practical experiences shows that, the average yield records of each field in the last five years shows significant variability, the lower (older) plots being less productive compared to the upper (recently expanded) plots. Fields vary in their capability to produce wheat crop because of differences in various factors, specifically soil quality. Average productivity (wheat crop yield) of the plots varies from 2224 kg per hectare to 4003 kg per hectare. Where, higher yields correspond with the upper fields adjoining the forest area and lower yields correspond with lower fields.

Unlike to the upper reach wet dark soils, the soils in the lower reach of the vast wheat field are inferior and economically less important. As the topsoil erodes from the fields, infiltration rate and water availability become limited. The subsoil does not absorb the rainfall as rapidly, leading to more surface water runoff and less available water for crop production.

During the field work the upper field was covered by young wheat, planted on February 19/20, 2001 Mexican variety. Similar to the previous year the seed intensity was 61.7 kg/acre (152.46 kg/ha), three weeks after plantation fertilizer (di-amonium phosphate DAP) is applied uniformly at a rate of 45 kg/acre (111.197 kg/ha). Similarly the lower field was planted on April 11/12, 2001 with Nyangume variety, with maturity period ranging 140-150 days, with seed intensity of 60 kg/acre (148.263 kg/ha), di-amonium phosphate (DAP) fertilizer is applied uniformly at a rate of 37.8 kg/acre (93.41 kg/ha) at the same time. The same type of tillage system is applied throughout the fields with average depth of 20-30 cm.

As a rule of thumb three weeks after plantation, herbicides and pesticides together with copper sulphate (0.5 kg/ha) are uniformly sprayed. A total of 204.5 liters of pesticide, herbicide and copper solutions are sprayed for each hectare containing 2.5 liters of Matril, 1 liter of Atacord and 0.5 liters of Kocide mixed with 200 litter water per hectare.

3.5. Soils

The soils belong to the loam to sandy clay loam Vitric ANDOSOLS. They are developed on thick volcanic ashes and tuffs. They are well-drained, high in organic matter (3.9 to 13.2 %) and have low bulk densities (0.72 to 1.52 g/cm³). The thickness of the A horizon varies (A_h) with altitude and slope steepness from 5 to 24 cm In the sampled upper wheat field the thick A horizon could well be related to the fact that the field was still under forest in 1994.

Organic matter content and topsoil depth (thickness of A horizon) increases with increasing elevation in upper field and towards the valley bottom in the lower field, the general trend of soil variability in Ndabibi soils shows an increase of black clay loam layer towards the upper field adjoining the forest areas and decreases and eventually terminates on the lower oldest plots in the Plateau.

Variability of soils within the Kijabe wheat fields

Soils developed on the upper edges of the Kijabe wheat fields are, well-drained, moderately deep-to-deep, brown and dark brown, friable, loam to sandy clay loam Vitric ANDOSOLS. They are grouped under the name Andic Phaeozems, rich in humus mainly in surface horizons and in the subsoil. The soils in the lower part of the wheat field adjoining the Ndabibi plain and lower volcanic plain are mainly Ando-calcaric Regosols, excessively drained to well drained, very deep, dark greyish brown to olive

grey, stratified, calcareous, loose fine sand to very friable fine sandy loam or silt. Below the upper layer (15-40 cm) soils are very porous and full of pumicieous gravel.

Soils in the upper edge of the upper wheat field are dark, and relatively thicker than the lower elevation areas. The reason for the observed soil heterogeneity in Kijabe soils, which can be easily detected at reconnaissance survey level, is complex.

Natural factors such as the variation in relief, climate, volcanic activities and underlying rocks and vegetation cover as well as human influences including differences in farming history, are the most important influencing factors. Above all hydraulic erosion plays a greater role in decreasing the thickness of the upper soil horizon towards the lower edges of the plain. Comparing with the upper fields adjoining to the existing thick forest, washing out the humus rich topsoil is more pronounced in the lower part of the Kijabe fields.

The most important soils in the study area are Andosols, which are well drained and deep, containing clay with an acid, humic topsoil. Their fertility status is inherently fair to good; however, as we go down to older lower fields intensive cultivation has mined them of their nutrients. Soils with a high acidity are marked by a low nutrient availability, and possible vulnerability to P-fixation and Mn and Al toxicities.

Laboratory texture analysis results reveals that, soils developed on the upper edges of the Kijabe Plateau are well drained, moderately deep to very deep, Black to very dark gray, with organic matter rich topsoil, and fine to medium sub-rounded weathered pumic increasing in intensity and size with increasing depth of sub soils. On the other hand, soils developed on lower edges of the Plateau comprising the lower wheat plot are moderately to excessively drained, deep, dark reddish brown to pale brown, sandy clay loam to sandy loam. Except in the small valleys, the subsoil of the elevated zones of the lower plots soils is very porous and contains intensive pumicieous gravel. According to the local inhabitants, soils in the lower plots tend to form crop emergence-restricting crusts i.e. a hard thin layer at the soil surface after rain during warm early sowing periods, where this is also confirmed by the field level studies, characterized by greater density and shear strength, but with finer pores and lower saturated hydraulic conductivity, than the underlying pumicieous gravelly soils.

Residue mulch left on the soil surface is commonly used as a means of moisture conservation reducing the potential of soil crusting. With increasing elevation towards the upper and more recent fields the soils organic matter content significantly increases in the plow layer (20-30 cm). This in turn may have an impact in lowering the probability of crusting compared to the lower plots.

Figure 8 Land use map of the study area

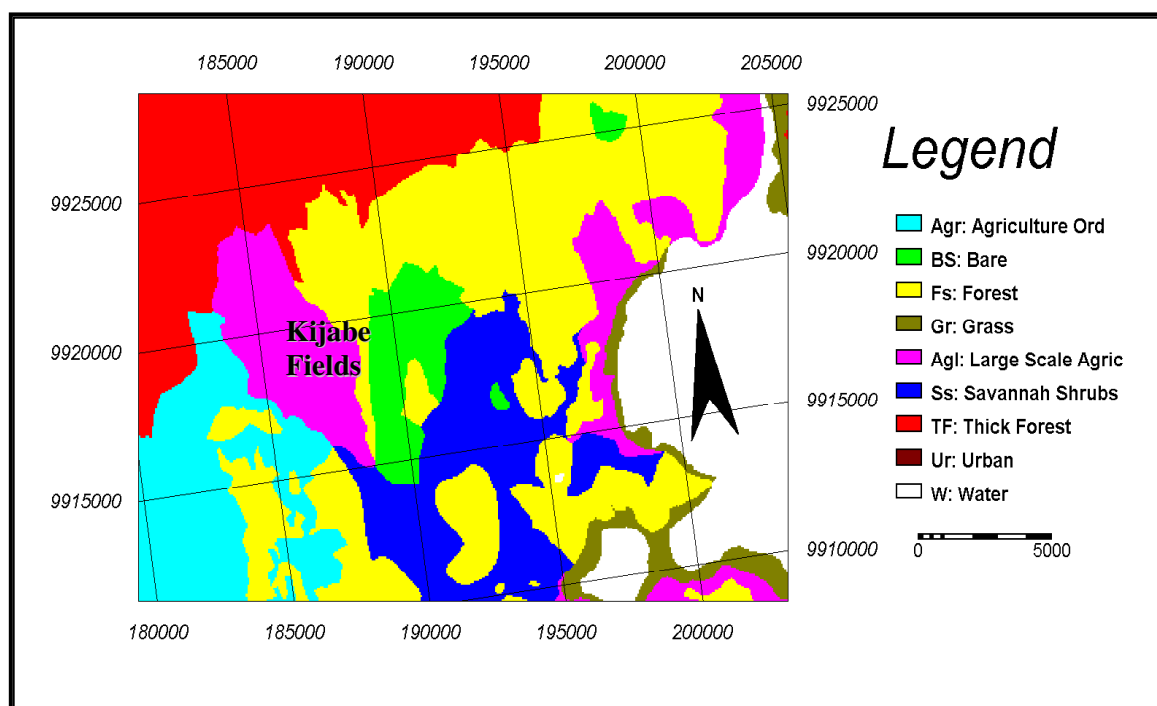


Figure 9 Geological map of the study area (sub-mapped from Clarke1990).

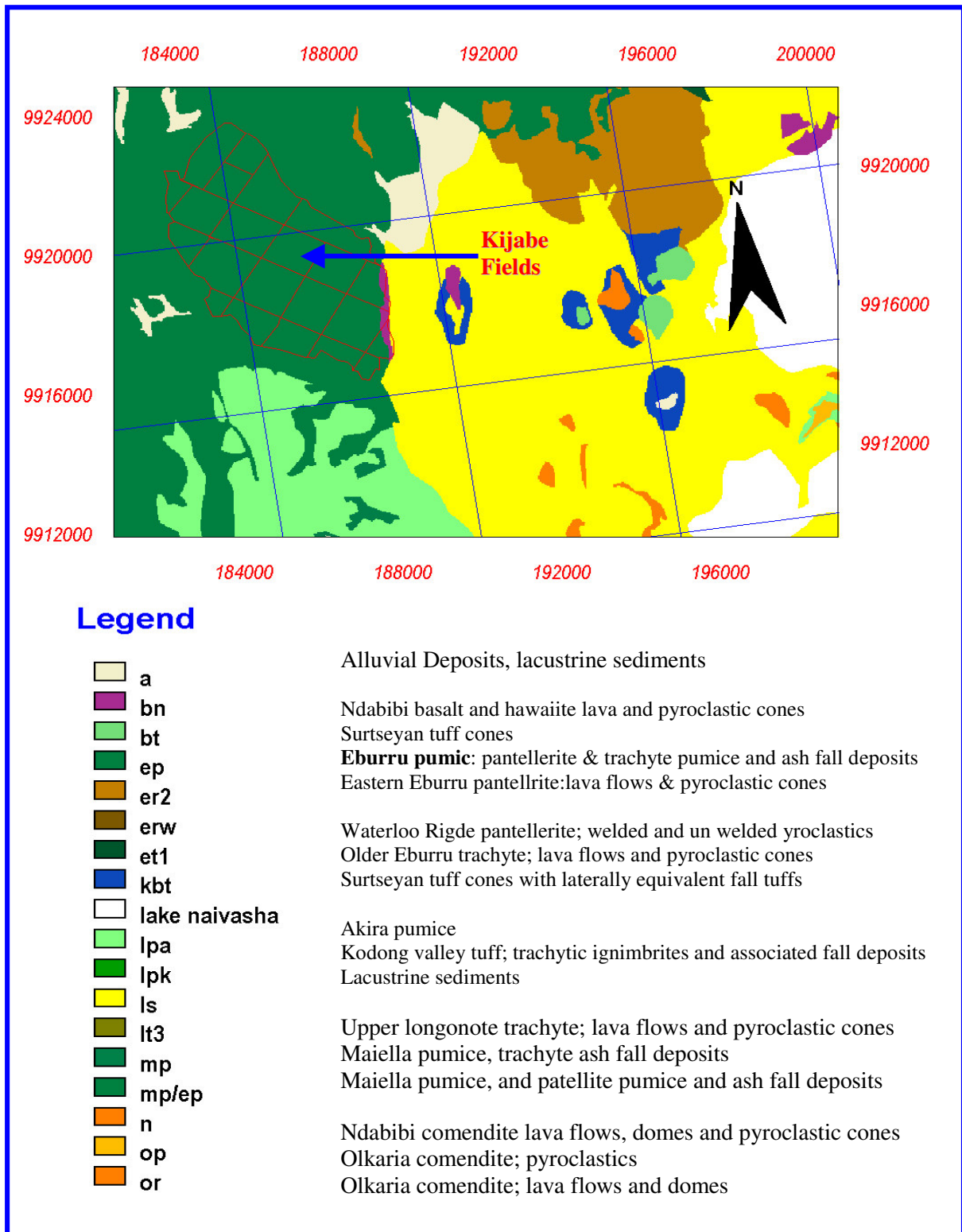
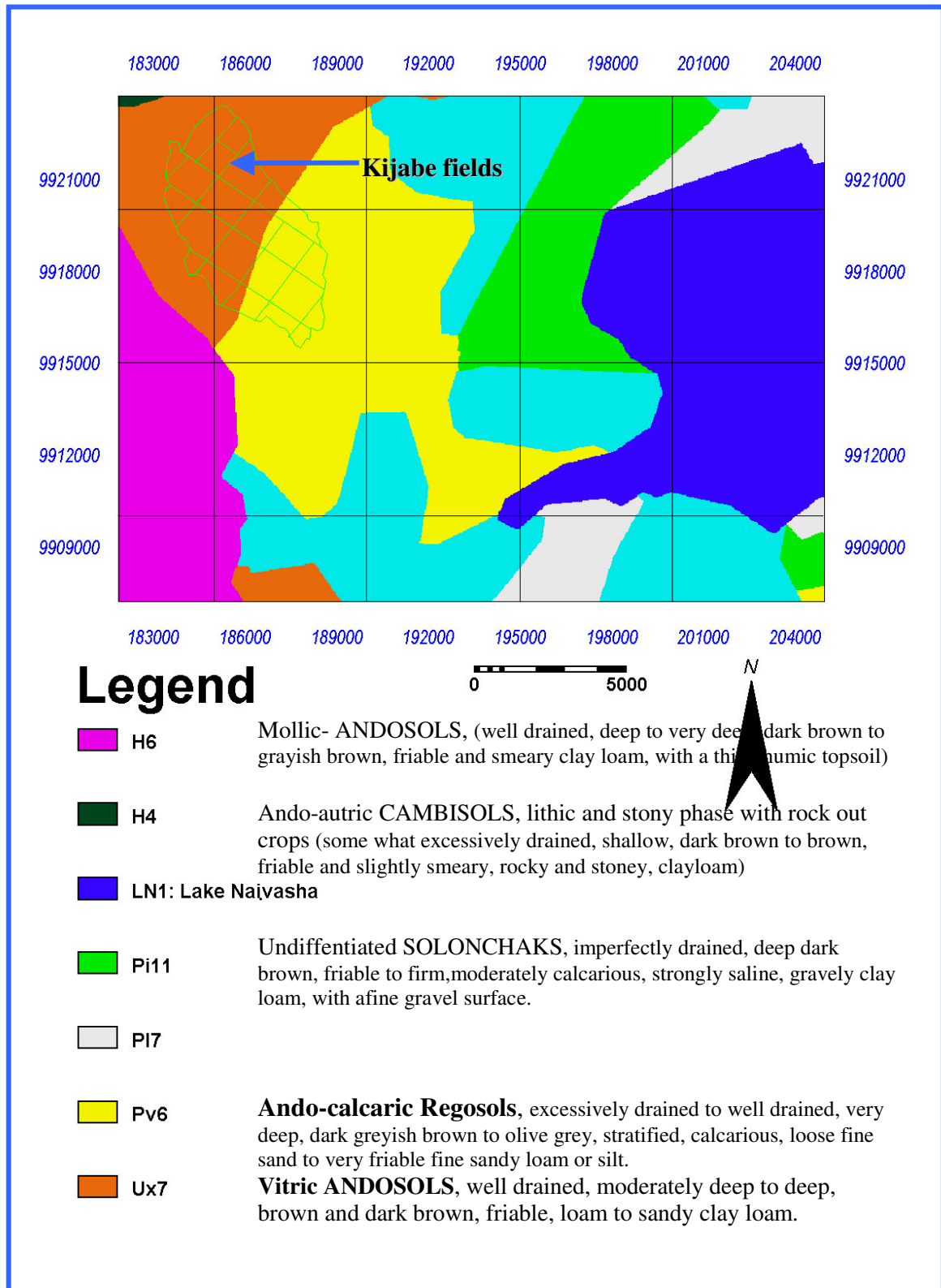


Figure 10 Soils map of the study area (Kijabe fields are indicated on the left side)



Chapter 4. Materials and methods

Two sampling fields consisted of a one square kilometer area, located 60 kilometers south west of Naivasha town were selected for sampling. With the exception of the upper edges of the field adjoining the forest area the main part of the remaining field has been cropped to wheat for more than 40 years following maize. During the satellite overpass the upper and lower fields were covered with a young wheat planted in April 9&10,2000 and April 7&8, 2000 with Mexica and Nyangume varieties and seeding rate of 152.5 and 148.26 kg/ha respectively. (As a rule of thumb the same combination of agricultural inputs are applied described in section 3.4.)

A systematic grid sampling system was used as a method of soil sampling to systematically reveal the observed variation in ET as in the upper plot based on the 60-meter pixels in the ETa map. Based on the prior Knowledge of the localized soil and topographic patterns of the lower field soil sampling along sections was considered as appropriate technique for the lower plot.

A regular grid consisting of 99 grid locations spaced on 100 ha experimental area of young wheat in the upper field and 25 sampling grid points in the lower field were set up as a regular sampling positions for the various soil parameters. Position and elevation of each grid points were determined using a GPS. Soil sampling for pH and EC determination was done at each point. Physical soil characteristic measurements such as soil moisture, saturated hydraulic conductivity, soil depth determination and profile observation were made using a transect across both the East-west and North-south the five sliced actual evapotranspiration patterns.

ILWIS.3 Remote sensing and GIS software was used to pre-process and analyze evapotranspiration estimates and for classifying the observed actual evapotranspiration patterns. Required measured weather data, including maximum and minimum air temperature and precipitation, wind speed; humidity was collected from previous studies. With the exception of the precipitation, which shows considerable spatial variation within the farm plots, all other weather data was assumed to be uniform over the adjoining weather stations (mainly the Oserian farm~24 km far).

Information on management practices (crop variety, planting date, planting density, planting depth and chemical applications) was obtained from the farm manager.

A field level soil survey of the Kijabe wheat fields established the presence of four distinct soils- Andic clay loam, sandy loam, sandy clay loam (over washed phase) and gravely sandy loam (eroded).

For the purpose of this study the topsoil sampling was done by aggregating into two main classes (horizons): first horizons 0-10 cm and second horizon 15-30 cm. Additional sampling points were identified based on the sliced spatial ETa variation (patterns) with special emphasis in the two extreme zones of the field i.e. the very high and very low ETa zones.

Soil profile description was made along the south north and east west transect lines, concentrated along the unique ETa gradient and unique soil type and topsoil depth combinations. Special emphasis was given to the topographic variation and the associated water movements, as they are the possible sources of soil erosion, soil heterogeneity and related ETa variations.

Saturated Hydraulic conductivity: Determination of Saturated Hydraulic conductivity using an inverse Auger-Hole Method. A hole was bored into the soil with known depth (commonly 30-45 cm), diameter and known distance between the soil and the reading point.

The hole has been filled with water till the top level and infiltration starts at the bottom and along the side walls of the hole, so the water level dropped down; when the infiltration rate becomes constant it's equal to hydraulic conductivity. After saturating the soil the shape of the graph was changed and the plotted function is the; $\log(h+0.5*r)$, with h =height of water column in the hole at time t (depth of hole + height of reading from the soil - measured water level from the top) versus time. The distance and time laps records were plotted using an inverse hall method (spread sheet) model, where the trend line equation is shown on the plot and the slope $(\log(h+0.5)/t)$ of the straight line used in K_s calculation.

$$K = 1.15 * \text{hole radius} * \text{slope}$$

And the daily hydraulic conductivity values were obtained by multiplying the hourly values by 24 i.e. $K_s \text{ (daily)} = -(\text{Hole diameter (cm)} * \text{slope} * 1.15 * 3600 * 24)$

Bulk density: A hole of about 20 cm diameter and 40 cm deep (about 2.5 l) was augured and the removed soil was dried (105°C) and weighed. The volume was measured by filling the hole with water after lining it with a special plastic bag.

Soluble cations: soluble Mg, Ca, K and Na were measured from the 1:5 soil water extract using the measuring apparatus called inductively coupled plasma-Atomic emission spectrometer (ICP-AES). The concentration of soluble cations which are considered to be readily available for extraction by plants was given in milligrams per liter extract, in this study the units are in mill equivalents of soluble cation per hundred gram of soil sample.

4.1. Field work and post field work

Preliminary Proposal Writing: The main tasks that were performed before the fieldwork are Proposal writing comprising literature review and collection of general site information. Preparatory Phase: During this period basic site information and data were collected including literature search land use, land cover, rainfall, soil, geology, and climate, etc. materials and equipment requirement for the field work were listed.

The primary ones are listed below:

Satellite imagery (TM image of May 18, 2000)

Topographic map of the area (1:50,000)

Exploratory soil map of Kenya

Geological Map of the study area (1:50,000)

Aerial photographs at a scale of (1:12,000)

Full set of Landsat TM image (May 18, 2000) was acquired from ITC-WREM database and sub-mapped using corners to concentrate on the target area. The Landsat7 image, which was initially Geo-referenced by using the thermal band (B6) and panchromatic band (B8) with tm6h_00s (14 tie points with sigma 0.54 pixels) and tm8_00 respectively, and coordinate system NAIV.

The coordinate system NAIV has the following parameters:

Minimum X, Y (166000, 9889400)

Maximum X, Y (251750, 9992350)

Projection: UTM

Zone: 37

Datum: Arc 1960

Datum area: Mean

Ellipsoid: Clarke 1880 with parameters $a=6378249.145$, $1/f=293,465000000$

In order to proceed with the energy balance method of estimation of actual evapotranspiration values using the set of geo-referenced satellite images all other bands were resampled to a 60 meters pixel size i.e. the resolution of the thermal band.

Atmospheric and geometric corrections were performed using the following steps:

Digital numbers (DN) were converted to spectral radiance.

Calculation of spectral reflectance at the top of the atmosphere,

Calculation of broadband reflectance at the top of the atmosphere

and Calculation of the broadband albedo (see figure 14).

Aerial photo interpretation: Before going out to the field, aerial photo interpretation, using the 1:12,500 photos were done on the Ndabibi area wheat fields. Older aerial photos were used to collect past histories of the fields including the previous land use.

Preliminary analysis and classification of the ETa patterns were made based on the NDVI and estimates of actual evapotranspiration computed based on the May 18 2000 TM images. Preliminary sampling design was prepared based on the observed variations of actual evapotranspiration estimates. Five major ETa patterns were identified in the upper wheat plot and three in the lower wheat plot.

4.2. Field sampling and laboratory work.

4.2.1. Sampling procedure

After a careful survey of the area and preliminary images & AP interpretations the proposed sampling strategy was updated to suit the topographic conditions of the area. Grid sampling and landscape directed soil sampling were chosen for the upper and lower wheat plots respectively to reveal the observed ETa patterns and reconnaissance level soil survey i.e. observed micro topographic variations.

For this study 99 sampling points for determining soil variables were selected in the upper wheat field and 25 in the lower wheat field. A total of 124 GPS points were acquired from the both fields. The accuracy of the GPS points was in the range of 5-7 m, enough number of satellite signals were Used for a reasonable accuracy of the GPS guided "Go-to" sampling approaches for each point. However, relocation of some of the sampling points (total of 7) which fall on or near to farm boundaries, big trees and house yards were made by shifting towards the centre of the wheat fields. ETa map with pixel size of 60 meters was used as a base during the entire sampling procedure. The details of the sampling procedures and soil variables are discussed in chapter 6.

4.2.2. Variables

pH and EC were selected in the upper field based on the grid system (80 m apart) and the observed within field ETa variability patterns. 11 of them are in the "very high ETa " (VH ETa), 24 in the "higher performance" (H ETa), and 37 in the " medium level performance "(M ETa), 16 in the "lower ETa value "(L ETa) and 11 in the "very low ETa "(VL ETa) zones of the same field and crop age.

Soil properties, which are less expensive to carry out such as the pH, EC soil moisture measurements were made at each grid point. Other soil properties which are relatively expensive and time consuming, such as the saturated hydraulic conductivity (Ks), Bulk density (Bd), percentage of organic matter (%OM), topsoil depth (A_h), soil texture and determination of soluble cations were mainly limited on the observed extreme zones of ETa as well as along the transect of the field in order to check the within field variation of each parameter between the observed zones and across both east west and south north transects.

The sampling method in the lower wheat field was done by dividing the field in to three ETa patterns i.e. high, medium and low, 25 sampling points were selected based on the topographic and soil texture variability along a valley cross section. Similar to the upper wheat field among the 25 sampling points EC, pH and soil moisture content were sampled at each point while the other soil parameters are systematically done in the 14 points selected across the transect along the localized valley corresponding with the three ETa patterns.

Soil physical properties such as: bulk density (Bd), saturated hydraulic conductivity (Ksat), soil characterization and moisture content (MC), particle size (texture), slope, depth of the top soil and soil chemical properties such as: the readily available nutrients in Milli equivalents per 100 gram of soil sample (Magnesium, sodium, Potassium and calcium) and percentage of organic carbon and organic matter are being measured on the various performance patterns and with two horizons.

Sampling fields were selected based on the spatial variation of actual evapotranspiration patterns (low, medium and optimum ETa values) identified in the map and the ground conditions. Field observations including measurements of electrical conductivities, soil texture, soil moisture, pH and ionic concentration of soil-water extract analysis of targeted locations were carried out in the Sulmac lab.

Spatial variation in the daily ETa values was taken as a reference for identifying the relative ETa patterns. Observed soil and topographic variations were considered during the planning of the sampling scheme to evaluate the influence of the soil texture and topographic variations in the final analysis.

The sample size determination was optimised for both sampling fields with respect to the given field work period.

During the field sampling 2-4 sample cores were collected from each sampling point to a depth of 0-10 cm and 15-30 cm for determining pH, EC, Bd, Ks, soluble cations (Mg²⁺, Ca²⁺, Na⁺ and K⁺), organic

matter content and soil texture. Other parameters such as the slope gradient and topsoil depth were also measured during the fieldwork.

Soil pH, EC variability across the sliced five actual evapotranspiration patterns was measured by the author, in Sulmac farm Laboratory Naivasha_Kenya. The soil analysis, which is known as, the potentiometric measurement of supernant suspension of 1:5 soils: liquid (water) mixture.

Laboratory analyses of soil samples

After the fieldwork additional Soil samples were analysed in the ITC soil laboratory. The samples collected from the identified ETa zones. Three soil cores, were collected within 1-m radius of each sample position and combined, oven dried and analysed for standard soil properties, including potassium, pH, organic matter, calcium, magnesium, sodium and texture.

4.3. Research method

- Report writing including review of relevant literature .
- Existing data; inventory of available data series (previous studies);
- Literatures review in the areas such as: evapotranspiration, soil information and statistical methods, site specific management, Soil dynamics and Agricultural-Organic chemicals.
- RS&GIS-based reference materials and soft wares.

Statistical reference materials and soft wares used for this study include: Mintab.13, Surfer7, ASTER and LANDSAT.7 TM Images, ILWIS.3, Flow4 and Microsoft excel.

Research methods: selected sampling fields (based on the ETa variation and ground conditions)

- ✓ Establish statistical experimental set-up. (Multivariate analysis, stepwise regression and analysis of variance between different soil and crop set-ups and soil characteristics). (See chapter 8)
- ✓ Small questionnaire for the farmers own declaration of the agricultural practices (spatial input application), land use and history of the within field yield variability.
- ✓ Description of the statistical relationship of the major soil fertility parameters, (mainly: Bulk density, Organic Mater content and pH) and the specific soil variability and ETa was analyzed.
- ✓ RS/GIS based land use /cover of the basin; estimation of ETa map for the study area; a spatial distribution of soil fertility ranges and detailed information of the land use; crop growth stage and agricultural management of the target areas.

Figure 11 Data analysis method (spatial analysis)

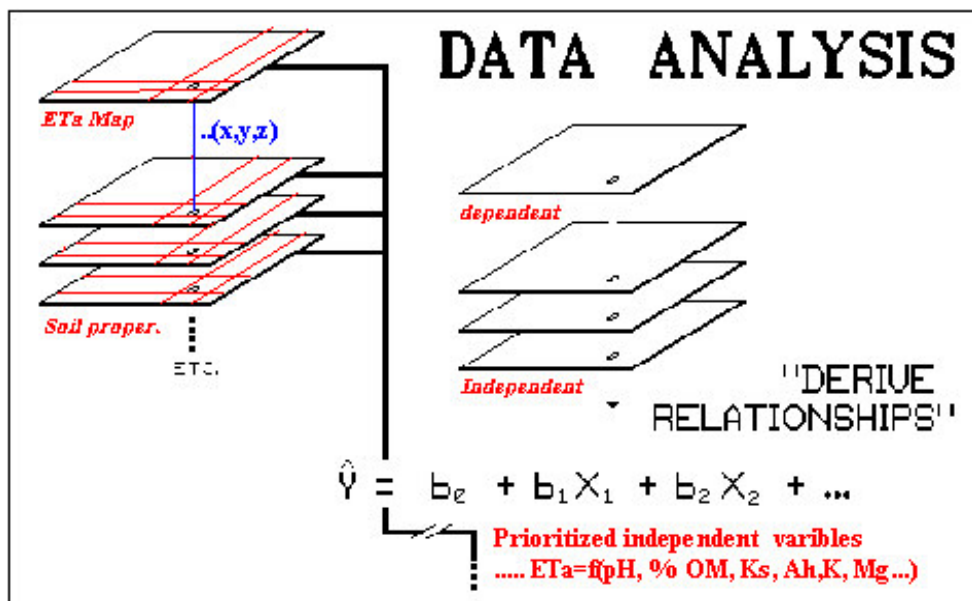
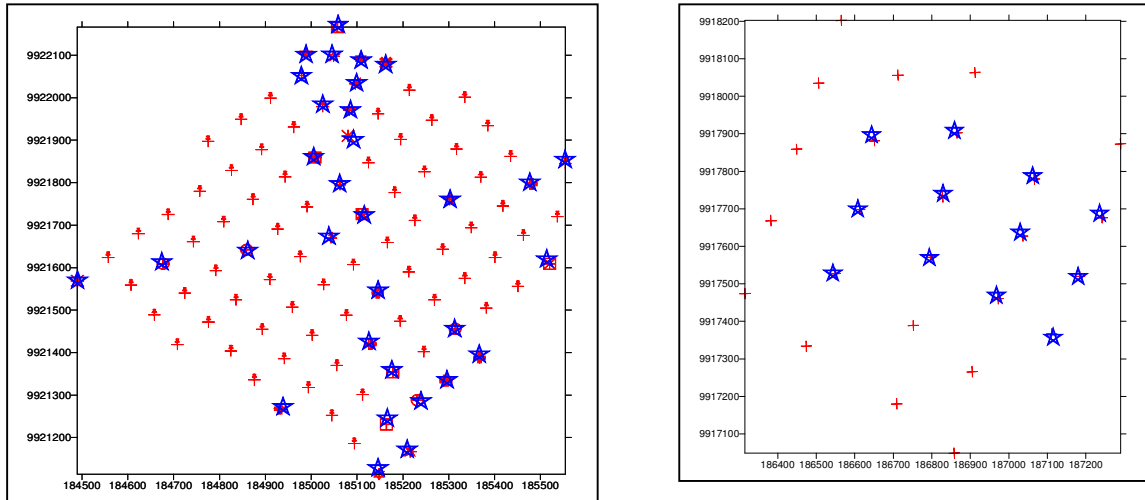


Figure 12 Location of sampling points for both upper and lower wheat fields (respectively)



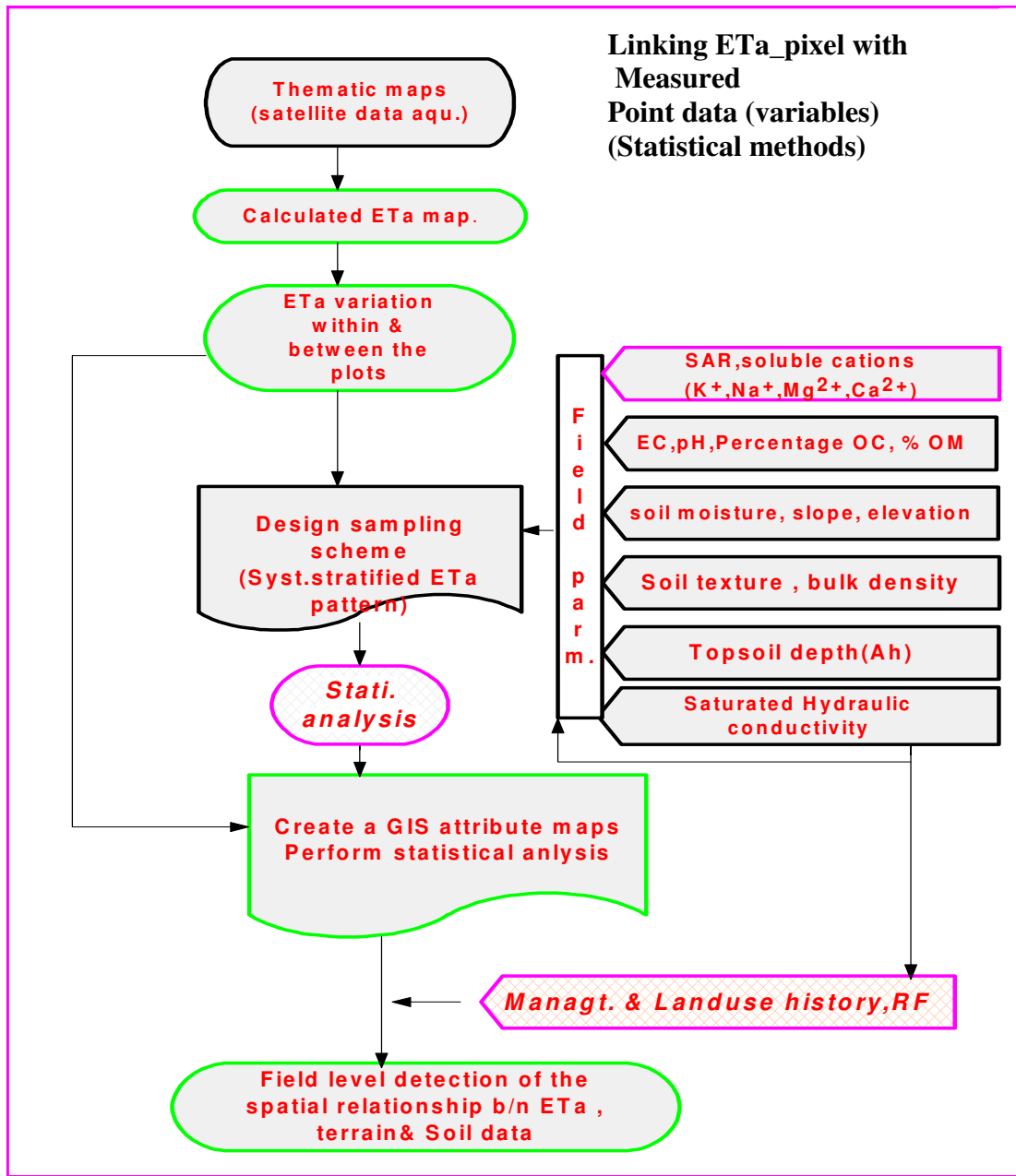
The sampling points were made with special emphasis on the two extreme ETa zones, namely the very high and very low ETa zones consisting 11 observation points each.

Since crop performance and the corresponding ETa rates considerably vary with space and time, relating the spatial within and between field variation of actual evapotranspiration with soil and topographic conditions could allow us to associate some, but not all.

Statistical relationship of the major soil fertility parameters and pixel based ETa values i.e. indicating the relevance of the spatial variability of soil topographic variables towards the reduced ETa values are modelled (see chapter 8).

The sampling scheme was designed to evaluating the spatial variability of key soil properties such as bulk density and organic matter levels in different ranges and the relationship of the available nutrients and other parameters with actual evapotranspiration map. Document and evaluate the Key spatial ETa variability attributes for the selected pixels in the targeted field.

Figure 13 Flow diagram (methodology and materials)



In an attempt to better characterize the data, different statistical models were tested and the best descriptive methods are selected for analysis and display. Other standard statistical methods are also found important in analysis of the relationship of different parameters within the given data set. Correlation of ETa and other variables in this context is displayed using the Pearson product moment coefficient of correlation (also called the correlation coefficient or correlation) for pairs of variables. The correlation coefficients are used as a measure of the degree of linear relationship between two variables. The p value obtained within the correlation coefficients is used to test whether the evidence is sufficient or not. Methodologies of the principal component analysis and stepwise regression are given in chapters 7 and 8.

Chapter 5. Analysis of evapotranspiration (RS & GIS applications)

(Estimating local wheat evapotranspiration using Landsat TM imagery)

5.1. Data acquisition and preprocessing (parameters used)

The Landsat-7 TM data of eight bands (Bands 1 to 8 including the panchromatic band) on the 18th of May 2000 were acquired and NDVI was computed from image digital numbers (DN) for visualization purposes as

$$NDVI_{DN} = \frac{(b4) - (b3)}{(b4) + (b3)}$$

The terms b3 and b4 denote red and near infrared channels

For simplicity and focusing in the Ndabibi area wheat fields the images were resampled to a 60m resolution TM bands and sub mapped. The resampling task was necessary in order to carry out an energy balance algorithm, which takes the thermal band (band 6) as a main input. As a result of the lower spatial resolution of the thermal band, the other visible and IR bands were resampled to the lower resolution.

At-satellite spectral planetary albedos, r_p , near nadir reflectance from both surface and atmosphere above it has been calculated from the following relation:

$$r_p(\lambda_i) = \frac{\pi * L_{\lambda_i} d^2}{K(\lambda_i) \cos \phi_{su}}$$

Where L_{λ_i} is the measured spectral radiance from the TM sensor, d is the earth-sun distance in astronomical units (AU) and ϕ_{su} is the solar zenith angle. One AU as noted in Markham and Barker (1985b) is the mean Earth-Sun distance L_{λ_i} , based on the pre launch absolute calibration of the internal calibration system of the TM, has been obtained by

$$L_{\lambda=LMIN_{\lambda}} + \left(\frac{LMAX_{\lambda} - LMIN_{\lambda}}{255} \right) QCAL$$

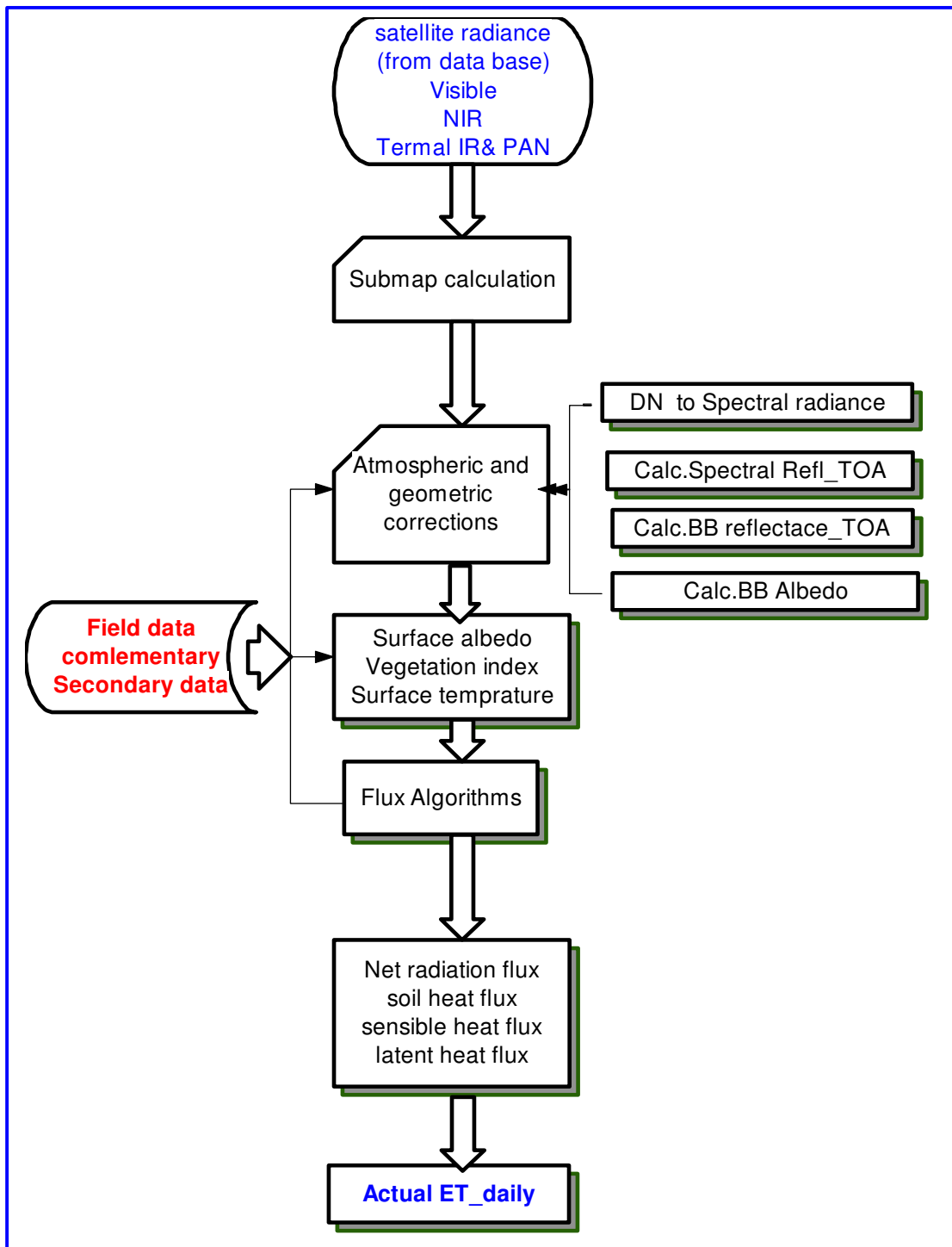
Or

$$L_{\lambda_i} = a + \frac{(d - a) * DN}{255}$$

Where QCAL is radiometrically calibrated digital radiances found in TM tapes in units of DN, and

$a = LMIN_{\lambda}$ and $d = LMAX_{\lambda}$ are dated constants (appendix G) used in TM ground processing which reflect the radiance at DN=0 and DN=255, respectively.

Figure 14 Estimation of actual evapotranspiration patterns



5.2. Data analysis

In order to convert the DN of the thermal band (Band 6) to surface temperature, two Procedures are required. Firstly, each DN has been converted to the spectral radiance L_i and secondly, the spectral radiance is converted to surface brightness temperature.

Radiant temperature is being computed using the spectral radiance by using the following relation:

$$T_R = \frac{K_2}{\ln\left(\frac{K_1}{L_i} + 1\right)}$$

T_R : radiant temperature in Kelvin

K_1 : Calibration constant (666.09 watts/(meter squared *ster* μm))

K_2 : Calibration constant (1282.71 watts/(meter squared *ster* μm ,^o K)

L : spectral radiance in watts/(meter squared*ster* μm)

The Kinetic temperature at the top of the atmosphere has been computed from the radiant temperature map using the following relation:

$$T_{toa} = \epsilon_o^{0.25} T_R$$

Here, the symbol ϵ_o represents the spectral emissivity.

In computing the Kinetic temperature approximate values of surface temperature were compared with recorded average values and the signal at the map and relative surface water temperature was taken for comparison with the lake surface temperature.

The thermal infrared surface emissivity ϵ_o has been estimated on the basis of NDVI using the relation:

$$\epsilon_o = 1.009 + 0.047 \ln(\text{NDVI})$$

The relationship between ϵ_o and NDVI is valid for the NDVI values between 0.16 and 0.74 i.e. not valid for water bodies with negative NDVI values. For water bodies a constant emissivity $\epsilon_o = 1$ is assigned after masking.

However, when using the above equation since the relationship between ϵ_o and NDVI is valid for the NDVI values between 0.16 and 0.74 i.e. not valid for water bodies with negative NDVI values. A special modification was made using a conditional equations to mask the water bodies by assigning a constant emissivity $\epsilon_o = 1$.

The NDVI map was derived from the spectral planetary reflectance as follows:

$$NDVI_{TOA} = \frac{r_p(b4) - r_p(b3)}{r_p(b4) + r_p(b3)}$$

$$NDVI_{ground} = -0.043 + (1.008 NDVI_{toa})$$

Where $NDVI_{ground}$ and $NDVI_{toa}$ are the Normalized difference vegetation indexes at the ground and at the top of the atmosphere and $r_p(b4)$ and $r_p(b3)$ are spectral planetary reflectance's derived from TM bands 4 and 3 respectively.

Broadband reflectance at the top of the atmosphere, which is the weighted average of all the single band reflectance values, has been computed using the relation:

$$r_p = \frac{\sum W_i r_p(\lambda_i)}{\sum W_i}$$

Where W_i : the band wise calibration constants $K(\lambda_i)$ [$mWcm^{-2} \mu m^{-1}$]

$r_p(\lambda_i)$: narrow band planetary albedos

The weights for the different bands are computed as the ratio of the amount of incoming short-wave radiation from the sun in a particular band and the sum of incoming short-wave radiation for all the bands.

The surface albedo is then calculated from using both the planetary albedo and the double way atmospheric transmittance using the relation:

$$r_o = \frac{r_p - r_{mini}}{\tau^2}$$

In this relation the terms r_p and r_{mini} represent the pixel-by-pixel values of the broadband planetary albedo and the smallest value of the total image in this case the albedo of a water body respectively.

τ Represents atmospheric transmittance

τ^2

$$T_{toa} = \epsilon_o^{0.25} T_R$$

In order to convert the DN of the thermal band (Band 6) to surface temperature, two Procedures are required. Firstly, each DN has been converted to the spectral radiance as follows:

$$L_{\lambda_i} = a + \frac{d - a}{255} * DN$$

Where the terms: L_{λ_i} ($mWcm^2sr^{-1} \mu m^{-1}$): the spectral radiance of the i _th band of the TM at the top of the atmosphere, DN: the digital numbers of each pixel of the map (band i), and a and b are given by Markham and Barker (1987)

Figure 15 Images showing NDVI (a), surface temperature (b) and radiated temperature (c) of the study area on Landsat TM image window of 18 May 2000 (blue colour is part of lake Naivasha)

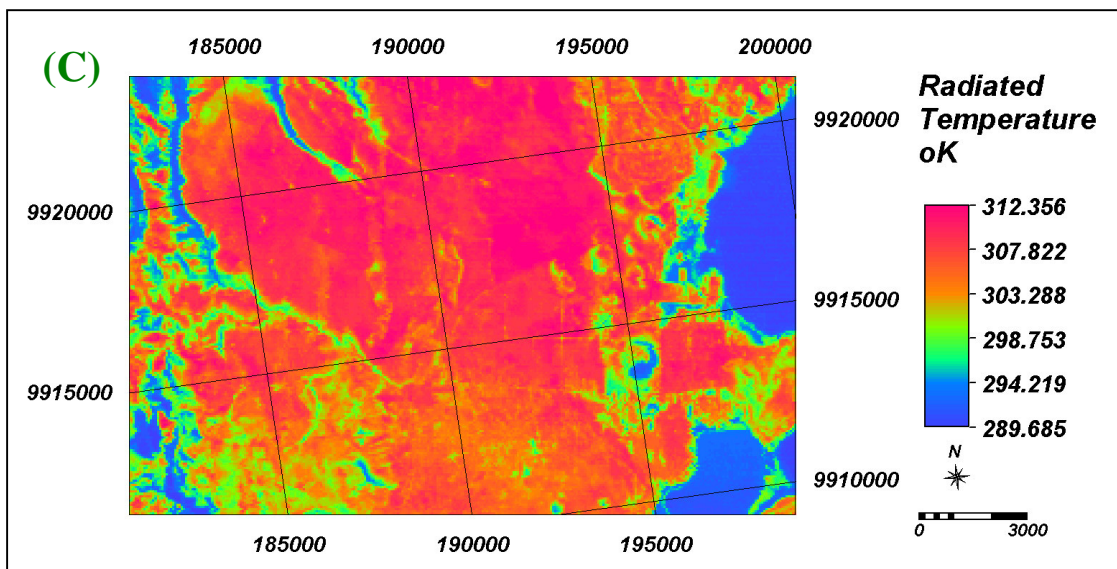
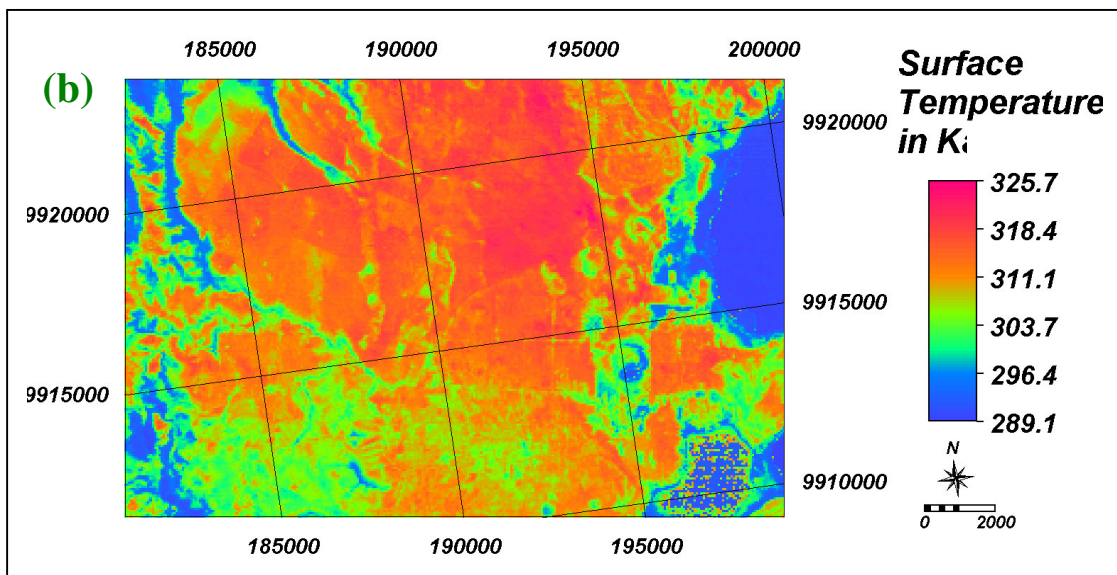
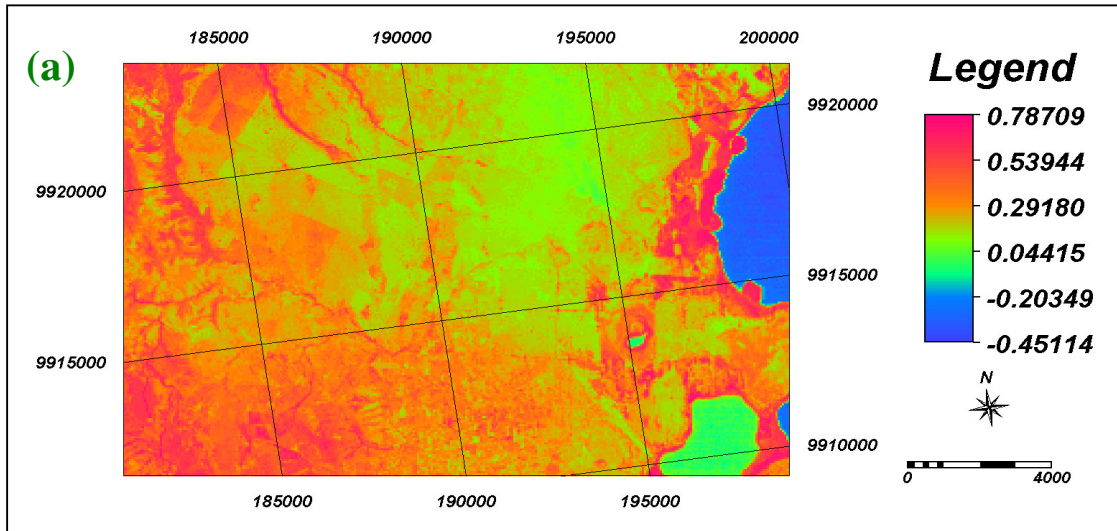
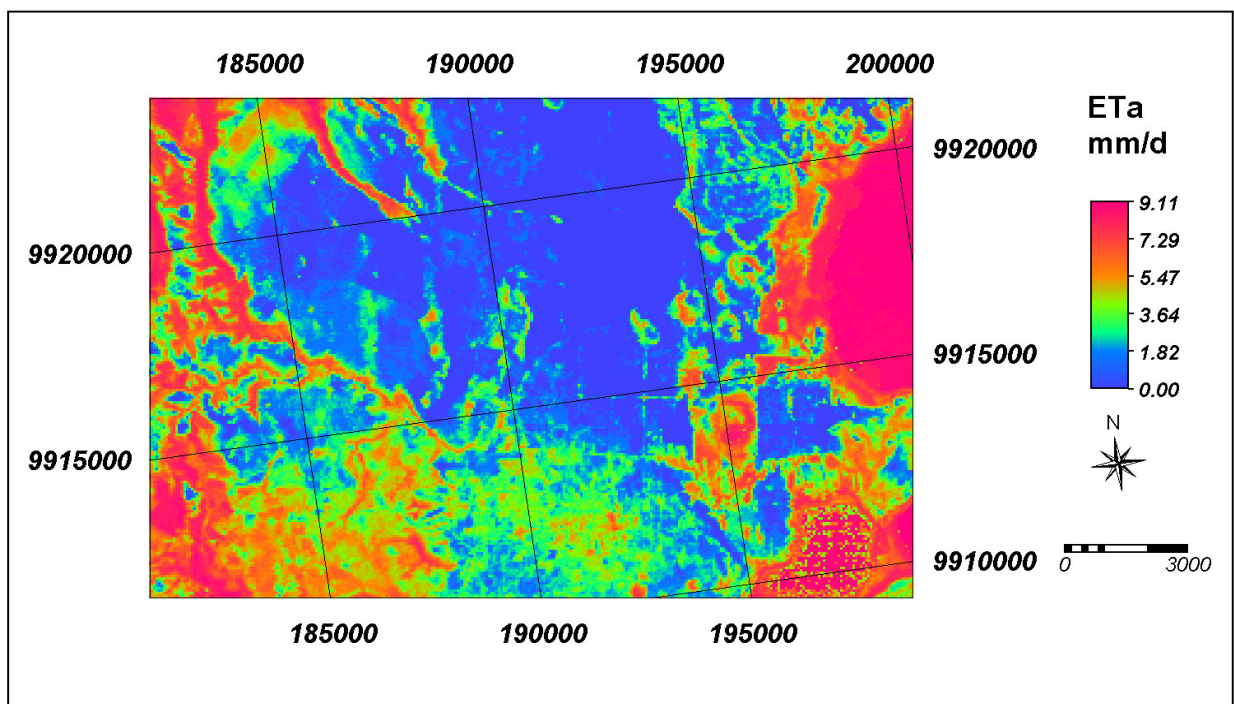
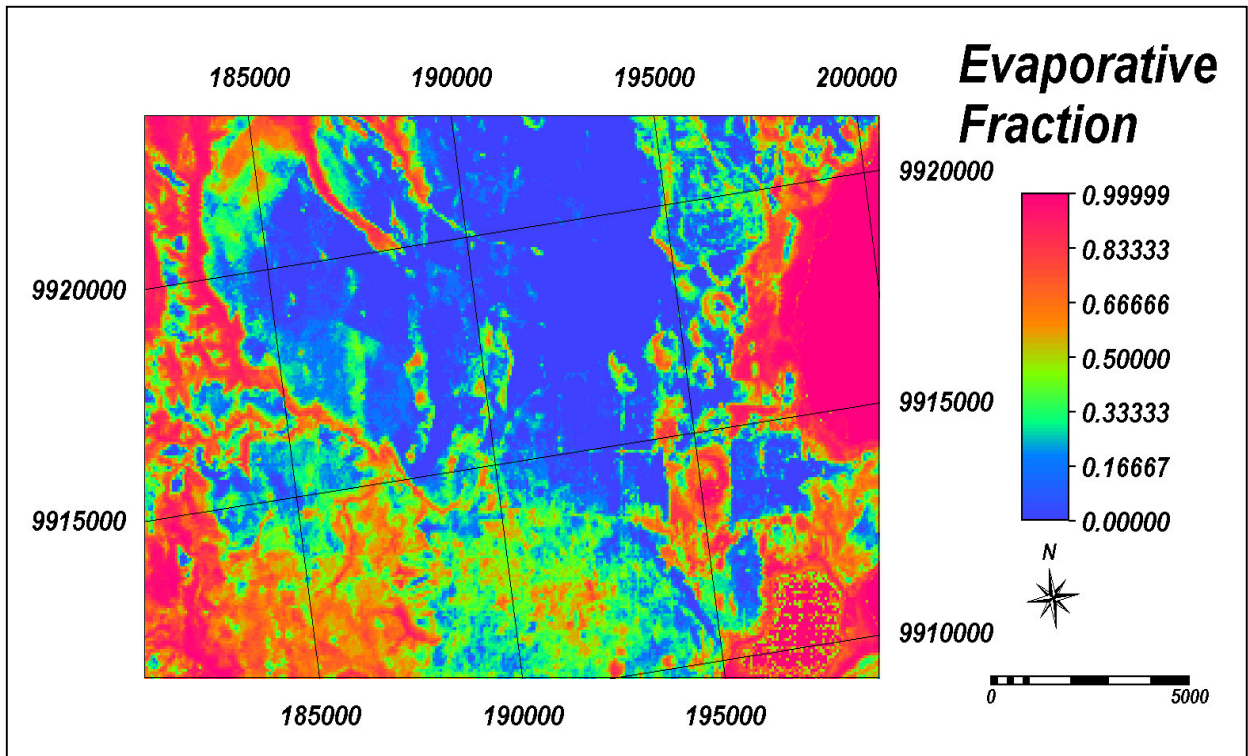


Figure 16 Images showing evaporative fraction and daily ETa values of the study area on Landsat TM image window of 18 May 2000 (part of lake Naivasha is indicated on the right side)



From the above ETa map (figure16) it is shown that maximum evapotranspiration is observed in the near by tick forest areas, forested gentle valleys traversing the wheat fields and of course the Lake evaporation.

The year 2000 was a dry year in the Naivasha area; in the map wide arable and grazing lands were bare and dry with limited evaporative fraction and the corresponding ETa except in the upper Kijabe fields and depressions (drainage lines) with thicker alluvial deposits.

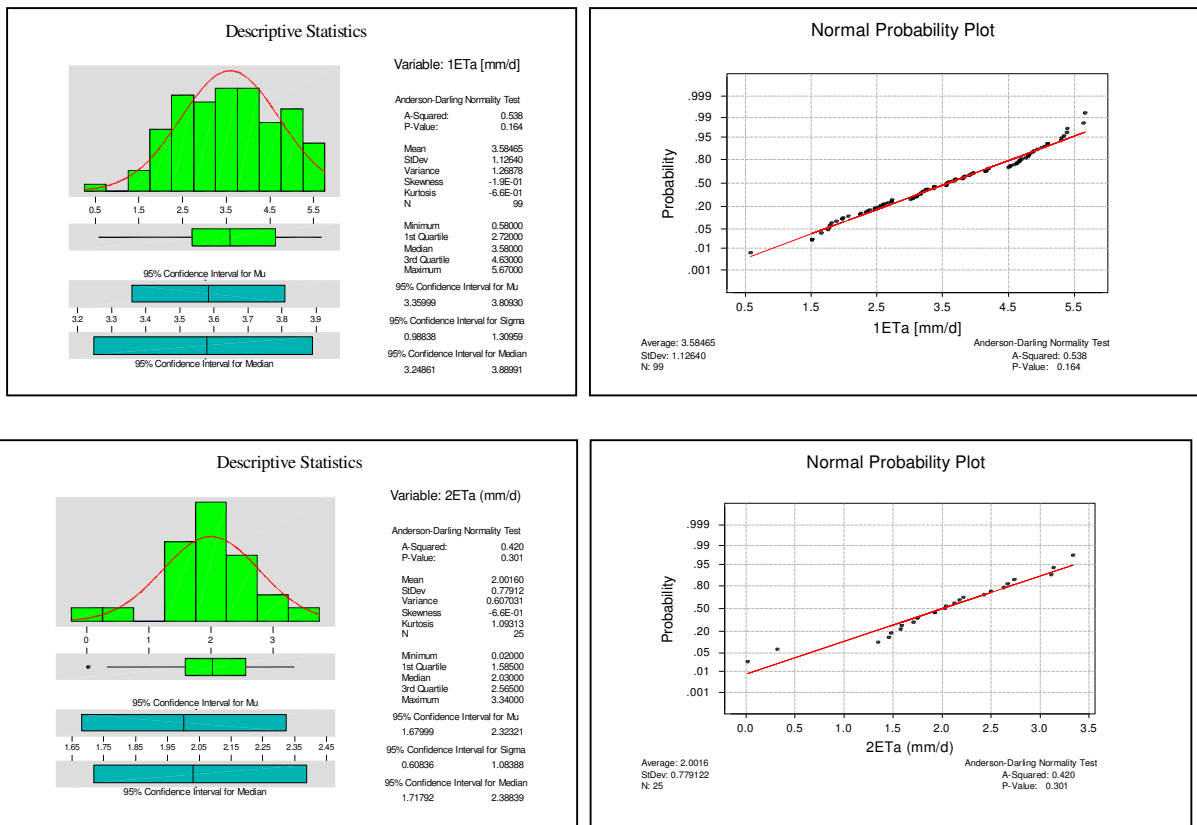
5.3. Classification of crop performance zones

5.3.1. Variation between fields

In this section statistical analysis were performed by considering ETa as a continuous variable. Two-sample t-test was chosen to check the variation of ETa between the two fields.

a) Upper wheat field

Figure 17 Descriptive statistics and normal probability plot of ETa (Both fields)



From the normal probability plot and descriptive statistics graphs above actual evapotranspiration samples in both fields are normally distributed at 95% confidence level, there fore two-sample t-test can be performed to check the significance of the spatially distributed ETa values.

Table 3 Two-sample T test for upper field ETa [mm/d] vs. lower field ETa (mm/d)

	N	Mean	StDev	SE Mean
Upper field ETa [mm/d]	99	3.58	1.13	0.11
Lower field ETa [mm/d]	25	2.002	0.779	0.16

Difference = μ 1ETa [mm/d] - μ 2ETa (mm/d)
 Estimate for difference: 1.583
 95% CI for difference: (1.110, 2.056)

T-Test of difference = 0 (vs not =): T-Value = 6.63 **P-Value = 0.000** DF = 122
 Both use Pooled StDev = 1.07

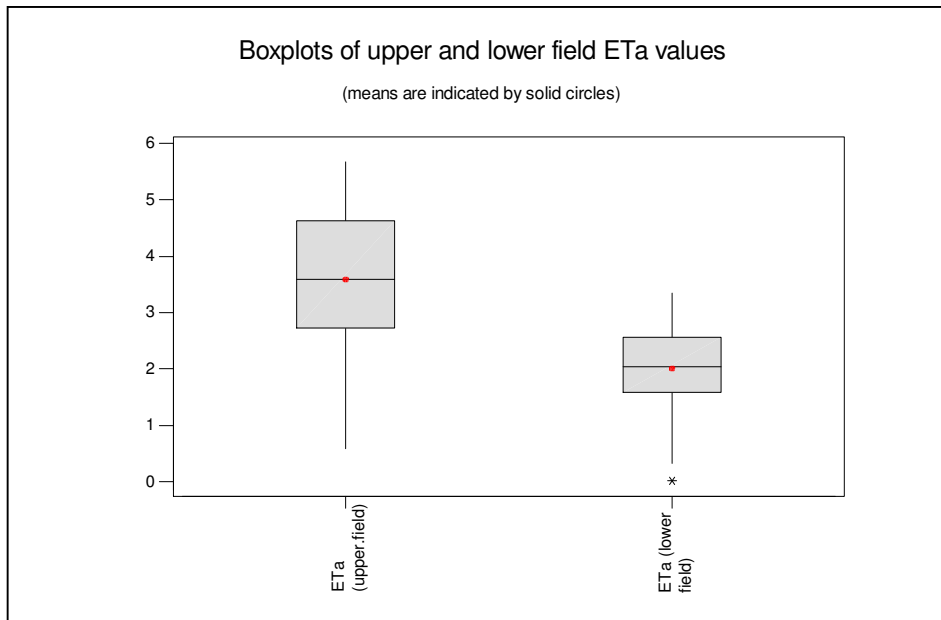


Figure 18 Box plot to compare the variability of ETa in both fields

The most commonly used statistical method for evaluating the differences in the means of two data groups is the t-test, therefore based on the Minitab's T-test procedures The two-sample t-confidence interval and test procedures were used to make inferences about the difference between two population means (ETa_upper wheat field in mm/day and ETa_Lower wheat field in mm/day), based on data from two independent, random samples.

For the purpose of testing the variation of the means of the daily actual evapotranspiration rates of the two wheat fields, where the null hypothesis H_0 : is there is no significant ETa variation between these two fields of the same crop type and age under a uniform management and the alternative hypothesis H_1 : there is a significant variation between the actual rates of evapotranspiration. Since the two independent sample sets are normally distributed, two-sample t-procedures was used.

As it is shown in table 3 the p-value is less than the commonly chosen α -levels (0.05), there fore we can conclude that there is enough evidence for a difference in ETa values across the upper and lower wheat fields at 95% confidence interval.

The "box-and -whisker" plots on the other hand shows a useful picture of ETa data distributions in both the upper and lower plots, allowing us to eyeball the overall differences among the two actual evapotranspiration Map surfaces.

5.3.2. Within field variability

The actual evapotranspiration map was used to identify spatial ETa patterns across the fields. The TM image taken on 18 May 2000 was the reference for estimating the ETa values and grouping in to classes of similar ETa values using supervised classification technique in ILWIS 3.0 software. Pixels of similar ETa values grouped as performance patterns across the sampling plots after trying various ranges of values.

Based on the observed variability ranges in the two wheat fields two types of performance ranges has been done as follows: During the classification estimated actual evapotranspiration values in the range of 2.5 to 3 mm/day is considered as average rate for wheat grown around Naivasha area.

5.3.2.1. Upper wheat field

The spatial variability of actual evapotranspiration values in the upper wheat field (fig.19) ranging from 1.5 to 5.6 mm/day with mean value of 3.2 mm/day and pooled standard deviation of 0.284.

Figure 19 within field variability patterns (upper field)

- 19a: Kijabe wheat field sliced ETa patterns
- 19b: ETa in the upper field & surrounding fields
- 19c: clipped upper field ETa Map.

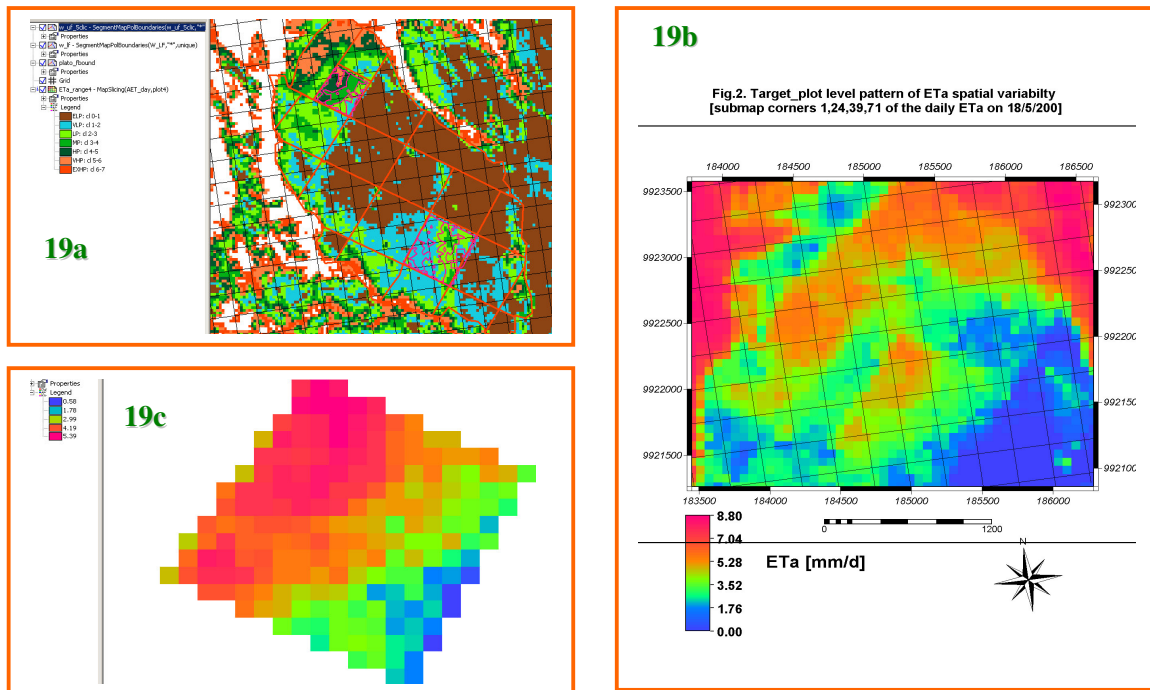


Figure 20 3D views of actual evapotranspiration and NDVI patters

(Upper wheat field, Landsat TM image window of 18 may 2000)

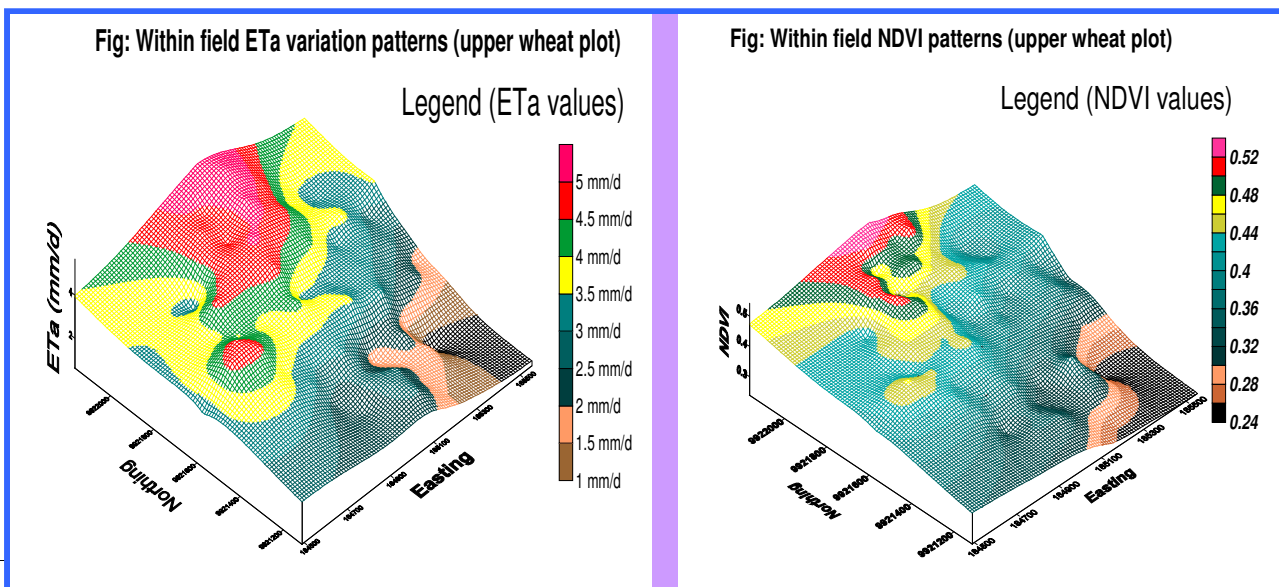
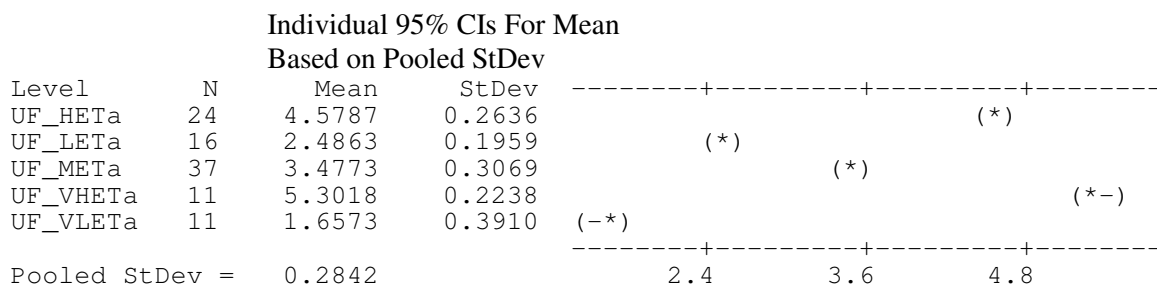


Table 4 One-way Analysis of variance of the sliced actual evapotranspiration zone (Upper wheat field)

Analysis of variance

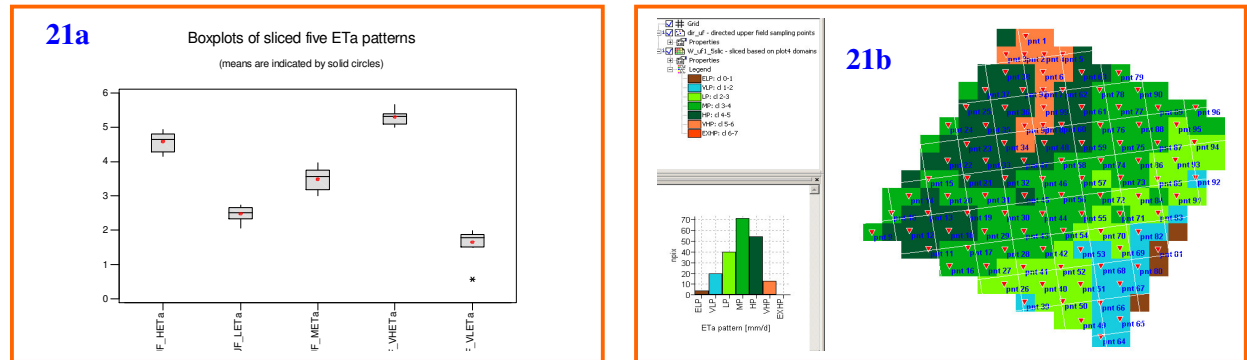
One-way ANOVA: UF_HETa, UF_LETa, UF_METa, UF_VHETa, UF_VLETa

Analysis of Variance between the upper wheat field actual evapotranspiration (ETa) five patterns					
Source	DF	SS	MS	F	P
Factor	4	116.7457	29.1864	361.26	0.000
Error	94	7.5943	0.0808		
Total	98	124.3401			



The above ANOVA table shows that there is significant difference between the 5 ETa patterns at 95% confidence interval.

Figure 21 Box plot and sliced crop performance zones (Upper wheat field)



An analysis of variance (ANOVA) was done to investigate whether a differentiation of ETa in 5 classes in the upper field made sense, the classes were:

- VHETa (Very high evapotranspiration zone, 5-6 mm/day and mean 5.3 mm/day)
- HETa (high evapotranspiration zone, 4-5 mm/day and mean 4.57 mm/day),
- METa (Medium evapotranspiration zone, 3-4 mm/day and mean 3.48 mm/day)
- LETa (Low evapotranspiration zone, 2-3 mm/day and mean 2.49 mm/day),
- VLETa (Very low evapotranspiration zone, 1-2 mm/day and mean 1.66 mm/day)

ETa shows a highly significant difference at 95% confidence interval.

The results are shown in table 4 by the box and whisker plot of figure 21a

The maps of the ETa classes of the upper field is shown in figure 21b

The distribution of ETa was normal and therefore an analysis of variance was done to investigate whether 5 classes of ETa by splitting the observed range in equal intervals, were meaningful. That proved to be the case. The ETa segmentation assisted in the sampling design to ensure a good density in the highest and lowest class

5.3.2.2. Lower wheat fields

The spatial variability of actual evapotranspiration values in the Lower wheat field (fig.22-23) ranging from 0.2 to 3.4 mm/day with mean value of 2.01 mm/day and pooled standard deviation of 0.422.

Figure 22 within field variability patterns (lower field)

- 22a: Lower field ETa pattern
- 22b: lower field sliced ETa pattern
- 22c: Kijabe area ETa (sliced) patterns
- 22d: Polygon zed ETa zones

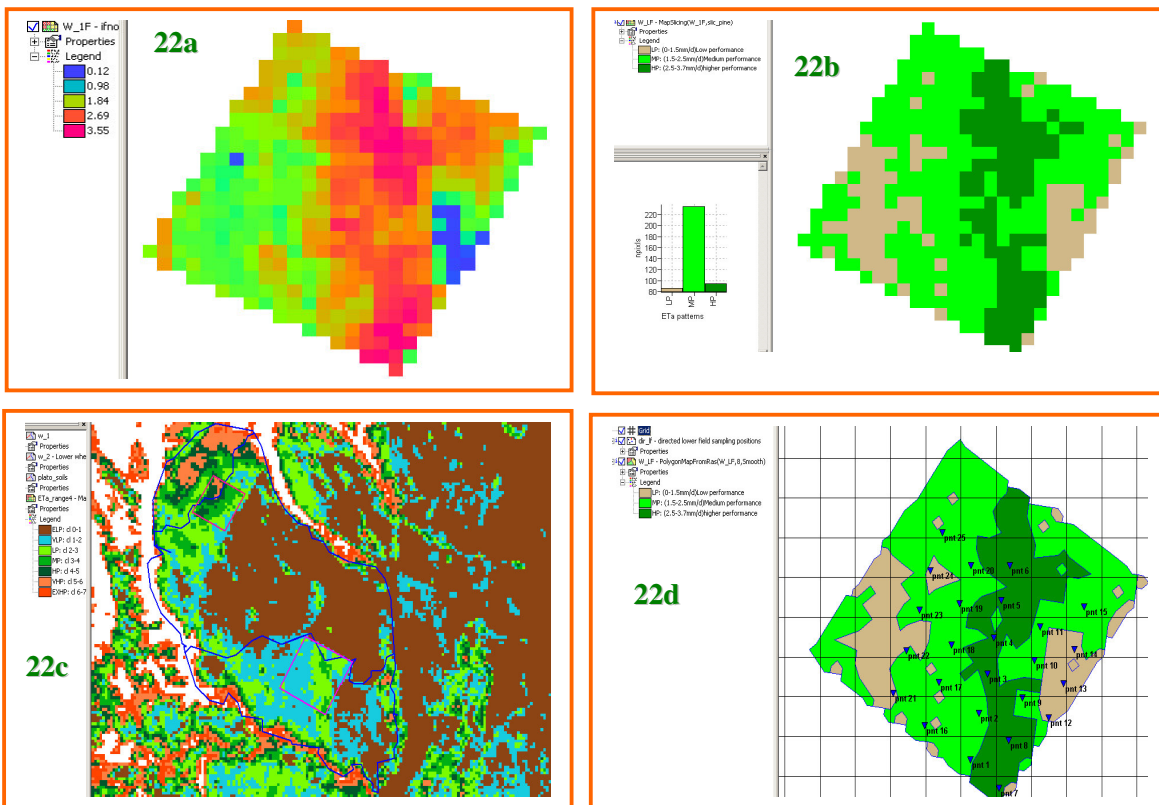
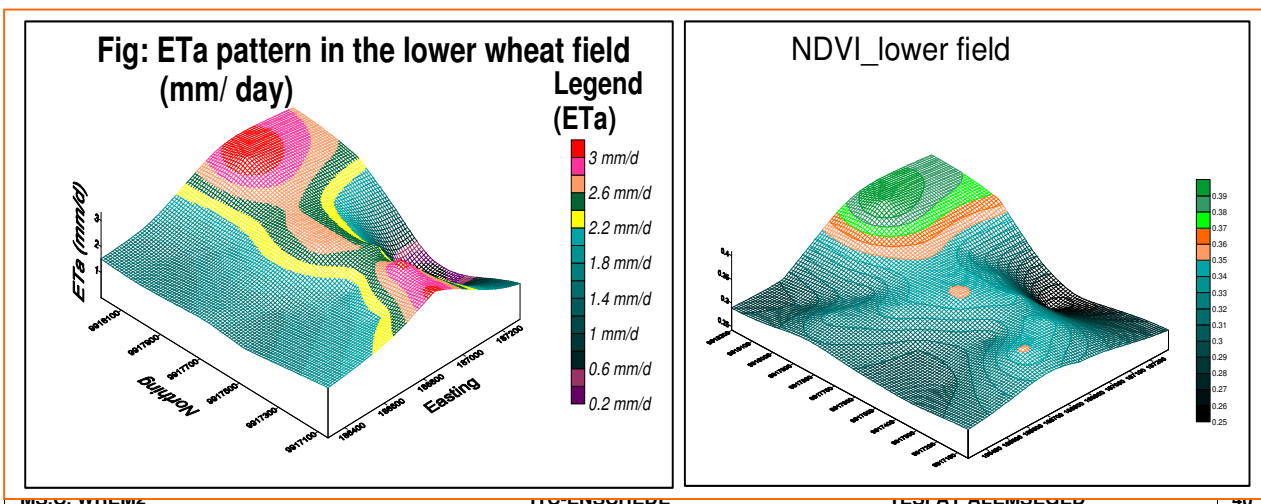


Figure 23 ETa and NDVI patterns of the lower field



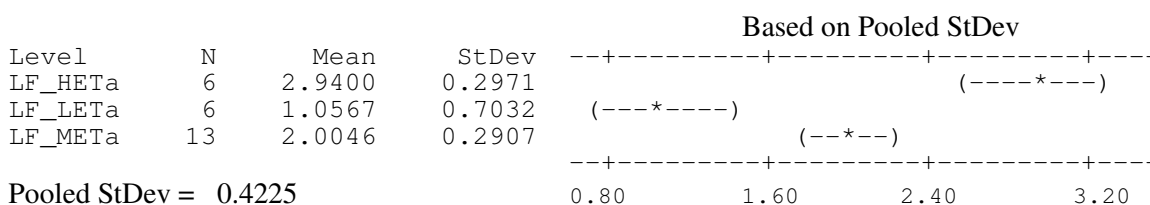
Analysis of variance

Table 5 One-way Analysis of variance of the sliced actual evapotranspiration zone (Lower wheat field)

One-way ANOVA: LF_HETa, LF_LETa, LF_METa

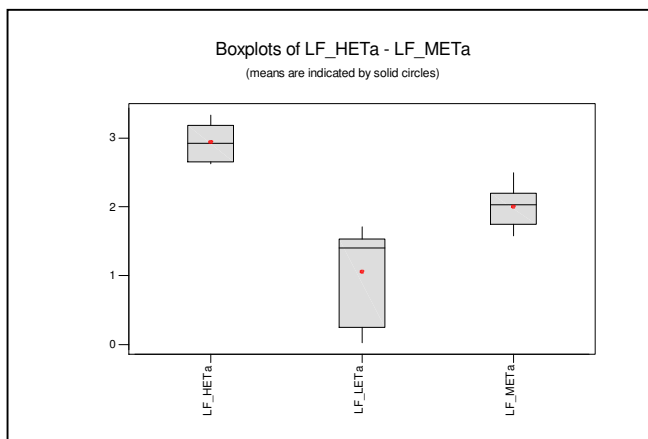
Analysis of Variance between the Lower wheat field actual evapotranspiration (ETa) three patterns					
Source	DF	SS	MS	F	P
Factor	2	10.641	5.321	29.80	0.000
Error	22	3.928	0.179		
Total	24	14.569			

Individual 95% CIs For Mean



The above ANOVA table shows that there is significant difference between the 3 ETa patterns at 95% confidence interval.

Figure 24 Box plot and sliced crop performance zones (Lower wheat field)



The analysis of variance (ANOVA) for the Lower wheat field observed actual evapotranspiration three patterns classified based on the observed within field variations showed significant differences.

The classes are:

- i.e. HETa (high evapotranspiration zone, 2.5-3.7 mm/day and mean 2.94 mm/day),
- METa (Medium evapotranspiration zone, 1.5-2.5 mm/day and a mean of 2.0 mm/day)
- and LETa (Low evapotranspiration zone, 0-1.5 mm/day and mean 1.06 mm/day)

Similar to the upper wheat field since the distribution of ETa was proved normal and the analysis of variance was done to investigate whether the 3 classes of ETa range sliced in equal intervals, were meaningful. That proved to be the case. The ETa segmentation assisted in the sampling design to ensure a good density in the highest and lowest class.

Chapter 6. Statistical analysis, single variables

6.1.Upper field

6.1.1. Introduction (sampling scheme, variables and acronyms)

Sampling scheme

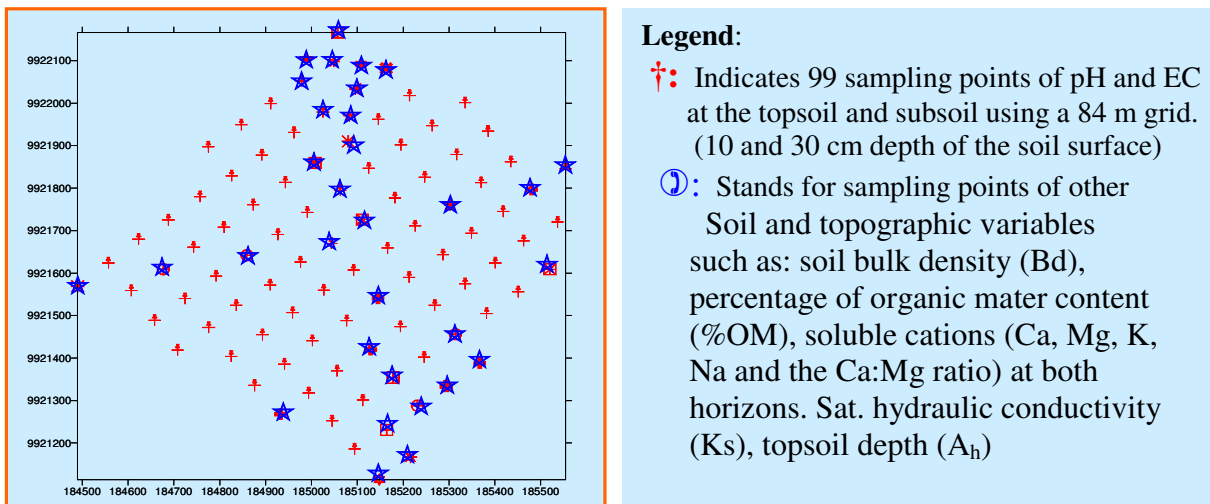
Geo-referenced data obtained on the study fields included soil pH, electrical conductivity, soil moisture content, saturated hydraulic conductivity, bulk density, topographic elevation, and a number of soil properties. Listed below. The existing topographic map scale 1:40,000 was not found appropriate for analysing the micro relief and contours within the sampling area because of its coarser size, there for field level measured elevation data was used in the regression table.

Soil sampling was conducted on an 84.8-m grid in September of 2001; on wheat field of 1 Km². During the satellite over pass of 18 May 2000 the wheat was about 6 weeks old. An Auger was used to collect soil samples ranging from 10 to 45 centimetres depth. Three soil cores obtained within 1-m radius of each geo-referenced sampling position were combined, oven dried and analysed for pH, electrical conductivity and bulk density in Sulmac lab. Additional samples were taken to The Netherlands and further analysis was made on other chemical properties of the soil.

Standard soil properties such as Organic matter percentage of 38 paired soil samples, measurement of pH and EC as well as the determination of other essential cations (Mg²⁺, Ca²⁺, Na⁺ and K⁺) was made using the ICP.(see chapter 4)

Ninety nine sampling positions were chosen in the upper wheat field based on a combined grid and evapotranspiration pattern out of which 16 oriented on south-east and east-west transect are chosen as permanent observation points for major soil properties requiring more time, such as the hydraulic conductivity, Bd, %OM, depth of top soil and other essential cations.

Figure 25 Location of sampling points for upper wheat field



The sampling points were made to specially concentrate on the two extreme zones of ETa, namely the very high and very low ETa zones consisting 11 observation points each.

The analysis of the upper field is discussed first followed by the lower field.

In this chapter actual evapotranspiration data of each sampling position (see chapter 4) were regressed against soil physical and chemical variables.

First analysis of the chemical variables was done; they are soil pH, electrical conductivity, soluble Cations, organic matter content measured at two soil horizons i.e. 10 and 30 cm depth.

Acronyms of soil and topographic parameters.

<i>Soil chemical properties</i>	<i>acronyms</i>
Soil pH at 10 cm depth	(pH_10)
Soil pH at 30 cm depth	(pH_30)
Electrical conductivity at 10 cm depth	(EC 10)
Electrical conductivity at 30 cm depth	(EC 30)
Percentage of organic matter content at 10 cm depth	(%OM_10)
Percentage of organic matter content at 10 cm depth	(%OM_30)
Percentage of organic matter content at 70 cm depth	(%OM_70)
Soluble Ca content in milliequivalents per 100-gram soil at 10 cm depth	(Ca_10)
Soluble Calcium content in milliequivalents per 100-gram soil at 30 cm depth	(Ca_30)
Soluble Magnesium content in milliequivalents per 100-gram soil at 10 cm depth	(Mg_10)
Soluble Magnesium content in milliequivalents per 100-gram soil at 30 cm depth	(Mg_30)
Soluble potassium content in milliequivalents per 100-gram soil at 10 cm depth	(K_10)
Soluble potassium content in milliequivalents per 100-gram soil at 30 cm depth	(K_10)
Soluble sodium content in milliequivalents per 100-gram soil at 10 cm depth	(Na_10)
Soluble sodium content in milliequivalents per 100-gram soil at 30 cm depth	(Na_30)
Calcium-Magnesium ratio at 10 cm depth of the soil horizon	(Ca:Mg_10)
Calcium-Magnesium ratio at 30 cm depth of the soil horizon	(Ca:Mg_30)

Note: The numbers in front of each acronym indicates 1 for upper field & 2 for the lower field.

<i>Soil physical properties</i>	<i>acronyms</i>
Soil bulk density at 10-20 cm depth	(Bd 10-20)
Soil bulk density at 40-50 cm depth	(Bd 40-50)
Saturated hydraulic conductivity in cm per day	(Ks cm/d)
Topsoil depth	(ds=A _h),
Slope percent (steepness)	(slope%)
Percentage of sand in soil samples	(%sand).

6.1.2. Chemical parameters (upper field)

It is generally known that topsoil chemical properties are variable both in space and time since it is indirect contact with human activities mainly chemical inputs and climatic factors (rainfall, sunshine, wind, temperature, etc.). The rooting depth of wheat is concentrated on the upper most 40 cm of the soil.

Because of this, most of the field level surveys and laboratory analysis was made on the topsoil. The soil samples used for Chemical analysis are mainly taken from the first 10-30 cm depth.

Table 6 Correlations of soil chemical parameters (upper field)

	ETa	pH_10	pH_30	EC_10	EC_30	%OM_10	%OM_30	%OM_70
pH_10	0.638							
	<u>0.000</u>							
pH_30	0.319	0.647						
	<u>0.001</u>	0.000						
EC 10	0.180	0.202	0.210					
	0.074	0.045	0.037					
EC 30	0.015	0.049	0.073	0.876				
	0.883	0.631	0.475	0.000				

%OM_10	0.759	0.648	0.618	-0.117	-0.243			
	<u>0.000</u>	0.000	0.000	0.552	0.213			
%OM_30	0.728	0.577	0.547	0.246	0.059	0.687		
	<u>0.000</u>	0.001	0.003	0.207	0.765	0.000		
%OM_70	0.613	0.459	0.364	-0.011	-0.017	0.474	0.631	
	<u>0.026</u>	0.114	0.221	0.972	0.957	0.102	0.021	
Ca_10	0.648	0.640	0.599	0.432	0.079	0.462	0.553	0.048
	<u>0.000</u>	0.000	0.001	0.019	0.684	0.013	0.002	0.877
Ca_30	0.602	0.732	0.678	0.138	-0.119	0.566	0.521	0.074
	<u>0.001</u>	0.000	0.000	0.476	0.537	0.002	0.005	0.809
K_10	0.372	0.381	0.486	0.486	0.305	0.239	0.365	0.172
	<u>0.047</u>	0.042	0.008	0.008	0.108	0.222	0.056	0.575
K_30	0.292	0.356	0.481	0.173	0.093	0.348	0.495	0.091
	0.125	0.058	0.008	0.369	0.630	0.070	0.007	0.767
Mg_10	0.622	0.551	0.572	0.514	0.203	0.404	0.502	0.374
	<u>0.000</u>	0.002	0.001	0.004	0.290	0.033	0.006	0.208
Mg_30	0.676	0.583	0.550	0.458	0.227	0.341	0.621	0.525
	<u>0.000</u>	0.001	0.002	0.013	0.236	0.075	0.000	0.065
Na_10	0.098	0.091	-0.030	0.068	-0.140	-0.003	-0.045	-0.170
	0.613	0.637	0.879	0.727	0.469	0.988	0.821	0.578
Na_30	0.001	0.008	0.177	0.373	0.230	-0.091	-0.000	-0.047
	0.997	0.966	0.359	0.046	0.230	0.646	0.998	0.879
Ca:Mg10	0.267	0.329	0.217	0.059	-0.130	0.225	0.277	-0.516
	0.161	0.081	0.259	0.760	0.503	0.250	0.154	0.071
Ca:Mg30	0.247	0.428	0.365	-0.142	-0.272	0.426	0.220	-0.193
	0.196	0.020	0.051	0.463	0.154	0.024	0.260	0.527

	Ca10 (m)	Ca30	K10	K30	Mg10	Mg30	Na10	Na30	Ca:Mg10
Ca30	0.768								
	0.000								
K10	0.729	0.472							
	0.000	0.010							
K30	0.528	0.419	0.595						
	0.003	0.024	0.001						
Mg10	0.796	0.585	0.679	0.276					
	0.000	0.001	0.000	0.147					
Mg30	0.667	0.396	0.642	0.490	0.798				
	0.000	0.034	0.000	0.007	0.000				
Na10	0.367	0.202	0.059	-0.117	0.395	0.190			
	0.050	0.294	0.759	0.545	0.034	0.323			
Na30	0.329	0.097	0.264	0.151	0.374	0.243	0.524		
	0.081	0.617	0.167	0.433	0.045	0.203	0.004		
Ca:Mg10	0.600	0.484	0.240	0.477	0.006	0.065	0.132	0.090	
	0.001	0.008	0.210	0.009	0.976	0.740	0.495	0.644	
Ca:Mg30	0.403	0.804	0.038	0.185	0.078	-0.201	0.049	-0.080	0.552
	0.030	0.000	0.844	0.337	0.686	0.295	0.802	0.680	0.002

Cell Contents: Pearson correlation

P-Value

The Pearson correlation analysis above indicates that there is significant positive correlation between the response variable ETa and soil chemical predictors (pH, %OM, Mg, Ca in both horizons and k in the upper soil horizon) at 95% confidence Interval (underlined figures)

6.1.2.1. Soil pH

The pH measurement was made using the standard FAO guide for 99 samples corresponding to the 99 sampling points. (See chapter 4), at soil depths of 10 and 30 cm. Across the five ETa patterns, the "very

high ETa " (VH ETa), "high ETa " (H ETa), "medium ETa value " (M ETa), "lower ETa value " (L ETa) and "very low ETa " (VL ETa), the measured pH ranges between 5.44 and 6.55 with a median of 6.06 and mean 6.04 in the upper horizon (at 10 cm depth).

The soil pH variation in the lower soil horizon (at 20-30 cm depth), increases in most observation points, ranging between 5.84 and 6.6 with a median of 6.23 and mean 6.24 in the upper horizon (at 10 cm depth).

The main trend of increase of soil pH from 10 to 30 is mainly pronounced in the lower elevation areas experiencing lower ETa values, at some sample sites in the lower elevation area the pH at 30 cm is even less than the pH at 10 cm.

It can also be noted that on gentle slopes the pH is higher than the steeper slopes, which may be explained by excessive leaching of cations in the steeper and sandy clay loam soils.

Based on the available old aerial photos (1995), historical records of the farm shows that the upper edges of the farm was a forest area before it was fenced as part of the Kijabe wheat farm, and the pH seems to follow this trend. Compared to the rest of the fields, this area shows a distinct variation in other soil properties such as the soil organic matter content; saturated hydraulic conductivity and bulk density.

Figure 26 scatter plot of ETa regressed by pH_10 cm depth (Upper field)

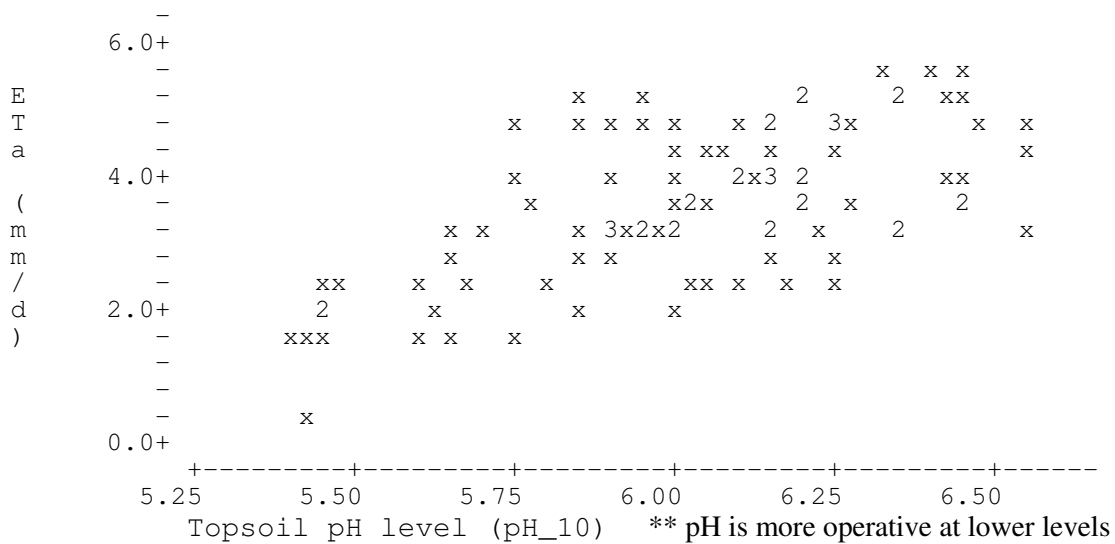


Figure 27 scatter plot of ETa regressed by %pH_30 cm depth (upper field)

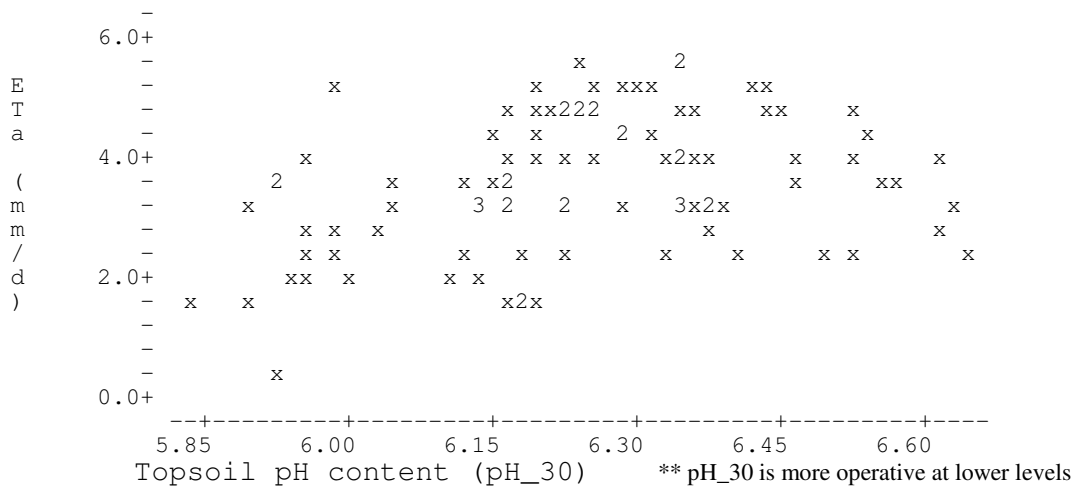
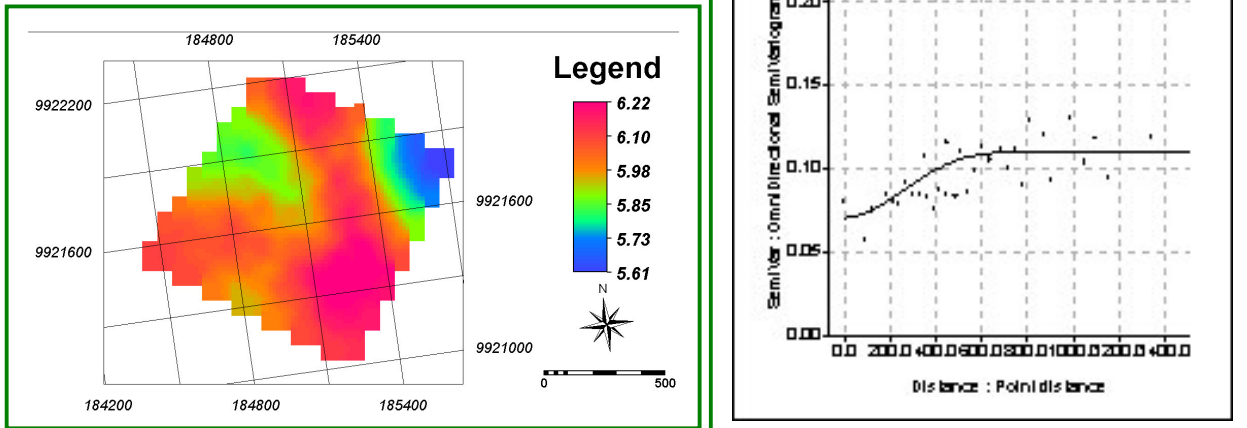


Figure 28 Soil pH map of the upper field (using ordinary Kriging).

U.Field	Model	Nugget	Sill	Range
pH_10	Gaussian	0.07	0.11	350



The semi variogram for pH_10 shows that the range value is about 6 pixels (350 m), which means that, with the density of our sample points, interpolation by Kriging (see figure 28) is meaningful. However, the high nugget value indicates a strong local variation of the pH_10 at short distances. This implies that part of the variation appearing in scatter plots of ETa against pH can be explained by the nugget value.

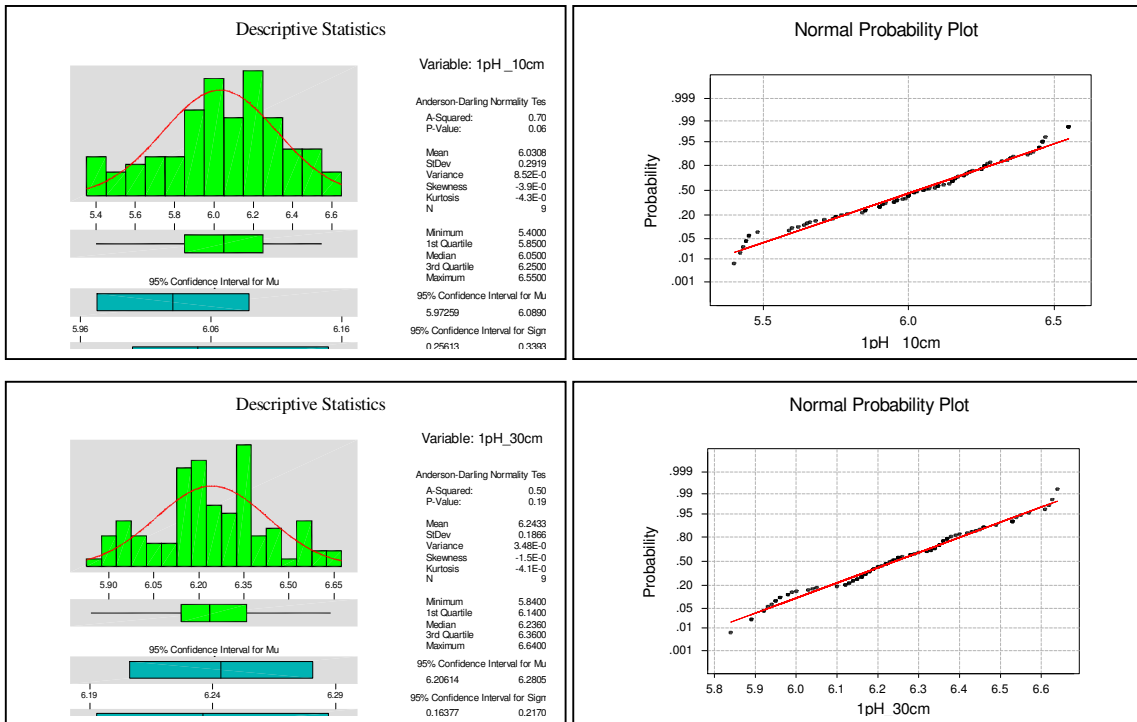
Plate 1 Partial view of the Upper Kijabe field covered by 52 days old wheat (september 20, 2001)



As it is indicated in the above scatter plots (figures 26-27) the relationship of the actual evapotranspiration values and soil acidity levels is more pronounced in the lower pH values (mainly <6.0), a slightly linear increase of actual evapotranspiration values in the lower pH range indicates that there is positive relationship between the predictor pH and the response ETa. The cloud of points observed at higher pH ranges indicates that there is relatively less effect on ETa at pH>6.

Figure 29 Descriptive statistics and normal probability plots for all samples in the upper field

Descriptive statistics and normal probability plots (fig.29.1)_pH.

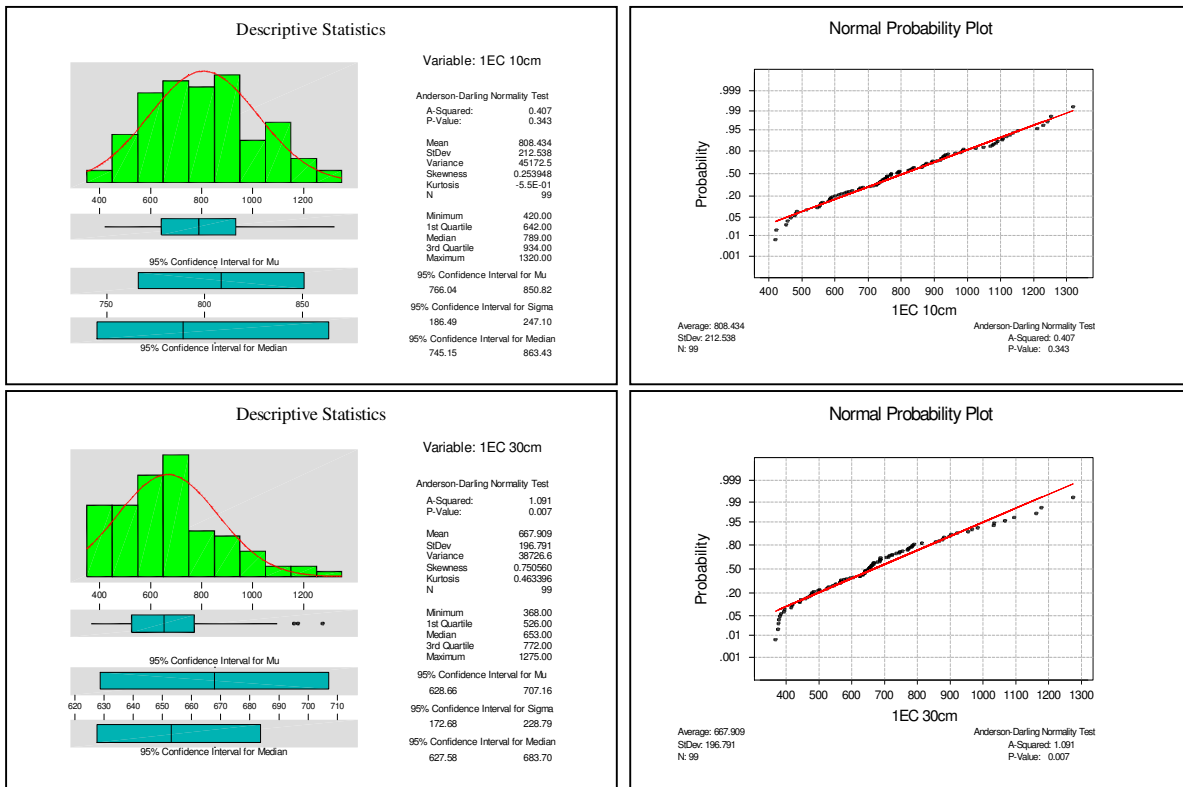


6.1.2.2. Electrical conductivity (EC)

Soil electrical conductivity for both fields was measured (see chapter 4) in Sulmac laboratory. Some soil samples were analyzed in ITC laboratory, The Netherlands after 45 days, which showed an average of 6.2 % increase. For consistency and data sufficiency purposes, however, the data, which was used for this study, is only the previously measured (Sulmac lab.) ones. The distribution of the variable EC_10 is normally distributed at 95% confidence interval. The mean (807 μ s/cm) and median (789 μ s/cm) are more or less similar with slightly higher values in the medium ETa zone i.e. the middle of the field. The distribution of EC_30 is normal after log transformation (see table 8&9). The mean of EC_30 is (668 μ s/cm) and median (658 μ s/cm).

As it is shown in the above correlation table (table 6) EC in the two horizons significantly correlated (R2 = 0.876) and with soluble cations (Ca²⁺, Mg²⁺, K⁺, Na⁺) at 95% confidence interval.

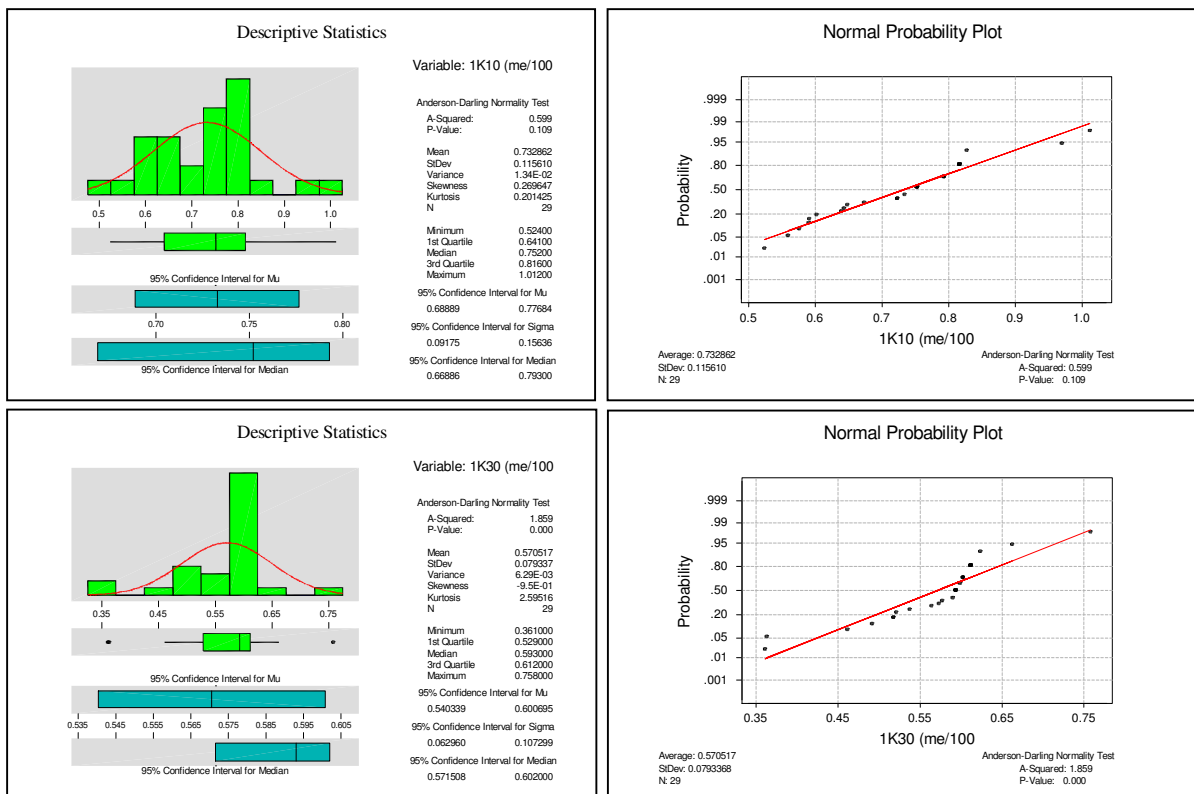
Descriptive statistics and normal probability plots (fig.29.2)_EC.



6.1.2.3. Soluble cations (Na, Mg, K, Ca and Ca:Mg ratio)

Concentrations of soluble cations were measured in ITC laboratory using the ICP-AES method (see chapter 4). Initially the measurements were made in milligram per liter soil extract, the results were later converted in to units of me/ 100-gram soil sample. Out of the 29 measured samples the distribution of the variables Mg, Ca_30, K_10 and Ca:Mg ratio are normally distributed at 95% confidence interval. While the rest were also normally distributed after log transformation except for Na in both horizons (see table 8&9).

Descriptive statistics and normal probability plots (fig.29.3)_soluble cations.



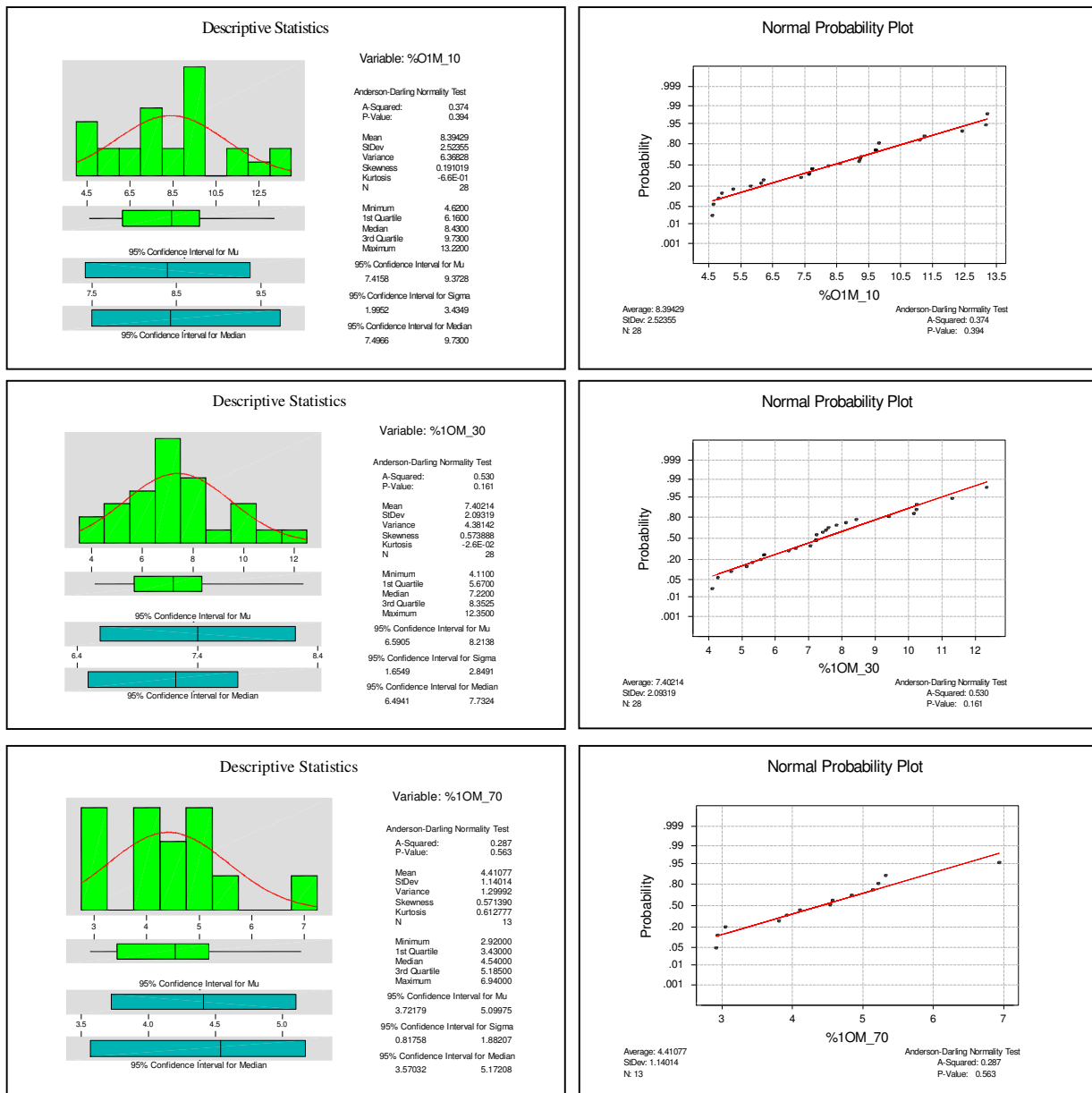
6.1.2.4 Organic matter content

Organic matter content in the soils of the upper wheat field decreases with increasing depth and with increasing elevation towards the upper edges of the field, which are recently converted (forest areas). Organic matter content of the upper soil horizon (10 cm) in the upper wheat field ranges from 4.6-13.2% (w/w) where the mean is 8.39 and median 8.43.

Organic matter content distribution of soils at 30 cm depth ranges from 4.11-12.35% (w/w) with mean 7.4 and median 7.22. Similarly although very few (13 samples) some measurement of OM was made at soil depth of 70 centimetres, the measured values range from 2.92 in the lower steeply portions of the upper field to 6.94 % in the upper flatter areas.

%OM_10, %OM_30 and %OM_70 are normally distributed and significantly correlated with ETa, pH, Ks, soil depth and slope steepness at 95% confidence interval.

Figure 30 Descriptive statistics and normal probability plot for soil %OM in the upper wheat field.



6.1.3. Physical Variables (upper field)

In this section interpretations and figures of the soil physical data are given based on the Anderson-darling normality test and Pearson correlations of the measured physical variables with ETa.

Correlations: ETa [mm/d], Bd 10-20 cm, Bd 40-50 cm, Ks cm/d, ds=Ah, slop %
 Table 7 Correlation Pearson of ETa and physical soil parameters (Upper field)

	ETa [mm/d]	Bd 10-2	Bd 40-50	Ks cm/d	ds=Ah	slop %
Bd 10-2	-0.765	<u>0.001</u>				
Bd 40-5	-0.621	0.874	<u>0.013</u>	<u>0.000</u>		
Ks cm/d	-0.562	0.496	0.647	<u>0.002</u>	0.060	<u>0.009</u>
ds=Ah	0.588	-0.239	-0.122	-0.213	<u>0.027</u>	0.411
slop %	-0.605	0.342	0.183	0.129	-0.654	<u>0.017</u>
%sand	-0.489	0.567	0.376	0.081	-0.240	0.254
	0.054	0.028	0.167	0.767	0.408	0.362

Cell Contents: Pearson correlation
 P-Value

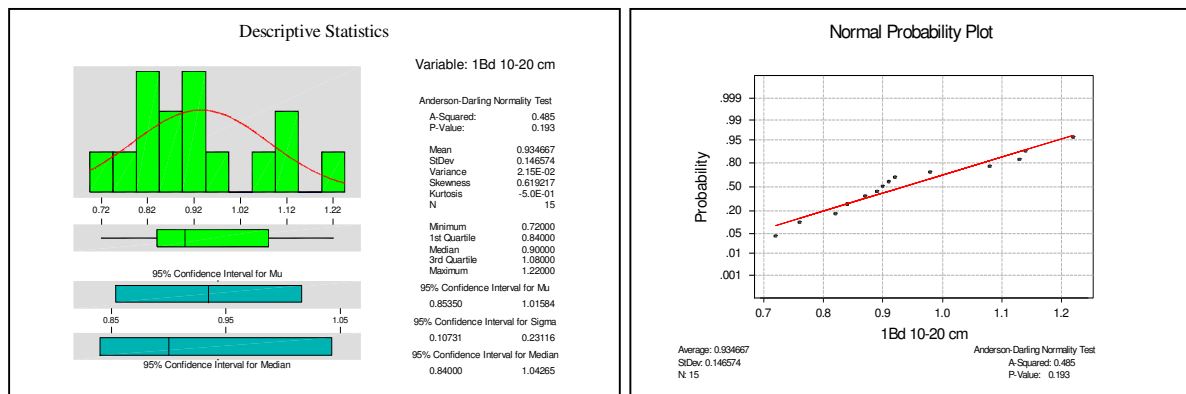
The correlation analysis above indicates that there is significant positive correlation between the response variable ETa and soil physical predictors, soil depth (Ah_horizon) and negative correlation with Bd in both horizons, Ks, slope%, and sand% at 95% confidence interval (underlined figures).

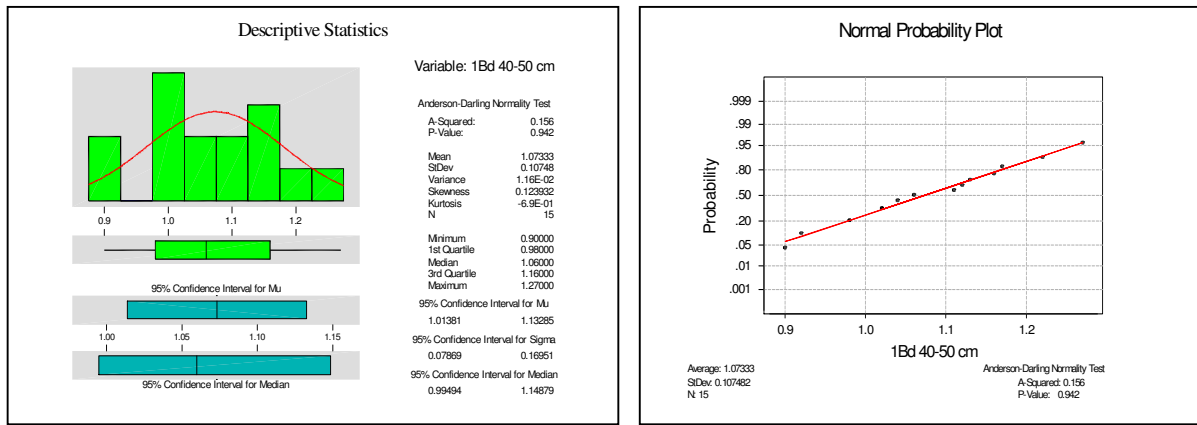
6.1.3.1. Bulk density (Bd)

Similar to other soil variables, bulk density test were made in Sulmac laboratory, as it is shown in the plot of descriptive statistics the data set of bulk density from both horizons is normally distributed. The bulk density of the upper field is generally very low with values ranging from 0.72-1.22 g/ cm2 in the upper soil horizon (Bd_10-20cm) and 1.07-1.27 g/cm2 in the lower horizon (Bd_40-50 cm).

The Bd results were negatively correlated with %OM and ETa and positively correlated with saturated hydraulic conductivity values at 95% confidence level.

Descriptive statistics and normal probability plots (fig.29.4)_Bd.

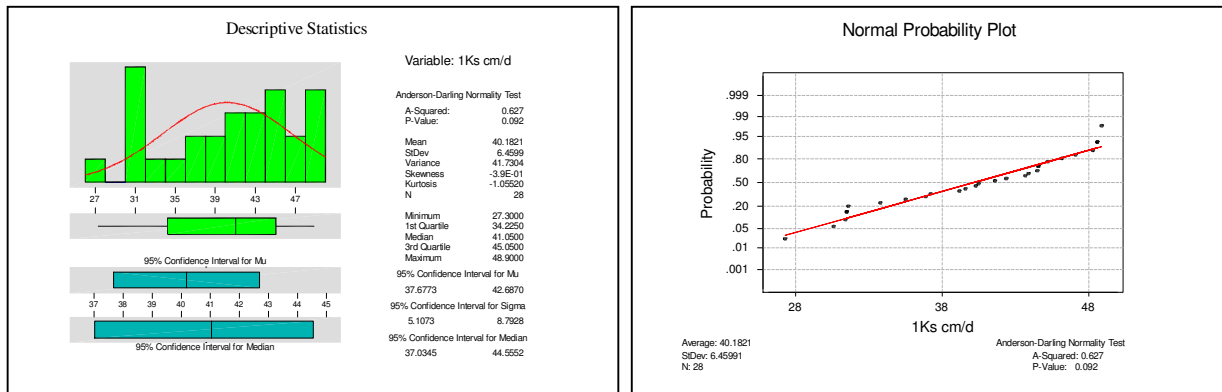




6.1.3.2. Saturated hydraulic conductivity

28 saturated hydraulic conductivity (Ks) tests were done using the inverse augur hall method (see chapter 4) in the upper field across the east west and south north transects. As it can be seen in the saturated hydraulic conductivity results, soils in the upper field are excessively drained to well drained. The general trend of variations in Ks is more pronounced along the south-north direction with decreasing rate. Ks is negatively correlated with ETa and positively correlated with bulk density at the lower soil horizon (Bd_40-50cm) at 95% confidence interval. The data set is normally distributed (table 5) with mean 40.18 cm/day and median 41.05cm/day.

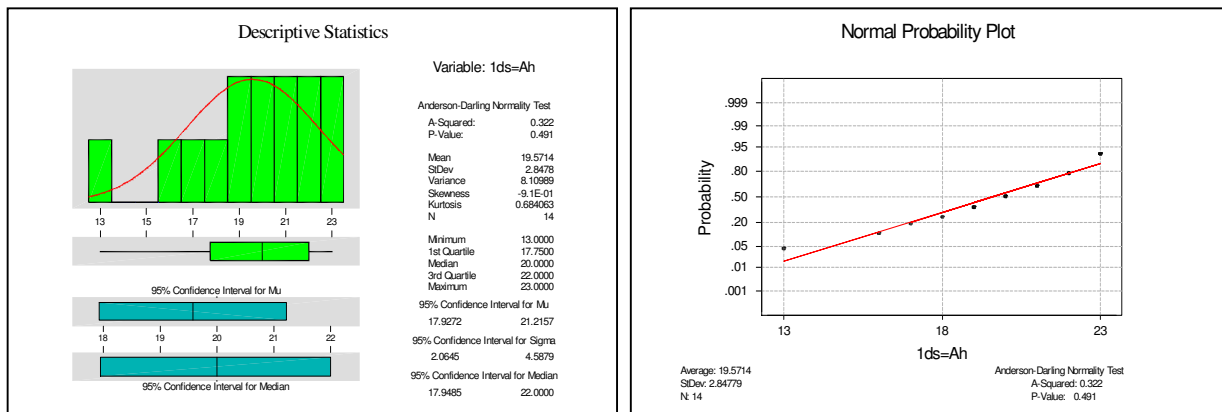
Descriptive statistics and normal probability plots (fig.29.5)_Ks.



6.1.3.4. Soil profile

The soil thickness variations (Ah) observed among the 14 observation points are normally distributed with mean 19.57 and median 20 cm. The Analysis shows that of the Ah horizon thickness and ETa was positively correlated at 95% confidence level. Wheat transpiration in the upper less steeper, with relatively thicker soils were greater than those of lower portion of the field with

Descriptive statistics and normal probability plots (fig.29.6)_Ah.

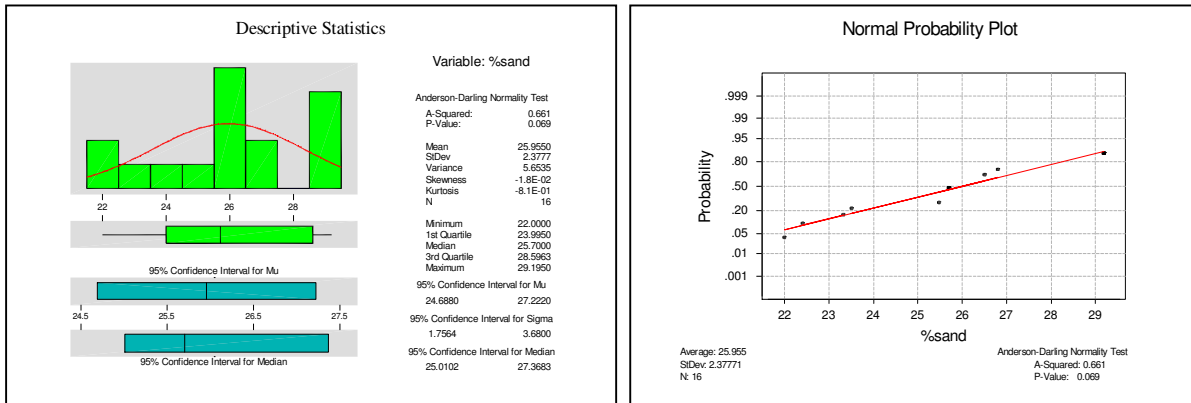


soils of higher slopes and relatively thinner A horizon thickness. The better transpiration (crop response) with the soils of thicker A_h horizon in the upper portion of the field can be partly attributed to the soil uniformity and better water- and nutrient-holding capacity compared with the lower soils.

6.1.3.5. Texture

Percentage of sand by weight of 16 mixed soil samples was determined to compare the relationship of soil texture with ETa patterns. The analysis result shows that there is a significant positive correlation with the bulk density at 95% confidence interval.

Descriptive statistics and normal probability plots (fig.29.7)_%sand.



6.1.3.6. Topographic effects

The slope steepness variations (slope%) observed among the 15 samples are normally distributed with mean 6.67 and median 6 percent. The Analysis shows that the slope steepness was negatively correlated with topsoil depth (A_h) and ETa at 95% confidence interval. Wheat transpiration in the upper less steeper and relatively thicker soils were greater than those of lower portion of the field with soils of steeper slopes and relatively thinner A horizon thicknesses. The better transpiration (crop response) with the soils of gentle slope and thicker A_h in the upper portion of the field can be partly attributed to the soil uniformity and better water- and nutrient-holding capacity compared with the lower soils.

Descriptive statistics and normal probability plots (fig.29.8)_slope%.

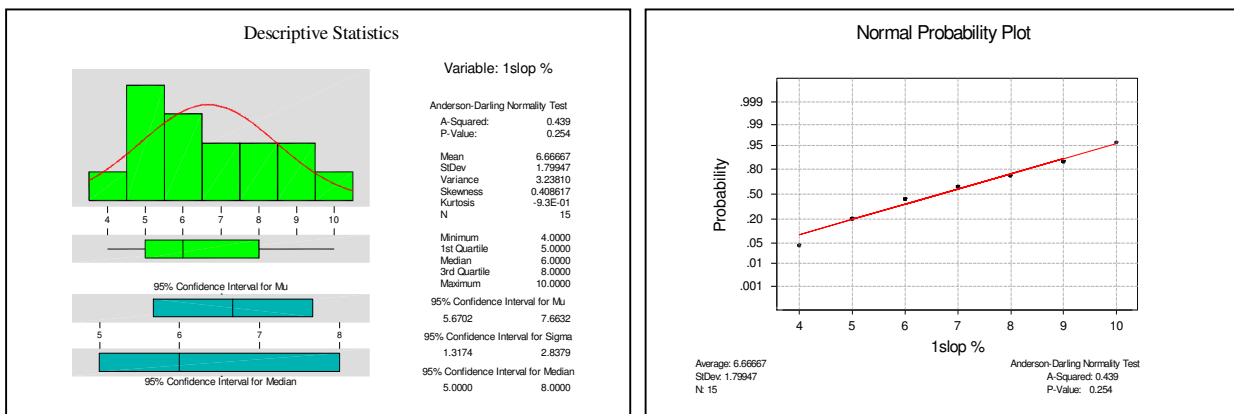


Table 8 Analysis results of chemical and physical predictors in the upper wheat field at $\alpha = 0.05$

Parameters	Predictor	Depth [cm]	# of Samples	Mean	Median	Anderson-Darling Normality test	
						Normality	P-value
Chemical	Ca	10	29	4.013	4.44	NN	0.014
Chemical	Ca	30	29	2.798	2.97	N	0.063
Chemical	%OM	10	28	8.394	8.43	N	0.394
Chemical	%OM	30	28	7.402	7.22	N	0.161
Chemical	%OM	70	13	4.41	4.54	N	0.563
Chemical	pH	10	99	6.03	6.05	N	0.066
Chemical	pH	30	99	6.24	6.636	N	0.199
Chemical	EC	10	99	808	789	N	0.343
Chemical	EC	30	99	667	526	NN	0.007
Chemical	Na	10	29	2.562	2.74	NN	0.029
Chemical	Na	30	29	3.367	3.24	NN	0.013
Chemical	Mg	10	29	0.6397	0.67	N	0.129
Chemical	Mg	30	29	0.488	0.53	N	0.103
Chemical	K	10	29	7.329	7.52	N	0.109
Chemical	K	30	29	5.705	5.93	NN	0.01
Chemical	Ca:Mg_10	10	29	6.1872	6.01	N	0.068
Chemical	Ca:Mg_30	30	29	4.9793	4.8	NN	0.014
	ETa	--	99	3.585	3.58	N	0.164
Physical	ds [Ah]	--	14	19.57	20	N	0.491
Physical	slope%	--	15	6.67	6	N	0.254
Physical	Bd	20-30	15	0.928	0.9	N	0.193
Physical	Bd	40-50	15	1.067	1.06	N	0.942
Physical	Ks	--	28	40.18	41.05	N	0.092

Table 9 Analysis results of log transformed chemical and physical predictors in the upper wheat field at $\alpha = 0.05$

Parameters	Predictor	Depth [cm]	# of Samples	Mean	Median	Anderson-Darling Normality Test	
						Log transformed Values	P-value
Chemical	Ca	10	29	-1.10E-01	-5.00E-02	NN	0.03
Chemical	EC	30	99	2.807	2.81	N	0.249
Chemical	Na	10	29	-6.00E-01	-5.68E-01	NN	0.04
Chemical	Na	30	29	-4.80E-01	-4.90E-01	NN	0.018
Chemical	K	30	29	-2.50E-01	-2.36E-01	N	0.08
Chemical	Ca:Mg_30	30	29	0.678	0.68	N	0.13

Where N=normally distributed
 NN=not normally distributed

6.1.4. NDVI and altitude (upper field)

Correlations: 1ETa [mm/d], 1NDVI_gr, 1Elv masl
 1ETa [mm 1NDVI_gr
 1NDVI_gr 0.947
0.000
 1Elv mas 0.887 0.895
0.000 0.000

Cell Contents: Pearson correlation including P-Value

The correlation analysis above indicates that there is significant positive correlation between the response variable ETa, elevation, and NDVI at 95% confidence Interval (underlined figures)

6.2.Lower field.

6.2.1 Sampling scheme

Similar to the upper field Geo-referenced data obtained on the lower study fields included soil pH, electrical conductivity, soil moisture content, saturated hydraulic conductivity, bulk density, topographic elevation, and a number of soil properties.

Soil sampling was conducted on a 120-m grid in September of 2001, on a matured wheat field. An Auger was used to collect soil samples ranging from 10 to 45 centimeters depth. Three soil cores obtained within 1-m radius of each geo-referenced sampling position were combined, oven dried and analyzed for pH, electrical conductivity and bulk density in Sulmac lab. Where other samples were taken to The Netherlands for further analysis of standard soil properties such as %OM, soluble cations, e.t.c.

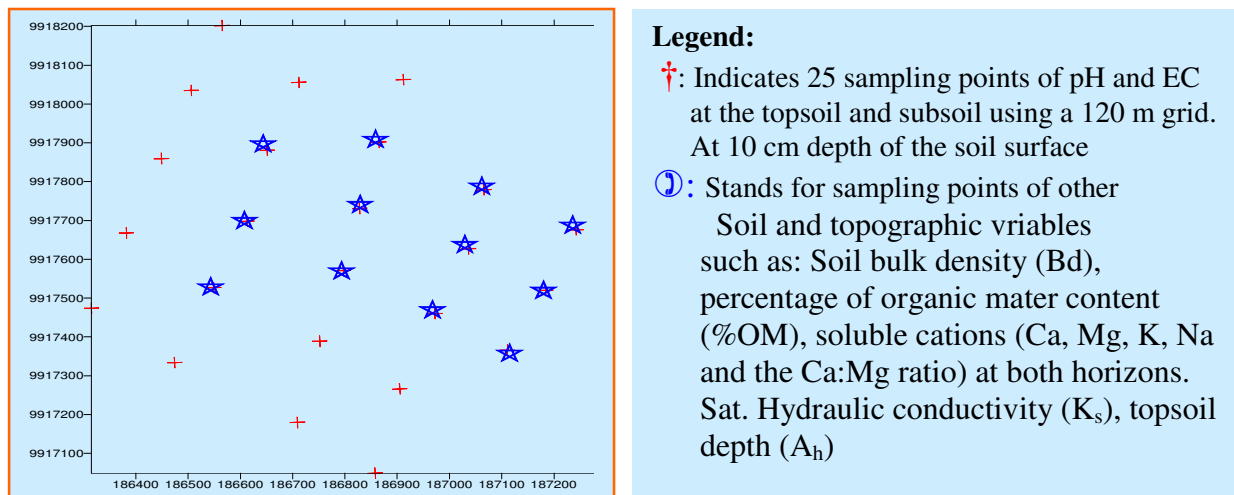
25 sampling positions were chosen in the lower wheat field based on a combined grid and evapotranspiration pattern based on grid tuned by the variation in topographic variations.

Among the 25 sampling positions distributed along the topographic and observed three ETa patterns 12 locations aligning across the small valley transect were used as permanent observation points for major soil properties requiring more time and cost.

The sampling points were made to specially concentrated on the two extreme zones of ETa, namely the very high and very low ETa zones consisting of 10 observation points each.

Actual evapotranspiration data for each sampling position were regressed against soil and topographic variables-pH, topsoil depth, elevation, EC, saturated hydraulic conductivity, and bulk density.

Figure 31 Location of sampling points for the lower wheat field



6.2.2. Chemical parameters (lower wheat field)

Similar to the upper field (see section 6.2.1.) because of its importance to wheat growth, most of the field level surveys and laboratory analysis was made on the topsoil. The soil samples used for Chemical analysis are mainly taken from the first 10-30 cm depth.

Correlations: ETa (mm/d), pH_10cm, EC_10cm, %OM_10cm, Ca10 (me/10, K10 (me

Table 10 Correlation (Pearson) of soil chemical variables.

	ETa	pH_10	EC_10cm	%OM_10	Ca_10	K10	Mg10	Na10
pH_10	0.646							
	<u>0.000</u>							
EC_10	0.187	0.377						
	0.371	<u>0.063</u>						
%OM_10	0.303	0.547	0.473					
	0.254	0.028	<u>0.064</u>					
Ca10	0.506	0.644	0.737	0.626				
	<u>0.046</u>	0.007	0.001	<u>0.009</u>				
K10	0.011	0.022	-0.030	-0.299	0.060			
	0.968	0.936	0.911	0.261	<u>0.824</u>			
Mg10	0.562	0.536	0.660	0.639	0.845	0.253		
	<u>0.023</u>	0.032	0.005	0.008	0.000	<u>0.344</u>		
Na10	-0.151	-0.042	0.057	0.072	0.123	-0.624	-0.072	
	0.577	0.877	0.834	0.791	0.651	0.010	<u>0.790</u>	
Ca:Mg	-0.150	0.189	0.161	-0.058	0.286	-0.264	-0.267	0.323
	0.580	0.484	0.552	0.832	0.283	0.323	0.318	<u>0.222</u>

Cell Contents: Pearson correlation

P-Value

The Pearson correlation analysis above indicates that there is significant positive correlation between the response variable ETa and soil chemical predictors (pH, Mg, Ca) at 95% confidence Interval (underlined figures)

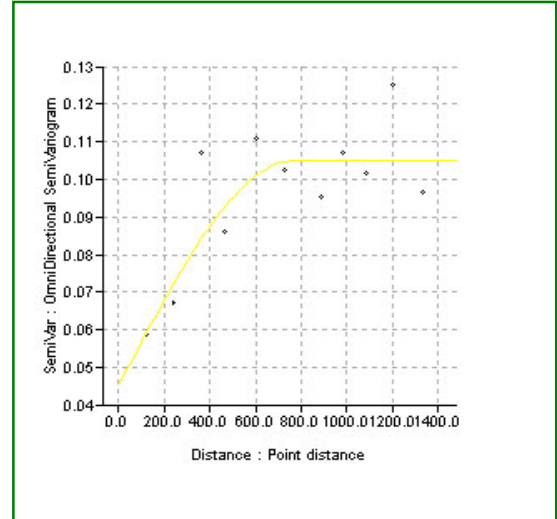
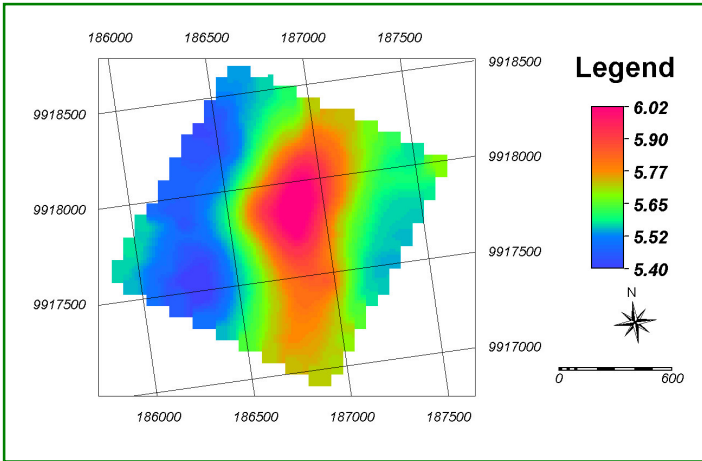
6.2.2.1. Soil pH

The pH measurement was made using the standard FAO guide for 25 samples corresponding to the 25 sampling points. (See chapter 4), at soil depths of 10 and 30 cm. Across the three ETa patterns, the "high ETa " (H ETa), "medium ETa value " (M ETa), and "lower ETa value " the measured pH ranges between 5.24 and 6.34 with a median of 6.06 and mean 6.04 in the upper horizon (at 10 cm depth).

The soil pH variation in the lower soil horizon (at 20-30 cm depth) is normally distributed at 95% confidence interval, in most sampling points pH increases with depth, ranging between 5.84 and 6.6 with a median of 5.64 and mean 5.73 in the lower horizon (at 30 cm depth).

Figure 21. soil pH map lower wheat field (using ordinary Kriging).

L.Field	Model	Nugget	Sill	Range
pH_10	Spherical	0.045	0.105	770



The soil pH variation of the lower wheat field is poorly defined by the above semi variogram, thus the map gives a general trend only.

Plate 2 Partial view of the Lower Kijabe field covered by 112 days old (matured) wheat (October 3, 2001)



Figure 32 Descriptive statistics and normal probability plots for the lower field samples
Descriptive statistics and normal probability plots (fig.32.1)_pH.

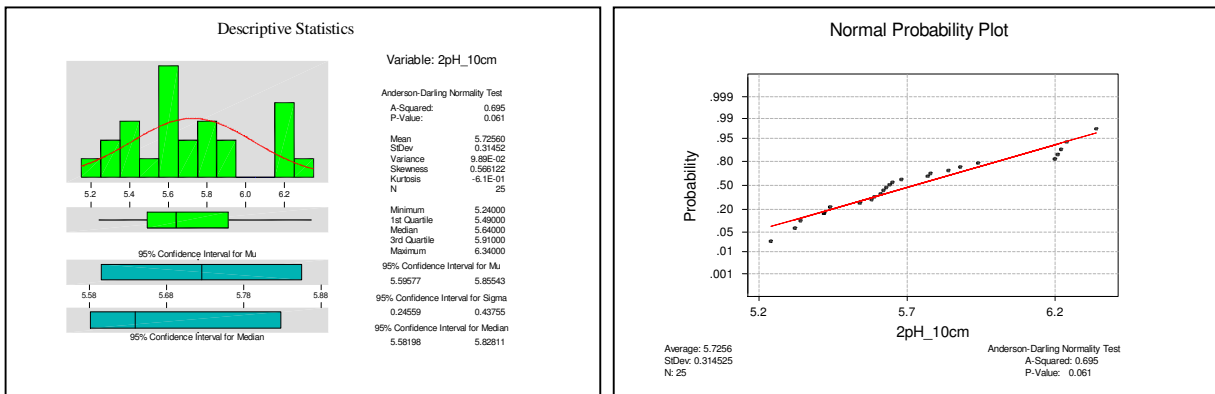
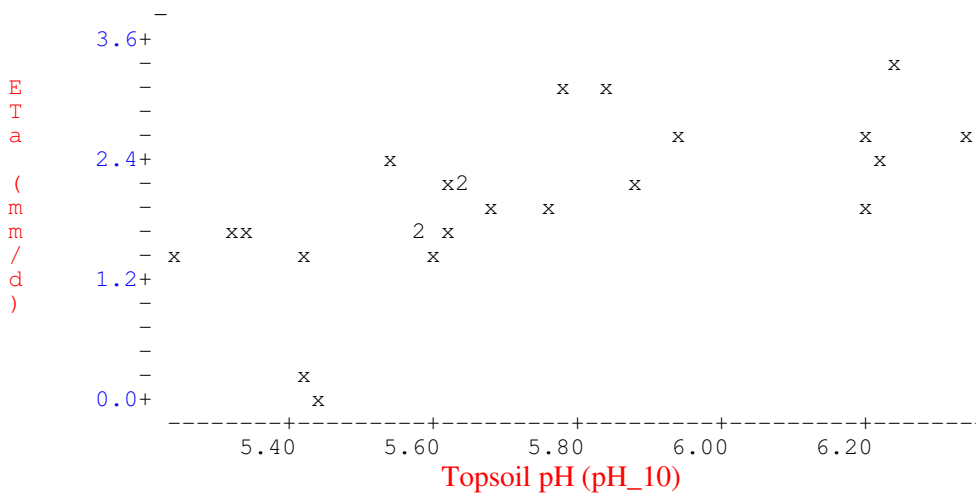
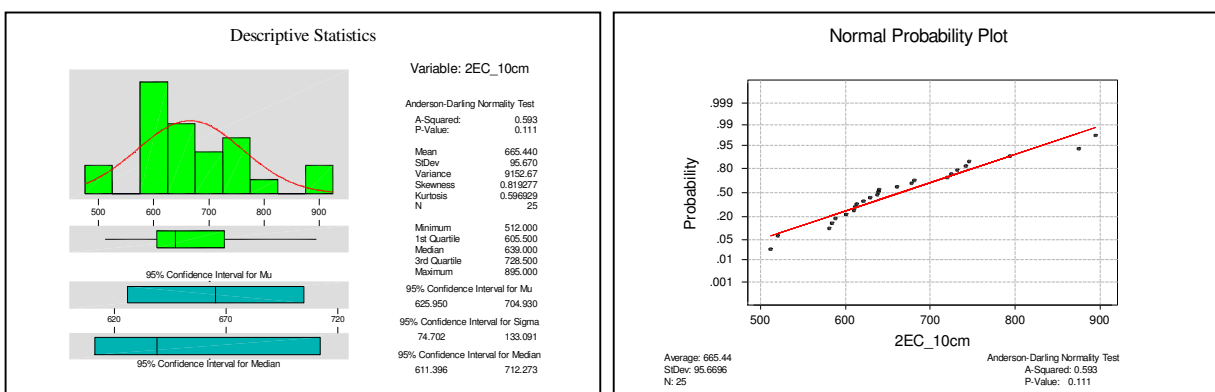


Figure 33 scatter plot of ETa regressed by pH_10 (Lower field)



6.2.2.2. Electrical conductivity (EC)

Similar to the upper field Soil electrical conductivity for the lower field was measured (see chapter 4) in Sulmac laboratory. The distribution of the variable EC_10 is normally distributed at 95% confidence interval. The mean (665.4 μ s/cm) and median (639 μ s/cm) are more or less similar with slightly higher values in the higher ETa zones i.e. the upper middle portion of the field. Descriptive statistics and normal probability plots (fig.32.2)_EC.

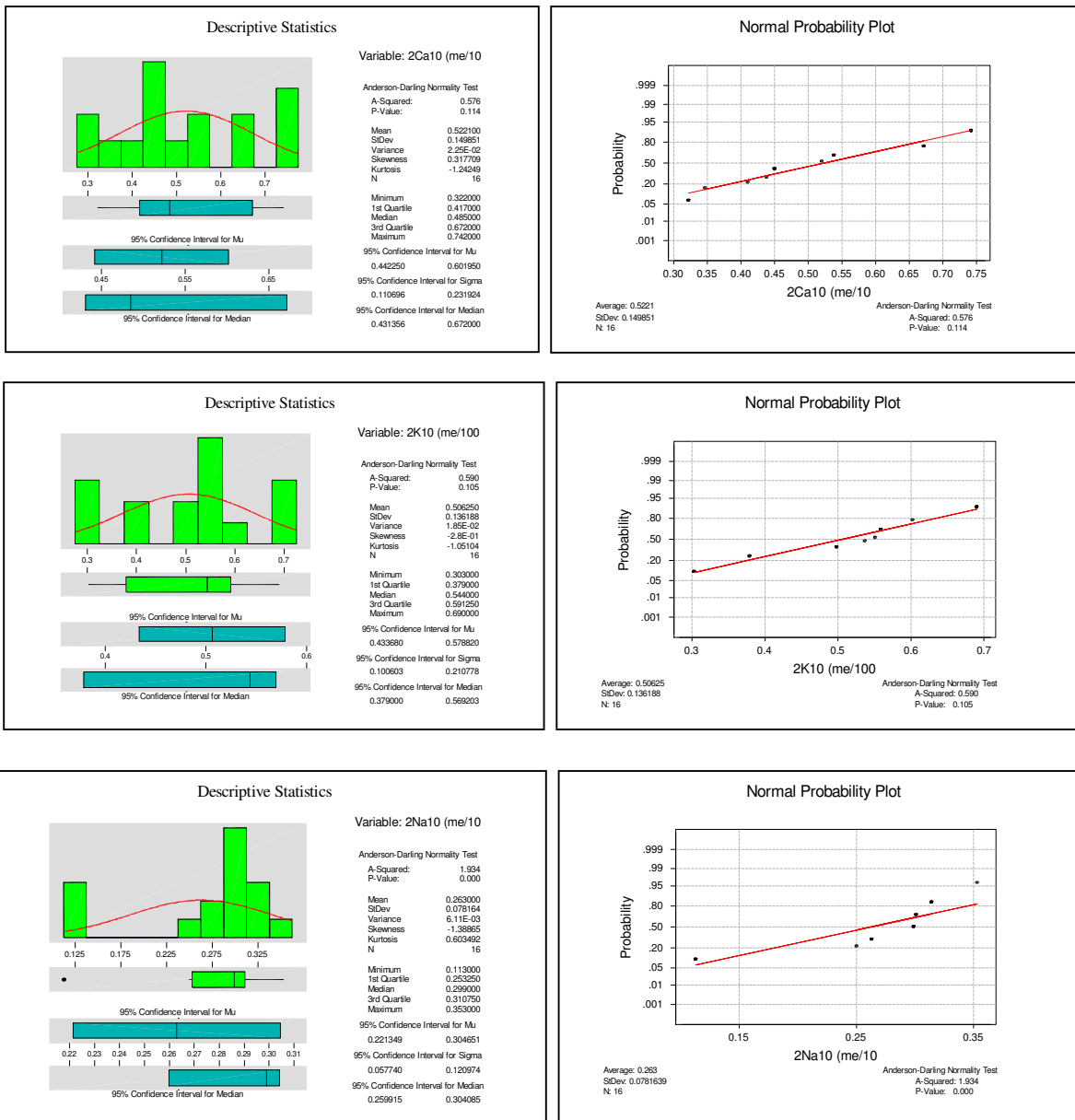


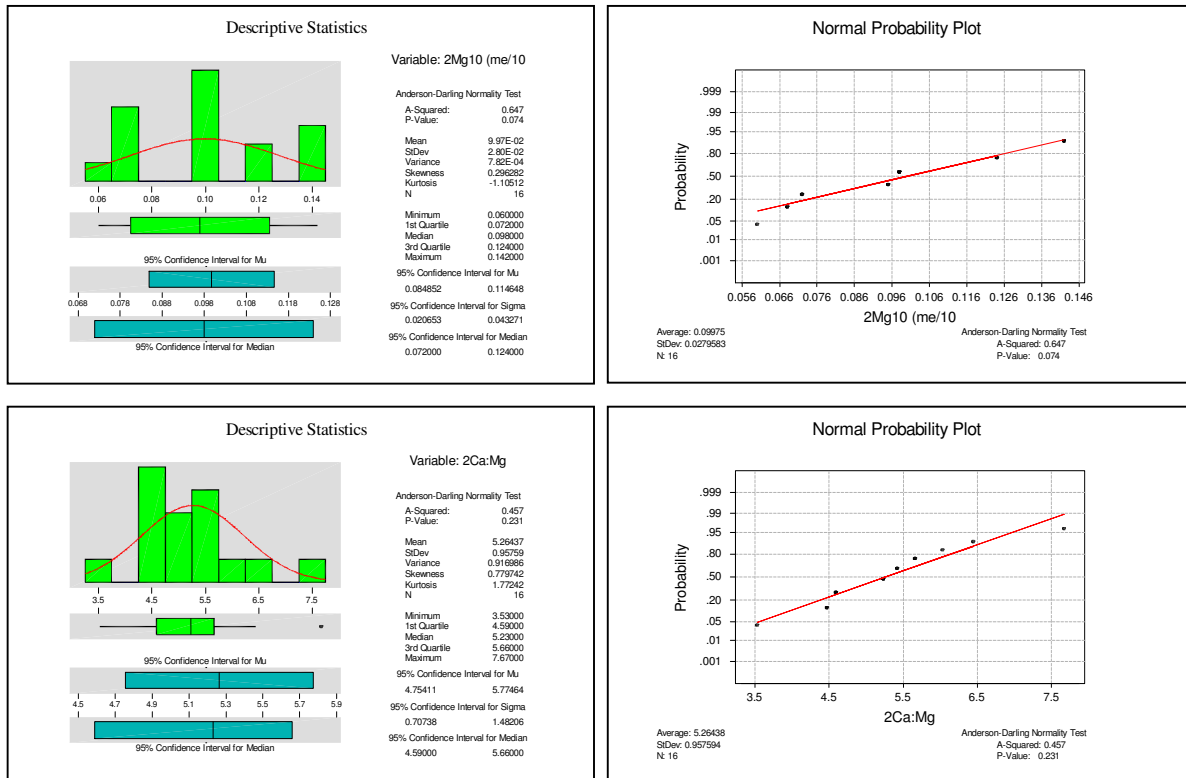
6.2.2.3. Soluble cations (Na, Mg, K, Ca and Ca:Mg ratio)

Similar to the upper field Concentrations of soluble cations were measured in ITC laboratory. Using the ICP-AES method (see chapter 4). Initially the measurements were made in milligram per liter of saturated soil extract (ppm); the results were later converted in to units of me/ 100-gram soil sample. Out of the 16 measured samples the distribution of the variables Mg, Ca, K and Ca:Mg ratio at 10 cm soil depth are normal at 95% confidence interval. Only Na was not normally distributed even after log transformation (see table 13).

In the lower field soluble cation concentrations were not measured for the lower soil horizon i.e. 30 cm.

Descriptive statistics and normal probability plots (fig.32.3)_soluble cations (all).



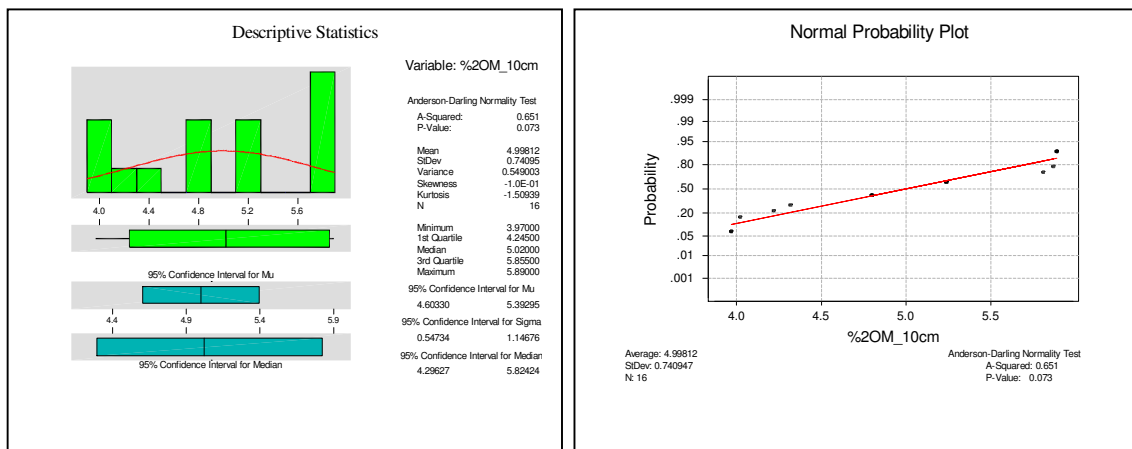


6.2.2.4. Organic matter content

Organic matter content in the soils in the lower wheat field decreases with increasing elevation towards the upper edges of the field, which are highly eroded. Organic matter content of the upper soil horizon (10 cm) in the lower wheat field ranges from 3.97-5.89% (w/w) where the mean is 4.99 and median 5.02.

%OM₁₀ is normally distributed and significantly correlated with Ca and Mg at 95% confidence interval, the correlation of %OM₁₀ with ET_a was unexpectedly insignificant which could be explained by the seasonal water logging effect in the lower portion of the field during the emergence stage of the crop.

Descriptive statistics and normal probability plots (fig.32.4)_%OM.



6.2.3. Physical parameters (lower wheat field)

In this section interpretations and figures of the soil physical data descriptions are given based on the Anderson-darling normality test and Pearson correlations of the measured physical variables with ET_a.

Table 11 Correlation (Pearson) analysis of soil physical Variables

	ETa (mm)	Bd_H1	Bd_H2	Ks [cm/d]	ds=Ah	slop%
Bd_H1	-0.764 <u>0.000</u>					
Bd_H2	-0.493 <u>0.012</u>	0.879 <u>0.000</u>				
Ks [cm/d]	0.527 0.067	-0.785 <u>0.000</u>	-0.893 <u>0.000</u>			
ds=Ah	0.131 0.532	-0.521 <u>0.008</u>	-0.638 <u>0.001</u>	0.437 <u>0.029</u>		
slop%	0.068 0.745	0.364 0.074	0.604 <u>0.001</u>	-0.469 <u>0.018</u>	-0.824 <u>0.000</u>	
%sand	-0.791 <u>0.011</u>	0.879 <u>0.002</u>	0.909 <u>0.001</u>	-0.934 <u>0.000</u>	-0.623 0.073	0.841 <u>0.005</u>

Cell Contents: Pearson correlation P-Value

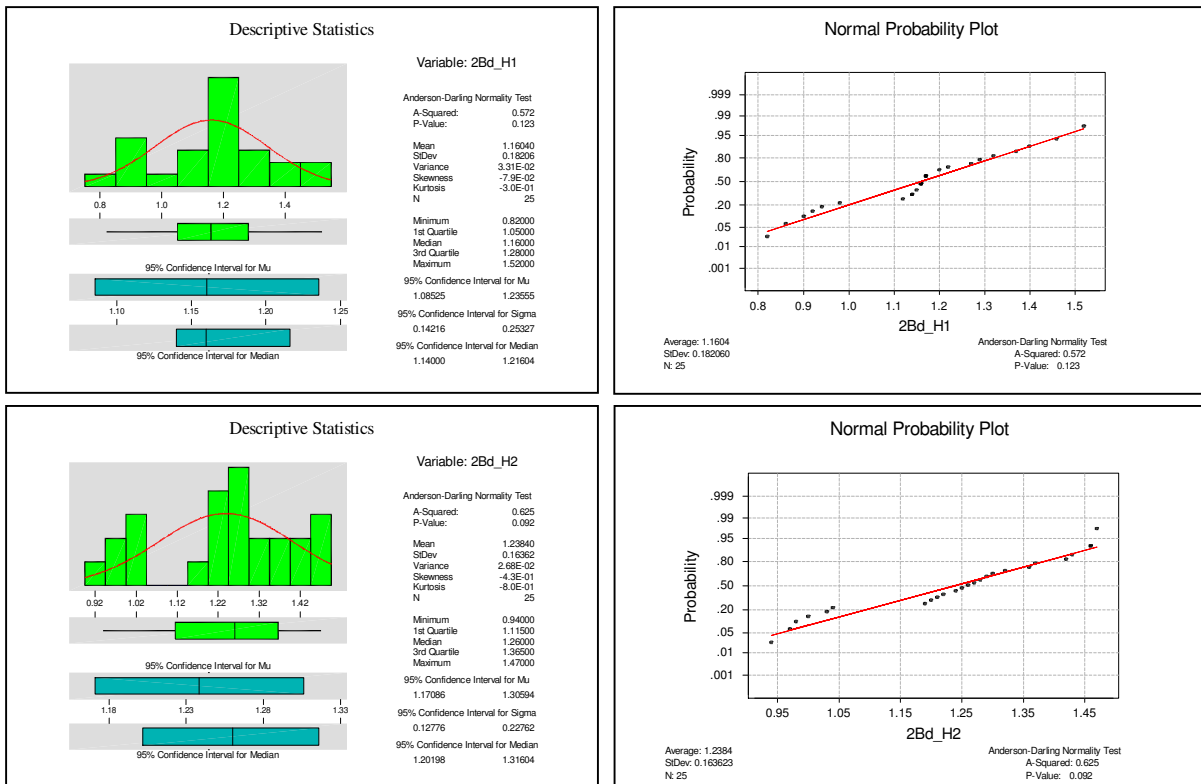
The Pearson correlation analysis above indicates that there is significant negative correlation between the response variable ETa and soil physical predictors (Bd in both horizons and % sand in the upper horizon) at 95% confidence Interval (underlined figures)

6.2.3.1. Bulk density

Similar to upper field, as it is shown in the plot of descriptive statistics the data set of bulk density from both horizons is normally distributed. The bulk density of the upper field is generally very low with values ranging from 0.82-1.52 g/ cm2 in the upper soil horizon (Bd_10-20cm) and 0.94-1.47 g/cm2 in the lower horizon (Bd_40-50 cm).

The Bd results were negatively correlated with %OM and ETa and positively correlated with saturated hydraulic conductivity values at 95% confidence level.

Descriptive statistics and normal probability plots (fig.32.5)_Bd.



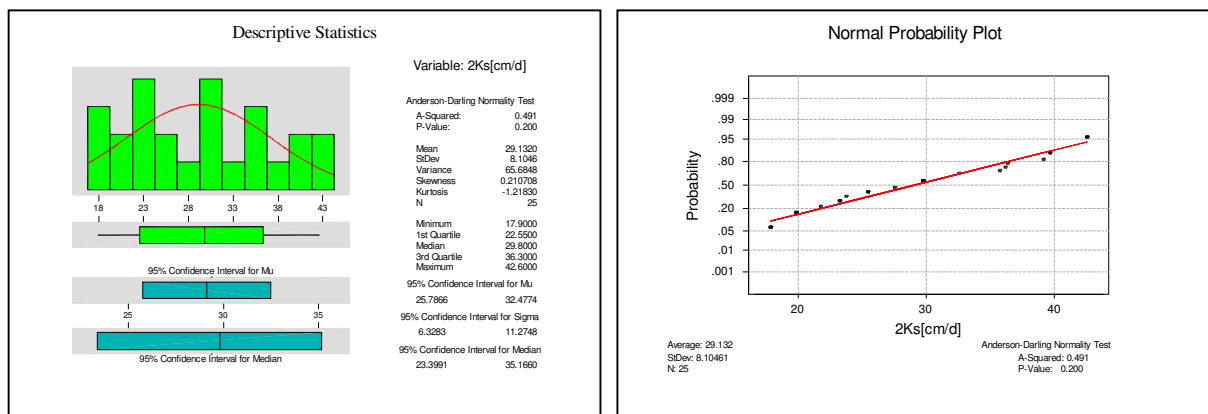
6.2.3.2 Saturated hydraulic conductivity

25 saturated hydraulic conductivity (Ks) tests were done using the inverse augur hole method (see chapter 4) in the lower field across the valley cross section. Soils in the lower field are excessively drained to well drained as it can be seen in the saturated hydraulic conductivity results.

The general trend of variations in Ks is an increased rate of Ks in the lower horizon especially in both elevated portions of the field where the soil type abruptly changes in to a gravely pumic 10-30 centimeters below the hard upper surface.

Ks is negatively correlated with ETa and soil depth (A_h) (at 95% confidence interval. The data set is normally distributed with mean 29.132-cm/day and median 29.8 cm/day.

Descriptive statistics and normal probability plots (fig.32.6)_Ks.

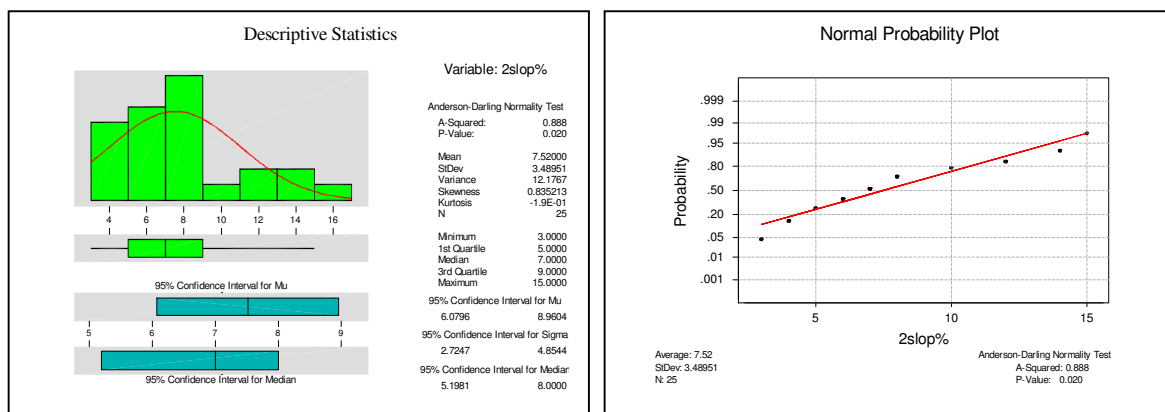


6.2.3.4. Topographic effects

The slope steepness variations (slope%) observed among the 25 samples are not normally distributed even after log transformation. Slope steepness ranges 3-15% with mean 7.52 and median 7 percent. The Analysis shows that the slope steepness was positively correlated with bulk density and negatively correlated with topsoil depth (A_h) at 95% confidence interval.

With the exception of the previously water logged portion of the lower field, Wheat transpiration in the lower alluvial thicker soils was greater than those of upper steeper slopes and relatively thinner A-horizon thicknesses. The better transpiration (crop response) with the soils of gentle slope and thicker A_h in the middle portion of the field can be partly attributed to the soil uniformity and better water- and nutrient-holding capacity compared with the lower soils.

Descriptive statistics and normal probability plots (fig.32.7)_slope%.

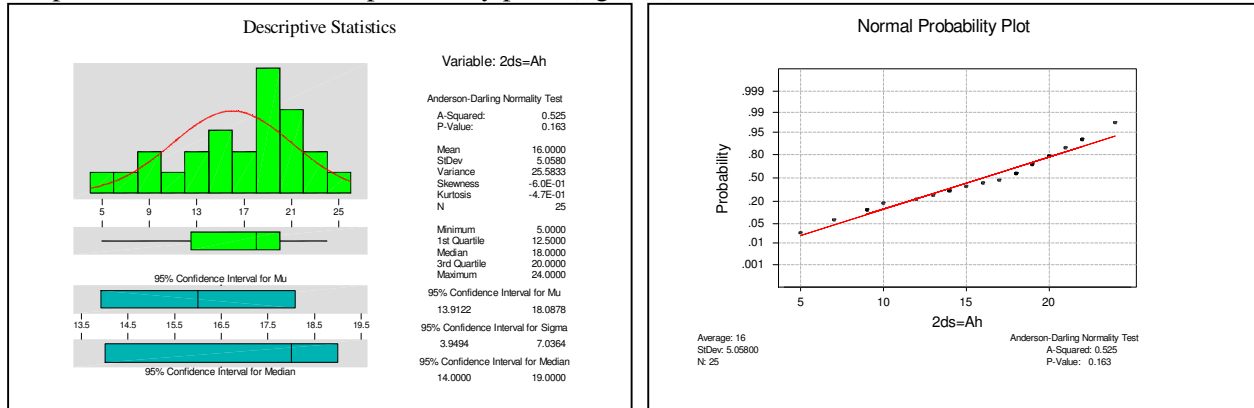


6.2.3.5. Soil profile

The soil thickness variations (A_h) observed among the 14 observation points are normally distributed with mean 16 and median 18 cm. The Analysis shows that the correlation of the A_h horizon thickness and ET_a was not significant which could be explained by the water logging effect in the lower portion of the thick alluvial deposits.

The better transpiration (crop response) with the soils of the remaining thicker gently sloping alluvial deposits of the field can be partly attributed to the soil uniformity and better water- and nutrient-holding capacity compared with the side soils.

Descriptive statistics and normal probability plots (fig.32.8)_Ah.



6.2.3.6. Texture

Percentage of sand by weight of 3 mixed soil samples was determined to compare the over all variation of soil texture with three ET_a patterns. Soil samples were collected from the centers of four randomly selected pixels from each of the identified ET_a patterns and mixed with equal weight before analysis.

The percentage of sand in three mixed soil samples shows that there is a negative correlation with ET_a i.e. the mean sand% of the High ET_a , medium ET_a and Low ET_a pixels is 31.03%, 42.67% and 44.06% respectively.

Descriptive statistics and normal probability plots (fig.32.9)_sand%.

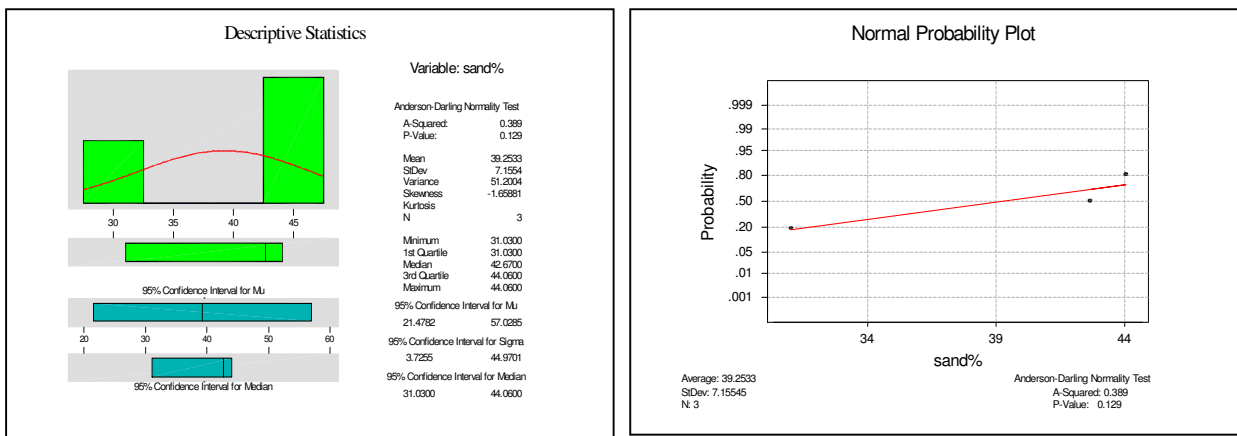


Table 12 Analysis results (summary) of chemical and physical predictors in the lower wheat field at $\alpha = 0.05$

Parameters	Predictor	Depth [Cm]	# Of Samples	Mean	Median	Anderson-Darling	
						Normality test	
						Normality	P-value
Chemical	Na	10	16	2.63	2.99	NN	0
Chemical	Mg	10	16	9.97E-02	0.098	N	0.074
Chemical	K	10	16	5.063	5.44	N	0.105
Chemical	Ca	10	16	0.5221	0.485	N	0.114
Chemical	%OM	10	16	4.998	5.02	N	0.73
Chemical	EC	10	25	665.4	639	N	0.111
Chemical	pH	10	25	2.002	2.03	N	0.61
Chemical	Ca:Mg	10	16	5.2644	5.23	N	0.231
	ETa	--	25	5.6	5.58	N	0.301
Physical	ds [Ah]	--	25	16	18	N	0.163
Physical	slope%	--	25	7.52	7	NN	0.02
Physical	Ks	--	25	29.132	29.8	N	0.2
Physical	Bd_H1	20-30	25	1.1604	1.16	N	0.123
Physical	Bd_H2	40-50	25	1.2484	1.26	N	0.092

Table 13 Analysis results of log transformed chemical and physical predictors in the lower wheat field at $\alpha = 0.05$

Parameters	Predictor	Depth [Cm]	# Of Samples	Mean			
					④	⑥	①
					①	④	⑤
					③	①	⑤
					③	①	⑤

Where N=normally distributed & NN=not normally distributed

6.2.4. NDVI and altitude (lower field)

Correlations: 2ETa (mm/d), 2Elv masl, 2NDVI_gr

2ETa (mm) 2Elv masl
 2Elv masl -0.351
0.085

2NDVI_gr 0.847 -0.427
0.000 0.033

Cell Contents: Pearson correlation including the P-Values

The correlation analysis above indicates that there is significant positive correlation between the response variable ETa and elevation and NDVI at 95% confidence Interval (underlined figures).

The above correlation analysis shows that there is an interrelationship among the various soil physical and chemical parameters, where the relationship of one parameter with the actual evapotranspiration values could at the same time bring about similar values of correlation to the other.

Actual evapotranspiration shows significant correlation with pH, EC, Bd, Ks, as well as calcium and magnesium ions) at 95% confidence interval. The correlation of the bulk density shows a decrease with soil depth from 10 to 40 centimeters. However, unlike to the upper field, ETa doesn't show significant correlation with %OM, slope steepness, topsoil depth (A_h) and other essential cations namely Mg²⁺, Ca²⁺, Na⁺ and K⁺ at 95% confidence interval.

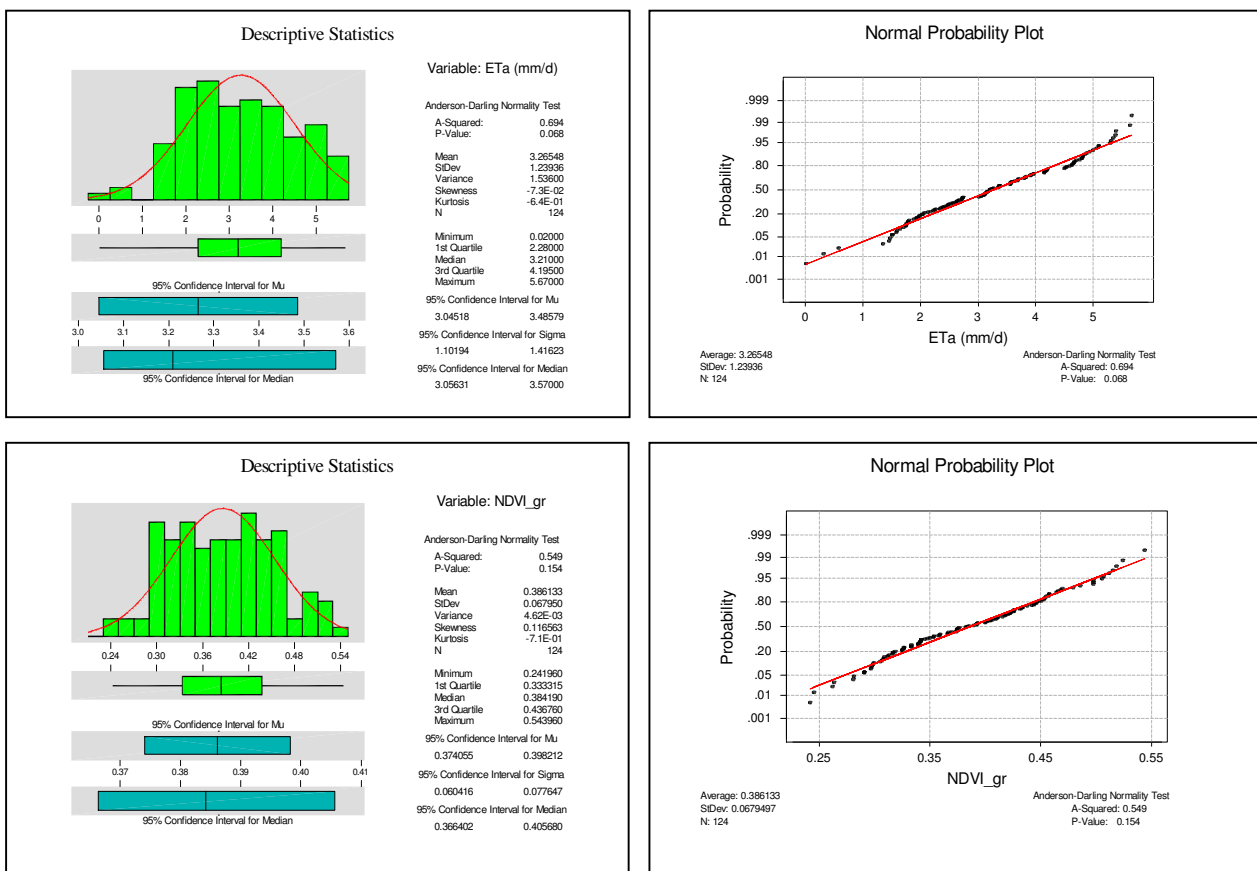
6.3. Mixed data (both fields)

6.3.1. Introduction

In this section the data sets of the two sampling wheat fields are mixed for analysis purposes. Mixed data of both fields is used to visualize the relationship between the uniformly measured soil and topographic parameters and the pixel level ETa values across the two fields.

Similar to the field level (separate) data sets, here mixed data of the two fields is checked for normal distribution before proceeding to the multivariate statistical analysis. Summary of the normality test of each soil and topographic variables is given in a tabulated form (see tables 16-17).

Figure 34 Descriptive statistics and normal probability plots for NDVI and ETa (mixed data).



6.3.2. Chemical variables

In this section the Chemical variables measured in the upper rooting zone (0-10 cm) are used for common type of analysis corresponding to the two fields. As it is shown in the previous sections (sections 6.1 & 6.2) there is a considerable variation of topsoil chemical properties between the two fields.

To mention some; %OM is significantly correlated with ETa in the upper field at 95% confidence interval but not in the lower field and Mg_30 is main ETa predictor in the upper field while an alternative predictor in the lower field (chapter 7). However, correlation result of %OM of the mixed data is highly correlated with ETa (see table 10) and Mg_30 remains as an alternative parameter in the final model.

Table 14 Correlation (Pearson) of chemical variables (mixed data i.e. upper & lower wheat fields)

	ETa	pH_10	EC 10cm	%OM_10	Ca10	K10	Mg10	Na10
pH_10	0.697							
	0.000							
EC 10	0.294	0.298						
	0.001	0.001						
%OM_10	0.774	0.609	0.125					
	0.000	0.000	0.417					
Ca10	0.682	0.639	0.542	0.625				
	0.000	0.000	0.000	0.000				
K10	0.476	0.342	0.445	0.505	0.700			
	0.001	0.021	0.002	0.000	0.000			
Mg10	0.668	0.574	0.572	0.556	0.842	0.641		
	0.000	0.000	0.000	0.000	0.000	0.000		
Na10	-0.002	0.026	0.039	-0.028	0.201	-0.231	0.139	
	0.988	0.865	0.800	0.856	0.185	0.127	0.363	
Ca:Mg	0.120	0.344	-0.101	0.226	0.311	-0.067	-0.019	0.135
	0.432	0.021	0.509	0.140	0.038	0.663	0.903	0.378

Cell Contents: Pearson correlation including the P-Values

6.3.2.1. Soil pH

As it is shown both in the descriptive plots below and the statistical summary tables 16& 17, pH values of the mixed data set are not normally distributed even after log transformation. The variation of the acidity level of the two fields could be explained by the difference in the histories of the two plots i.e. the lower field is one of the oldest and highly eroded plots in the entire Kijabe fields, While the upper field is a recently deforested area, there fore high organic matter replenished by vegetable and plant residue could buffer against potential acidification.

Soil pH is significantly correlated with ETa at 95% confidence interval (see table 14).

Figure 35 Descriptive statistics and normal probability plot of soil pH at 10 cm. (Mixed data)

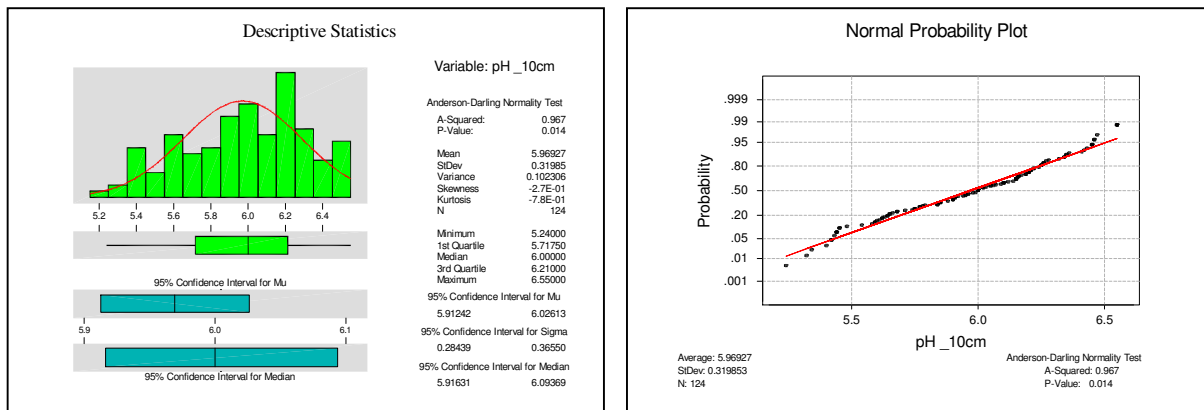
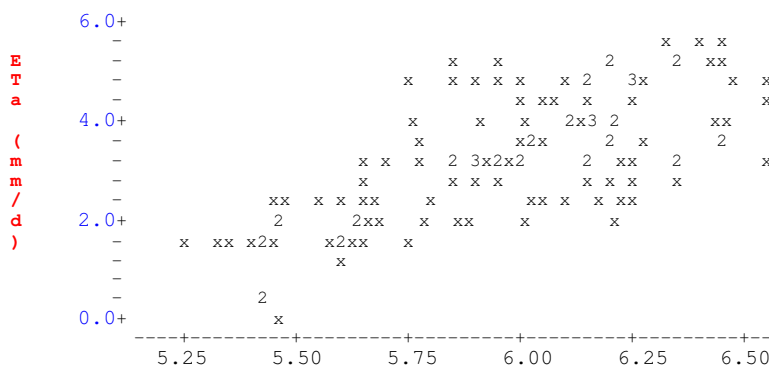


Figure 36 scatterplot of ETa regressed by pH_10 (Mixed field data)



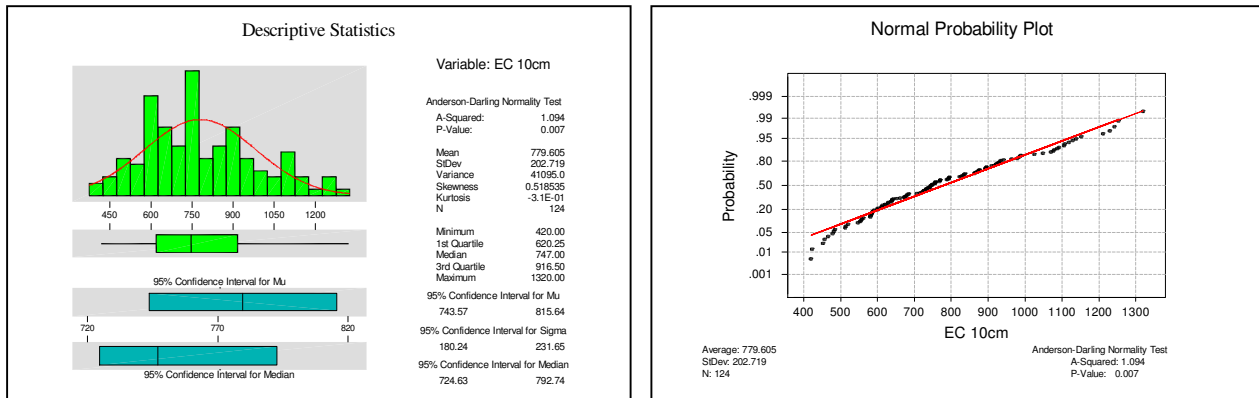
Topsoil pH (pH₁₀) ** pH₁₀ is more operative at lower levels

6.3.2.2 Electrical conductivity (EC)

Similar to pH, the mixed data set of EC for both fields are not normally distributed. Therefore log transformation was performed (see table 17), EC values for the mixed data set showed normality after transformation.

Soil EC is significantly correlated with ETa at 95% confidence interval.

Figure 37 Descriptive statistics and normal probability plot of EC at 10 cm depth (mixed data)



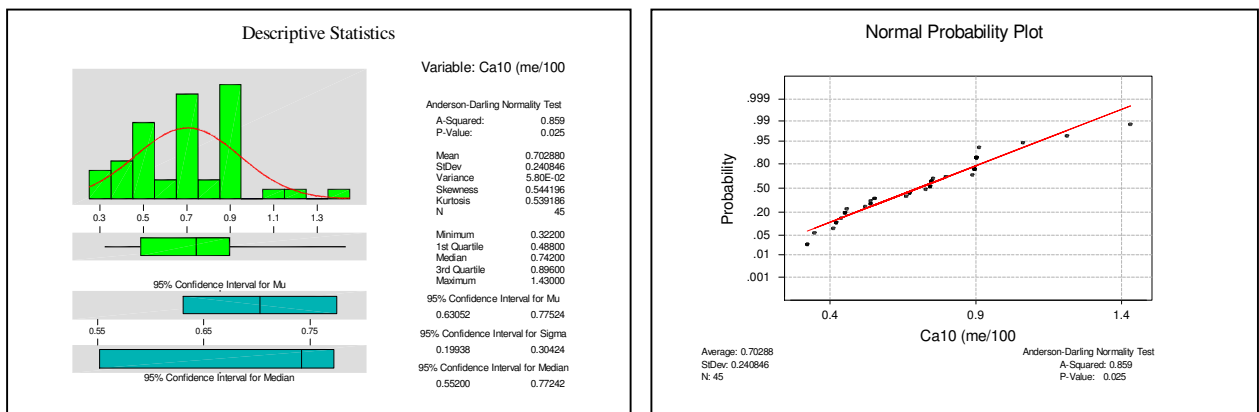
6.3.2.3 soluble cations (Na, Mg, K, Ca & Ca:Mg ratios)

Descriptive statistics and probability plots of mixed values (both upper and lower field) soluble cations in me/ 100-gram soil sample were done (see figure 38) to check the distribution of each variable before proceeding to multivariate and stepwise regression methods.

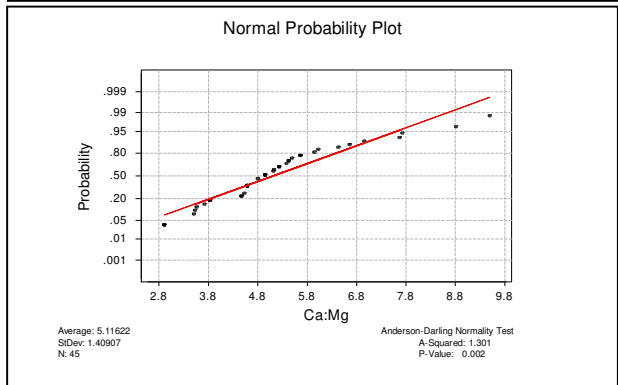
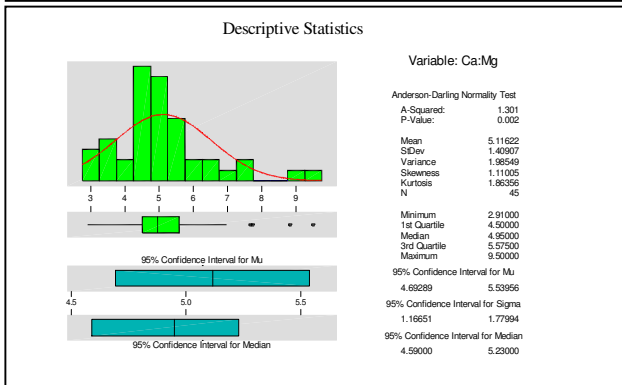
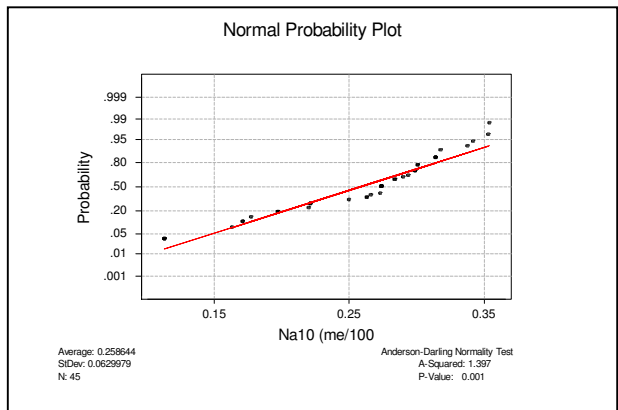
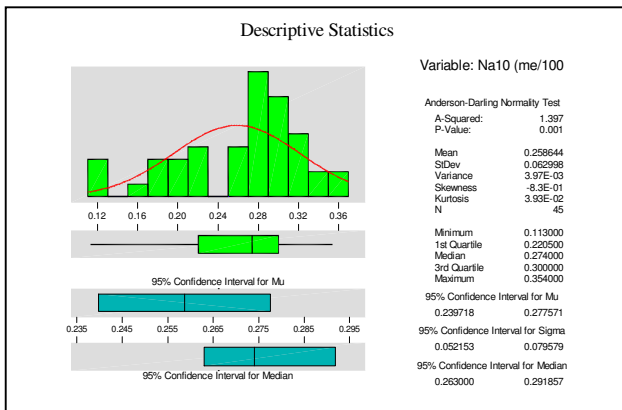
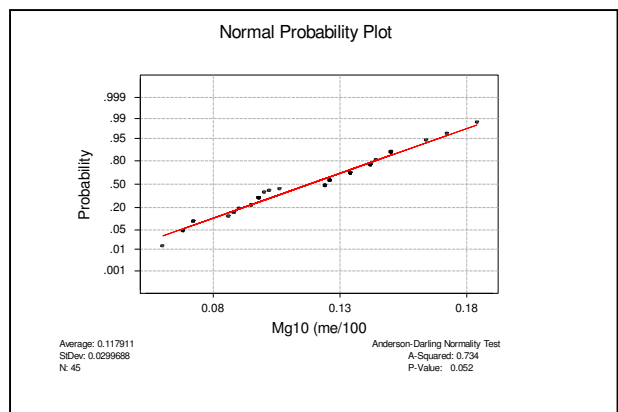
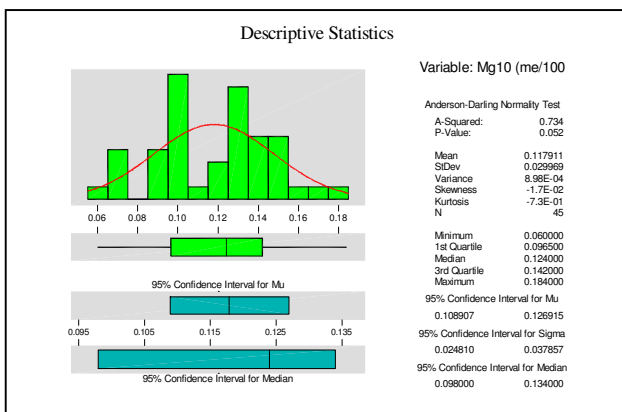
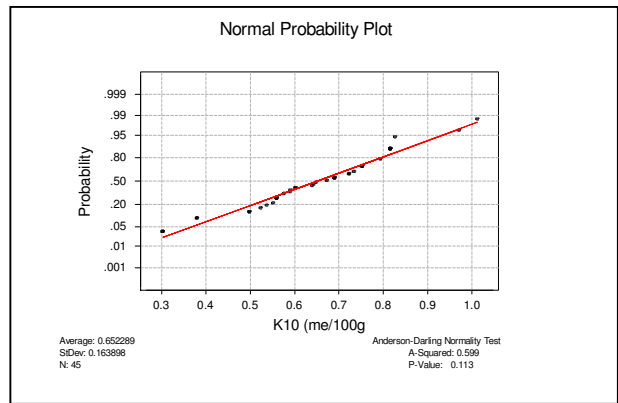
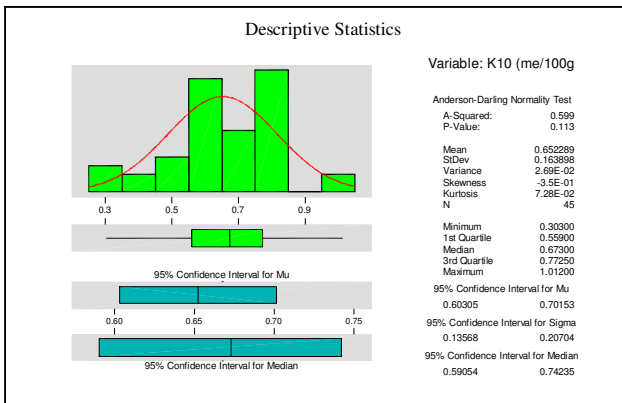
In both fields 45 samples were analyzed for each variable (chapter 4). Except Mg and K data set the distribution of the variables Ca, Na and Ca:Mg ratio are not normally distributed at 95% confidence interval, even after log transformation.

Soluble cations (Ca, Mg and K) are significantly correlated with ETa at 95% confidence interval.

Figure 38 Descriptive statistics and normal probability plots of all soluble cations (mixed data)



(Descriptive statistics & normality plot of soluble cations) Continued ...figure 38.



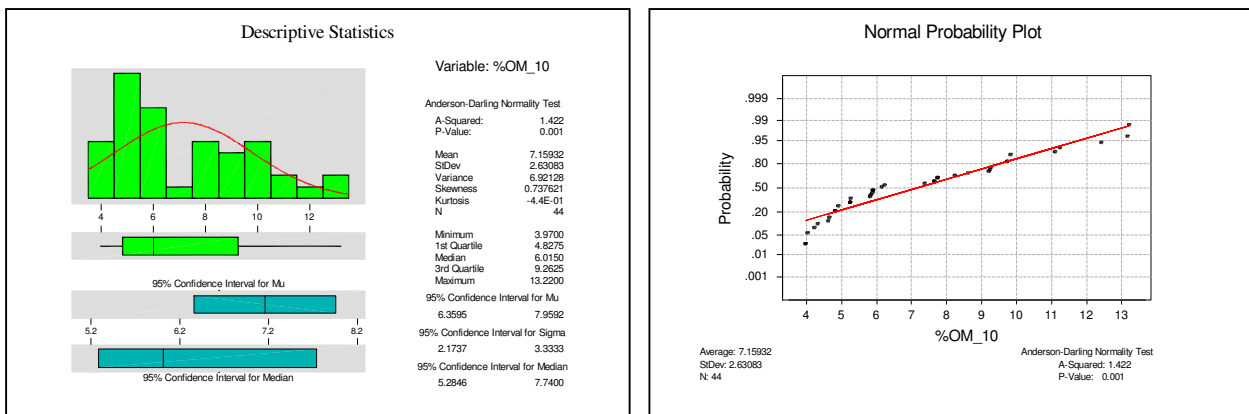
6.3.2.4 Organic matter content

Organic matter content of the soils in both upper and lower fields showed significant variation. According to the previously done farm level soil fertility tests as a general trend organic matter content of the soils decreases with the farm age. The mean and median of organic matter content of soils in the upper field are 8.39 and 8.43 and for the lower field is 4.99 and 5.02 respectively.

As it is shown below (figure 39) the distribution of the mixed data set for the organic matter content of soils at 10 cm depth is not normally distributed even after log transformation. The mean and median of the mixed data set is 7.15 and 6.02 respectively.

Soil %OM is significantly correlated with ETa at 95% confidence interval.

Figure 39 Descriptive statistics and normal probability plot of %OM_10 (mixed data).



6.3.3 Soil Physical variables (mixed data)

Similar to the previous sections, interpretations and figures of soil physical variables as well as descriptions are given based on Anderson-darling normality test and Pearson correlations. of the measured physical variables with ETa.

Table 15 Correlation (Pearson) of physical variables (both fields)

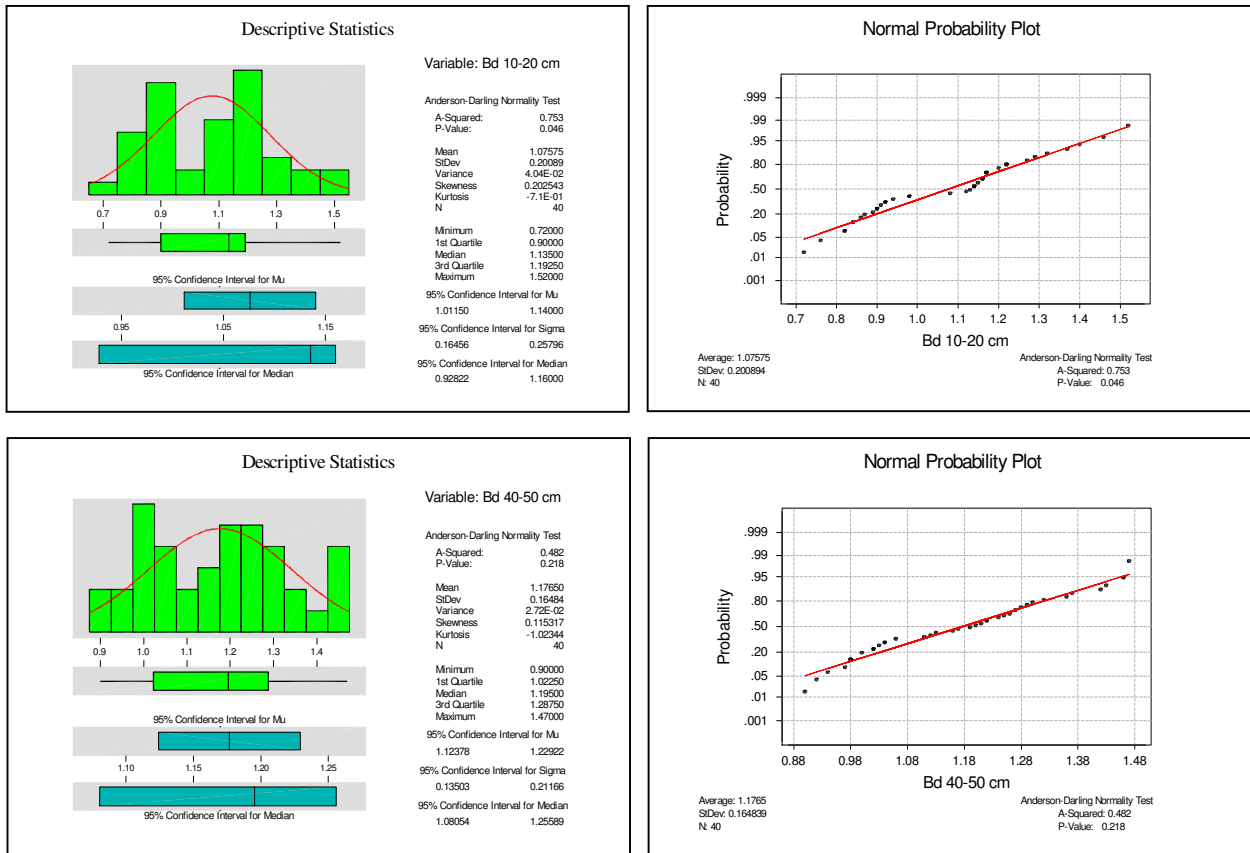
	ET	Bd 10-20	Bd 40-50	Ks .cm/d	ds (Ah)
Bd 10-20	-0.798				
	0.000				
Bd 40-50	-0.627	0.906			
	0.000	0.000			
Ks cm/d	0.178	-0.604	-0.648		
	0.202	0.000	0.000		
ds (Ah)	0.400	-0.558	-0.628	0.446	
	0.012	0.000	0.000	0.004	
slope %	-0.197	0.370	0.529	-0.357	-0.788
	0.224	0.019	0.000	0.024	0.000

Cell Contents: Pearson correlation P-Value

6.3.3.1. Bulk density (Bd)

The bulk density distribution of the mixed data set ranges from 0.72-1.52- g/cm^3 in the upper soil horizon (Bd_10-20cm) and 0.90-1.47 g/cm^3 in the lower horizon (Bd_40-50 cm). The mean and median of the bulk density variables in the upper horizon (Bd_10-20cm) is 1.075 and 1.135 g/cm^3 respectively. Similarly the mean and median of the bulk density of the lower soil horizon (Bd_40-50cm) is 1.177 and 1.195 g/cm^3 Respectively. Soil Bd in both horizons is negatively correlated with ETa and Positively correlated with topsoil depth at 95% confidence interval.

Figure 40 Descriptive statistics and normal probability plot of *Bd* in both horizons (mixed data)



6.3.3.2 Saturated hydraulic conductivity (Ks)

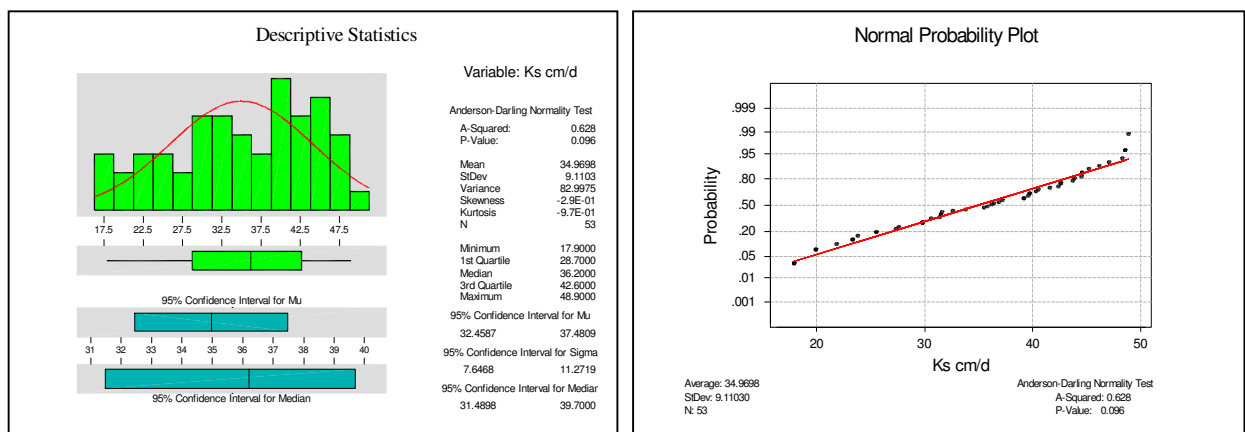
In both fields a total of 53 saturated hydraulic conductivity (Ks) tests were done using the inverse augur hall method (see chapter 4). The rate of saturated hydraulic conductivity is higher in the upper field and generally Ks increases with depth.

Compared to the subsoil (>20 cm depth) Ks is extremely low in the upper part of the soil in the lower field, due to the formation of a very hard silt loam layer. However, the Ks value abruptly increases with increasing depth towards the gravely sandy loam soils.

Ks is negatively correlated with Bd in both horizons at 95% confidence interval.

The data set is normally distributed with mean 34.97-cm/day and median 36.2 cm/day.

Figure 41 Descriptive statistics and normal probability plot of Ks (mixed data)

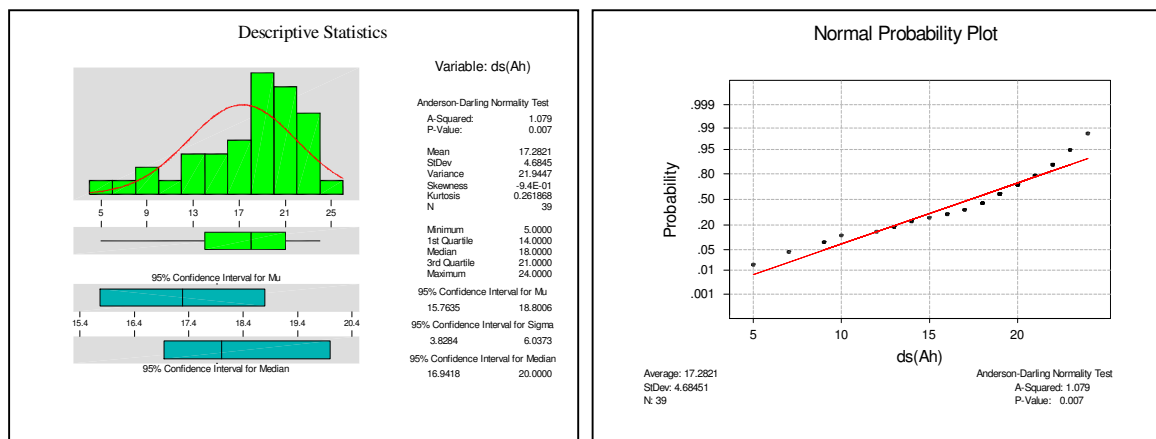


6.3.3.4. Soil profile

As it is shown in the descriptive statistics (figure 42) because of the higher variation of soil thickness (A_h) between the two fields, two distinct shapes are observed with minimum of 5 and maximum 24 cm. As a result the data (39 observation points) of both fields are not normally distributed even after log transformation (see table 17).

The Analysis shows that A_h horizon thickness is positively correlated with ET_a and K_s , and negatively correlated with bulk density and slope steepness at 95% confidence interval. Better transpiration (crop response) in the soils with relatively thicker topsoil and gently sloping can be partly attributed to the soil uniformity and better water- and nutrient-holding capacity compared with the soils at the side slope.

Figure 42 Descriptive statistics and normal probability plot of topsoil depth (mixed data)

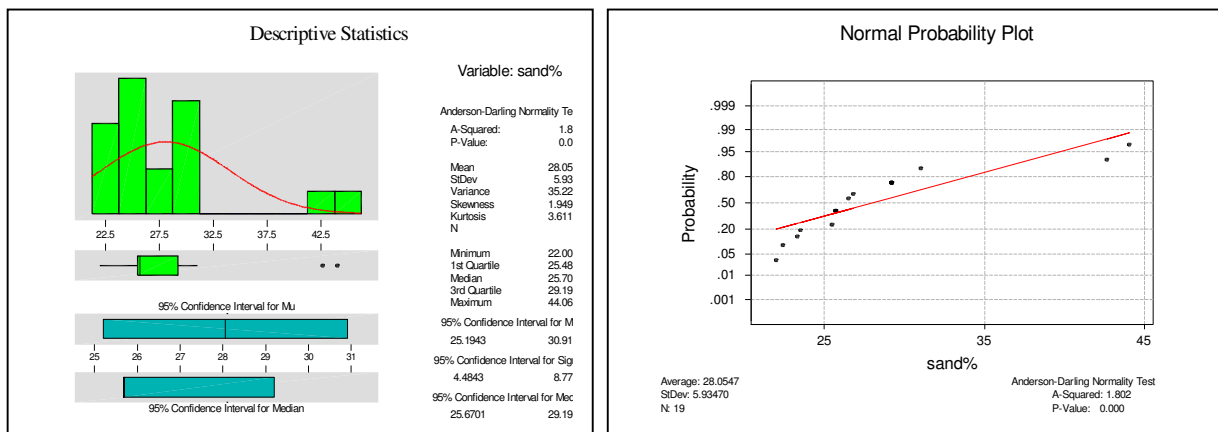


6.3.3.5. Texture

As it was mentioned in the previous field level descriptions percentage of sand by weight, 19 mixed soil samples were determined to compare the over all variation of soil texture along with the observed ET_a patterns. Soil samples were collected from the centers of four randomly selected pixels from each of the identified ET_a patterns and mixed using equal weights before analysis.

The higher percentage of sand in the mixed soil samples corresponds with low ET_a zones of the fields and lower sand percent corresponds with higher ET_a . Higher sand percentages were observed in the subsoil's of the steeper areas of the lower wheat field.

Figure 43 Descriptive statistics and normal probability plot of sand percentages (mixed data)



6.3.3.6. Topographic effects

The slope steepness variations (slope%) observed among the 40 samples are normally distributed with mean 7.2 and median 7 percent. Original slope% data values are not normally distributed; therefore log transformation was necessary.

After log transformation slope% showed normality (see table 17). The Analysis shows that the slope steepness was negatively correlated with topsoil depth (A_h) and K_s and positively correlated with bulk density at 95% confidence interval.

Figure 44 Descriptive statistics and normal probability plot of slope percentages (mixed data)

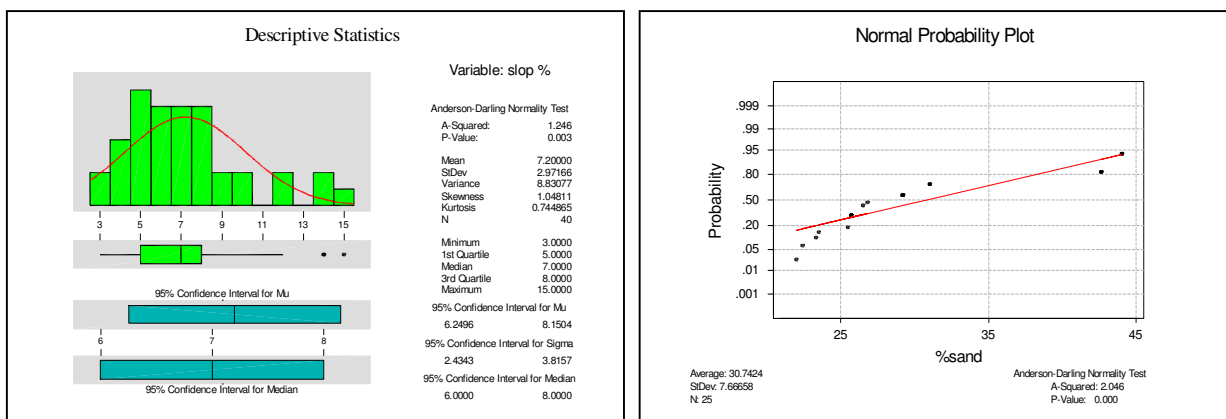


Table 16 Analysis results of chemical and physical predictors in the both wheat fields (mixed) at $\alpha = 0.05$

Parameters	Predictor	Depth [cm]	# of Samples	Mean	Median	Anderson-Darling Normality test	
						Normality	P-value
Chemical	Na	10	45	2.586	2.74	NN	0.001
Chemical	Mg	10	45	0.11791	0.124	N	0.052
Chemical	K	10	45	0.65229	0.673	N	0.113
Chemical	Ca	10	45	3.0457	3.71	NN	0.009
Chemical	%OM	10	44	7.159	6.015	NN	0.01
Chemical	EC	10	124	779.61	747	NN	0.07
Chemical	pH	10	124	5.96	6	NN	0.014
Chemical	Ca:Mg	10	45	5.116	4.95	NN	0.002
	ETa	--	124	3.265	3.21	N	0.068
Physical	ds [Ah]	--	39	17.2821	18	NN	0.007
Physical	slope%	--	40	7.2	7	NN	0.003
Physical	Ks	--	53	34.97	36.2	N	0.096
Physical	Bd_H1	20-30	40	1.075	1.135	NN	0.046
Physical	Bd_H2	40-50	40	1.1765	1.19	N	0.218

Table 17 Analysis results of log transformed chemical and physical variables (mixed data) at $\alpha = 0.05$

Parameters	Predictor	Depth [cm]	# of Samples	Mean	Median	Anderson-Darling (Log transformed data)	
						Normality	P-value
Chemical	Na	10	45	-6.00E-01	-6.60E-01	NN	0
Chemical	Ca	10	45	-1.80E-01	-1.30E-01	NN	0.01
Chemical	%OM	10	44	0.8209	0.77	NN	0.014
Chemical	EC	10	124	2.8775	2.87	N	0.522
Chemical	pH	10	124	0.7756	0.78	NN	0.013
Physical	ds [A _h]	--	39	1.213	1.26	NN	0.001
Physical	Slope %	--	40	0.8336	0.85	N	0.466
Physical	Bd_H1	20-30	40	4.49E-02	0.06	N	0.072

Where N=normally distributed
 NN=not normally distributed

6.3.4. NDVI and altitude

Correlations: ETa (mm/d), NDVI_gr, Elv masl

	ETa (mm/d)	NDVI_gr
NDVI_gr	0.951 <u>0.000</u>	
Elv masl	0.641 <u>0.000</u>	0.611 <u>0.000</u>

Cell Contents: Pearson correlation
 P-Value

The correlation analysis above indicates that there is significant positive correlation between the response variable ETa with elevation and NDVI at 95% confidence Interval (underlined figures)

Chapter 7. Multivariate analysis

7.1. Introduction

Results were obtained by using the following procedure. In the previous section actual evapotranspiration of May 18, 2000 was regressed against 14 soil and topographic variables-Bulk density, pH, EC, soluble cations (Mg^{2+} , Ca^{2+} , Na^+ , K^+ and Ca:Mg ratio), organic matter, topsoil depth, saturated hydraulic conductivity, slope and texture.

The result of the previous regression analysis indicates that there is colinearity among the predictors since some of the parameters are highly correlated among each other, e.g. Slope is highly correlated with topsoil depth and Magnesium and calcium are correlated with pH.

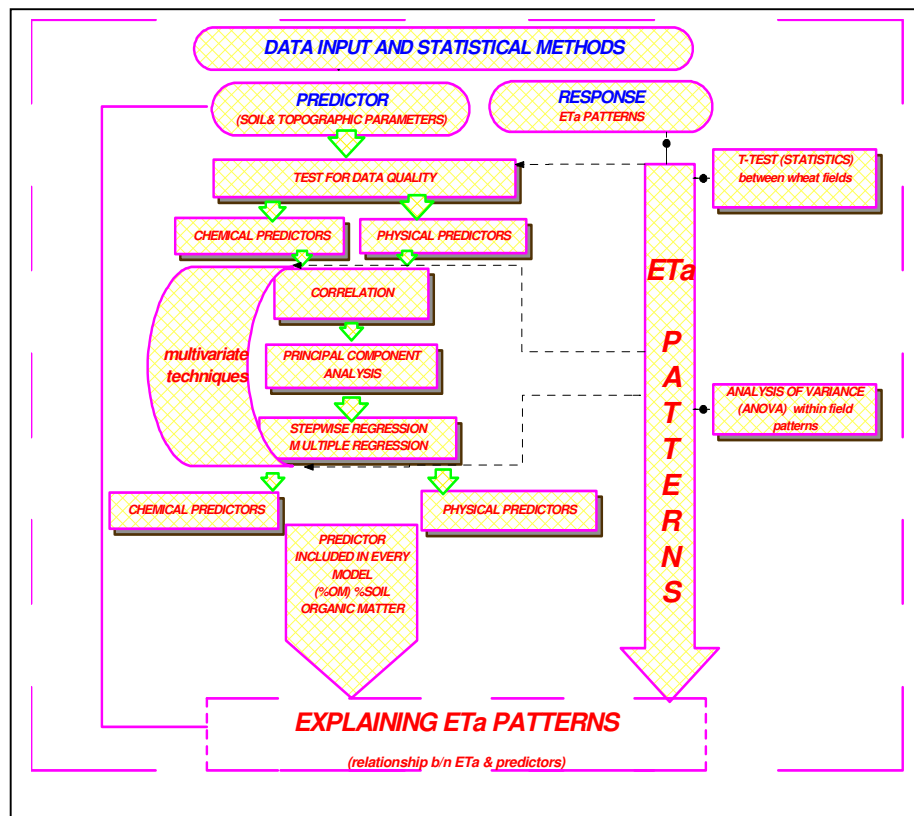
To further guard against over fitting and identify the most dominant predictors affecting ET_a , principal component analysis was used to visualize the relative role of the soil and topographic predictors in determining crop performance, before applying a stepwise regression.

A stepwise regression procedure was followed to analyze the data set using the Minitab software for all the multiple measurements of the predictors to analyze the data covariance structure, reduce the data dimension, and design appropriate data groups for stepwise regression (see figure 45).

Principal component analysis was therefore performed to understand the underlying structure of each data set and form a smaller number of uncorrelated variables (to avoid multi-co linearity in regression),

The data sets of both wheat fields were analyzed individually but they were also grouped. The correlation matrix was used to standardize the measurements. The measurements were standardized since the variables have different units.

Figure 45 Statistical analysis steps (Multivariate statistics)



7.2. Upper wheat field

As it is mentioned in the introductory procedures (section 7.1) in this section, following principal component analysis, actual evapotranspiration was regressed against the chemical, physical and finally combined predictors based on stepwise regression analysis.

7.2.1. Principal Component Analysis

Table 18 Principal component analysis (upper field)

14 cases used 85 cases contain missing values

Eigenvalue	6.1233	3.7195	2.3076	1.4360	1.2639	0.5934
Proportion	0.360	0.219	0.136	0.084	0.074	0.035
Cumulative	0.360	0.579	0.715	0.799	0.874	0.908

Eigenvalue	0.5565	0.3685	0.2505	0.1783	0.1167	0.0516
Proportion	0.033	0.022	0.015	0.010	0.007	0.003
Cumulative	0.941	0.963	0.978	0.988	0.995	0.998

Variable	PC1	PC2	PC3	PC4	PC5	PC6
pH_10c	-0.330	-0.126	-0.136	0.060	-0.118	-0.523
pH_30cm	-0.323	0.018	-0.048	-0.118	0.310	-0.041
EC 10cm	0.025	0.448	0.214	-0.183	0.113	0.011
EC 30cm	0.096	0.348	0.304	-0.340	0.167	0.123
Bd 10-2	0.255	0.304	-0.260	0.007	0.133	-0.112
Bd 40-5	0.174	0.276	-0.400	0.164	0.199	0.143
Ks cm/d	0.082	0.248	-0.186	0.533	0.140	-0.002
ds=Ah	-0.263	-0.005	-0.065	-0.192	0.469	-0.226
slop %	0.316	-0.140	-0.020	0.285	-0.219	0.094
%OM_10	-0.301	-0.130	-0.073	0.089	0.246	0.623
%OM_30	-0.290	-0.180	0.242	0.270	0.091	0.314
Ca10 (m)	-0.269	0.228	-0.269	-0.093	-0.352	0.173
Ca30 (m)	-0.274	-0.008	-0.427	0.035	0.035	-0.117
K10 (me)	-0.207	0.397	-0.008	-0.054	-0.284	0.107
Mg10 (m)	-0.276	0.323	-0.006	0.216	-0.142	0.018
Mg30 (m)	-0.252	0.151	0.336	0.155	-0.337	-0.109
Ca:Mg10	0.038	-0.162	-0.377	-0.490	-0.311	0.251

Variable	PC7	PC8	PC9	PC10	PC11	PC12
pH_10c	-0.110	0.166	0.011	-0.407	0.063	-0.099
pH_30cm	0.550	-0.236	0.082	0.249	-0.286	0.058
EC 10cm	-0.105	0.274	0.039	-0.428	-0.189	0.418
EC 30cm	0.162	-0.037	0.339	-0.256	0.226	-0.325
Bd 10-2	-0.164	-0.321	0.208	0.191	0.095	-0.063
Bd 40-5	-0.244	-0.107	-0.178	-0.002	0.366	0.026
Ks cm/d	0.326	0.627	0.203	0.133	-0.055	-0.069
ds=Ah	-0.537	0.169	0.192	0.312	-0.205	0.108
slop %	-0.192	-0.216	0.481	-0.165	-0.510	0.121
%OM_10	-0.214	0.053	-0.028	-0.219	-0.217	-0.445
%OM_30	-0.028	-0.067	0.235	0.035	0.443	0.559
Ca10 (m)	-0.017	0.088	-0.123	0.052	-0.058	0.037
Ca30 (m)	0.171	-0.263	0.407	-0.349	0.154	0.002
K10 (me)	0.019	-0.150	0.051	0.235	-0.210	0.119
Mg10 (m)	-0.086	-0.194	-0.285	-0.136	-0.108	0.060
Mg30 (m)	-0.217	0.048	0.331	0.293	0.205	-0.354
Ca:Mg10	0.004	0.333	0.249	0.107	0.106	0.127

The *first principal component* has a variance (eigen value) of 6.1233 and accounts for 36 % of the total variance. The coefficients listed under PC1 show how to calculate the principal component scores:

$$PC1 = |-0.330 * pH_{-10}| + |-0.323 * pH_{-30}| + \dots$$

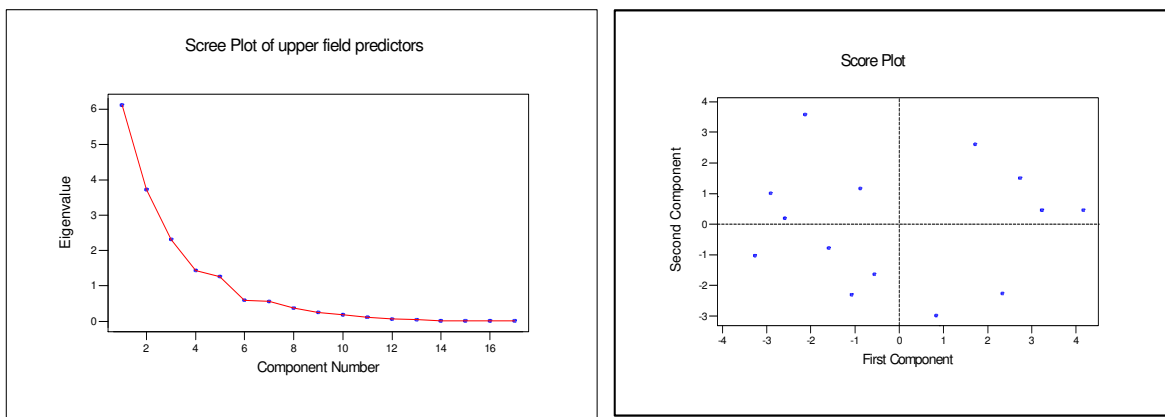
It should be noted that the interpretation of the principal components is subjective, however, obvious patterns emerge quite often. For instance, one could think of the first principal component as representing %OM_10, pH at both horizons and slope% and %OM_30 and Bd_10 to some extent, because the coefficients of these terms have the same sign and are not close to zero.

The *second principal component* has variance 3.7195 and accounts for 21.9 % of the data variability. It is calculated from the original data using the coefficients listed under PC2. This component could be thought of as contrasting level of EC and Mg_10 with K_10 to some extent.

Together, the first two and the first three principal components represent 57.9% and 71.5%, respectively, of the total variability. Thus, most of the data structure can be captured in three or four underlying dimensions. The remaining principal components account for a very small proportion of the variability and are probably less important.

The eigen value (scree) plot provides this information visually. Using pH_10, pH_30, EC_10, EC_30, Bd_20, Bd_50, Ks, slop%, %OM_10, %OM_30, Ca_10, Ca_30, K_10, Mg_10, Mg_30 and Ca:Mg ratio at 10cm depth,

Figure 46 Eigen values and Scree plot (upper field variables)



The above PC analysis shows that among others chemical parameters such as pH, %OM and Magnesium as well as physical parameters such as bulk density are important field parameters, therefore grouping variables with similar properties a better fit of the model with the observed data structure.

7.2.2. Procedures followed in stepwise regression

To perform a stepwise regression the predictors were grouped in to two main categories: namely the chemical and physical soil properties.

Chemical: Ca, Mg, K, Na, OM.

Physical: OM, Bd, Ks, slope, Topsoil depth

Stepwise regression was chosen to simplify the analysis through removing and adding variables and to identify the most useful subset of the predictors in the regression model.

The stepwise information table consists of:

- Alpha-to-Enter, this is the value that determines if any of the predictors not currently in the model should be added to the model.
- Alpha-to-Remove, this is the value that determines if any of the predictors in the model should be removed from the model.
- Summary line, which includes the response name, the number of independent variables or predictors considered, and the number of observations used in the analysis.

For the purpose of screening of the main ETa limiting factors using the stepwise regression method, Alpha-to-Enter and Alpha-to-Remove is considered to be **0.15**. Thus, for each chemical and physical predictor at each step of the procedure, a predictor was added to the model, if it has the smallest p-value among those predictors with p-values less than 0.15. Similarly, at each sequential step of the procedure, a predictor was only removed from the model if it has the largest p-value among those predictors with p-values greater than 0.15.

In this model a subset of 9 Chemical predictors including the response parameter i.e. actual evapotranspiration (ETa), are being used for the first regression step.

Considering the special linkage and effects it has with other soil properties, the *soil organic matter content* is used as a common predictor to be included in every model made in the stepwise regression.

Model selection statistics was performed using the MINITAB statistical software and the result of the stepwise regression analysis for the upper field chemical, physical and combined predictors is displayed in a tabular form below (see table 19-21).

The resulting stepwise table includes statistics that were used for model selection.

The statistics include:

- S, which is an estimate of the standard deviation of the error term in the model. In general, the smaller the S, the better the model fits the data.
- R-Sq, this is the proportion of the variation in the response data. The larger the R, the better the model fits the data.

R-sq was used as a coefficient of determination for the models presented in the table. The coefficient of determination for a model represents the proportion of variation in the response data that is explained by the predictors in the model. It is calculated as the ratio of the sums of squares for regression over the total sums of squares.

R is one of the criteria used to check whether the model fits the data well. However, it was not used as a sole criterion for model selection because R can be made artificially high by simply including too many terms in the model.

- *Adjusted R (Adj. R-sq)*: The adjusted R-value for all the models displayed in the table. The adjusted R is a modified version of R that has been adjusted for the number of predictors in the model. Unlike the R, when a new predictor is introduced into the model, the adjusted R may get smaller. In general, the higher the value, the better the model fits the data.
- *C-p*, which is another statistic for assessing how well the model, fits the data. C-p should be close to the number of predictors contained in the model.

The Mallows' C-p statistic for all the models listed in the table. The C-p statistic is expressed as the summation of the mean-squared errors of the fitted response values divided by the variance of the error term.

For a model with p parameters, the variance portion equals p. A reasonable norm for judging the C-p value of a model is $C-p = p$.

- A C-p much larger than p indicates that the bias is large.
- A C-p below p suggests that the mean-square error of the model being considered is smaller than the mean-square error of the full model.

PRESS: The sum of squares of the prediction errors, where the prediction error for the i^{th} observation is calculated in two steps:

- Fit a regression model without the i^{th} observation. From this model, obtain the predicted value of the i^{th} output, and obtain a fitted value for the response using the model.
- Subtract the predicted value from the response value. This error is a true prediction error with the predicted value being independent of the response. In general, the smaller the PRESS, the better the model fits the data.

- *R-sq(pred)*, which is another R-like statistic that reflects how well the model will predict future data. *Predicted R (R-Sq (pred))*: the predicted R indicates how well the model will fit future data. It is a measure of goodness-of-prediction as opposed to R, which is a measure of goodness-of-fit.

R (predicted) safeguards against over fitting a model, therefore, models were mainly selected according to R (predicted) instead of R, which may be misleading. R (pred) is much better than R (adjusted) for comparing models because it is calculated on observations that are not in the model.

Best alternative predictor table

Alternative predictors are those predictors that are not entered into the model at each step. The best alternative predictors are the alternative predictors with the smallest p-values among all the predictors not included in the model. Based on the given P-values it was possible to decide how many best alternative predictors will be displayed for each step.

The p-values of the best alternative predictors are greater than the p-value of the entered predictor(s), but are the smallest among the predictors not included in the model. The p-value for each best alternative predictor represents how significant the predictor would be if it replaced the entered predictor in the model,

7.2.3. Stepwise Regression (upper wheat field chemical parameters)

Alpha-to-Enter: 0.15 Alpha-to-Remove: 0.15
 Response is ETa [mmd] on 7 predictors, with N = 28
 N(cases with missing observations) = 71 N(all cases) = 99

Table 19 Stepwise Regression of upper wheat plot chemical Parameters

Step	1	2	3
Constant	-1.595	-14.849	-13.139
%OM_10	0.325	0.142	0.222
T-Value	3.04	1.72	2.95
P-Value	0.005	0.097	0.007
%OM_30	0.312	0.197	0.044
T-Value	2.42	2.13	0.47
P-Value	0.023	0.044	0.646
pH_10c		2.61	1.94
T-Value		5.26	4.04
P-Value		0.000	0.001
Mg30 (m			24.7
T-Value			3.06
P-Value			0.006
S	1.02	0.709	0.610
R-Sq	65.64	84.05	88.67
R-Sq(adj)	62.89	82.05	86.70
C-p	51.2	14.0	6.1
PRESS	31.6686	17.0861	12.6065
R-Sq(pred)	58.11	77.40	83.32
best alt.			
Variable	1Mg30 (m		1pH_30cm
T-Value	4.31		1.47
P-Value	0.000		0.156
Variable	1Ca10 (m		1Mg10 (m
T-Value	2.62		1.25
P-Value	0.015		0.224

Fro table 19 the best predictors in the chemical parameters model is indicated in the third step of the model, i.e. predictors with p-value below Alpha 0.15 are percentage of soil organic matter at 10 cm depth, pH at 10 cm depth and soluble magnesium concentration in mill equivalents per 100 gram soil at 30 cm depth.

These statistics was used to compare how well the model fits the data at every step.

The above chemical parameters data indicates that, S and PRESS decreases from step 1 to step 3, R-sq and R-sq (adj) and R_sq(pred) increase from step 1 to step 3, and C-p becomes closer to the number of predictors in the model.

Taken together, these statistics indicate that the step 3 model, containing the predictors **%OM_10**, **%OM_30**, **pH_10** and **Mg_30**, provides a better fit for the data.

For the above chemical parameters data, two alternative predictors were requested:

- At the second step, among the five predictors not included in the model, Mg_30 and Ca_10 were the two best alternative predictors, with p-values of 0.000 and 0.015 respectively.
- At the third (final) step, only four predictors (pH_30, Mg_10, K_10, Ca_10 and Ca_30) are not included in the model. Therefore, pH_30 and Mg_10 were listed as the two best alternative predictors.

7.2.4. Stepwise Regression (upper wheat field physical parameters)

Alpha-to-Enter: 0.15 Alpha-to-Remove: 0.15
 Response is ETa [mm/d] on 7 predictors, with N = 14
 N(cases with missing observations) = 85 N(all cases) = 99

Table 20 Stepwise Regression of upper wheat plot physical Parameters

Step	1	2	3
Constant	-1.222	1.568	7.563
%OM_10	0.21	0.12	0.14
T-Value	1.53	0.96	1.15
P-Value	0.154	0.361	0.281
%OM_30	0.35	0.34	0.04
T-Value	1.37	1.52	0.13
P-Value	0.197	0.160	0.896
slop %		-0.30	-0.26
T-Value		-2.04	-1.96
P-Value		0.069	0.082
Bd 10-2			-4.1
T-Value			-1.76
P-Value			0.113
S	0.972	0.858	0.780
R-Sq	59.16	71.13	78.51
R-Sq(adj)	51.74	62.47	68.96
C-p	4.5	2.8	2.6
PRESS	19.5649	14.2282	13.0353
R-Sq(pred)	23.18	44.13	48.82
best alt.			
Variable	1Bd 10-2	1Bd 40-5	
T-Value		-1.82	-1.74
P-Value		0.098	0.116
Variable	1Bd 40-5	1Ks	cm/d
T-Value		-1.82	-1.36
P-Value		0.099	0.207

The physical predictors model i.e. step three indicates that the predictors with p-value below Alpha 0.15 are **slope steepness** and **bulk density at 10 cm** depth.

The above physical parameters data indicates that, S and PRESS decreases from step 1 to step 3, R and R(adj) and R-sq(pred), increase from step 1 to step 3, and C-p becomes closer to the number of predictors in the model. Taken together, these statistics indicate that step 3 model, containing the predictors **Bd_10** and **slope%**, provides a better fit for the data.

For the above physical parameters data, two alternative predictors were requested:

- At the second step, among the four predictors not included in the model, Bd_50 and Bd_10 were the two best alternative predictors, with p-values of 0.099 and 0.098 respectively.
- at the third step, only three predictors (Bd_50, depth of the Ah and Ks) are not included in the model. Therefore, **Bd_50** and **Ks** were listed as the two best alternative predictors,

7.2.5. Stepwise Regression of upper wheat plot in general (chemical and physical Parameters)

Alpha-to-Enter: 0.15 Alpha-to-Remove: 0.15
 Response is ETa on 6 predictors, with N = 15
 N(cases with missing observations) = 84 N(all cases) = 99

Table 21 Stepwise Regression of the upper wheat plot in general
 (Chemical and physical Parameters)

Step	1	2	3	4
Constant	-1.339	-15.671	-14.179	-7.167
%OM_10	0.198	0.114	0.204	0.227
T-Value	1.36	1.22	2.49	3.26
P-Value	0.200	0.246	0.032	0.010
%OM_30	0.40	0.21	-0.04	-0.27
T-Value	1.48	1.20	-0.25	-1.56
P-Value	0.163	0.257	0.808	0.154
pH_10c		2.73	2.21	1.76
T-Value		4.43	4.17	3.62
P-Value		0.001	0.002	0.006
Mg30 (m			24.7	26.3
T-Value			2.67	3.37
P-Value			0.024	0.008
Bd 10-2				-3.1
T-Value				-2.27
P-Value				0.050
S	1.02	0.638	0.511	0.430
R-Sq	55.77	84.13	90.73	94.10
R-Sq(adj)	48.39	79.80	87.02	90.82
C-p	55.5	16.1	8.5	5.6
PRESS	20.7716	9.27604	6.48544	5.68330
R-Sq(pred)	26.32	67.10	77.00	79.84
best alt.				
Variable		Mg30 (m	Bd 10-2	1slop %
T-Value		2.86	-1.38	-0.65
P-Value		0.015	0.198	0.531
Variable		1Bd 10-2	1slop %	
T-Value		-2.12	-1.06	
P-Value		0.057	0.313	

The general model of *both chemical and physical predictors* in the upper wheat field i.e. step three indicates that the predictors with p-value below Alpha 0.15 are percentage of soil organic matter at 10 cm depth (**%OM_10**), pH at 10 cm depth (**pH_10**), bulk density at 20 cm depth (**Bd_20**) and soluble magnesium concentration in milli-equivalents per 100 gram soil at 30 cm depth (**Mg_30**).

As it is shown in Table 21, S and PRESS decreases from step 1 to step 4, R and R(adj) and R_sq(pred) increase from step 1 to step 4, and C-p becomes closer to the number of predictors in the model. Taken together, these statistics indicate that the step 4 model, containing the predictors **%OM_10**, **Mg_30**, **pH_10** and **Bd_20** provides a better fit for the overall upper wheat field data.

For the above general parameters data, one alternative predictor was requested:

- *At the second step*, among the three predictors not included in the model, **Bd_20** and **Mg_30** were the two best alternative predictors, with p-values of 0.057 and 0.015 respectively.

- *At the third step*, only two predictors (Bd₂₀ and slope% with p-values 0.198 and 0.313 respectively) are not included in the model. Therefore, Bd₁₀ and slope% were listed as the two best alternative predictors.
- *At the final (third) step*, only one predictor (**slope%**) is left as an alternative predictor with p-value of 0.531. as a result slope steepness is considered as the best alternative predictor in explaining the spatial variation of actual evapotranspiration in the upper wheat field.

7.3. Lower wheat field

Similar to the upper wheat field (section 7.2) in this section, actual evapotranspiration was regressed against the chemical, physical and finally combined (both chemical and physical) predictors based on stepwise regression analysis. However, first Principal component analysis was done to visualize the data structure (pattern) in the lower field.

7.3.1. Principal Component Analysis (Eigenanalysis of the Correlation Matrix)

16 cases used 9 cases contain missing values

Table 22 Principal component analysis (lower field)

Eigenvalue	6.9863	2.2379	1.3317	0.9613	0.6657	0.4743
Proportion	0.537	0.172	0.102	0.074	0.051	0.036
Cumulative	0.537	0.710	0.812	0.886	0.937	0.974

Eigenvalue	0.2299	0.0525	0.0355	0.0180	0.0049	0.0018
Proportion	0.018	0.004	0.003	0.001	0.000	0.000
Cumulative	0.991	0.995	0.998	0.999	1.000	1.000

Variable	PC1	PC2	PC3	PC4	PC5	PC6
2pH_10cm	0.254	-0.168	-0.229	-0.520	-0.016	-0.337
2EC_10cm	0.252	-0.101	-0.173	0.620	0.199	0.332
2Bd_H1	-0.343	0.106	-0.001	0.239	0.249	-0.284
2Bd_H2	-0.369	0.001	-0.015	0.078	-0.008	-0.205
2Ks[cm/d]	0.361	-0.043	-0.109	-0.085	-0.252	0.059
2ds=Ah	0.278	0.271	0.300	-0.138	0.401	-0.187
2slop%	-0.278	-0.280	-0.274	-0.297	-0.178	0.330
%2OM_10c	0.342	0.058	0.277	-0.133	0.261	0.017
2Ca10 (m)	0.327	-0.174	-0.317	0.154	-0.016	-0.099
2K10 (me)	-0.098	-0.569	-0.024	0.148	0.199	-0.546
2Mg10 (m)	0.302	-0.335	0.075	0.224	-0.234	-0.135
2Na10 (m)	0.081	0.511	-0.180	0.220	-0.536	-0.422
2Ca:Mg	0.036	0.257	-0.724	-0.072	0.438	-0.022

Variable	PC7	PC8	PC9	PC10	PC11	PC12
2pH_10cm	0.658	0.143	0.004	0.118	0.049	0.036
2EC_10cm	0.407	0.156	-0.293	0.198	0.177	-0.120
2Bd_H1	0.241	-0.125	-0.106	0.194	-0.695	0.248
2Bd_H2	0.034	0.647	0.020	-0.248	-0.096	-0.559
2Ks[cm/d]	-0.069	-0.164	-0.561	-0.450	-0.436	-0.206
2ds=Ah	-0.259	0.455	-0.409	0.060	0.095	0.291
2slop%	-0.264	0.213	-0.324	0.549	-0.123	0.014
%2OM_10c	-0.102	-0.179	0.192	0.446	-0.252	-0.605
2Ca10 (m)	-0.267	0.228	0.294	0.019	-0.237	0.263
2K10 (me)	-0.231	-0.287	-0.270	0.035	0.279	-0.127
2Mg10 (m)	-0.124	0.257	0.293	0.045	-0.189	0.062
2Na10 (m)	-0.077	-0.047	-0.135	0.352	0.159	-0.100
2Ca:Mg	-0.211	-0.083	0.124	-0.117	0.035	-0.136

The *first principal component* has variance (eigenvalue) 6.9863 and accounts for 53.7% of the total variance. The coefficients listed under PC1 show how to calculate the principal component scores:

$$PC1 = |-0.343 * Bd_{10}| + |-0.369 * Bd_{40}| + \dots$$

It should be noted that the interpretation of the principal components is subjective, however, obvious patterns emerge quite often. For instance, one could think of the first principal component as representing mainly physical predictors i.e. bulk density at both horizons, %OM₁₀ and Ks to some extent, since the coefficients of these terms have the same sign and are not close to zero.

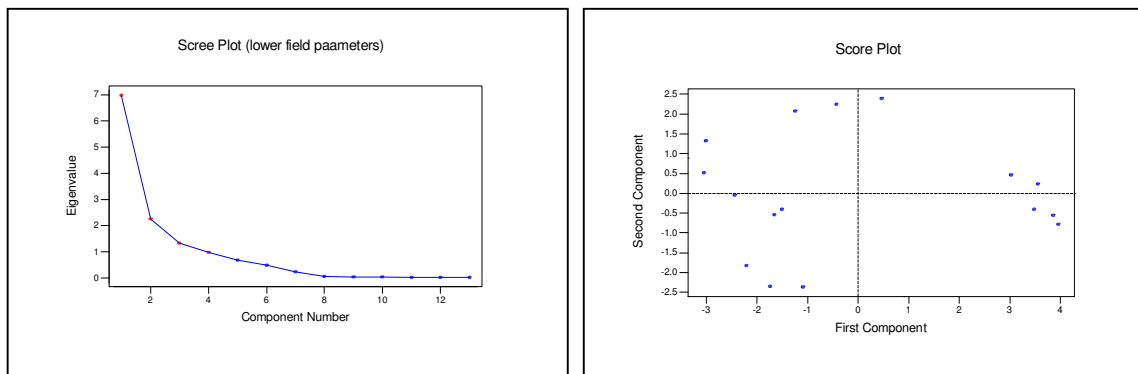
The *second principal component* has variance of 2.2379 and accounts for 17.2 % of the data variability. It is calculated from the original data using the coefficients listed under PC2. This component could be thought of as contrasting level of chemical predictors like K₁₀ and Na₁₀ with Mg₁₀ to some extent.

Together, the first two and the first three principal components represent 71 % and 81.2%, respectively, of the total variability. Thus, most of the data structure can be captured in three or four underlying dimensions. The remaining principal components account for a very small proportion of the variability and are probably less important.

The eigen value (scree) plot (fig.47) provides this information visually,

Similar to the upper wheat plot as it is shown in the correlation matrix (tables 6&7) of chapter 6 and from table 22 it is shown that there is a highly significant correlation among the predictors as well as between the predicted ETa values and the various predictors at 95% confidence interval

Figure 47 Eigen values and Scree plot (lower field variables)



The correlation results indicates that, there is a clear inter-relationship between various predictors which requires further statistical treatment to find out the most important factors limiting the spatial variation of actual evapotranspiration in the lower field. Before performing Standard stepwise regression that provides important indicators/coefficients for determination of appropriate statistical models the data set was reorganized in a suitable subgroups with similar characteristics.

Therefore similar to the upper field Predictors were grouped in to two main categories: namely the chemical and physical soil properties.

1. *Chemical*: pH, EC, Ca, Mg, K, Na, OM
2. *Physical*: Bd, Ks, slope, topsoil depth

Stepwise regression was chosen to simplify the analysis through removing and adding variables and to identify a useful subset of the predictors in the regression model. This procedure was chosen to generate a model by including variables in or excluding variables from the model based on the specified Alpha-to-Enter and Alpha-to-Remove values as it is indicated in section (7.2.2.).

7.3.2. Stepwise Regression

The procedures of stepwise regression are already explained in the previous section (section 7.1.2.)

7.3.2.1 Chemical predictors

Alpha-to-Enter: 0.15 Alpha-to-Remove: 0.15
 Response is ETa (mm/d) on 4 predictors, with N =16
 N(cases with missing observations) = 9 N(all cases) = 25

Table 23 Stepwise Regression of lower field chemical parameters

Step	1	2	3
Constant	0.2265	-9.7194	-7.7001
%OM_10c	0.36	-0.08	-0.34
T-Value	1.19	-0.28	-1.06
P-Value	0.254	0.786	0.308

pH_10cm	2.09	1.73	
T-Value	2.69	2.27	
P-Value	0.018	0.043	
Mg10 (m)		14.0	
T-Value		1.65	
P-Value		0.125	
S	0.868	0.722	0.678
R-Sq	9.17	41.72	52.49
R-Sq(adj)	2.69	32.75	40.61
C-p	9.6	3.8	3.3
PRESS	15.1091	10.8398	9.60501
R-Sq(pred)	0.00	6.73	17.36
best alt.			
Variable	Mg10	Ca10	
T-Value	2.10	0.74	
P-Value	0.056	0.473	
Variable	Ca10		
T-Value	1.69		
P-Value	0.114		

As it is shown in table23 the smaller R and R(adj) and R_sq(pred) values indicates relatively weaker fitness of the chemical predictors in the lower wheat field. The exclusion of the %OM_10 from the model could be an indication of the temporal instability of the yield/ETa patterns in some specific spots i.e. susceptible to water logging, 3 outliers out of 25 total samples with exceptionally low ETa values were included in the data corresponding to the water logged pixels.

The chemical predictors model i.e. step three indicates that the predictors with p-value below Alpha 0.15 are pH and Mg measured in the upper rooting zone.

Table23 shows that, S and PRESS decreases from step 1 to step 3, R and R(adj) and R_sq(pred) increase from step 1 to step 3, and C-p becomes closer to the number of predictors in the model. Taken together, these statistics indicates that the step3 model, containing the predictors **pH_10** and **Mg_10** provides a better fit for the data.

For the above chemical parameters data, one alternative predictor was requested:

•The *third iteration step* indicates that %OM_10 is not included in the model. However, **Ca_10** was selected as best alternative predictor, with p-value of 0.473.

The result of the above stepwise regression of chemical predictors signifies that temporal and spatial stability of actual evapotranspiration cannot be assumed; and spatial stability of evapotranspiration patterns across growing seasons is a big challenge for multiple-year ETa patterns,

7.3.2.2 Physical predictors

Alpha-to-Enter: 0.15 Alpha-to-Remove: 0.15
 Response is 2ETa (mm on 4 predictors, with N = 16
 N(cases with missing observations) = 9 N(all cases) = 25

Table 24 Stepwise Regression of lower field physical parameters

Step	1	2	3
Constant	0.2265	14.4301	7.5085
%2OM_10c	0.36	-1.00	-0.34
T-Value	1.19	-4.47	-1.49
P-Value	0.254	0.001	0.163
2Bd_H1		-6.48	-9.46
T-Value		-7.59	-9.85
P-Value		0.000	0.000
2Bd_H2			5.7
T-Value			3.93
P-Value			0.002
S	0.868	0.386	0.266
R-Sq	9.17	83.29	92.69

R-Sq (adj)	2.69	80.72	90.86
C-p	137.6	17.5	4.0
PRESS	15.1091	2.80062	1.54241
R-Sq (pred)	0.00	75.90	86.73
best alt.			
Variable	2Ks [cm/d		2Ks [cm/d
T-Value	3.45		-1.37
P-Value	0.004		0.195
Variable	2Bd_H2		
T-Value	-2.19		
P-Value	0.048		

The above physical parameters data indicates that, S and PRESS decreases from step 1 to step 3, R and R(adj) and R_sq(pred) increase from step 1 to step 3, and C-p becomes exactly the same as the number of predictors in the model. Taken together, these statistics indicate that the step 3 model, containing the predictors **Bd_10** and **Bd_30** provides a better fit for the data.

For the above physical parameters data, one alternative predictor was requested:

- At the second step, among the three predictors not included in the model, Bd_50, and Ks were the two best alternative predictors, with p-values of 0.048 and 0.004, respectively.
- At the final (third) step, only one predictor (**Ks**) is left as an alternative predictor with p-value of 0.195.as a result saturated hydraulic conductivity is considered as the best alternative physical predictor in explaining the spatial variation of actual evapotranspiration in the lower wheat field.

7.3.2.3. Mixed data

Alpha-to-Enter: 0.15 Alpha-to-Remove: 0.15

Response is ETa (mm/d) on 5 predictors, with N = 16

N(cases with missing observations) = 9 N(all cases) = 25

Table 25 Stepwise Regression lower field of general soil properties
(Chemical and physical Parameters)

Step	1	2	3	4
Constant	0.2265	14.4301	7.5085	1.9742
%OM_10c	0.36	-1.00	-0.34	-0.31
T-Value	1.19	-4.47	-1.49	-1.73
P-Value	0.254	0.001	0.163	0.111
Bd_H1		-6.48	-9.46	-8.79
T-Value		-7.59	-9.85	-11.08
P-Value		0.000	0.000	0.000
Bd_H2			5.7	5.9
T-Value			3.93	5.14
P-Value			0.002	0.000
pH_10cm				0.75
T-Value				2.88
P-Value				0.015
S	0.868	0.386	0.266	0.210
R-Sq	9.17	83.29	92.69	95.83
R-Sq (adj)	2.69	80.72	90.86	94.31
C-p	206.0	30.1	9.6	4.0
PRESS	15.1091	2.80062	1.54241	1.07368
R-Sq (pred)	0.00	75.90	86.73	90.76
best alt.				
Variable	pH_10cm		Mg10 (m)	
T-Value	2.69		1.46	
P-Value	0.018		0.171	
Variable	Bd_50		Mg10 (m)	
T-Value	-2.19		-0.27	
P-Value	0.048		0.795	
Variable	Mg10 (m)			
T-Value	2.10			
P-Value	0.056			

The above general parameters data indicates that, S and PRESS decreases from step 1 to step 4, R and R(adj) and R_sq(pred) increase from step 1 to step 4, and C-p becomes exactly the same as the number

of predictors in the model. Taken together, these statistics indicate that step 3 model, containing the predictors **Bd_10**, **Bd_30** and **%OM_10** provides a better fit for the data.

One alternative predictor was requested to be included in the table:

- At the second step, among the three predictors not included in the model, **Bd_50**, **Mg_10** and **pH_10** were the three best alternative predictors, with p-values of 0.048, 0.056 and 0.018 respectively.
- At the third step, only two predictors **pH_10** and **Mg_10** with p-value of 0.171 and 0.795 respectively were not included in the model.
- At the fourth (final) step, only **Mg_10** appeared as the only alternative predictor, with P-value of 0.917.

7.4. Combined data (both fields)

7.4.1. Principal Component Analysis

Eigen analysis of the Correlation Matrix

30 cases used 94 cases contain missing values

Table 26 Principal component analysis (combined data)

Eigenvalue	6.3918	1.6793	1.3433	1.2649	0.7271	0.5027
Proportion	0.492	0.129	0.103	0.097	0.056	0.039
Cumulative	0.492	0.621	0.724	0.821	0.877	0.916

Eigenvalue	0.3729	0.2296	0.2061	0.1501	0.0863	0.0302
Proportion	0.029	0.018	0.016	0.012	0.007	0.002
Cumulative	0.945	0.962	0.978	0.990	0.996	0.999

Variable	PC1	PC2	PC3	PC4	PC5	PC6
pH_10cm	0.282	0.208	-0.298	0.176	0.333	0.262
EC 10cm	0.242	-0.418	0.252	-0.259	-0.175	-0.275
Bd 10-20	-0.324	-0.136	-0.091	-0.391	-0.259	-0.005
Bd 40-50	-0.321	-0.161	-0.259	-0.312	-0.156	0.136
Ks cm/d	0.313	-0.050	0.121	-0.123	0.293	-0.584
ds (Ah)	0.305	0.262	0.175	-0.001	-0.454	-0.005
slop %	-0.277	-0.255	-0.322	0.178	0.397	-0.176
%OM_10	0.299	0.072	-0.269	0.136	-0.335	0.234
Ca10 (me)	0.351	-0.148	-0.227	-0.211	0.085	-0.019
K10 (me/)	0.222	-0.536	-0.295	-0.056	-0.099	0.238
Mg10 (me)	0.341	-0.238	-0.014	-0.083	0.168	0.210
Na10 (me)	0.049	0.311	0.144	-0.692	0.367	0.326
Ca:Mg	0.074	0.367	-0.626	-0.230	-0.160	-0.450

Variable	PC7	PC8	PC9	PC10	PC11	PC12
pH_10cm	0.474	-0.199	-0.364	0.371	-0.189	-0.009
EC 10cm	0.123	0.388	-0.410	0.427	0.055	-0.014
Bd 10-20	0.211	-0.265	-0.009	0.085	-0.106	0.488
Bd 40-50	-0.061	-0.359	0.038	0.312	0.074	-0.620
Ks cm/d	-0.237	-0.525	0.115	0.071	-0.303	-0.012
ds (Ah)	0.056	-0.454	-0.344	-0.223	0.465	0.022
slop %	-0.308	-0.072	-0.411	-0.031	0.477	0.191
%OM_10	-0.674	0.064	-0.032	0.333	-0.148	0.116
Ca10 (me)	0.044	0.175	-0.004	-0.378	0.132	-0.448
K10 (me/)	0.041	-0.127	-0.093	-0.431	-0.314	0.196
Mg10 (me)	0.108	-0.089	0.579	0.267	0.516	0.230
Na10 (me)	-0.262	0.092	-0.188	-0.089	0.003	0.129
Ca:Mg	0.138	0.239	0.133	-0.007	0.076	0.135

The first principal component has variance (eigenvalue) 6.3918 and accounts for 49.2 % of the total variance. The coefficients listed under PC1 show how to calculate the principal component scores:

$$PC1 = |-0.324 * Bd_{10}| + |-0.321 * Bd_{40}| + ..$$

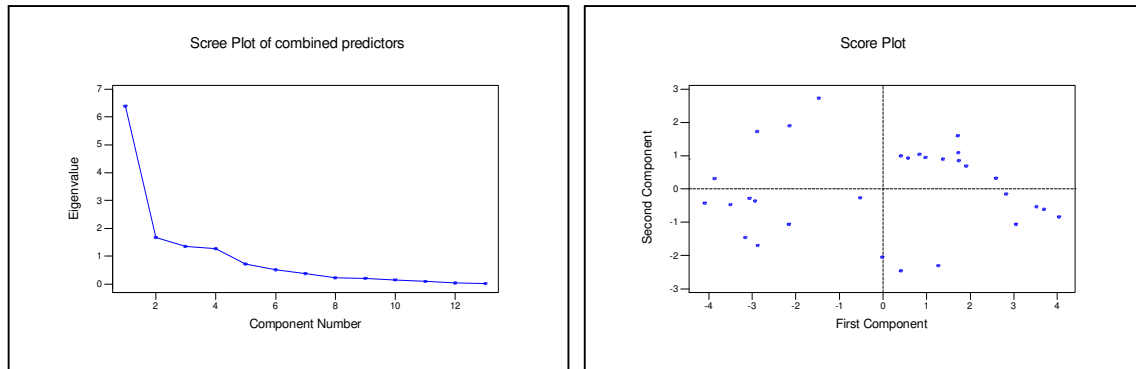
As it shown in the (table 26) obvious patterns of chemical and physical parameters are indicated. For instance, one could think of the *first principal component* as representing the **Bd_20** and **Bd_50** and **slope%** to some extent, since the coefficients of these terms have the same sign and are not close to zero.

The *second principal component* has variance 1.6793 and accounts for 12.9 % of the data variability. It is calculated from the original data using the coefficients listed under PC2.

This component could be thought of as contrasting level of all soluble cations, depth of the topsoil with EC_10 to some extent. Together, the first two and the first three principal components represent 62.1% and 72.4%, respectively, of the total variability. Thus, most of the data structure can be captured in three or four underlying dimensions.

The remaining principal components account for a very small proportion of the variability and are probably less important. The eigen value (scree) plot above provides this information visually.

Figure 48 Eigen values and Scree plot (mixed field variables)



As it was explained in the previous field level models (sections 7.1. & 7.2.) further statistical treatment is required to find out the most important ETa limiting factors for the combined data set.

As it was done in the previous field level procedures data set was grouped into two main categories: namely the soil chemical and physical properties, namely the chemical and physical soil properties.

1. *Chemical*: pH, EC, Ca, Mg, K, Na, OM
2. *Physical*: Bd, Ks, slope, topsoil depth

The procedures followed on interpreting the stepwise regression model are explained in section (7.2.2.).

7.4.2. Stepwise Regression

The same step was followed in the case of mixed data set, of both the lower and upper wheat fields where actual evapotranspiration of both fields was regressed against the mixed chemical, physical and finally combined (both chemical and physical) predictors based on stepwise regression analysis. However, first Principal component analysis was done to visualize the data structure (pattern) in the case of a mixed data sets (both fields' data set)

7.4.2.1. Chemical predictors

Alpha-to-Enter: 0.15 Alpha-to-Remove: 0.15
 Response is ETa (mm/ on 6 predictors, with N = 44
 N(cases with missing observations) = 80 N(all cases) = 124

Table 27 Stepwise Regression mixed fields (chemical soil properties)

Step	1	2	3
Constant	-0.4051	-13.5594	-12.6308
%OM_10	0.466	0.266	0.235
T-Value	7.92	4.85	4.17
P-Value	0.000	0.000	0.000
pH_10cm		2.46	2.17
T-Value		5.95	5.00
P-Value		0.000	0.000
Mg10 (me			8.6
T-Value			1.79
P-Value			0.081
S	1.01	0.752	0.732
R-Sq	59.90	78.50	80.09
R-Sq (adj)	58.95	77.45	78.60

C-p	35.8	2.7	1.7
PRESS	48.0515	26.6928	25.8154
R-Sq(pred)	55.43	75.24	76.05
best alt.			
Variable	Mg10 (me	K10 (me/	
T-Value		3.13	1.56
P-Value		0.003	0.127
Variable	Ca10 (me	EC 10cm	
T-Value		2.98	1.45
P-Value		0.005	0.155

The chemical predictors model i.e. step three indicates that the predictors with p-value below Alpha 0.15 are percentage of soil organic matter at 10 cm depth (**%OM_10**), pH at 10 cm depth, (**pH_10**) and **Mg_10**.

The above chemical parameters data (table 27) indicates that, S and PRESS decreases from step 1 to step 3, R and R(adj) and R_sq(pred) increase from step 1 to step 3, and C-p becomes closer to the number of predictors in the model. Taken together, these statistics indicate that the step 3 model, containing the predictors **%OM_10**, **pH_10** and **Mg_10** provides a better fit for the data.

For the above chemical parameters data, two alternative predictors were requested:

- *At the second step*, among the five predictors not included in the model, Mg_10 and Ca_10 were the two best alternative predictors, with p-values of 0.03 and 0.005, respectively.
- *At the third (final) step*, only two predictors (K_10 and EC_10) are not included in the model. Therefore, **K_10** and **EC_10** were listed as the two best alternative chemical predictors.

7.4.2.2. Physical predictors

Alpha-to-Enter: 0.15 Alpha-to-Remove: 0.15

Response is ETa (mm/ on 4 predictors, with N = 30

N(cases with missing observations) = 94 N(all cases) = 124

Table 28 Stepwise Regression mixed fields (physical soil properties)

Step	1	2	3
Constant	0.2038	4.9723	3.7781
%OM 10	0.371	0.201	0.139
T-Value	5.89	2.93	2.24
P-Value	0.000	0.007	0.034
Bd 10-20		-3.47	-8.91
T-Value		-3.79	-4.79
P-Value		0.001	0.000
Bd 40-50			6.3
T-Value			3.23
P-Value			0.003
S	0.903	0.742	0.639
R-Sq	55.30	70.84	79.20
R-Sq(adj)	53.70	68.68	76.79
C-p	27.7	11.1	3.0
PRESS	26.9345	18.3280	14.1616
R-Sq(pred)	47.22	64.08	72.25
best alt.			
Variable	Bd 40-50	ds (Ah)	
T-Value		-1.95	-1.82
P-Value		0.062	0.080
Variable	ds (Ah)		
T-Value		-0.34	
P-Value		0.738	

The physical predictors model i.e. step three indicates that the predictors with p-value below Alpha 0.15 are percentage of soil organic matter at 10 cm depth, Bd at 10 cm depth and at 30 cm depth.

The above chemical parameters data indicates that, S and PRESS decreases from step 1 to step 3, R and R(adj) and R_sq(pred) increase from step 1 to step 3, and C-p becomes closer to the number of

predictors in the model. Taken together, step3 model, containing the predictors **%OM_10**, **Bd_10** and **Bd_50** provides a better fit for the data.

For the above physical parameters data, one alternative predictor was requested:

- *At the second step*, among the five predictors not included in the model, **Bd_50** and topsoil depth were the two best alternative predictors, with p-values of 0.062 and 0.738, respectively.
- *At the third (final) step*, only one predictor (**topsoil depth**) is not included in the model. Therefore, topsoil depth was considered as the best alternative in this step.

7.4.2.3. Mixed predictors (both chemical & physical)

Alpha-to-Enter: 0.125 Alpha-to-Remove: 0.125
 Response is ETa (mm/ on 5 predictors, with N = 31
 N(cases with missing observations) = 93 N(all cases) = 124

Table 29 Stepwise Regression mixed fields (mixed soil properties)

Step	1	2	3	4	5
Constant	0.1535	-12.7085	-6.6676	-7.1472	-7.2605
%OM_10	0.387	0.222	0.162	0.113	0.091
T-Value	5.95	3.82	2.65	2.01	1.59
P-Value	0.000	0.001	0.013	0.055	0.125
pH_10cm		2.35	1.75	1.69	1.54
T-Value		5.02	3.38	3.70	3.34
P-Value		0.000	0.002	0.001	0.003
Bd 10-20			-2.02	-6.55	-6.49
T-Value			-2.15	-3.77	-3.83
P-Value			0.040	0.001	0.001
Bd 40-50				5.1	5.4
T-Value				2.97	3.20
P-Value				0.006	0.004
Mg10 (me					6.7
T-Value					1.50
P-Value					0.146
S	0.939	0.693	0.652	0.574	0.561
R-Sq	55.00	76.33	79.80	84.91	86.16
R-Sq (adj)	53.45	74.64	77.56	82.59	83.39
C-p	54.3	17.7	13.5	6.2	6.0
PRESS	30.0670	16.7090	14.4564	12.0049	11.7076
R-Sq (pred)	47.05	70.57	74.54	78.86	79.38
best alt.					
Variable		Bd 10-20	Mg10 (me	Mg10 (me	
T-Value		-3.98	1.43	0.95	
P-Value		0.000	0.163	0.351	
Variable		Mg10 (me	Bd 40-50		
T-Value		2.65	-0.61		
P-Value		0.013	0.547		

The general combined wheat fields predictors model i.e. step three indicates that the predictors with p-value below Alpha 0.125 are **pH_10**, **Bd_10**, **%OM_10** and **Bd_30**

The above chemical and physical (combined) parameters data indicates that, S and PRESS decreases from step 1 to step 4, R and R(adj) and R_sq(pred) increase from step 1 to step 4, and C-p becomes closer to the number of predictors in the model. Taken together, these statistics indicate that the step 4 model, containing the predictors: **%OM_10**, **pH_10**, **Bd_10** & **Bd_40** provides a better fit for the data.

For the above chemical parameters data, one alternative predictor was requested:

- *At the second step*, among the three predictors not included in the model, **%OM_10** and **pH_10** were the two best alternative predictors, with p-values of 0.001 and 0.000, respectively.

- *At the third step*, only two predictors (Bd_40 and Mg_10) were not included in the model. Therefore, Bd_40 and Mg_10 were listed as the two best alternative predictors.
- *At the final fourth step*, only one predictor (**Mg_10** with p-value of 0.351) is not included in the model. Therefore, Mg_10 was listed as the best alternative predictor for both the upper and lower wheat fields together.

Chapter 8. Results

The distributions of the variables were first examined using the Anderson-Darling test for normality at the 95 % confidence limit (Minitab, 2000. VIA. Technologies, inc.) Not all variables adhered to that criterion, and therefore Pearson correlation was used. The distribution of ETa was normal and therefore an analysis of variance was done to investigate whether 5 classes of ETa by splitting the observed range in equal intervals, were meaningful. That proved to be the case. The ETa segmentation assisted in the sampling design to ensure a good density in the highest and lowest class, but during the remainder of the statistical analysis ETa was treated as a continuous variable. After that correlation matrices were made and the r and P-value statistics were examined.

The data set containing all variables were used for further analysis.

Two parameter t-test was used to check the between fields variation of ETa pattern.

A principal component analysis was done to investigate the over all data structure for variables that contributed much to the first 4 principal components (together they contained 82.1% of the total variance) and a selection was made of the variables for stepwise multiple regression, by trying to avoid the co-linearity problem. The variables finally chosen were those that had high coefficients in the PC analysis.

The final steps in the regression analysis consisted of 4 iterations using a recommended threshold value with the result that at the fourth iteration only the strong variables survived. However, it was thought wise in this type of analysis with many somewhat interdependent variables to discuss also the “best alternative” Predictor.

The resulting regression equations were used to compare predicted ETa values with those calculated by the surface energy balance equation of the satellite overpass of the previous year, considered as the “observed” ETa. They are mentioned and illustrated below.

The physical single variables that had significant correlation with the ETa values for the upper field are, bulk density, slope percent, topsoil depth and saturated hydraulic conductivity and for the lower field bulk density in both horizons.

A good relationship (**R2 = 0.847 & 0.947**) between ETa and the vegetation index used (the Normalized Difference Vegetation Index, NDVI) exists but the NDVI was not included as a variable in the stepwise regression because NDVI is calculated from the satellite data and is included in the ETa calculation.

It is known that wheat growth is sensitive to aluminum toxicity at low pH. Therefore, the data set was split up in pH<6 and pH>6. Perhaps the toxicity effect may not be excluded, when the segmented data set is inspected.

The first principal component (PC) and second PC of the data set for the upper field contained variables with fairly high factor loadings (> 0.30) of both physical and chemical nature. For the lower field the first and second PC's separated respectively the physical and chemical variables.

The main results of the stepwise multiple regressions are shown graphically in figures 49a, 49b and 50. for the data sets of the upper field, the lower fields and combined data set respectively.

8.1. Upper field regression results

For the **upper field** the multiple regression analysis yielded the following relationship for the **physical** variables (**R² = 78.5**):

$$ETa \text{ (predicted)} = 7.58 - 0.26 \% \text{slope} - 4.1 * Bd_{10}$$

Where, Bd_{10} is the bulk density at 10 cm soil depth.

The best alternative predictors in this analysis are Bd_{40} and K_s

For the **chemical** variables (**R2 =88.67**):

$$ETa \text{ (predicted)} = -13.4 + 0.22 * \% OM_{10cm} + 1.94 pH_{10} + 24.7 * Mg_{30cm}$$

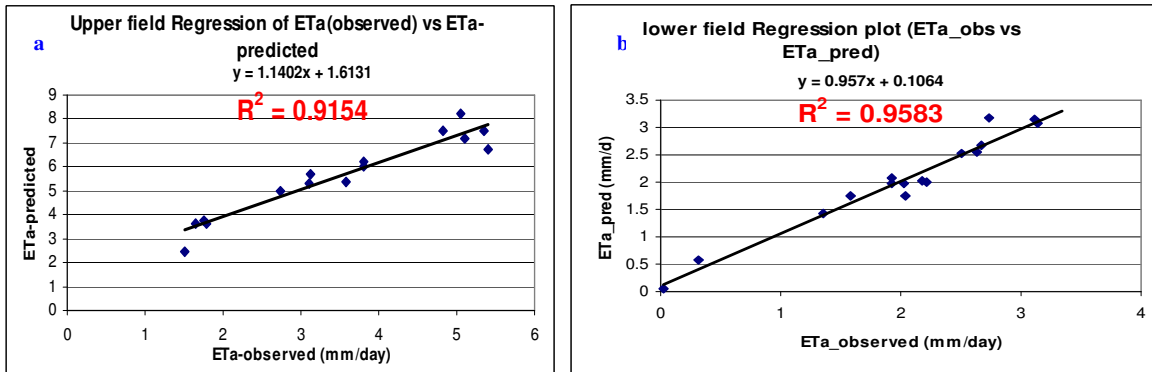
Where, OM_{10} is the organic matter content at 10 cm depth and Mg_{30} is the magnesium content at 30 cm. The best alternative predictors in this analysis are pH_{30} and Mg_{10} .

When *both physical and chemical* data were **combined** (see figure 49a) the equation (**R2 = 94.10**) is:

$$ETa \text{ (predicted)} = \%OM_{10} * 0.227 + 1.76 * pH_{10} + 26.3 * Mg_{30} - 3.1 * Bd_{10} - 7.167$$

The best alternative predictor in this analysis is **slope%**.

Figure 49 Regression plot of the Observed (satellite derived) against predicted ETa values (Upper field (Fig a) and lower field (Fig b))



8.2. Lower field regression results

For the **lower field** the results were as follows:

For the **physical** variables (**R2 = 92.69**):

$$ETa \text{ (predicted)} = -9.46 * Bd_{10} + 5.7 * Bd_{40} + 7.51$$

The best alternative predictor in this analysis is K_s .

For the **chemical** variables (**R2 = 52.49**):

$$ETa \text{ (predicted)} = 1.73 * pH_{10} + 14 * Mg_{30} - 7.7$$

The best alternative predictor in this analysis is Ca_{10} .

When *both physical and chemical* data were **combined** (figure 48b) the equation (**R2 = 95.83**) is:

$$ETa \text{ (predicted)} = -0.31 * \%OM_{10} + 0.75 * pH_{10} + 5.9 * Bd_{40} - 8.79 * Bd_{10} + 1.97$$

The best alternative predictor in this analysis is Mg_{10} .

8.3. Combined data (fields) regression results

Combination of the data sets for both fields provides a general background of the relationships in the wheat farm. The equations obtained were:

For the **physical** variables (**R2 = 79.2**):

$$ETa \text{ (predicted)} = -0.2 * \%OM_{10} - 3.47 * Bd_{10} + 6.3 * Bd_{40} + 4.97$$

The best alternative predictor in this analysis is topsoil depth (A_h).

For the **chemical** variables (**R2 = 80.09**):

$$ETa \text{ (predicted)} = 0.235 * \%OM_{10} + 2.17 * pH_{10} + 8.6 * Mg_{30} - 12.63$$

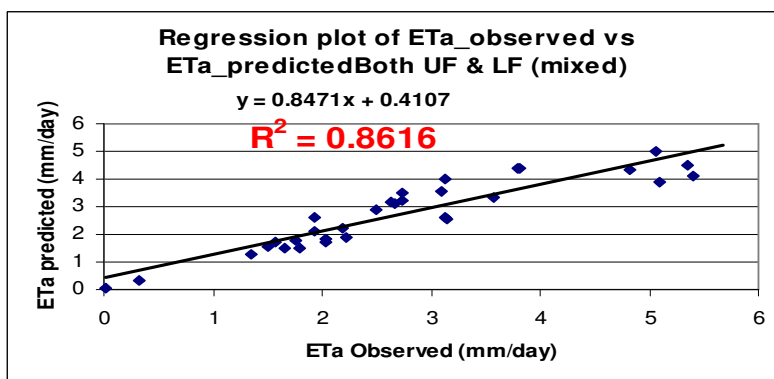
The best alternative predictors in this analysis are K_{10} and.

When *both physical and chemical* data were **combined** (figure 50) the equation (**R2 = 86.16**) is:

$$ETa \text{ (predicted)} = 0.113 * \%OM_{10} + 1.69 * pH_{10} - 6.55 * Bd_{10} - 7.147$$

The best alternative predictor in this analysis is Mg_{10} .

Figure 50 Regression plot of the Observed (satellite derived) against predicted ETa values (Both fields)



Chapter 9. Discussion

The single variables that were found significantly related to ETa in both fields were bulk density, organic matter content, soluble Mg content and soil pH in the rooting depth. For the upper field it was found that ETa was related to soil chemical parameters such as the soil pH and availability of soluble cations as compared to the lower field that is explained dominantly by soil physical variables i.e. bulk density and slope percent.

More over, the most important soil variables that limit transpiration of the young wheat crop throughout the study area are: Bulk density, organic matter content and soil pH. Bulk density is negatively correlated with ETa in both fields which can be explained by the sensitivity of wheat crops to soil compaction as they are known as monocot cool season grass having only fine roots and no taproot to penetrate compacted soils i.e. higher bulk density.

Major portion of the lower field, according to the farm manger, soil compaction and crusting could possibly prevent crop emergence since wheat seedling shoots are sensitive to soil compaction, the difference of the mechanical strength of this field as compared to the upper field is considered during plowing.

According to the local inhabitants (senior farm workers), soils in the lower plots tend to form crop emergence-restricting crusts i.e. a hard thin layer at the soil surface after rain, during warm early sowing periods, where this is also confirmed by the field level studies, characterized by greater density and shear strength, but with finer pores and lower saturated hydraulic conductivity, than the underlying pumicaceous gravelly soils.

The positive relationship between the organic matter content of soils can be explained by the important role of organic matter in enhancing soil aggregation, increasing structural stability and water holding capacity, contributing to the nutrient holding capacity and buffering against potential acidification. More over, organic matter binds toxic substances to the soil complex, e.g. an excess of Al and Fe; and provides the soil with N, P and S and other nutrients, which were stored in the upper ground.

Similarly, as wheat is sensitive to soil acidity, the direct relationship of ETa with soil pH can be mainly explained by the lower pH level in some portion of the fields with $\text{pH} < 6$, where availability of plant nutrients could be limited in this pH range.

Besides, The primary effect of low pH values could be related to the availability of toxic elements and plant nutrients. Toxic elements like aluminum and manganese could possibly be one of the major causes of crop stress in the relatively acidic portions of the fields.

It is known that these elements are the main problems in Andisols since they dissolve more readily and are more available for plant uptake at low pH. More over, in soils with low pH the primary problem for wheat production is aluminum toxicity, which results in poor root development.

It is quite likely that other variables, not measured, could explain the ET_a pattern even better, such as soil moisture during a longer dry period (as happened during the satellite overpass) or pF, or water holding capacity of the root zone as well as the CEC.

Some contrasting evidence can be noted when relationships between the upper field and lower field are studied. For example, ET_a is positively correlated with percentage of organic matter and soluble potassium content and negatively correlated with saturated hydraulic conductivity in the upper field, but not so in the lower field. This can be attributed to the strong local topographic influences in the lower field, brought out by the selection of the sample pixels. Also the number of samples is lower for the lower field, which means that outliers play an important role. For example, the colluvial soils of the small valley bottom have good chemical and physical properties for a wheat crop, but because of water logging during 2000 after sowing, the ET_a values were low.

The good ET_a-NDVI relationship is no surprise because the NDVI is sensitive to covers of LAI < 3 and the wheat crop during overpass was young. In fact, if only the relative spatial patterns of crop performance are of interest, the NDVI is an adequate and simple substitute for ET_a, at least when the crop is young.

The results of the stepwise regression for the upper field show that two simple physical variables, namely slope steepness and bulk density explain 78.5 % of the variation of ET_a. The correlation matrix showed that slope steepness is associated with topsoil depth and organic matter with pH, topsoil depth, soluble cations and slope steepness (see chapter 6). The bulk density can also be regarded as an inverse indicator of the moisture holding capacity being the best alternative both in the lower and upper fields. For the lower field ET_a is reasonably well associated with the bulk density at two depths, but not with slope, which is surprising, but probably related to the limited sample set and the outliers due to water logging at early crop stage.

Two of the chemical predictors of the ET_a of the upper field, namely pH and Mg, could be associated with higher annual rainfall of the area, causing rapid weathering of the underlying volcanic ashes and leaching of soluble basic cations from the highly porous sand clay loam soils in the lower portion of the field. This phenomenon could intern result free Al and Fe ions in the soil.

The presence of relatively higher amount of other cations, particularly Ca and K on the other hand can affect the availability of Mg. During this study it was observed that Ca:Mg ratio was exceeding beyond the threshold limit of 5:1 (Booker Tate, 1991) in some pixels which could explain the importance of magnesium in affecting wheat transpiration.

The toxicity effect of low pH on the wheat crop in the upper field, although statistically weak, could also contribute to the prediction. Organic matter can be regarded as a physical variable, because of its effect on the water holding capacity and as a chemical variable because of its association with high cation adsorption and supply and availability of nutrients. The other effect of pH is the well-known association of pH and nutrient availability (Booker Tate, 1991).

The best alternative variables namely saturated hydraulic conductivity (K_s) and topsoil depth (A_t) are also associated with other variables such as the organic matter content and bulk density, may be associated with the relative variation of soil moisture holding capacity of the soils, limiting wheat transpiration during the dry seasons like the time of satellite overpass.

The ET_a samples of the lower field are not well related to chemical variables.

A combination of physical and chemical variables for the upper field, namely OM₁₀, pH, Mg and Bd of the upper soil horizon explains much of the variation of ET_a in the sample set. The alternative set replaces OM₃₀ with slope steepness.

It is interesting to note that for the lower field the combination of variables improves the correlation with ET_a, and OM, pH of the upper soil layer and Bd's at two depths were found to be strongest predictors. The alternative predictor in this case is soluble Magnesium content in the rooting depth.

The presence of the variables OM and Bd could well point to the desirability of including more direct soil moisture variables. The improvement of the correlation for the lower field by including OM and pH besides the Bd's is noteworthy. Only one typical chemical variable, Mg, remained in the final regression result (for the upper field), which is somewhat surprising. Probably, fertilizer application, based on soil analysis, has suppressed limiting factors in this well managed farm.

When both data sets are combined, the variation of ETa in the sample set can be reasonably well explained by OM, pH and Bd's at two depths only. The relevance of these variables has been mentioned. The relevance of these variables has been mentioned.

Chapter 10. Conclusions and Recommendations

10.1. Conclusions

Remote sensing imagery with ETa analysis allowed for identification of spatial patterns of crop transpiration. The multivariate statistical model including correlation and stepwise regression provided validation of ETa patterns as well as soil and topographic effects on wheat transpiration.

For the well-managed Ndabibi wheat farm in Kenya, the actual evapotranspiration pattern (ETa) calculated by satellite data for an image during the dry year 2000 was explained chiefly by three simple variables, sampled during the next year with adequate rainfall. They were organic matter content, pH and bulk density of the soil in the rooting zone. It is likely that appropriate fertilizer application has subdued the effects of chemical variables, which could have played a role in other conditions. If soil variables more directly related to soil moisture could have been included, it could have changed the outcome of the regression analysis

Results of Stepwise regression model (see chapter 8 &9) were able to reasonably predict the ETa within and across the two fields, of the day of the satellite overpass. The results indicate the potential of this approach for use in yield map prediction, field characterization and interpretation in the context of site-specific agriculture.

Analysis results indicate that prevalence of Chemical predictors in explaining ETa variation in the upper field (88.6%) as compared to the physical predictors, which explain 78.5 % of the variations (see chapter 8). The reverse is true in the lower field i.e. Chemical parameters explain only 52.49% of the ETa variation, while physical predictors explain 92.69% of the variation.

The combined data set of both fields and both Chemical and physical parameters have an equivalent role in predicting ETa. The stepwise regression results indicate that about 79.2% of the variation could be explained by physical parameters namely: OM & Bd, while chemical parameters (%OM, pH and soluble Mg) explain 80.1% of the variation.

The final result of the stepwise regression shows that soil pH, organic matter content and bulk density of soils in the rooting zone could explain about 86.16% of the variation of ETa in both fields.

There could be particular portions of a field which are high-ETa (yielding) parts in one year are the lowest-ETa (yielding) parts in the following year, therefore yield limiting factors of importance to a specific field may not be consistent from year to year and from place to place.

The stepwise regression model could be mainly used to provide average ETa estimates in areas considered homogeneous in topography and weather. Topography is an important factor in crop development and transpiration, especially in areas (such as the lower field) where water logging is a problem in some occasions of heavy rainfall and flooding, causing the year-to-year variation.

Despite the existence of dominant ETa controlling factors present in both fields such as soil bulk density, organic matter and pH, extrapolation of explanatory relationships derived from a single-year analysis of ETa patterns may not be able to accurately describe conditions in the nearby fields. Since annual weather patterns, and other ETa-limiting factors are dynamic and complex, multiple-year ETa patterns could be used to better characterize a specific field as a function of the most dominant and more stable ETa-predictors.

Nevertheless, careful collection and utilization of routine site characterization data (multiple year ETa maps & soil and topographic data) including historical information will likely determine the success of the applicability of this approach for site specific management. Equally important will be the involvement of the farm manager throughout the process of identification of ETa patterns, analysis and interpretation.

Despite poor experimental conditions much of the variation of the ETa of the sample pixels can be explained by the mentioned three variables. This suggests that a single image with ETa values is more worth than just an instantaneous view controlled by weather conditions preceding the satellite overpass.

ETa estimates showed significant variation both within and across the two sampling fields at 95 % confidence interval. The high correlation between the values of the satellite vegetation index and the ETa values indicates that the vegetation index image can be used as a substitute for the ETa image of the wheat farm.

10.2.Recommendations

Future studies

- ✓ Multiple year images are more important for explaining ETa patterns using soil and topographic parameters.
- ✓ Multiple ETa maps (at least 2 or 3 images should be acquired during important crop growth stages e.g. Flowering stage)
- ✓ Right time ground survey data (soil sampling and management information) should be collected for better results.
- ✓ Additional soil and crop parameters should be included in the modeling-Process, such as right time soil moisture content, pF, CEC, Cu, Al toxicity effects. e.t.c.
- ✓ Together with the soil parameters integration of hydrological models that can simulate water flow in the field can better predict future ETa values.

As stated in Section (10.1), the method described makes it possible to explain satellite derived single-day actual evapotranspiration patterns of the previous year using soil and topographic data sampled the –next- year, as given in this study. However, since this modeling has been carried out with a limited data set under a particular set of environmental conditions, further study is necessary to extend this approach to broader set of soil, topography and management conditions.

Field management

- ✓ Field management should consider the variation of native soil properties and topographic characteristics of the different zones of the field.

- ✓ Laboratory test of important soil properties such as pH, Al and soluble Mg concentrations is recommended
- ✓ Soil compaction (bulk density) variations and periodic soil crusting are observed in the lower field; therefore designing special management system is recommended in this portion of the field. Special tillage system e.g. variable depth and frequency of tillage and application of organic matter are recommended to this field to improved Crop performance.
- ✓ In view to the significant variation in soil fertilities (%OM), zone specific application of chemical fertilizer is recommended.
- ✓ Application of urea as a top dressing may aggravate the acidity of some portions of the field with $\text{pH} < 6$, therefore it is recommended to make zone specific alternatives in this regard.

References

- A. Giesske (2001). Introduction to Geostatistics. Lecture Note. Enschede: International institute of Geo-information science and earth observation, water resource and environmental management division, The Netherlands.
- A.O. Thompson M.Sc 1958. and R. G. Dodson M.Sc: "Geology of the Naivasha area", explanation degree sheet 43 s.w. Nairobi, 8th November 1958. Agri-Growth, Inc. RR1 Box 33 Hollandale, MN 56045 (507) 889-4371 FAX: (507) 889-4381 E-mail: info@agrigrwth.com Access Date: 1 August, 2001.
- Allen, R.G., M. Smith, W.O. Pruitt and L.S. Pereira 1996b. "Modifications of the FAO crop coefficient approach." In: C.R. Camp, E.J. Sadler and R.E. Yoder (Ed.), *Evapotranspiration and Irrigation Scheduling* (Proc. of the International Conference November 1996), ASAE, 124-132.
- Allen, R.G., W.O. Pruitt, J.A. Businger, L.J. Fritschen, M.E. Jensen and F.H. Quinn 1996a. "Evaporation and Transpiration." Chapt. 4. In: *Hydrology Handbook*, ASCE, 28, 125-252.
- Aziz Moameni 1999, "Soil quality changes under long-term wheat cultivation in the Marvdashat plain, south-central Iran" PhD thesis, University of Ghent, Belgium. pp.284
- Bastiaanssen, W.G.M. 1995. "Regionalization of surface flux densities and moisture indicators in composite terrain." PhD thesis, Agricultural University of Wageningen, The Netherlands, pp. 273.
- Bastiaanssen, W.G.M. 1998. "Remote sensing in water resources management: The state of the art." International Water Management Institute, Colombo, Sri Lanka, pp. 118.
- Bastiaanssen, W.G.M. 2000. SEBAL-based sensible and latent heat fluxes in the integrated Gediz Basin, Turkey. *J. of Hydrol.* 229: 87-100
- Bastiaanssen, W.G.M. and R.A. Roebeling 1993. "Analysis of land surface exchange processes in two agricultural regions in Spain using Thematic Mapper simulator data." In: Bolle, Feddes and Kalma (Ed.), *Exchange processes at the land surface for a range of space and time scales*, IAHS Publ., 212, 407-416.
- Bastiaanssen, W.G.M., Thiruvengadachari S., Sakthivadivel .R, Molden .D.J. 1999. "satellite remote sensing for estimating productivities of land and water" international water management institute (IWMI), colombo, sri lanka pp.181-196.
- Booker 1991, *tropical soil manual: a handbook for soil survey and agricultural land evaluation in the tropics and subtropics* / ed. by J.R. Landon. -Harlow; Thame : Longman Scientific & Technical ; Booker Tate, 1991. - 474 p. ; 24 cm. - ISBN 0-582-00557-4 631.47 (213.5)
- Brady N.C., 1996 "the nature and properties of soils" 11 th edition, pp 72-73, A Simon and Schuster company, upper Saddle River, New Jersey 07458, USA
- Brutsaert, W. 1975. "On a derivable formula for long-wave radiation from clear skies." *Water Resour. Res.*, 11, 742-744.
- Caselles, V., M.M. Artigao, E. Hurtado, C. Coll and A. Brasa 1998. "Mapping actual evapotranspiration by combining LANDSAT TM and NOAA-AVHRR images: Application to the Barrax Area, Albacete, Spain." *Rem. Sens. Environ.*, 63, 1-10.
- Cereals. - Rome: FAO, 1977. - 51 p.; 21 cm. - ISBN 92-5-100150-2 (Better farming series; 15) (FAO economic and social development series; 3/15) 633.1
- Clarke, M. C. G., Woodhall, D. G. , Allen, D., and Darling, G. *Geological, Volcanological and Hydrogeological Controls on the Occurrences of Geothermal Activity in the Area Sur-rounding Lake Naivasha, Kenya.* (1990). Nairobi: Ministry of Energy. 138 pp.
- Cliff synder, 2001 *efficient fertilizer management, Soil pH Management, western fertilizer handbook*, 8th edition, California , USA. pp.20.
- Clothier, B. E. 2001, *Infiltration. in Soil and Environmental Analysis: Physical Methods.* Keith A. Smith and Chris E. Mullins, Editors. Marcel Dekker, inc.: New York.
- Darling, W.G., Allen, D.J., and Armannsson, H. *Indirect Detection of Subsurface Outflow From a Rift Valley Lake.* *Jornal of Hydrology*, 1990. 113: p. 231-305.
- Dingman, S.L. 1994. "Physical Hydrology." Prentice-Hall, Inc., Simon & Schuster / A Viacom Company, New Jersey, pp. 575.

- Euroconsult (1989). "Agricultural compendium for rural development in the tropics and subtropics". - Third revised edition. – The Netherlands Ministry of Agriculture and Fisheries, The Hague: Elsevier, 1989. - 740 p. ; 25 cm.
- FAO (1988a). Nature and Management of Tropical Peat Soils. FAO Soils Bulletin No. 59. Rome: Food And Agriculture Organization of the United Nations.
- FAO (1998). Topsoil Characterization for Sustainable Land Management. Rome: Food and Agricultural Organization of the United Nations, Land and Water Development Division.
- FAO 1998, "Crop evapotranspiration" Guidelines for computing crop water requirement, FAO irrigation and drainage paper 56 by Richard G Allen, part I & II, Rome, Italy. pp.281.
- FAO. Soil Map of the World. (1988b). Revised Legend, Reprinted with Corrections. Rome: Food And Agriculture Organization of the United Nations. Report Number, 60.
- Farah, H.O. and W.G.M. 2001. "Estimation of regional evaporation under different weather conditions from satellite and meteorological data in the Lake Naivasha Basin." PhD thesis Wageningen University and ITC, ISBN 90-5808-331-4, Enschede, The Netherlands.
- Farah, H.O. and W.G.M. Bastiaanssen 1998. "Spatial variations of surface parameters and evaporation in the Lake Naivasha Basin estimated from remote sensing measurements without ground data." Formation of Andosols pp. 271-289. Wageningen Agricultural University, The Netherlands.
- Henri D. Grissino-Mayer and Valdosta State University. Introduction to Soil Science grissino@valdosta.edu. A Regional University of the University System of Georgia .Access Date:14 July, 2001.
- IWMI home page, International water management institute, Colombo sirilanka.www.cgiar.org/iwmi/index..ht Access Date:26 October, 2001.
- Jackson, R.D., J.L. Hatfield, R.J. Reginato, R.J. Idso and P.J. Pinter 1983. "Estimation of daily evapotranspiration from one time-of-day measurements." Agri. Water Manag., 7, 351-362.
- Jackson, R.D., M.S. Moran, L.W. Gay and L.H. Raymond 1987. "Evaluating evaporation from field crops using airborne radiometry and ground-based meteorological data." Irrig. Sci., 8, 81-90.
- Jackson, R.D., S.B. Idso, R.J. Reginato and P.J. Pinter 1980. "Remotely sensed crop temperatures and reflectances as inputs to irrigation scheduling." In: Proceedings: ASCE, Irrigation and Drainage division, Specialty Conference, Boise, Idaho New York, 390-397.
- John VanDyk , Integrated Crop Management Newsletter April 20, 1999, Iowa State University and Iowa State University Extension. www.ent.iastate.edu/ipm/icm/default.html Access Date:10 August, 2001.
- K.A. Sudduth 1998 "Integrating spatial data collection, modeling and analysis for precision Agriculture" USDA-Agricultural research service cropping systems & water quality Research,Colombia, Missouri, USA. June 1998.
- K.A.Sudduth, Integrating spatial data collection, modeling and analysis for precision agriculture, (presented at the first international conference on geo-spatial information in Agriculture and forest, Lake Buena vista, Florida, 1-3 June 1998). USDA-Agricultural research service cropping systems & water quality research, Colombo, Missouri,USA. pp.8.
- Ledgard, M. B. Geological Map of Longonot Volcano, The Greater Olkaria and Eburru Volcanic Complexes, and Adjacent Areas. (1988). Naivasha, Kenya: Government of Kenya Ministry of Energy Geothermal Section.
- Mausbach. M.J. 1991, SSSA Spatial Variabilities of soils and landforms, special publication Number 28, 1991, proceedings of an international symposium, soil science of America, Inc. Madison, Wisconsin, USA. pp.270.
- Meijerink, A.M.J., H.A.M. De Brouwer, C.M. Mannaerts and C.R. Valenzuela 1994. "Introduction to the use of Geographic Information Systems for practical hydrology." ITC, The Netherlands, pp. 243.
- Mekonnen G.Michael & Wim G.M. Bastiaanssen.2000, a new simple method to determine crop coefficients for water allocation planning from satellite: results from Kenya, Irrigation and Drainage systems 14: 237-256,2000., Kluwer academic publishers, the Netherlands.
- Minitab statistical software, 2000. System manufacturer Microsoft Corporation VIA Technologies, inc. Version 13.1 Minitab statistical software, USA
- Moran, M. S. and R. D. Jackson, 1991, Assessing the spatial distribution of evapotranspiration using remotely sensed inputs, J. Environ.Qual, 20, 725-737,1991.

- Moran, M.S., Clarke, T.R., Inoue, Y. & Vidal, A. (1994) Estimating crop water deficit using the relation between surface-air temperature and spectral vegetation index, remote sensing of environment. 49 (2), pp. 246-263.
- Nico van Breemen and Peter Buurman, 1998 "Soil Formation". Kluwer academic publishers Formation of Andosols pp.271-289. Wageningen Agricultural University, The Netherlands.
- Parodi .G. (2001) Satellite hydrology, lecture note. Enschede: International institute of Geo-information science and earth observation, water resource and environmental management division, The Netherlands.
- Pedro A. Sanchez 1976, properties and management of soils in the tropics, department of soil science North Carolina state university. USA
- Roerink G.J.& Bastiaanssen, W.G.M 1997 "Relating Crop water consumption to irrigation water supply by remote sensing" winand starring center for integrated land, soil and water research (SC-DLO), Wageningen The Netherlands. pp 445-467.
- Rossiter, D. G. A Compendium of On-Line Soil Survey Information. URL: http://www.itc.nl/~rossiter/research/rsrch_ss.html, Access Date: 25 December, 2001.
- Sombroek, W.G., Brown, H.M.H., and Van Der Pouw, B.J.A. Exploratory Soil Map and Agro-climatic Zone Map of Kenya. (1980). Exploratory Soil Survey Report No. E, Including Map. Nairobi: Kenya Soil Survey (KSS).
- The Precision Farming Primer Berry & Associates// Spatial Information Systems 2000 South College, Suite 300, Fort Collins, Fort Collins, Colorado, USA 80525 Web Site: www.inovativegis.com/basis Access Date:10 August, 2001.
- Thomas H. Wonnacott & Ronald J. Wonnacott, introductory statistics for business and economics, fourth edition wiley series in probability and mathematical statistics, New york, 1990
- Thompson, A.O. and Dodson, R.G. Geology of the Naivasha Area. (1963). Geology and Mines Report No. 55. Nairobi, Kenya.
- Trottman, Damali K. (1998). Modelling Groundwater Storage Change in Response to Fluctuating Levels of Lake Naivasha Kenya: Modelling Groundwater Storage Change in Response to Fluctuating Levels of Lake Naivasha Kenya. Master of Science (MSc) Thesis. International Institute for Aerospace Survey and Earth Science (ITC). Water Resources Department. Enschede, 78 pp.
- Webster, R. and Oliver, M. A. (1990). Statistical Methods in Soil and Land Resource Survey. Spatial Information Systems, ed. P. H. T. Beckett, P. A. Burrough, M. F. Goodchild, and P. Switzer. New York: Oxford University Press.

Appendix

Appendix A Soil profile description

The soil distribution in the Kijabe plateau

Soil profile NAIV/2001/LF_TA/002 Lower wheat field sampling pt.9

Information on soil profile site

Date of examination	September 30, 2001
Authors	Tesfay Alemseged Tesfay
Location	Lower part of the Kijabe Ltd. Wheat Farm on the Ndabibi Plateau; UTM 186972, 9917460 ARC 1960
Elevation	2,112 m above sea level
Geopedological unit	Lf - Higher convex part of undulating mesa belonging to (tilted) step-faulted plateau
Topography	Sloping (12-15 %) with a convex slope form.
Micro-topography	Nil
Parent material	Eburru pumic (Ep), pantellerite & trachyte pumic and ash fall deposits
Land use	Large-scale rainfed wheat (<i>Triticum aestivum</i>) fertilized (young crop in pre-tasseling stage); average crop cover >85% of soil surface.
Natural vegetation	Cleared at site but remnants of pin forest occur along upper boundary of wheat plot.

General information on soil profile

C) Soil profile description

Classification (WRB 1998)

Human influence	Clearing of vegetation and wheat cultivation; fertilization and pesticide application on crop
Effective depth	120+ cm
Rock outcrops / surface stoniness	Nil gravels of pumic
Evidence of erosion	Sheet erosion
Sealing / crusting	The first 10-15 cm
Cracks
Drainage (natural) class	Excessively drained
Internal drainage	Never saturated, well drained
External drainage	Neither receiving nor shedding water
Depth of ground water table	Below 1.20 m
Moisture condition	Dry throughout

Horizon	Depth (cm)	Description
Ah	0-7	Strong brown (7.5YR 5/6) (dry), gravely <u>sandy loam</u> (field), moderate to coarser sub-angular blocky structure, friable, non-sticky, slightly plastic, moderately fine sub-rounded and partially weathered pumic, fine and very few channel and interstitial pores, few to very few very fine to fine roots, no microbial activities, pH 6.
2Ah1	7-45	Brown (7.5YR4/4), dry, gravely <u>Loamy sand</u> (field), weak, coarse sub-angular blocky structure, very friable, non sticky, non plastic, full of moderate to courser sub-rounded and weathered pumic, very fine and very few channel pores, very few very fine roots, no microbial activities, pH 5.5
2BA	45-95	Light brown (7.5 YR 6/3), dry, gravely <u>Loamy sand</u> (field), full of fresh pumic gravel; pH 6,
2Bt	95-120+	Pinkish gray (7.5 YR7/2), dry, <u>massive fresh pumic gravel</u> (field), very courser, fresh pumic gravel, pH 6,

Note : Bt2 and Bt3 are examined by angering; disturbed samples taken of all horizons.

Additional remarks: The depth of the profile is too shallow, it is mainly composed of volcanic materials i.e. fresh pumic gravels erupted from the near by volcanoes, modified by the action of water and wing erosions, this zone of the Kijabe field is one of the oldest plots in the plateau for its use as an arable land, water erosion has been the main problem in this zone for many years, until the last five years, before the construction of the existing terraces.

Soil profile NAIV/2001/JT-TA/001

Information on soil profile site

Date of examination	September 29, 2001
Authors	Tesfay Alemseged Tesfay, Somia Mohammed Ahmed, Jessica Torrion and Rob Hennemann
Location	Upper part of the Kijabe Ltd. Wheat Farm on the Ndabibi Plateau; UTM 185121, 9922092 ARC 1960
Elevation	2,307 m above sea level
Geopedological unit	Lf - Higher convex part of undulating mesa belonging to (tilted) step-faulted plateau
Topography	Sloping (5-10 %) with a convex slope form.
Micro-topography	Nil
Parent material	Eburru pumic (Ep), pantellerite & trachyte pumic and ash fall deposits
Land use	Large-scale rainfed wheat (<i>Triticum aestivum</i>) fertilized (young crop in pre-tasseling stage) ; average crop cover >80% of soil surface.
Natural vegetation	Cleared at site but remnants of dry montane forests occur along upper boundary of

wheat plot.

General information on soil profile

C) Soil profile description

Classification (WRB 1998)

Human influence	Clearing of vegetation and wheat cultivation; fertilization and pesticide application on crop
Effective depth	190+ cm
Rock outcrops / surface stoniness	Nil
Evidence of erosion	None
Sealing / crusting	None
Cracks
Drainage (natural) class	Well drained
Internal drainage	Never saturated, well drained
External drainage	Neither receiving nor shedding water
Depth of ground water table	Below 1.90 m
Moisture condition	Moist throughout

Horizon	Depth (cm)	Description
Ah	0-21	Black (7.5 YR 2.5/1) (moist), <u>sandy loam</u> (field), weak to moderate very fine to fine sub-angular blocky structure, friable, non-sticky, slightly plastic, few fine sub-rounded and weathered pumic, fine and very few channel and interstitial pores, few to very few very fine to fine roots, no microbial activities, pH 5.0
2Ah1	21-55	Black (7.5 YR 2.5/1), moist, <u>clay loam</u> (field), weak, fine to medium sub-angular blocky structure, very friable, sticky, plastic, few fine to moderate sub-rounded and weathered pumic, very fine and few channel pores, very few very fine roots, no microbial activities, pH 5.0
2Ah2	55-92	Very dark gray (7.5 YR 3/1), moist, <u>clay loam</u> (field), very weak fine to medium sub-angular blocky structure, very friable, sticky, plastic, many fine to medium sub-rounded sub-rounded pumic, very fine and few channel pores, very few very fine roots, no microbial activities, pH 5.0
2BA	92-120	Very dark gray (7.5 YR 3/1), moist, <u>sandy clay</u> (field), very sticky, very plastic, pH 4.5
2Bt	120-190+	Dark brown (7.5 YR3/4), moist, <u>sandy clay</u> (field), very sticky, very plastic, pH 4.5

Note : Bt2 and Bt3 are examined by auguring; disturbed samples taken of all horizons;

Additional remarks: The depth of the profile very deep, it is mainly composed of organic materials mainly in the upper 30 cm, the main parent material of the soil is a volcanic tuff erupted from the near by volcanoes, modified by the intensive vegetation covers as well as action of slight water erosion and grazing, this zone of the Kijabe field is the youngest one of the recently deforested plots for cattle grazing and finally for crop production, Due to its elevation and the convex shape of the contours, compared to the lower plots of the Kijabe wheat fields this part of the Plato is less affected by water erosion.

Soil profile NAIV/2001/UF-TA/002 upper wheat field sp.67

Information on soil profile site

Date of examination	September 30, 2001
Authors	Tesfay Alemseged Tesfay
Location	Upper part of the Kijabe Ltd. Wheat Farm on the Ndabibi Plateau; UTM 185231, 9921288 ARC 1960
Elevation	2,230 m above sea level
Geopedological unit	Lf - Higher convex part of undulating mesa belonging to (tilted) step-faulted plateau
Topography	Sloping (8-10 %) with a convex slope form.
Micro-topography	Nil
Parent material	Eburru pumic (Ep), pantellerite & trachyte pumic and ash fall deposits
Land use	Large-scale rainfed wheat (<i>Triticum aestivum</i>) fertilized (young crop in pre-tasseling stage); average crop cover >80% of soil surface.
Natural vegetation	Cleared at site but remnants of dry montane forests occur along upper boundary (near to housing compound) of wheat plot.

General information on soil profile

C) Soil profile description

Classification (WRB)

Human influence	Clearing of vegetation and wheat cultivation; fertilization and pesticide application on crop
Effective depth	180+ cm
Rock outcrops / surface stoniness	Nil
Evidence of erosion	None
Sealing / crusting	None
Cracks
Drainage (natural) class	Excessively drained
Internal drainage	Never saturated, well drained
External drainage	Neither receiving nor shedding water
Depth of ground water table	Below 1.30 m
Moisture condition	Moderately Moist throughout

Horizon	Depth (cm)	Description
Ah	0-13	Black (7.5 YR 2.5/1) (moist), <u>clay loam</u> (field), weak to moderate very fine to fine sub-angular blocky structure, friable, sticky, plastic, few fine sub-rounded and weathered pumic, fine and very few channel and interstitial pores, few to very few very fine to fine roots, no microbial activities, pH 5.0
2Ah1	13-48	Very dark brown (7.5 YR 2.5/2), moist, <u>sandy loam</u> (field), weak, fine to medium sub-angular blocky structure, very friable, non-sticky, slightly plastic, few fine to moderate sub-rounded and weathered pumic, very fine and few channel pores, very few very fine roots, no microbial activities, pH 4.5
2Ah2	48-92	Very dark gray (7.5 YR 2.5/3), moist, <u>sandy loam</u> (field), very weak fine to medium sub-angular blocky structure, very friable, slightly sticky, plastic, many fine to medium sub-rounded sub-rounded pumic, very fine and few channel pores, very few very fine roots, no microbial activities, pH 5.
2BA	92-110	Very dark gray (7.5 YR 3/1), slightly moist, <u>sandy clay</u> (field), slightly sticky, slightly plastic, pH 5
2Bt	110-180+	Strong brown (7.5 YR4/6), slightly moist, <u>sandy clay</u> (field), slightly sticky, slightly plastic, pH 5.

Note : Bt2 and Bt3 are examined by augering; disturbed samples taken of all horizons.

Soil profile NAIV/2001/JT-TA/003 upper wheat field SP 13.

Information on soil profile site

Date of examination	October 1, 2001
Authors	Tesfay Alemseged Tesfay
Location	Upper north-eastern part of the Kijabe Ltd. Wheat Farm on the Ndabibi Plateau; UTM 184677, 9921609 ARC 1960
Elevation	2,264 above sea level
Geopedological unit	Lf - Higher convex part of undulating mesa belonging to (tilted) step-faulted plateau
Topography	Sloping (6-8 %) with a convex slope form.
Micro-topography	Nil
Parent material	Eburru pumic (Ep), pantellerite & trachyte pumic and ash fall deposits
Land use	Large-scale rainfed wheat (<i>Triticum aestivum</i>) fertilized (young crop in pre-tasseling stage); average crop cover >80% of soil surface.
Natural vegetation	Cleared at site but remnants of dry montane forest occurs along eastern and upper boundary of wheat plot.

General information on soil profile

C) Soil profile description

Classification (WRB)

Human influence	Clearing of vegetation and wheat cultivation; fertilization and pesticide application on crop
Effective depth	180+ cm
Rock outcrops / surface stoniness	Nil
Evidence of erosion	Slight/sheet
Sealing / crusting	None
Cracks
Drainage (natural) class	Well drained
Internal drainage	Never saturated, well drained
External drainage	Neither receiving nor shedding water
Depth of ground water table	Below 1.40 m
Moisture condition	Moist throughout

Horizon	Depth (cm)	Description
Ah	0-20	Black (7.5 YR 2.5/1) (moist), clay <u>loam</u> (field), weak to moderate very fine to fine

		sub-angular blocky structure, friable, non-sticky, slightly plastic, few fine sub-rounded and weathered pumic, fine and very few channel and interstitial pores, few to very few very fine to fine roots, no microbial activities, pH 5.0
2Ah1	21-65	Black (7.5 YR 2.5/1), moist, sandy clay (field), weak, fine to medium sub-angular blocky structure, very friable, sticky, plastic, few fine to moderate sub-rounded and weathered pumic, very fine and few channel pores, very few very fine roots, no microbial activities, pH 5.0
2Ah2	65-78	Very dark gray (7.5 YR 3/2), moist, sandy clay (field), very weak fine to medium sub-angular blocky structure, very friable, sticky, plastic, many fine to medium sub-rounded pumic, very fine and few channel pores, very few very fine roots, no microbial activities, pH 5.0
2BA	78-110	Very dark gray (7.5 YR 3/2), moist, <u>sandy clay loam</u> (field), very sticky, very plastic, pH 4.5
2Bt	110-140+	Dark brown (7.5 YR3/4) , moist, <u>sandy clay</u> loam (field), very sticky, very plastic, pH 4.5

Note : Bt2 and Bt3 are examined by angering; disturbed samples taken of all horizons.

Soil profile NAIV/2001/UF-TA/004 Upper wheat field SP 95

Information on soil profile site

Date of examination	October 2, 2001
Authors	Tesfay Alemseged Tesfay
Location	Upper north-western part of the Kijabe Ltd. Wheat Farm on the Ndabibi Plateau; UTM 185480, 9921797 ARC 1960
Elevation	2,246 m above sea level
Geopedological unit	Lf - Higher convex part of undulating mesa belonging to (tilted) step-faulted plateau
Topography	Sloping (9-12 %) with a convex slope form.
Micro-topography	Nil
Parent material	Eburru pumic (Ep), pantellerite & trachyte pumic and ash fall deposits
Land use	Large-scale rainfed wheat (<i>Triticum aestivum</i>) fertilized (young crop in pre-tasseling stage) ; average crop cover >80% of soil surface.
Natural vegetation	Cleared at site but remnants of dry montane forest occur along upper and lower boundary of wheat plot.

General information on soil profile

C) Soil profile description

Classification (WRB 1998)

Human influence	Clearing of vegetation and wheat cultivation; fertilization and pesticide application on crop
Effective depth	180+ cm
Rock outcrops / surface stoniness	Nil
Evidence of erosion	Slight/sheet
Sealing / crusting	None
Cracks
Drainage (natural) class	Well drained
Internal drainage	Never saturated, well drained
External drainage	Neither receiving nor shedding water
Depth of ground water table	Below 1.50 m
Moisture condition	Moist throughout

Horizon	Depth (cm)	Description
Ah	0-17	Black (7.5 YR 2.5/1) (moist), <u>clay loam</u> (field), weak, fine to medium sub-angular blocky structure, very friable, sticky, plastic, few fine to moderate sub-rounded and weathered pumic, very fine and few channel pores, very few very fine roots, no microbial activities, pH 5.0
2Ah1	17-45	Very dark brown (7.5 YR 5/3), moist, <u>sandy clay</u> (field), weak to moderate very fine to fine sub-angular blocky structure, friable, non-sticky, slightly plastic, few fine sub-rounded and weathered pumic, fine and very few channel and interstitial pores, few to very few very fine to fine roots, no microbial activities, pH 5.5.
2Ah2	45-86	Very dark brown (7.5 YR 5/2), moist, <u>sandy clay</u> (field), weak to moderate very fine to fine sub-angular blocky structure, friable, non-sticky, slightly plastic, few fine sub-rounded and weathered pumic, fine and very few channel and interstitial pores, few to very few very fine to fine roots, no microbial activities, pH 5.5.
2BA	86-120	Very dark gray (7.5 YR 3/1), moist, <u>sandy clay loam</u> (field), non-sticky, slightly plastic, pH 5.5
2Bt	120-150+	Dark brown (7.5 YR3/4), moist, <u>sandy clay loam</u> (field), non-sticky, slightly plastic, pH 5.5

Note : Bt2 and Bt3 are examined by augering; disturbed samples taken of all horizons.

Soil profile NAIV/2001/UF-TA/005 upper wheat field SP 58

Information on soil profile site

Date of examination	October 2, 2001
Authors	Tesfay Alemseged Tesfay.
Location	Upper part of the Kijabe Ltd. Upper Wheat Farm on the Ndabibi Plateau; the central position of the plot, UTM 185111, 9921726 ARC 1960
Elevation	2,252 m above sea level
Geopedological unit	Lf - Higher slightly convex part of undulating mesa belonging to (tilted) step-faulted plateau
Topography	Sloping (7-10 %) with a convex slope form.
Micro-topography	Nil
Parent material	Eburru pumic (Ep), pantellerite & trachyte pumic and ash fall deposits
Land use	Large-scale rainfed wheat (<i>Triticum aestivum</i>) fertilized (young crop in pre-tasseling stage) ; average crop cover >85% of soil surface.
Natural vegetation	Cleared at site but remnants of dry montane forest occur along upper and lower boundaries of the wheat plot.

General information on soil profile

C) Soil profile description

Classification (WRB 1998)

Human influence	Clearing of vegetation and wheat cultivation; fertilization and pesticide application on crop
Effective depth	130+ cm
Rock outcrops / surface stoniness	Nil
Evidence of erosion	None
Sealing / crusting	None
Cracks
Drainage (natural) class	Well drained
Internal drainage	Never saturated, well drained
External drainage	Neither receiving nor shedding water
Depth of ground water table	Below 1.30 m
Moisture condition	Moist throughout

Horizon	Depth (cm)	Description
Ah	0-22	Black (7.5 YR 2.5/1) (moist), <u>clay loam</u> (field), weak, fine to medium sub-angular blocky structure, very friable, sticky, plastic, few fine to moderate sub-rounded and weathered pumic, very fine and few channel pores, very few very fine roots, no microbial activities, pH 6.0
2Ah1	22-42	Black (7.5 YR 2.5/1), moist, <u>sandy loam</u> (field), weak to moderate very fine to fine sub-angular blocky structure, friable, non-sticky, slightly plastic, few fine sub-rounded and weathered pumic, fine and very few channel and interstitial pores, few to very few very fine to fine roots, no microbial activities, pH 5.5
2Ah2	42-75	Very dark gray (7.5 YR 3/1), moist, <u>sandy loam</u> (field), weak to moderate very fine to fine sub-angular blocky structure, friable, non-sticky, slightly plastic, few fine sub-rounded and weathered pumic, fine and very few channel and interstitial pores, few to very few very fine to fine roots, no microbial activities, pH 5.5
2BA	75-110	Very dark gray (7.5 YR 3/1), moist, <u>sandy clay loam</u> (field), slightly sticky, non-plastic, pH 5.5
2Bt	110-130+	Dark brown (7.5 YR3/4), moist, <u>sandy clay loam</u> (field), slightly sticky, non-plastic, pH 6.

Note : Bt2 and Bt3 are examined by augering; disturbed samples taken of all horizons;

Soil profile NAIV/2001/LF-TA/002 lower wheat field sp 4

Information on soil profile site

Date of examination	October 3, 2001
Authors	Tesfay Alemseged Tesfay.
Location	Lower part of the Kijabe Ltd. The depression/ small valley part of the Wheat Farm, Ndabibi Plateau; UTM 186828, 9917731 ARC 1960
Elevation	2,087 m above sea level
Geopedological unit	Lf - Higher convex part of undulating mesa belonging to (tilted) step-faulted plateau
Topography	Sloping (3-5 %) with a concave slope form.
Micro-topography	Nil
Parent material	Eburru pumic (Ep), pantellerite & trachyte pumic and ash fall deposits
Land use	Large-scale rainfed wheat (<i>Triticum aestivum</i>) fertilized (young crop in pre-tasseling stage); average crop cover >90% of soil surface.
Natural vegetation	Cleared at site but remnants of dry montane trees occur along upper boundary of wheat plot.

General information on soil profile

C) Soil profile description

Classification (WRB 1998)

Human influence	Clearing of vegetation and wheat cultivation; fertilization and pesticide application on crop
Effective depth	200+ cm
Rock outcrops / surface stoniness	Nil
Evidence of erosion	None
Sealing / crusting	None
Cracks
Drainage (natural) class	Poorly drained
Internal drainage	Occasionally saturated, weakly drained
External drainage	Receiving seasonal floods and shedding.
Depth of ground water table	Below 2 m
Moisture condition	Moist throughout

Horizon	Depth (cm)	Description
Ah	0-19	Dark brown (7.5 YR 3/4) (moist), <u>sandy clay loam</u> (field), weak to moderate fine sub-angular blocky structure, friable, non-sticky, slightly plastic, few fine sub-rounded and weathered pumic, fine and very few channel and interstitial pores, few to very few very fine to fine roots, no microbial activities, pH 5.5; Abrupt smooth boundary to
2Ah1	19-68	Strong brown (7.5 YR 5/6), moist, <u>clay loam</u> (field), weak, fine to medium sub-angular blocky structure, very friable, sticky, plastic, few fine to moderate sub-rounded and weathered pumic, very fine and few channel pores, very few very fine roots, no microbial activities, pH 6. Abrupt smooth boundary to
2Ah2	68-97	Strong Brown (7.5 YR 4/6), moist, <u>clay loam</u> (field), very weak fine to medium sub-angular blocky structure, very friable, sticky, plastic, many fine to medium sub-rounded fresh pumic gravels, very fine and few channel pores, very few very fine roots, no microbial activities, pH 6. Abrupt smooth boundary to
2BA	97-135	Brown (7.5 YR 5/2), moist, <u>sandy clay</u> (field), slightly sticky, non plastic, pH 5.5
2Bt	135-200+	Brown (7.5 YR 5/2), moist, <u>sandy clay</u> (field), very sticky, non plastic, pH 5.5

Note : Bt2 and Bt3 are examined by augering; disturbed samples taken of all horizons.

Additional remarks: When receiving higher depth of precipitation and due to the concave structure of the contours in the depression (small valley), this part of the lower wheat field is usually exposed to water logging problems.

The depth of the profile is very deep, it is mainly composed of alluvial deposits rich in organic materials in the upper 30 cm, the main parent material of the soil is a volcanic tuff erupted from the near by volcanoes, modified by the water erosion and cattle grazing, this zone of the Kijabe field is the oldest one of the initially deforested plots for cattle grazing and crop production, Due to its topographic nature i.e. depression and concave shape of the contours, the soil color and texture is entirely different from the adjoining plots across the small valley.

Soil profile NAIV/2001/LF-TA/003 Lower wheat field SP 17

Information on soil profile site

Date of examination	September 31, 2001
Authors	Tesfay Alemseged Tesfay.
Location	Lower part of the Kijabe Ltd. Wheat Farm on the Ndabibi Plateau, opposite to the pin trees; UTM 186549, 9917527 ARC 1960
Elevation	2,094 m above sea level
Geopedological unit	Lf - Higher convex part of undulating mesa belonging to (tilted) step-faulted plateau
Topography	Sloping (5-10 %) with a convex slope form.
Micro-topography	Nil
Parent material	Eburru pumic (Ep), pantellerite & trachyte pumic and ash fall deposits
Land use	Large-scale rainfed wheat (<i>Triticum aestivum</i>) fertilized (young crop in pre-teaseling stage); average crop cover >90% of soil surface.
Natural vegetation	Cleared at site but remnants of dry montane forest dispersed through out the plot.

General information on soil profile

C) Soil profile description

Classification (WRB)

Human influence	Clearing of vegetation and wheat cultivation; fertilization and pesticide application on crop
Effective depth	130+ cm
Rock outcrops / surface stoniness	Nil moderate
Evidence of erosion	sheet
Sealing / crusting	Highly crusted
Cracks
Drainage (natural) class	Well drained
Internal drainage	Never saturated, well drained
External drainage	Neither receiving nor shedding water
Depth of ground water table	Below 1.20 m
Moisture condition	Dry and hard throughout

Horizon	Depth (cm)	Description
Ah	0-15	Light brown (7.5 YR 6/4) (dry), gravely <u>sandy loam</u> (field), weak to moderate very fine to fine sub-angular blocky structure, friable, non-sticky, slightly plastic, few fine sub-rounded and weathered pumic, fine and very few channel and interstitial pores, few to very few very fine to fine roots, no microbial activities, pH 5.0
2Ah1	21-55	Strong brown (7.5 YR 5/6), slightly moist, <u>clay loam</u> (field), weak, fine to medium sub-angular blocky structure, very friable, sticky, plastic, few fine to moderate sub-rounded and weathered pumic, very fine and few channel pores, very few very fine roots, no microbial activities, pH 4.5.
2BA	55-88	Brown (7.5 YR 5/3), dry, gravely <u>sandy clay</u> (field), non sticky, non plastic, Fresh pumic gravel; no roots pH 4.5
2Bt	88-120+	Gray (7.5 YR5/1), dry, gravely <u>sandy clay</u> (field), non sticky, on plastic, fresh pumic gravel; no roots, pH 4.5.

Note : Bt2 and Bt3 are examined by augering; disturbed samples taken of all horizons;

Appendix B Statistical methods

Principal components analysis: In a multivariate statistical analysis (parameters) principal component analysis is helpful to understand the underlying data structure and/or form a smaller number of uncorrelated variables (for example, to avoid multicollinearity, potential over fitting in regression). "Principal components computed using the correlation matrix is preferably used to test whether it makes sense to standardize variables (the usual choice when variables are measured by different scales)". More over, it is required to understand the underlying data structure before performing principal components analysis i.e. correlation matrix is used to standardize the measurements if they are not measured with the same scale.

Regression analysis: is used to investigate and model the relationship between a response variable and one or more predictors. Minitab software by VIA technologies, inc. USA, provides various least squares and logistic regression procedures,

- Least-squares procedure is applicable when the response variable is continuous.
- Logistic regression is useful when the response variable is categorical.

"Both least-squares and logistic regression methods estimate parameters in the model so that the fit of the model is optimized. Least squares minimize the sum of squared errors to obtain parameter estimates. Where as Minitab's logistic regression commands obtain maximum likelihood estimates of the parameters".

Stepwise regression: removes and adds variables to the regression model for the purpose of identifying a useful subset of the predictors. Minitab provides three commonly used procedures: standard stepwise regression (adds and removes variables), forward selection (adds variables), and backward elimination (removes variables).

Analysis of Variance (ANOVA) technique computes a confidence interval and performs a hypothesis test for the equality, or homogeneity, of variance of two samples. ANOVA is a statistical method commonly used for determining whether the means of two or more data sets, with each group in a separate column are equal or not. One-way unstacked ANOVA is an appropriate method of performing a multiple comparison for data sets of different size.

Application of Geo-statistics: Soils vary both in space and time. Knowledge about the soil spatial variability is a crucial element to quantify the pedogenic concepts and better understand the causal factors of soil distribution patterns and landscape evolution (Wilding and Drees, 1983).

Several techniques have been devised to quantify / estimate spatial variability. But, there is no theoretical answer to which estimator is best. One has to check against the validation. "Geo-statistics is basically a technology for estimating the values at unsampled places of properties that vary in space, whether in one, two or three dimensions, from more or less pairs sample data" (Webster and Oliver, 1990).

"The semi-variogram is the basic geo-statistical tool for visualizing, modeling and exploiting the spatial autocorrelation of a regionalized variable. As the name implies, the semi-variance is a measure of variance. A straightforward way of measuring how a variable z changes in value between site x and a site $(x+h)$ a distance h apart is the following relation" (Meer, 1999).

$$\gamma^*(h) = \frac{\sum \{z(x) - z(x+h)\}^2}{2n}$$

Where $\gamma^*(h)$ is the semi variance for distance h .

Kriging technique is a method of estimating values of regionalized variables at unvisited sites based on the knowledge of the data at hand. Estimated values in Kriged surface of a certain unvisited point is a result of a linear sum of the data but in which the data carry different weights according to their positions in relation to the unknown point to one another. The development of an appropriate variogram model requires numerous correct decisions. These decisions can only be properly addressed with an intimate knowledge of the data at hand, and a competent understanding of the data genesis (i.e. the underlying processes from which the data are drawn). Among the various methods of estimating values at unvisited sites, linear Kriging, trend surface, moving average and nearest point are commonly used ones.

Surfer's default linear variogram takes the form: $\gamma_{(h)} = C_o + S * h$

Where C_o : is the unknown nugget effect, and
 S : is the unknown slope.

Solving for these two unknown parameters is performed using two defining equations. According to theory, the expected value of the sample variance is the average value of the variogram between all possible pairs of sample locations (Barnes, 1991); this yields one equation. Equating the experimental sample variogram for nearest neighbors to the modeled variogram generates the second equation.

Thus, it can be defined as: $Var = C_o + S * D_{avg}$
 $G_{nn} = C_o + S * D_{nn}$

Where D_{nn} = average distance to the nearest neighbors.
 D_{avg} = average inter-sample separation distance.
 G_{nn} = one half the averaged squared difference between nearest neighbors.
 Var = sample variance.

Solving the two equations for the two unknown parameters, and checking for unreasonable values, gives the following final formulae (used in Surfer 7 software).

$$S = \max \left[\frac{Var - G_{nn}}{D_{avg} - D_{nn}}, 0 \right] \qquad C_o = \max \left[\frac{G_{nn} * D_{avg} - Var * D_{nn}}{D_{avg} - D_{nn}}, 0 \right]$$

Appendix C. Naivasha weather data (Temperature and wind speed graphs)

Figure * Wind speed Record (May 18, 2000), source Oserian farm Naivasha.

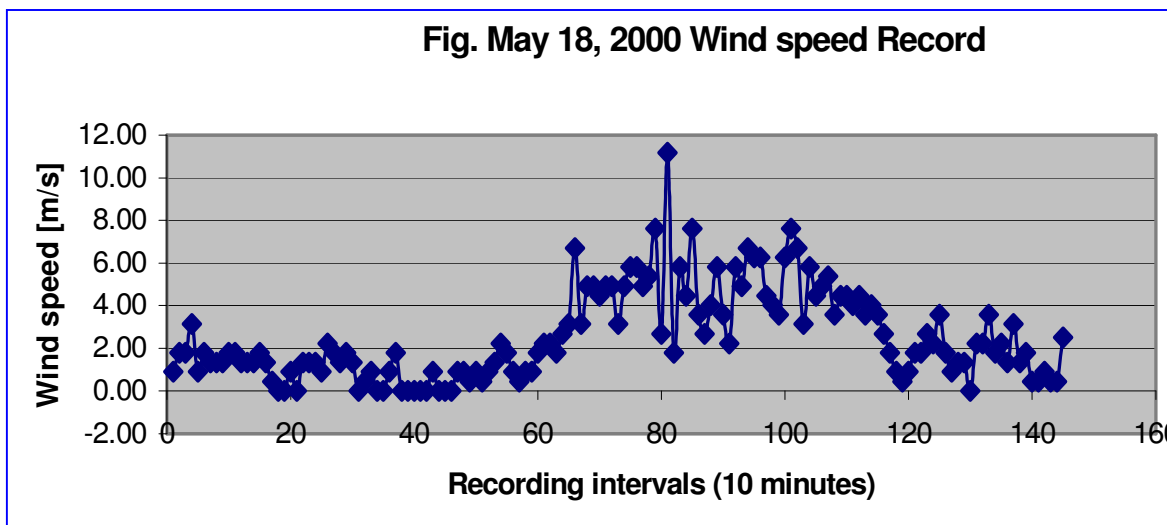


Figure 51 Temperature, Relative humidity and wind speed, source Oserian farm Naivasha.

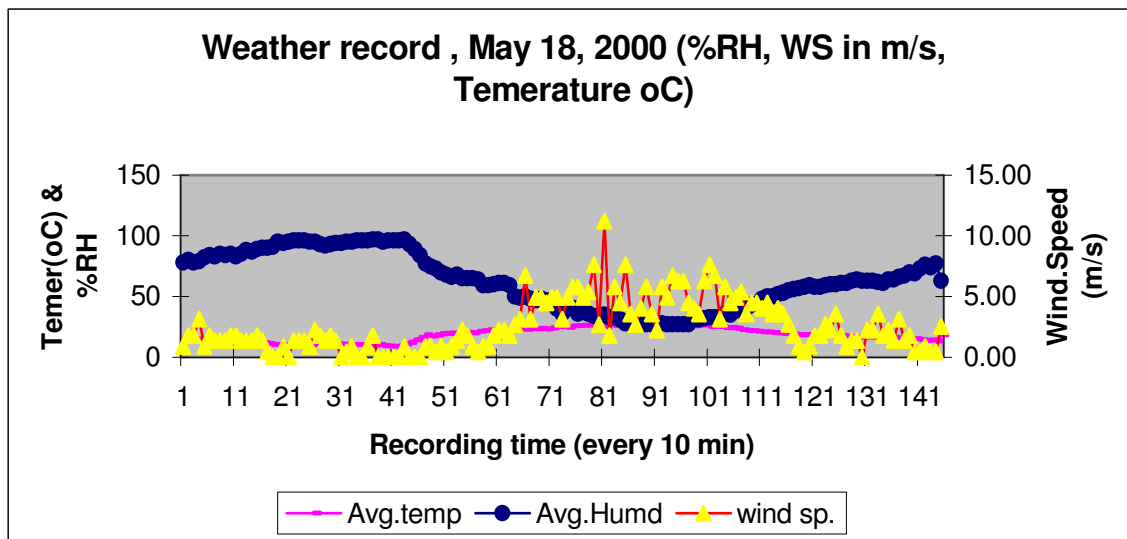
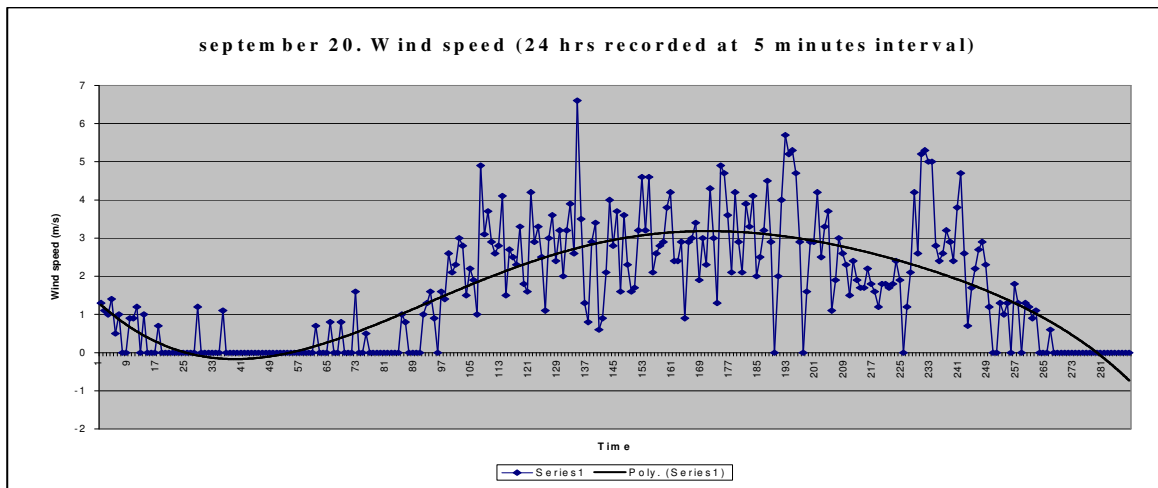


Figure 52 Fieldwork time wind speed record (sept. 20, 2001), source Oserian farm Naivasha



Appendix D LANDSAT-ETM+ Image Preprocessing

a) Characteristics of the LANDSAT system

LANDSAT 7 was launched on April 15, 1999 from the Western Test Range at Vandenberg Air Force Base on a Delta-II launch vehicle. ETM+ instrument is an eight-band multispectral scanning radiometer capable of providing high-resolution image information of the Earth's surface. It detects spectrally-filtered radiation at visible, near-infrared, short-wave, and thermal infrared frequency bands from the sun-lit Earth. Nominal ground sample distances or "pixel" sizes are (15 meters) in the panchromatic band; (30 meters) in the 6 visible, near and short-wave infrared bands; (60 meters) in the thermal infrared band. The satellite orbits the Earth at an altitude of approximately (705 kilometers) with a sun-synchronous 98-degree inclination and a descending equatorial crossing time of 10 a.m. A three-axis attitude control subsystem stabilizes the satellite and keep the instrument pointed toward Earth to within 0.05 degrees.

The Landsat-7 system operates in a sun-synchronous orbit with an orbit track repeat cycle of 16 days completing 233 orbits.

b) Bandwidths in nanometers

TM AND ETM+ SPECTRAL BANDWIDTHS								
Bandwidth (μ) Full Width - Half Maximum								
Sensor	Band 1	Band 2	Band 3	Band 4	Band 5	Band 6	Band 7	Band 8
TM	0.45 - 0.52	0.52 - 0.60	0.63 - 0.69	0.76 - 0.90	1.55 - 1.75	10.4 - 12.5	2.08 - 2.35	N/A
ETM+	0.45 - 0.52	0.53 - 0.61	0.63 - 0.69	0.78 - 0.90	1.55 - 1.75	10.4 - 12.5	2.09 - 2.35	.52 - .90

c) Nominal orbit parameters for the Landsat-7 spacecraft include:

Parameter	Value
Launch Date:	April 15, 1999
Orbit:	Sun Synchronous, Near Polar
Nominal Altitude:	705 Kilometers, Near Circular
Inclination:	98.2 Degrees
Nodal Period:	98.8 Minutes
Equatorial Crossing Time:	10:00 a.m., Local (Descending)

For ETM+ bands, the following values of $E_{sun\lambda_i}$ have been given by Markham and Barker (1987):

d) $E_{sun\lambda_i}$ values in watts/(meter squared*micro.m)

Band 1	Band 2	Band 3	Band 4	Band 5	Band 7	Band 8
1970	1843	1555	1047	227.1	80.53	1368

Appendix E Field data (upper and lower fields) a) upper field

Easting	Northing	Elv masl	ETa [mm/d]	NDVI_gr	pH_10cm	pH_30cm	EC 10cm	EC 30cm	Bd 10-20 cm	Bd 40-50	Ks cm/d	ds=Ah	slop %	%OM_10	%OM ₃₀	%OM_70
184658	9921489	2260	4.18	0.41524	5.9	6.17	744	577	*	*	*	*	*	*	*	*
184927	9921691	2258	4.15	0.43772	6.15	6.25	864	724	*	*	*	*	*	*	*	*
184873	9921761	2263	4.52	0.46554	6.26	6.28	1118	876	*	*	*	*	*	*	*	*
184943	9921814	2264	4.89	0.49749	6.26	6.45	1092	880	*	*	*	*	*	*	*	*
184892	9921878	2266	4.86	0.51523	6.55	6.53	1077	968	*	*	*	*	*	*	*	*
184962	9921931	2268	4.5	0.44618	6.55	6.54	877	654	*	*	*	*	*	*	*	*
184979	9922052	2275	4.8	0.45757	6.27	6.24	919	723	*	*	*	*	*	*	*	*
184976	9921626	2252	4.2	0.45082	6.05	6.28	827	712	*	*	*	*	*	*	*	*
184991	9921743	2256	4.8	0.45324	6.25	6.35	757	585	*	*	*	*	*	*	*	*
185063	9921795	2258	4.54	0.4111	6.15	6.32	611	524	*	*	*	*	*	*	*	*
185182	9921777	2257	4.15	0.43288	6.1	6.23	677	565	*	*	*	*	*	*	*	*
184607	9921559	2263	4.71	0.44638	5.95	6.19	789	641	*	*	*	*	*	*	*	*
185125	9921847	2262	4.67	0.42582	5.75	6.24	822	656	*	*	*	*	*	*	*	*
185195	9921902	2263	4.59	0.45525	6.07	6.2	729	634	*	*	*	*	*	*	*	*
185146	9921962	2267	4.94	0.45757	6	6.36	909	754	*	*	*	*	*	*	*	*
185214	9922018	2269	4.77	0.44865	5.9	6.26	875	688	*	*	*	*	*	*	*	*
185025	9921979	2270	4.82	0.49769	6.47	6.43	896	772	*	*	*	*	*	*	*	*
184677	9921609	2264	4.82	0.46412	6.25	6.25	769	605	0.92	1.11	44.6	20	6	11.25	9.41	3.81
184724	9921540	2261	4.64	0.44427	6.15	6.21	726	567	*	*	*	*	*	*	*	*
184792	9921593	2262	4.17	0.44225	5.75	5.95	546	476	*	*	*	*	*	*	*	*
184809	9921708	2263	4.2	0.45707	6	6.15	941	498	*	*	*	*	*	*	*	*
184757	9921780	2255	4.66	0.45294	6.09	6.22	742	651	*	*	*	*	*	*	*	*
184826	9921829	2266	4.68	0.46796	6.16	6.22	1106	814	*	*	*	*	*	*	*	*
184847	9921949	2274	4.63	0.50565	5.85	6.17	979	687	*	*	*	*	*	*	*	*
184876	9921336	2240	2.24	0.31645	5.68	6.18	1129	1163	*	*	*	*	*	*	*	*
185382	9921505	2234	2.07	0.29881	5.45	5.96	672	565	*	*	*	*	*	*	*	*
185335	9921575	2231	2.72	0.34206	5.66	5.99	934	922	*	*	*	*	*	*	*	*
185401	9921624	2230	2.59	0.35929	6.25	6.53	585	378	*	*	*	*	*	*	*	*
185451	9921556	2226	2.26	0.2975	6.06	6.64	1242	898	*	*	*	*	*	*	*	*
185463	9921676	2227	2.67	0.36978	6.16	6.62	635	445	*	*	*	*	*	*	*	*
185537	9921720	2234	2.48	0.33339	6.17	6.4	591	421	*	*	*	*	*	*	*	*
185480	9921797	2246	2.73	0.37633	6.26	5.95	652	465	0.9	1.06	48.9	17	9	4.8	7.42	*
184994	9921318	2242	2.63	0.34165	5.9	6.03	1107	1034	*	*	*	*	*	*	*	*
184941	9921386	2244	2.47	0.35012	6.1	6.33	1152	1275	*	*	*	*	*	*	*	*
185094	9921186	2229	2.57	0.30678	5.48	5.98	478	376	*	*	*	*	*	*	*	*
185045	9921252	2230	2.72	0.34206	5.85	6.37	514	382	*	*	*	*	*	*	*	*
185112	9921301	2236	2.54	0.30869	5.79	6.22	620	396	*	*	*	*	*	*	*	*
185056	9921370	2240	2.34	0.31585	5.59	6.12	600	460	*	*	*	*	*	*	*	*
185246	9921402	2234	2.36	0.37381	5.45	5.96	420	375	*	*	*	*	*	*	*	*
185194	9921474	2249	2.39	0.33329	6.02	6.49	556	418	*	*	*	*	*	*	*	*
184490	9921569	2263	3.12	0.40012	6.15	6.37	749	662	0.84	1.02	39.6	20	5	9.24	7.6	*
184893	9921455	2241	3.01	0.37461	5.95	6.22	795	678	*	*	*	*	*	*	*	*
184836	9921524	2254	3.68	0.40385	6	5.93	482	384	*	*	*	*	*	*	*	*
184910	9921572	2243	3.69	0.42562	5.77	5.92	456	394	*	*	*	*	*	*	*	*
184859	9921642	2256	3.8	0.43388	6	6.19	989	661	0.89	1.17	45.2	19	5	11.1	8.12	4.54
185002	9921441	2244	3.1	0.37542	5.65	5.89	628	547	*	*	*	*	*	*	*	*
184959	9921507	2248	3.37	0.40516	5.9	6.14	834	642	*	*	*	*	*	*	*	*
185027	9921560	2240	3.59	0.40203	6.2	6.57	748	660	*	*	*	*	*	*	*	*
185043	9921670	2248	3.37	0.40949	6.34	6.37	724	637	*	*	*	*	*	*	*	*

EXPLAINING SATELLITE-DERIVED ACTUAL EVAPOTRANSPIRATION PATTERNS IN HOMOGENEOUSLY CROPPED LARGE FIELDS

Easting	Northing	Elv masl	Eta [mm/d]	NDVI_gr	pH_10cm	pH_30cm	EC 10cm	EC 30cm	Bd 10-20 cm	Bd 40-50 cm	Ks cm/d	ds=Ah	slop %	%OM_10	%OM30	%OM_70
185077	9921488	2246	3.05	0.35879	6.55	6.627	984	706	*	*	*	*	*	*	*	*
185145	9921541	2247	3.58	0.36615	6.45	6.46	1079	782	1.14	1.22	48.6	21	5	7.38	6.4	4.11
184557	9921624	2265	3.93	0.43388	6.46	6.61	733	641	*	*	*	*	*	*	*	*
185092	9921607	2245	3.57	0.38963	6.45	6.55	838	687	*	*	*	*	*	*	*	*
185166	9921659	2250	3.24	0.39185	6	6.16	768	667	*	*	*	*	*	*	*	*
185111	9921726	2252	3.81	0.39306	6.1	6.46	587	502	0.91	1.12	43.7	22	7	13.22	10.17	4.57
185269	9921524	2247	3.17	0.34165	5.71	6.35	557	442	*	*	*	*	*	*	*	*
185213	9921590	2246	3.16	0.36615	5.91	6.35	715	648	*	*	*	*	*	*	*	*
185287	9921643	2246	3.27	0.37461	5.96	6.39	674	530	*	*	*	*	*	*	*	*
185226	9921711	2251	3.36	0.37461	5.98	6.17	706	565	*	*	*	*	*	*	*	*
185302	9921760	2252	3.1	0.37381	6	6.13	642	541	0.87	1.02	31.5	19	9	9.27	7.84	3.05
185247	9921826	2260	3.97	0.42229	6.15	6.36	987	668	*	*	*	*	*	*	*	*
185317	9921879	2259	3.64	0.42229	6.05	6.12	1025	786	*	*	*	*	*	*	*	*
184623	9921680	2255	3.91	0.43096	6.21	6.34	1138	882	*	*	*	*	*	*	*	*
185263	9921947	2260	3.91	0.42582	6.16	6.53	867	640	*	*	*	*	*	*	*	*
185335	9922001	2259	3.57	0.39185	6.03	6.16	792	625	*	*	*	*	*	*	*	*
185349	9921694	2246	3.21	0.38318	5.91	6.35	584	526	*	*	*	*	*	*	*	*
185418	9921745	2245	3.06	0.39306	6.14	6.29	562	479	*	*	*	*	*	*	*	*
185370	9921813	2249	3.7	0.40657	6.19	6.04	892	716	*	*	*	*	*	*	*	*
185435	9921862	2251	3.37	0.4111	5.85	6.22	1320	1033	*	*	*	*	*	*	*	*
185385	9921934	2256	3.21	0.3852	6.22	6.14	755	653	*	*	*	*	*	*	*	*
185554	9921845	2245	3.56	0.41856	6.28	6.16	735	686	*	*	*	*	*	*	*	*
184688	9921725	2259	3.83	0.42401	6.21	6.38	1254	856	*	*	*	*	*	*	*	*
184708	9921419	2247	3.84	0.40062	6.12	6.33	931	775	*	*	*	*	*	*	*	*
184776	9921472	2248	3.56	0.42058	6.02	6.15	739	568	*	*	*	*	*	*	*	*
184743	9921661	2258	3.97	0.42229	6.42	6.35	963	785	*	*	*	*	*	*	*	*
184775	9921897	2269	3.17	0.41745	6.35	6.36	794	634	*	*	*	*	*	*	*	*
184825	9921404	2240	3.21	0.38217	5.92	6.05	758	625	*	*	*	*	*	*	*	*
185057	9922166	2272	5.67	0.54396	6.41	6.35	422	416	*	*	41.6	*	*	13.17	11.31	5.33
185008	9921859	2268	5.1	0.46937	5.96	6.3	1212	985	*	*	43.9	*	*	9.2	12.35	*
185080	9921910	2270	5.06	0.44396	6.35	6.2	1088	867	0.76	0.98	39.2	22	6	12.43	10.25	6.94
185049	9922098	2273	5.4	0.50696	6.32	6.34	862	745	0.84	0.98	31.5	23	5	9.73	7.22	*
184989	9922105	2274	5.31	0.5242	6.19	6.25	769	687	*	*	33.8	*	*	9.73	7.22	*
185108	9922092	2272	5.64	0.4856	6.46	6.236	755	596	*	*	35.5	*	*	9.83	7.52	*
185163	9922082	2274	5.3	0.51856	6.2	6.32	684	368	*	*	30.6	*	*	9.73	7.22	*
185096	9922033	2274	5.35	0.47945	6.43	6.42	832	747	0.72	0.9	27.3	21	4	8.24	10.24	4.84
185083	9921970	2271	5.39	0.49765	6.45	6.44	872	736	*	*	31.4	*	*	9.73	7.22	*
185010	9921859	2270	5.1	0.45324	6.36	6.28	921	791	0.82	0.92	31.6	*	7	8.62	8.43	5.15
184911	9921999	2274	5	0.5119	5.84	5.98	928	771	*	*	*	*	*	*	*	*
185148	9921114	2220	1.81	0.26333	5.99	6.13	466	552	*	*	36.9	*	*	7.64	4.27	*
185216	9921167	2222	1.51	0.26192	5.64	5.89	921	903	1.22	1.27	37.2	18	8	5.82	5.31	2.92
185164	9921231	2224	1.97	0.29942	5.85	5.94	552	485	*	*	40.3	*	*	7.74	5.67	*
184932	9921268	2237	1.99	0.34125	5.44	6.1	580	478	*	*	48.6	*	*	7.74	5.67	*
185314	9921456	2236	1.51	0.30819	5.4	6.18	1071	955	*	*	44.6	*	*	4.64	5.14	*
185520	9921609	2237	1.78	0.33349	5.44	6.16	484	442	*	*	42.4	*	*	6.22	4.67	*
185129	9921420	2248	1.65	0.30819	5.6	6.19	1230	1068	1.13	1.16	46.2	23	6	6.14	7.06	2.94
185231	9921288	2230	1.79	0.32482	5.43	6.18	1049	1096	0.98	1.04	44.5	13	8	5.26	7.24	5.22
185178	9921354	2235	1.76	0.31645	5.74	5.84	894	668	1.08	1.13	40.5	16	10	4.91	6.61	3.92
185294	9921334	2233	1.88	0.32492	5.62	6	928	1178	*	*	47.1	*	*	7.64	5.57	*
185367	9921388	2232	0.58	0.24519	5.42	5.92	452	472	*	*	48.3	*	*	4.62	4.11	*

EXPLAINING SATELLITE-DERIVED ACTUAL EVAPOTRANSPIRATION PATTERNS IN HOMOGENEOUSLY CROPPED LARGE FIELDS

Eastings	Northing	Elv masl	ETa [mm/d]	NDVI gr	Ca10 (me/100g)	Ca30 (me/100g)	K10 (me/100g)	K30 (me/100g)	Mg10 (me/100g)	Mg30 (me/100g)	Na10 (me/100g)	Na30 (me/100g)	% sand	Ca:Mg 10	Ca:Mg 30	% sand
184658	9921489	2260	4.18	0.41524	*	*	*	*	*	*	*	*	*			*
184927	9921691	2258	4.15	0.43772	*	*	*	*	*	*	*	*	*			*
184873	9921761	2263	4.52	0.46554	*	*	*	*	*	*	*	*	*			*
184943	9921814	2264	4.89	0.49749	*	*	*	*	*	*	*	*	*			*
184892	9921878	2266	4.86	0.51523	*	*	*	*	*	*	*	*	*			*
184962	9921931	2268	4.5	0.44618	*	*	*	*	*	*	*	*	*			*
184979	9922052	2275	4.8	0.45757	*	*	*	*	*	*	*	*	*			*
184976	9921626	2252	4.2	0.45082	*	*	*	*	*	*	*	*	*			*
184991	9921743	2256	4.8	0.45324	*	*	*	*	*	*	*	*	*			*
185063	9921795	2258	4.54	0.4111	*	*	*	*	*	*	*	*	*			*
185182	9921777	2257	4.15	0.43288	*	*	*	*	*	*	*	*	*			*
184607	9921559	2263	4.71	0.44638	*	*	*	*	*	*	*	*	*			*
185125	9921847	2262	4.67	0.42582	*	*	*	*	*	*	*	*	*			*
185195	9921902	2263	4.59	0.45525	*	*	*	*	*	*	*	*	*			*
185146	9921962	2267	4.94	0.45757	*	*	*	*	*	*	*	*	*			*
185214	9922018	2269	4.77	0.44865	*	*	*	*	*	*	*	*	*			*
185025	9921979	2270	4.82	0.49769	*	*	*	*	*	*	*	*	*			*
184677	9921609	2264	4.82	0.46412	1.212	0.824	0.97	0.758	0.172	0.15	0.354	0.319	22.4	7.05	5.49	22.4
184724	9921540	2261	4.64	0.44427	*	*	*	*	*	*	*	*	*			*
184792	9921593	2262	4.17	0.44225	*	*	*	*	*	*	*	*	*			*
184809	9921708	2263	4.2	0.45707	*	*	*	*	*	*	*	*	*			*
184757	9921780	2255	4.66	0.45294	*	*	*	*	*	*	*	*	*			*
184826	9921829	2266	4.68	0.46796	*	*	*	*	*	*	*	*	*			*
184847	9921949	2274	4.63	0.50565	*	*	*	*	*	*	*	*	*			*
184876	9921336	2240	2.24	0.31645	*	*	*	*	*	*	*	*	*			*
185382	9921505	2234	2.07	0.29881	*	*	*	*	*	*	*	*	*			*
185335	9921575	2231	2.72	0.34206	*	*	*	*	*	*	*	*	*			*
185401	9921624	2230	2.59	0.35929	*	*	*	*	*	*	*	*	*			*
185451	9921556	2226	2.26	0.2975	*	*	*	*	*	*	*	*	*			*
185463	9921676	2227	2.67	0.36978	*	*	*	*	*	*	*	*	*			*
185537	9921720	2234	2.48	0.33339	*	*	*	*	*	*	*	*	*			*
185480	9921797	2246	2.73	0.37633	0.66	0.518	0.524	0.491	0.102	0.108	0.318	0.3	23.32	6.47	4.80	23.32
184994	9921318	2242	2.63	0.34165	*	*	*	*	*	*	*	*	*			*
184941	9921386	2244	2.47	0.35012	*	*	*	*	*	*	*	*	*			*
185094	9921186	2229	2.57	0.30678	*	*	*	*	*	*	*	*	*			*
185045	9921252	2230	2.72	0.34206	*	*	*	*	*	*	*	*	*			*
185112	9921301	2236	2.54	0.30869	*	*	*	*	*	*	*	*	*			*
185056	9921370	2240	2.34	0.31585	*	*	*	*	*	*	*	*	*			*
185246	9921402	2234	2.36	0.37381	*	*	*	*	*	*	*	*	*			*
185194	9921474	2249	2.39	0.33329	*	*	*	*	*	*	*	*	*			*
184490	9921569	2263	3.12	0.40012	0.91	0.742	0.734	0.662	0.098	0.096	0.163	0.324	22	9.29	7.73	22
184893	9921455	2241	3.01	0.37461	*	*	*	*	*	*	*	*	*			*
184836	9921524	2254	3.68	0.40385	*	*	*	*	*	*	*	*	*			*
185002	9921441	2244	3.1	0.37542	*	*	*	*	*	*	*	*	*			*
184959	9921507	2248	3.37	0.40516	*	*	*	*	*	*	*	*	*			*
185027	9921560	2240	3.59	0.40203	*	*	*	*	*	*	*	*	*			*

EXPLAINING SATELLITE-DERIVED ACTUAL EVAPOTRANSPIRATION PATTERNS IN HOMOGENEOUSLY CROPPED LARGE FIELDS

Easting	Northing	Elv masl	ETa [mm/d]	NDVI gr	Ca10 (me/100g)	Ca30 (me/100g)	K10 (me/100g)	K30 (me/100g)	Mg10 (me/100g)	Mg30 (me/100g)	Na10 (me/100g)	Na30 (me/100g)	% sand	Ca:Mg 10	Ca:Mg 30	% sand
184859	9921642	2256	3.8	0.43388	1.062	0.554	0.827	0.521	0.164	0.108	0.29	0.311	26.5	6.48	5.13	26.5
185043	9921670	2248	3.37	0.40949	*	*	*	*	*	*	*	*	*	*	*	*
185077	9921488	2246	3.05	0.35879	*	*	*	*	*	*	*	*	*	*	*	*
185145	9921541	2247	3.58	0.36615	1.23	1.102	1.012	0.564	0.184	0.116	0.342	0.419	25.48	6.68	9.50	25.48
184557	9921624	2265	3.93	0.43388	*	*	*	*	*	*	*	*	*	*	*	*
185092	9921607	2245	3.57	0.38963	*	*	*	*	*	*	*	*	*	*	*	*
185166	9921659	2250	3.24	0.39185	*	*	*	*	*	*	*	*	*	*	*	*
185111	9921726	2252	3.81	0.39306	0.672	0.838	0.59	0.623	0.124	0.095	0.177	0.307	26.8	5.42	8.82	26.8
185269	9921524	2247	3.17	0.34165	*	*	*	*	*	*	*	*	*	*	*	*
185213	9921590	2246	3.16	0.36615	*	*	*	*	*	*	*	*	*	*	*	*
185287	9921643	2246	3.27	0.37461	*	*	*	*	*	*	*	*	*	*	*	*
185226	9921711	2251	3.36	0.37461	*	*	*	*	*	*	*	*	*	*	*	*
185302	9921760	2252	3.1	0.37381	0.888	0.668	0.639	0.577	0.1	0.096	0.266	0.298	23.5	8.88	6.96	23.5
185247	9921826	2260	3.97	0.42229	*	*	*	*	*	*	*	*	*	*	*	*
185317	9921879	2259	3.64	0.42229	*	*	*	*	*	*	*	*	*	*	*	*
184623	9921680	2255	3.91	0.43096	*	*	*	*	*	*	*	*	*	*	*	*
185263	9921947	2260	3.91	0.42582	*	*	*	*	*	*	*	*	*	*	*	*
185335	9922001	2259	3.57	0.39185	*	*	*	*	*	*	*	*	*	*	*	*
185349	9921694	2246	3.21	0.38318	*	*	*	*	*	*	*	*	*	*	*	*
185418	9921745	2245	3.06	0.39306	*	*	*	*	*	*	*	*	*	*	*	*
185370	9921813	2249	3.7	0.40657	*	*	*	*	*	*	*	*	*	*	*	*
185435	9921862	2251	3.37	0.4111	*	*	*	*	*	*	*	*	*	*	*	*
185385	9921934	2256	3.21	0.3852	*	*	*	*	*	*	*	*	*	*	*	*
185554	9921845	2245	3.56	0.41856	*	*	*	*	*	*	*	*	*	*	*	*
184688	9921725	2259	3.83	0.42401	*	*	*	*	*	*	*	*	*	*	*	*
184708	9921419	2247	3.84	0.40062	*	*	*	*	*	*	*	*	*	*	*	*
184776	9921472	2248	3.56	0.42058	*	*	*	*	*	*	*	*	*	*	*	*
184743	9921661	2258	3.97	0.42229	*	*	*	*	*	*	*	*	*	*	*	*
184775	9921897	2269	3.17	0.41745	*	*	*	*	*	*	*	*	*	*	*	*
184825	9921404	2240	3.21	0.38217	*	*	*	*	*	*	*	*	*	*	*	*
185057	9922166	2272	5.67	0.54396	0.896	0.594	0.752	0.593	0.134	0.116	0.274	0.365	25.7	6.69	5.12	25.7
185008	9921859	2268	5.1	0.46937	0.902	0.652	0.816	0.612	0.15	0.142	0.274	0.365	*	6.01	4.59	*
185080	9921910	2270	5.06	0.44396	0.902	0.652	0.816	0.612	0.15	0.142	0.274	0.365	25.7	6.01	4.59	25.7
185049	9922098	2273	5.4	0.50696	0.896	0.594	0.752	0.593	0.134	0.12	0.274	0.365	25.7	6.69	4.95	25.7
184989	9922105	2274	5.31	0.5242	0.896	0.594	0.752	0.593	0.134	0.12	0.274	0.365	*	6.69	4.95	*
185108	9922092	2272	5.64	0.4856	0.896	0.594	0.752	0.593	0.134	0.12	0.274	0.365	*	6.69	4.95	*
185163	9922082	2274	5.3	0.51856	0.896	0.594	0.752	0.593	0.134	0.12	0.274	0.365	*	6.69	4.95	*
185096	9922033	2274	5.35	0.47945	0.902	0.652	0.816	0.612	0.15	0.142	0.197	0.289	25.7	6.01	4.59	25.7
185083	9921970	2271	5.39	0.49765	0.902	0.652	0.816	0.612	0.15	0.142	0.197	0.289	*	6.01	4.59	*
185010	9921859	2270	5.1	0.45324	0.902	0.652	0.816	0.612	0.15	0.142	0.197	0.289	25.7	6.01	4.59	25.7
184911	9921999	2274	5	0.5119	0.728	0.538	0.559	0.361	0.142	0.1	0.273	0.299	*	5.13	5.38	*
185148	9921114	2220	1.81	0.26333	0.456	0.372	0.576	0.461	0.126	0.106	0.314	0.382	*	3.62	3.51	*
185216	9921167	2222	1.51	0.26192	0.752	0.546	0.643	0.537	0.098	0.082	0.294	0.369	29.195	7.67	6.66	29.195
185164	9921231	2224	1.97	0.29942	0.538	0.44	0.591	0.573	0.09	0.074	0.22	0.294	*	5.98	5.95	*
184932	9921268	2237	1.99	0.34125	0.552	0.35	0.602	0.363	0.106	0.094	0.284	0.323	*	5.21	3.72	*
185314	9921456	2236	1.51	0.30819	0.796	0.42	0.648	0.59	0.144	0.118	0.338	0.402	*	5.53	3.56	*
185520	9921609	2237	1.78	0.33349	0.552	0.39	0.673	0.599	0.086	0.086	0.284	0.322	*	6.42	4.53	*
185129	9921420	2248	1.65	0.30819	0.746	0.338	0.793	0.602	0.126	0.116	0.221	0.382	29.195	5.92	2.91	29.195
185231	9921288	2230	1.79	0.32482	0.746	0.338	0.793	0.602	0.126	0.116	0.221	0.382	29.195	5.92	2.91	29.195
185178	9921354	2235	1.76	0.31645	0.746	0.338	0.793	0.602	0.126	0.116	0.221	0.382	29.195	5.92	2.91	29.195
185294	9921334	2233	1.88	0.32492	0.42	0.322	0.723	0.517	0.088	0.084	0.171	0.264	*	4.77	3.83	*
185367	9921388	2232	0.58	0.24519	0.42	0.322	0.723	0.517	0.088	0.084	0.171	0.264	*	4.77	3.83	*

b) lower field

Easting	Northing	Elv	ETa	NDVI	pH	EC	Bd	Bd_H2	Ks[cm/d]	ds	slop	%OM_10cm	Ca10	K10	Mg10	Na10	Ca:Mg	%sand
		masl	(mm/d)	_gr	_10cm	_10cm	20-30cm	40-50 cm		Ah	%		soluble cations(me/100g)				ratio	
186797	9917571	2085	2.74	0.35314	5.94	725	0.86	1.04	39.7	22	5	5.89	0.742	0.559	0.142	0.299	5.23	31.03
186828	9917731	2087	2.67	0.34548	6.2	720	0.9	0.98	42.6	19	3	5.89	0.742	0.559	0.142	0.299	5.23	31.03
186865	9917902	2087	2.63	0.35798	6.34	794	0.94	1	42.6	20	5	5.89	0.742	0.559	0.142	0.299	5.23	31.03
186912	9918063	2090	3.34	0.4102	6.24	742	0.82	0.97	36.2	24	3 *	*	*	*	*	*	*	*
186858	9917049	2110	3.14	0.31867	5.84	610	1.12	1.32	29.8	5	15	3.97	0.5378	0.498	0.095	0.301	5.66	*
186905	9917266	2111	3.12	0.3479	5.78	681	1.14	1.37	29.8	7	14	3.97	0.5378	0.498	0.095	0.301	5.66	*
187111	9917366	2114	0.32	0.28137	5.42	732	1.46	1.46	17.9	10	10	4.02	0.438	0.551	0.068	0.25	6.44	44.06
187184	9917520	2115	0.02	0.24196	5.44	640	1.52	1.47	17.9	13	8	4.22	0.41	0.602	0.068	0.353	6.03	44.06
187242	9917676	2116	1.35	0.28067	5.61	661	1.37	1.46	19.9	9	7	4.32	0.346	0.537	0.098	0.299	3.53	44.06
186315	9917474	2106	1.48	0.2966	5.24	581	1.4	1.19	36.4	14	6 *	*	*	*	*	*	*	*
186382	9917668	2105	1.71	0.30506	5.34	621	1.17	1.22	32.6	17	7 *	*	*	*	*	*	*	*
186506	9918035	2108	1.46	0.29085	5.42	638	1.32	1.36	17.9	18	6 *	*	*	*	*	*	*	*
186709	9917180	2082	2.18	0.35355	5.88	895	0.92	0.94	39.7	18	4	5.87	0.672	0.379	0.124	0.263	5.42	*
186651	9917881	2092	1.93	0.31282	6.21	611	1.14	1.2	29.8	19	8	5.24	0.52	0.303	0.06	0.314	7.67	42.67
186712	9918056	2091	2.13	0.33954	5.65	512	1.15	1.24	27.6	22	7 *	*	*	*	*	*	*	*
186449	9917859	2107	1.59	0.32603	5.58	678	1.16	1.21	39.2	18	5 *	*	*	*	*	*	*	*
186565	9918202	2106	1.75	0.29085	5.32	588	1.22	1.28	23.8	20	4 *	*	*	*	*	*	*	*
186752	9917389	2083	1.93	0.31192	5.77	875	0.98	1.03	35.8	20	4	5.81	0.672	0.379	0.124	0.263	5.42	*
186972	9917460	2112	2.5	0.33944	6.22	629	1.17	1.3	25.5	12	12	4.8	0.45	0.69	0.098	0.113	4.59	*
187036	9917627	2113	2.03	0.32633	5.68	639	1.16	1.26	25.5	9	14	4.8	0.45	0.69	0.098	0.113	4.59	*
187066	9917779	2115	2.22	0.32635	5.64	613	1.27	1.43	19.9	14	12	4.8	0.45	0.69	0.098	0.113	4.59	*
187290	9917873	2113	2.43	0.36655	5.54	746	1.29	1.42	21.8	15	7 *	*	*	*	*	*	*	*
186474	9917334	2092	1.75	0.29085	5.62	601	1.2	1.29	23.3	16	8 *	*	*	*	*	*	*	*
186549	9917527	2094	1.58	0.2977	5.59	520	1.17	1.27	23.3	18	8	5.24	0.322	0.303	0.072	0.314	4.47	42.67
186613	9917698	2092	2.04	0.33984	5.63	584	1.16	1.25	29.8	21	6	5.24	0.322	0.303	0.072	0.314	4.47	42.67

Appendix F Summary of Analytical methods

Parameter	Description of measured Parameters			Unit	Method of determination/Analytical method		Comments /Observations
					Field Level Measurements/ analysis	Laboratory analysis	
Chemical parameters	Soil acidity	pH	Horizons (2)	--	Auguring	1:5 soil:H ₂ O extract	Variation in standing time showed
	Soil Alkalinity	EC	Horizons (2)	micro.s/cm	Auguring	1:5 soil:H ₂ O extract	Some variations in Measurement
	Soluble cations	Mg	Horizons (2)	Meq/100g	Auguring	Milli equivalents of cation Per 100 g Soil sample Saturation extract	Magnesium content of the extract was Very low
		Ca	Horizons (2)				
		K	Horizons (2)				
		Na	Horizons (2)				
Calcium-Magnesium Ratio	Ca:Mg Ratio	Horizons (2)	--			Some values (ratios) exceed 1:5	
Organic matter content	%OM	Horizons (2)	w/w % OM			Generally very high	
Physical parameters	Saturated hydraulic Conductivity	K _{sat}		Cm/day	Inverse Auger method		Results are very high
	Bulk density	Bd	Horizons (2)	cc/cm ³	insitu weighing of soil sample	Dry weight to total volume of soil	low
	Soil texture	Particle size	Horizons	% Sand, clay..	Auguring and sample preparation		
	Slope %	%			clinometer measurement		
	Depth of A _h	Cm		cm_depth	Mini pits		

Plate 3. Profile of the study area



**Eastern Kijabe Farm
(Traversing gentle valleys)**



**Upper field
(Terraces & dispersed acacia trees)**



Lower field-Low ETa zones (Oct. 3,2001)



Upper field-High ETa zone (Sept.18, 2001)



Figures 53 Visual comparison Kriged ETa topographic and %OM maps (lower field).

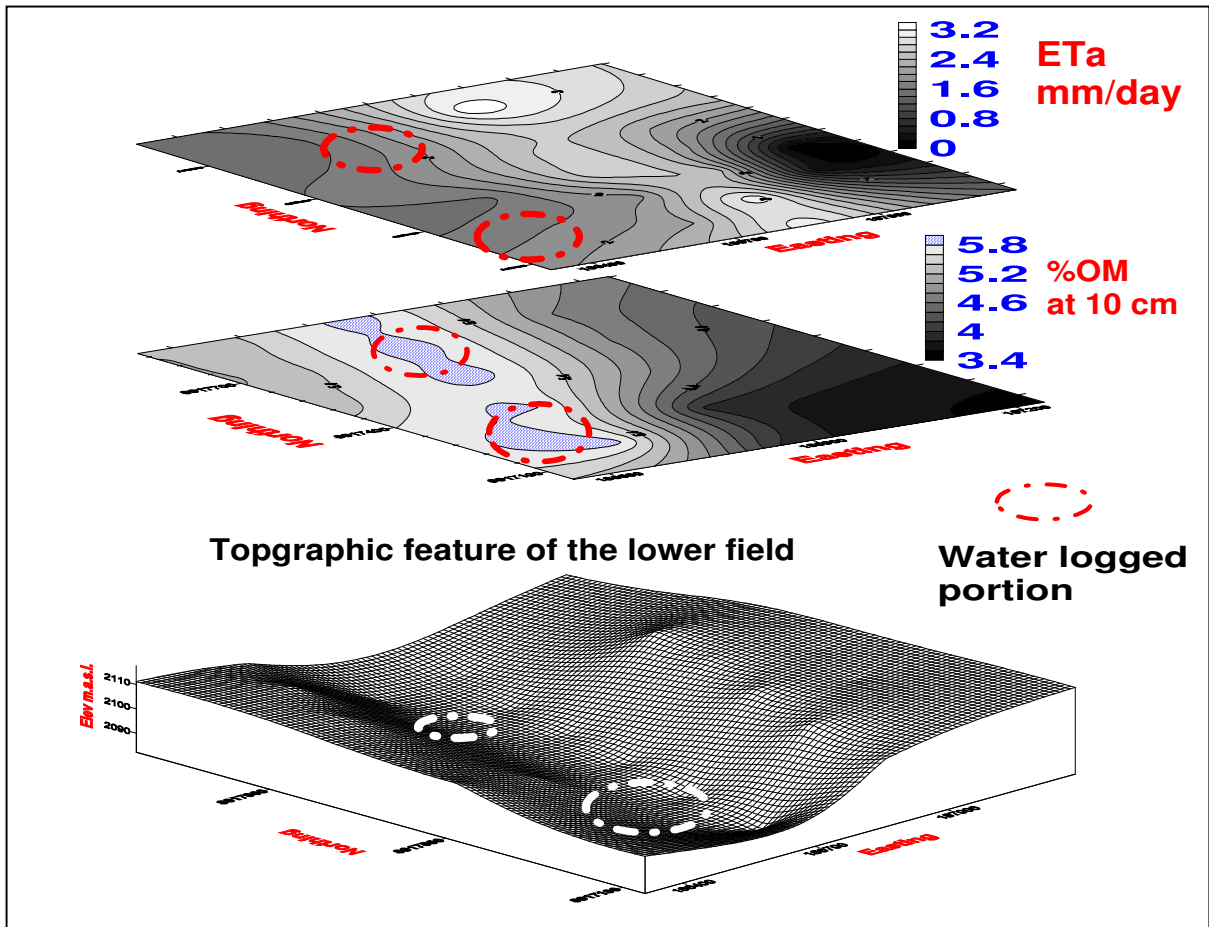


Figure 54 Visual comparison of Kriged ETa and bulk density Maps (lower field)

